

INFORMATION TO USERS

This manuscript has been reproduced from the microfilm master. UMI films the text directly from the original or copy submitted. Thus, some thesis and dissertation copies are in typewriter face, while others may be from any type of computer printer.

The quality of this reproduction is dependent upon the quality of the copy submitted. Broken or indistinct print, colored or poor quality illustrations and photographs, print bleedthrough, substandard margins, and improper alignment can adversely affect reproduction.

In the unlikely event that the author did not send UMI a complete manuscript and there are missing pages, these will be noted. Also, if unauthorized copyright material had to be removed, a note will indicate the deletion.

Oversize materials (e.g., maps, drawings, charts) are reproduced by sectioning the original, beginning at the upper left-hand corner and continuing from left to right in equal sections with small overlaps.

Photographs included in the original manuscript have been reproduced xerographically in this copy. Higher quality 6" x 9" black and white photographic prints are available for any photographs or illustrations appearing in this copy for an additional charge. Contact UMI directly to order.

**Bell & Howell Information and Learning
300 North Zeeb Road, Ann Arbor, MI 48106-1346 USA**

UMI[®]
800-521-0600

NOTE TO USERS

Page(s) not included in the original manuscript are unavailable from the author or university. The manuscript was microfilmed as received.

166

This reproduction is the best copy available.

UMI

University of Alberta

**Comparison of Several Air Dispersion Models at
Selected Sour Gas Processing Plants**

by

Verona M. Goodwin

**A thesis
submitted to the Faculty of Graduate Studies and Research
in partial fulfillment of the requirements for the degree of**

**Master of Science
in
Medical Sciences - Public Health Sciences**

Edmonton, Alberta

Spring 1999



**National Library
of Canada**

**Acquisitions and
Bibliographic Services**

**395 Wellington Street
Ottawa ON K1A 0N4
Canada**

**Bibliothèque nationale
du Canada**

**Acquisitions et
services bibliographiques**

**395, rue Wellington
Ottawa ON K1A 0N4
Canada**

Your file Votre référence

Our file Notre référence

The author has granted a non-exclusive licence allowing the National Library of Canada to reproduce, loan, distribute or sell copies of this thesis in microform, paper or electronic formats.

The author retains ownership of the copyright in this thesis. Neither the thesis nor substantial extracts from it may be printed or otherwise reproduced without the author's permission.

L'auteur a accordé une licence non exclusive permettant à la Bibliothèque nationale du Canada de reproduire, prêter, distribuer ou vendre des copies de cette thèse sous la forme de microfiche/film, de reproduction sur papier ou sur format électronique.

L'auteur conserve la propriété du droit d'auteur qui protège cette thèse. Ni la thèse ni des extraits substantiels de celle-ci ne doivent être imprimés ou autrement reproduits sans son autorisation.

0-612-40053-0

University of Alberta

Library Release Form

Name of Author: Verona M. Goodwin

Title of Thesis: Comparison of Several Air Dispersion Models at Selected Sour
Gas Processing Plants

Degree: Master of Science

Year this Degree Granted: 1999

Permission is hereby granted to the University of Alberta Library to reproduce single copies of this thesis and to lend or sell such copies for private, scholarly, or scientific research purposes only.

The author reserves all other publication and other rights in association with the copyright in the thesis, and except as herein before provided, neither the thesis nor any substantial portion thereof may be printed or otherwise reproduced in any material form whatever without the author's prior written permission.



16916 100 St.,

Edmonton, AB

T5X 4L6


Dec 22 1998

Date

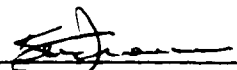
University of Alberta

Faculty of Graduate Studies and Research

The undersigned certify that they have read, and recommend to the Faculty of Graduate Studies and Research for acceptance, a thesis entitled *Comparison of Several Long Term Plume Dispersion Models at Selected Sour Gas Processing Plants* submitted by *Verona Marie Goodwin* in partial fulfillment of the requirements for the degree of *Masters of Science in Medical Sciences-Public Health Sciences*.



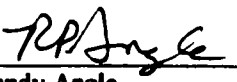
Dr. Tee Guidotti



Dr. Ken Froese



Dr. Warren Kindzierski



Dr. Randy Angle

Dec 17/98

Dedication

I dedicate this thesis to Sam and to my family who regularly reminded me of the importance of bushes, butterflies and breaks.

Abstract

A valid exposure indicator was needed to reliably categorize long-term exposures to airborne emissions from sour gas processing plants for a retrospective epidemiological study of emissions on cattle health (Scott, 1998). Predicted monthly sulphur dioxide concentrations from six models (long-term sector average, convective dispersion, modified climatological, mixed layer scaling, Gaussian plume dispersion (ISCLT3), and an exponential decay model) were compared with monthly sulphation values, wind speed- and convective velocity-adjusted sulphation values obtained from networks around 11 sour gas processing plants.. The preferred model for use in exposure assessments corresponded poorest overall (r , between -0.30 and 0.17). The convective dispersion and modified climatological model predictions corresponded best with the convective velocity-adjusted sulphation (r , between 0.40 and 0.73 and r , between 0.22 and 0.76, respectively). The recommendation that the ISCLT3 model be used for exposure assessment purposes should be revisited as simpler models perform better under a wide variety of conditions.

Acknowledgements

Many people helped me in many ways with this project. First, I extend my gratitude to Morgan Scott for his enthusiasm, generosity and overall encouragement and assistance. Randy Angle provided especially kind and helpful advice and direction throughout. The Alberta Environmental Protection staff provided great help accessing the processing plant files. I am appreciative of the Rimbey Agricultural Association and the Flagstaff District Agricultural staff for their interest, assistance and allowing me the opportunity to present and discuss my project proposal.

I very much appreciated the discussions with and assistance from Karen McDonald, David Wilson, Will Alexander, Henry Bertram, Hongmao Tang, Allan Clarke, Trevor Hilderman, and many other people helped to keep my interest piqued and my confusion at bay. I thank Tim Lambert for his humor and poetry, willingness to explain and discuss just about everything, and for overall motivational conversation. I am very grateful for the creative and supportive environment provided by Tee Guidotti and the Department of Public Health Sciences staff.

Financial and 'in kind' support is greatly appreciated from:
Smith Environmental Association; Island Lake Cow-Calf Operators; Natural Sciences and Engineering Research Council; Alberta Agricultural Research Institute; Agriculture Canada; Alberta Health; Alberta Dairy Control Board; Alberta Energy and Utilities Board; Alberta Environmental Protection; Northern Alberta Institute of Technology; and Environment Canada.

Table of Contents

Chapter 1.0	Introduction	1
1.1	Background	1
1.2	Emissions of Industrial Pollutants to the Atmosphere in Alberta	4
1.3	Sour Gas Plant Processing Practices	7
1.4	Waste Management Practices	13
1.5	Incineration and flaring are the two main methods of waste gas disposal	17
	1.5.1 Incineraton	17
	1.5.2 Flaring	18
1.6	Airborne Compounds Identified Around Sour Gas Processing Facilities	20
	1.6.1 The SCIEX™ Study	20
	1.6.2 Strosher Study	21
	1.6.3 Tollefson and Strosher Study	22
	1.6.4 Colley <i>et.al.</i> Study	23
	1.6.5 Strosher Flaring Emissions Studies	24
	1.6.6 Gnyp's Trace Element Studies	25
	1.6.7 Cooper and Peake Study	27
	1.6.8 Other Studies of Hydrocarbon Combustion Products	28
	1.6.8.1 Particulates	28
	1.6.8.2 Chlorine - Containing Compounds	28
1.7	Summary	32
Chapter 2.0	Exposure Assessment Approaches, Dilemmas and Problems	34
2.1	Rationale for Approach Taken	40
2.2	Sulphation Plates and Candles	41
	2.2.1. Comparison Studies of Candle and Huey Plate	43
	2.2.2 Accuracy	44
	2.2.3 Precision or Reproducibility	44
	2.2.4 Sensitivity	45
	2.2.5 Range of Application	45
	2.2.6 Interferences by Chemical or Physical Agents	46
	2.2.6.1 Chemical Agents	46
	2.2.6.2 Humidity	46
	2.2.6.3 Temperature	46
	2.2.6.4 Wind	47
	2.2.6.5 Shelter Configuration and Orientation	47
	2.2.6.6 Shelter Materials	48
	2.2.7 Field Comparisons	49

2.3	Summary	50
Chapter 3.0 Atmospheric Boundary Layers and Pollutant Dispersion Models		52
3.1	Structure and Dynamics of the Atmospheric Boundary Layer	53
3.1.1	Summary	61
3.2	Perspectives on Modelling Concepts in the Atmospheric Sciences	66
3.3	Gaussian Plume Dispersion Theory	72
3.3.1	Continuous Emissions	74
3.3.2	Conservation of Mass	74
3.3.3	Steady-State Meteorological Conditions	76
3.3.4	Crosswind and Vertical Concentrations Distributions	76
3.3.5	Sampling and Averaging Times	77
3.4	Use, Choice and Definition of Dispersion Parameters	78
3.5.	Dispersion Parameter Scheme Discrepancies	87
3.6	Model Validation Studies	91
3.6.1	Model Accuracy	91
3.7	Summary	98
Chapter 4.0 Methods		100
4.1	Dispersion Model Selection and Use	100
4.1.1.	Industrial Source Complex Long Term	101
4.1.2.	Long Term Sector Average Model	103
4.1.3.	Modified Climatological Model	107
4.1.4.	Convective Dispersion Model	110
4.1.5.	Mixed Layer Scaling Convection Model	113
4.1.6.	Exponential Decay Model	116
4.2	Sour Gas Processing Plant Data	117
4.3	Total Sulphation Data	120
4.4	Plume Rise Considerations	121
4.5	Statistical Analysis	122
Chapter 5.0 Results, Discussion, Conclusions and Recommendations		123
5.1	Model Predictions and Total Sulphation Comparisons	123
5.2	Processing Plant Characteristics	123
5.2.1	Plume Rise	123
5.2.2	Wind Speed	124
5.2.3	Sulphation Station Network Density and Layout	125
5.2.4	Topography	125
5.3	Between Model Comparisons	127

5.3.1	ISCLT3	128
5.3.2	LTSAM	129
5.3.3	CDM and MCM	130
5.4	Comparison of Sulphation and Wind-speed Adjusted Sulphation Values	132
5.5	Ensemble Average Correspondence	135
5.6	Identification of Other Sources of Error	135
5.7	Implications of Dispersion Modelling For Exposure Assessment Purposes	136
5.8	Conclusions and Recommendations	138
References		171

List of Tables

1.1	Composition of Produced Gas From Various Geologic Formations	7
1.2	Agents Commonly Used in Natural Gas Dehydration	9
1.3	Gas Treating Processes	10
1.4	Soil Contaminants at Gulf's Decommissioned Gas Plant	13
1.5	Amine Degradation Products Identified in Amine Solutions	15
1.6	Emission Rates of Metals from Gas Plant Incinerator Effluents	26
1.7	Combustion Conditions for Dioxin and Furan Formation	32
1.8	Expected Potentially Hazardous Air Emissions	33
3.1	Meteorological Conditions Associated with Point Source Emissions	64
3.2	Classification of Atmospheric Stability	81
3.3	Pasquill-Gifford Turbulence Typing Scheme	83
3.4	Predicted to Observed Concentrations Ratios Using Dispersion Models	93
4.1	Coefficients and Formulas Used in Model Calculations	106
4.2	Monthly Mean Maximum Afternoon Mixing Heights	110
4.3	Dickerson, Morgantown and Sudbury Model Testing Data Sets	112
4.4	Meteorology, Sulphation Station Network and Emissions Summary	119
5.1	Model-Predictions and Sulphation Correlations	165
5.2	Sour Gas Processing Plants' Incinerator Stacks Estimated Plume Rise	124

List of Figures

1.1	General Sour Gas Plant Process Flow Chart	8
2.1	Total Sulphation Candle and Holder	40
2.2	Huey Plate Configuration	40
3.1	Mid-latitude Boundary Layer Evolution in Summertime	54
3.2	Convective Boundary Layer Schematic	55
3.3	Large Eddy Diffusion in the Convective Boundary Layer	55
3.4	Evolution of Daily and Seasonal Temperature Profiles	56
3.5	Plume Dynamics for Different Release Times	57
3.6	Convective Circulations Corresponding to the Convective Velocity.	58
3.7	Decrease of Static Stability with Height at Night	59
3.8	Stably Stratified Boundary Layer Schematic	60
3.9	Appearance of Plumes from Continuously Emitting Stacks	63
3.10	Expected Downwind Ground Level Concentration Profiles	65
3.11	Horizontal and Vertical Gaussian Distributions	73
3.12	Turbulent Kinetic Energy Generation by Buoyancy and Shear	80
3.13	Turbulence Intensity, Temperature Profile, and Radiation During Unstable, Neutral, and Stable Atmosphere	81
4.1	Dimensionless Crosswind-Integrated Concentration Isoleths in a Convective Mixed Layer.	114
5.1 - 5.12	Plants # 1-14a – Scatter Plots of Wind-Speed Corrected Total Sulphation and Model-Predicted SO ₂ Concentrations	141 - 152
5.13 - 5.24	Plant # 1-14a – Scatter Plots of Convective Velocity Corrected Total Sulphation and Model-Predicted SO ₂ Concentrations	153 - 164
5.25	Correspondence Between Model Predictions and Total Sulphation	167
5.26 (a) - (k)	Seasonally Grouped Ensemble Average Predictions and Total Sulphation Ensemble Averages	168 - 170

List of Abbreviations

σ_y and σ_z	horizontal and vertical dispersion parameters, respectively
ABL	atmospheric boundary layer
ADRP	Acid Deposition Research Program
AEUB	Alberta Energy and Utilities Board
AEP	Alberta Environmental Protection
AERMOD	AERMIC Model
AMS	American Meteorological Society
API	American Petroleum Institute
ARC	Alberta Research Council
BL	boundary layer
°C	degrees in the Centigrade scale
C5 - C11	Alkanes containing 5 - 11 carbon atoms
CAPP	Canadian Association of Petroleum Producers
CBL	convective boundary layer
CDM	Convective Dispersion Model
cm ²	square centimeters
CO	carbon monoxide
CO ₂	carbon dioxide
COS	carbonyl sulphide
C _{obs}	observed concentration
C _{pred}	predicted concentration
CS ₂	carbon disulphide
CV	coefficient of variation (ratio of the standard deviation to the mean expressed as percent)
ERCB	Energy Resources Conservation Board
°F	degrees in the Fahrenheit scale
GSD	geometric standard deviation
HCl	hydrogen chloride or hydrochloric acid
H ₂ S	hydrogen sulphide
ISCLT	Industrial Source Complex Long Term
kph	kilometers per hour
LTSAM	Long - Term Sector Average Model
MCM	Modified Climatological Model
MLSCM	Mixed Layer Scaling Convective Model
mph	miles per hour
m/s	meters per second

NAPAP	National Acid Precipitation Assessment Program
NIOSH	National Institute of Occupational Safety and Health
NO₂	nitrogen dioxide
NO	nitric oxide
N₂O	nitrous oxide
NPRI	National Pollutant Release Inventory
oxy-PAH	oxygen containing polycyclic aromatic hydrocarbons
PAH	polycyclic aromatic hydrocarbons
PBL	planetary boundary layer
PbO₂	lead dioxide
PbSO₄	lead sulphate
PCDD	polychlorinated dibenzodioxin
PCDF	polychlorinated dibenzofuran
PDF	Probability Density Function
PG	Pasquill-Gifford
PGT	Pasquill-Gifford-Turner
pH	negative log of the hydrogen ion concentration
Pot Map	Potential Mapping
ppm	parts per million
ppb	parts per billion
ppt	parts per trillion
r_s	Spearman's rank correlation test statistic
RHS	generic mercaptan
R₁	Gradient Richardson number
SO₂	sulphur dioxide
SO₃	sulphite
SCRAM	Support Center for Regulatory Air Models
SD	standard deviation
SIC	Standard Industry Classification
SST	stably-stratified turbulence
STAR	Stability Array
TCDD	tetrachlorodibenzodioxin
²³⁴Th	radioisotope of thorium
TKE	Turbulence kinetic energy
US EPA	United States Environmental Protection Agency
VOC	volatile organic compound

Chapter 1

1.1 Background

Farmers have had longstanding concerns about the acute and chronic health effects of emissions from sour gas plant operations in Alberta. Recently, a retrospective epidemiological study of sour gas plant air emissions on long-term cattle health and productivity in Alberta was undertaken (Scott, 1998). A valid exposure measure or an indicator of exposure to airborne sour gas processing plant emissions was needed for this study. Since farm animals are increasingly exposed, both for short and long time periods to a wide variety of interacting and novel chemical, physical, and biological agents and processes throughout their lives, a credible exposure assessment strategy should consider all sources and types of exposure. The assessment also should attempt to prioritize and categorize the exposures based on agents of concern and on the nature of the processes and activities in their proximity. This is extremely difficult owing to the increasing number of agents of concern, the complexity of human and agricultural activities, industrial processing systems, and the meager toxicological information available on these topics.

To determine which agent or agents could best be used as an indicator of exposure to airborne sour gas plant emissions and to identify the potential chronic health hazards from airborne substances around sour gas processing plants, the literature pertaining to sour gas processing activities, agents, sources and extent of emissions was reviewed. The availability of ambient air monitoring methods and extent of monitoring activities around sour gas processing facilities was also reviewed with the aim of identifying agents emitted from processing plants that may impact animal health. The review was limited to airborne agents emitted into the atmosphere by plant processing activities. It did not consider chemical agents that may enter food or water systems, physical agents such as heat, cold, noise, light, and ionizing radiation, or biological agents such as viruses, bacteria, and parasites. It is recognized that these exposures, in addition to nutrition and

housing may also affect animal health.

The methods and approaches for assessing human exposure to potentially harmful airborne agents, although developed primarily for occupational settings, are believed to be generally applicable to animals and are outlined here. Assessing workers' exposure to airborne agents in occupational settings is typically done by measuring air concentrations of agents of concern close to the breathing zone for the time period corresponding to the agent's toxic properties. Other approaches include measuring substances in the areas in which the workers spend most of their time, noting the conditions and activities at the time of and for the duration of sampling in the surrounding areas, or combining these strategies. The success of these approaches is contingent upon several important factors. An investigator's knowledge of the sour gas plant processing methods, agents used and by-products likely to be present will, due to confidentiality concerns and trade secrets, inevitably limit the scope of agents considered for evaluation. For example, in addition to knowing the amount of agents going into the process, the investigators should have some knowledge of what chemicals and accompanying by-products are expected to be present, where they are expected, and in what form they are likely to be in (particles, gases, vapors, solids, aerosols, or mixtures or composites) to devise an efficient sampling strategy and to select the most suitable sampling and analytical method. Also, knowledge of the agents' physical-chemical properties (eg. density, size, shape, flammability, vapor pressure), and the conditions of their use (eg. enclosed, under pressure, increased temperature) in relation to the animal's activities will contribute to the development of an appropriate sampling strategy. The availability of validated air sampling and sensitive analytical methods appropriate to the time periods and ambient air concentrations of concern may also limit the investigator's ability to fully evaluate simultaneous exposures to the variety of environmental agents encountered.

While many monitoring and analytical methods for sulphur-containing gases have been developed and described in the literature, valid, accurate, sensitive and low cost air sampling methods for sulphur-containing gases suitable for use at remote outdoor

locations were not available at the outset of this study. However, for some sour gas processing plants, decades of historical data on monthly measures of sulphation as well as monthly site-specific wind direction and frequency, and emissions were available from Alberta Environment Protection. As well, a variety of plume dispersion models, which have been suggested for use in air pollution epidemiological studies as tools for categorizing exposures, have been made publicly available at the United States Environmental Protection Agency Support Center for Regulatory Air Models (US EPA SCRAM) Website (<http://www.epa.gov/ttn/scram>).

Under circumstances where personal sampling methods are not feasible or available, some researchers (Eifler *et. al.* 1981; Stinnett et al,1981; Wong and Bailey, 1993) suggest using a plume dispersion model, with the caveat that model evaluation be undertaken prior to its use. Plume dispersion models have been widely used to evaluate the impact of siting a facility by estimating the worst-case short- and long-term concentrations expected to be found around the site using historically-averaged meteorological data. Generally, a Gaussian plume dispersion model's estimate of the pollutant concentration at specific times and specific locations is poor (US EPA, 1993). Large error bounds, as much as a factor of 10 to 100 are expected, which can be reduced somewhat by using actual windspeed and wind direction data for the location of interest and by using accurate measures of atmospheric stability (Turner, 1994).

After reviewing the sour gas processing principles, practices, and emissions and the availability of air sampling, analytical methods and historical data, I concluded that the best readily-available choice of an indicator or surrogate for chronic exposure to sour gas processing emissions available was the total sulphation value. I also concluded that the least cost and most feasible approach to evaluating the validity of using a plume dispersion model to categorize exposures was to compare model-predicted sulphur dioxide concentrations to measured sulphation values. Thus, the main objective of this study was to determine the reliability and validity of using modelled air pollution concentrations for exposure categorization purposes. I evaluated the correspondence in

space and time between several long term dispersion models' predicted sulphur dioxide concentration and total sulphation values at selected sour gas processing plants by assessing the scatterplots for random, proportional and constant errors and linearity using the method of least squares regression and by calculating the Spearman Rank correlation coefficient.

1.2 Emissions of Industrial Pollutants to the Atmosphere in Alberta

In United States, Canada and Alberta, the atmosphere is the main environmental compartment into which industries dispose most wastes, including toxic and carcinogenic wastes (National Pollutant Release Inventory (NPRI) Summary Report, 1995; US EPA, 1991). In 1989, 43% of the total wastes produced (2.6 million tonnes) in the United States were released into the atmosphere, of which the chemicals industry (Standard Industry Classification (SIC) 28) was responsible for approximately half of the total (1.2 million tonnes) (US EPA, 1991). Of the total 2.6 million tonnes released into the environment, the proportion for each class of toxic substance that was released into the air is reported for 1989 as follows: organics – 68%; mineral acids and salts – 5%; metals – 4% (50% was released onto the land); halo-organics - 88%; and non-metals – 70%. Although mixtures and trade secrets together accounted for less than 0.2% of the Toxics Release Inventory total, 55% and 80% of the totals in each category, respectively, were emitted into the air (US EPA, 1991).

In Canada, 60% of the total waste produced by 1,754 industrial facilities and 54% of the toxic and carcinogenic wastes were released into the atmosphere in 1995. Of the 169,000 tonnes of total pollutant releases reported nation-wide to the 1995 National Pollutant Inventory Release Program, 102,000 tonnes were released into the air, and of the 14,000 tonnes of toxic and carcinogenic pollutants reported released, 54% (7,590 tonnes) were released on-site into the air. The crude petroleum and natural gas sector (SIC 07), the sixth largest contributor in Canada in 1994, emit about 5% of the total on-site releases.

From the 200 reporting industrial facilities in Alberta, 28,307 tonnes (65%) of the total 43,562 tonnes of pollutants (73 chemicals) were released to the air, 12,383 tonnes were to underground locations, 1,651 tonnes were to the land, and 1,183 tonnes to water. The conventional oil and natural gas industries (SIC code 0711) emitted 6,743 tonnes of pollutants to the atmosphere, most of which was carbon disulphide (3,590 tonnes), emitted by sour gas processing facilities, and, 36% of the 3590 tonnes (1,287 tonnes) was emitted by one facility. In Alberta, 262 tonnes of benzene (of which 124 tonnes was emitted by two facilities), 369 tonnes of toluene (of which 184 tonnes was emitted by two facilities), 347 tonnes of xylene (of which 207 tonnes were emitted by two facilities), 100 tonnes of cyclohexane (of which 75 tonnes was emitted by one facility), and 25 tonnes of ethyl benzene were released to the atmosphere in 1995 by the conventional oil and natural gas industries reporting to the NPRI (<http://www.npri-inrp.com>).

Picard *et.al.* (1992) summarized all fugitive volatile hydrocarbon emissions, including methane, by industry sector and type of primary resource. The gas processing sector contributes 7% of the total, emitting 8.4×10^4 tonnes of volatile hydrocarbon emissions (including methane) out of a total of 1.2×10^6 tonnes for the whole oil and gas industry. Recently, a working group on benzene emissions from glycol dehydrators report that there are an estimated 3500 glycol dehydrators in service in Canada, with Alberta accounting for 82% (2410/2939) and that the units are typically unattended and the emissions are not regularly monitored. In Alberta, the distribution of the 2410 dehydrating units from 86 reporting companies were as follows: 1484 at the well site, 421 at the compressors, 127 at batteries, 319 at the gas plants, and 58 at gas storage stations. The group estimates that 7% of glycol dehydrators with benzene emissions greater than 9 tonnes/year account for 41% of the total Canadian glycol dehydrator emissions (Working Group on Benzene Emissions From Glycol Dehydrators, 1997).

Concerns about sour gas processing plants' environmental and health impacts in Alberta have been documented in reports by Klemm (1972) and the Environmental Conservation Authority (1972, 1973). Attempts to address the concerns raised have been

undertaken in studies such as the Twin Butte Soils and Water Evaluation Task Force (1984), the Acid Deposition Research Program (ADRP) (Legge and Krupa, 1990), and within the ADRP, the Southwestern Alberta Medical Diagnostic Review (Spitzer, 1986).

The Acidifying Emissions Inventory (Picard *et.al.*, 1987, 1990) identified all sulphur dioxide emission sources in Alberta which were licensed by the provincial government agency (Alberta Environmental Protection) and all sour oil batteries approved by the Alberta Energy and Utilities Board (previously the Alberta Energy Resources Conservation Board) that emit sulphur dioxide at a rate of 0.2 tonnes per day or more. The inventory comprised 565 sources of sulphur dioxide which, based on available 1985-86 records, emitted a total of 1267 metric tonnes sulphur dioxide per day or approximately 460,000 tonnes per year (Picard *et.al.*, 1990, p 413-417). The petroleum industry accounted for 81.5% of the total, the electric utilities for 16.6% and pulp and paper, chemical and fertilizer industries accounted for the remaining. Within the petroleum industry sector, sour gas extraction plants account for 55.4% of the sulphur dioxide emissions; oil sands plants account for 34.5%, sour gas flaring plants 4.5%, and oil batteries, refineries and heavy oil plants account for the remaining (Picard *et.al.*, 1990, p 420-422).

Attempts to address specific concerns about the effects of acidifying emissions on livestock have been undertaken at a variety of forums. In 1992, a workshop was convened at the Alberta Environmental Center in Vegreville to review the anecdotal information and to discuss the harmful effects of acid forming emissions on livestock and to identify research needs and in 1996, an Acidifying Emissions Symposium was held in Red Deer. Recent literature reviews and discussion of the toxicological hazards of oilfield pollutants in cattle are found in the Alberta Cattle Commission Report (Alberta Environmental Centre, 1996) and in the Alberta Research Council Report (Chalmers, 1997), respectively.

1.3 Sour Gas Plant Processing Practices

Recovering and producing natural gas from geologic reservoirs for markets includes a variety of activities at the well production stage, gas transmission stage, processing and compression stage. Natural gas may occur in geologic formations dissolved within crude oil deposits, associated with crude oil, or dissolved within brines. The composition of produced gas varies with the geologic formation (Table 1.1).

Table 1.1. Composition of Produced Gas From Various Geologic Formations (after Hammond and Wessman, 1973)

Component	Beaverhill Lake	Viking/Cadomin	Triassic
Composition, Mole Percent			
Nitrogen	1.09	0.34	0.65
Carbon Dioxide	3.44	0.57	1.97
Hydrogen Sulphide	17.06	0.00	1.11
Methane	58.71	87.64	73.11
Ethane	7.85	5.61	14.55
Propane	3.15	2.97	6.36
<i>iso</i> -Butane	0.77	0.44	0.49
<i>n</i> -Butane	1.45	0.81	1.22
<i>iso</i> -Pentane	0.61	0.26	0.16
<i>n</i> -Pentane	0.64	0.24	0.22
Hexanes	1.18	0.37	0.09
Heptanes Plus	4.05	0.75	0.07

From the well-site to the processing plant and to the end user, natural gas production requires the use of many chemicals at various steps (drilling, cementing, completion, stimulation and production) in the processing stream. A description of sour gas processing has been given by various authors and organizations (Petroleum Extension Service, 1974; Curry, 1981; Klemm, 1972, Kohl and Riesenfeld, 1979) and an overview of the chemical compounds used in sour gas processing is found in the Alberta Cattle Commission Report (Alberta Environmental Centre, 1996). A general survey of the chemicals used, principally at the well-site, have been assembled and can be categorized according to their use as weighting agents, viscosifiers, dispersants, fluid loss additives, biocides, corrosion and scale inhibitors, surfactants, accelerators, retarders,

stabilizers, dehydrators, and defoamers (Brown, 1981; Borchardt, 1989; Cottle and Guidotti, 1990). Further, during drilling the presence of heat, pressure and the complex chemical mixing that occurs may lead to the formation of unrecognized toxic substances (Brown, 1981). As the gas-oil-mixture is recovered from the ground, further treatment is required to meet sales criteria and a variety of chemical agents are used throughout the processing system to purify the natural gas. Sour gas processing for commercial and residential markets is achieved by using many combinations of physical and chemical separation principles including: phase separation (fractionation), distillation and condensation, dehydration and chemical adsorption (where the gas stream contacts the chemicals in the solid phase) and absorption (the gas stream contacts the chemicals in the liquid phase), to remove unwanted substances and to purify the final product .

The produced gas is processed by separating the gas from free liquids (crude oil, hydrocarbon condensate, water) and entrained solids, removing condensable water and recoverable hydrocarbon vapors, and removing other undesirable components, such as hydrogen sulphide and carbon dioxide (Figure 1.1).

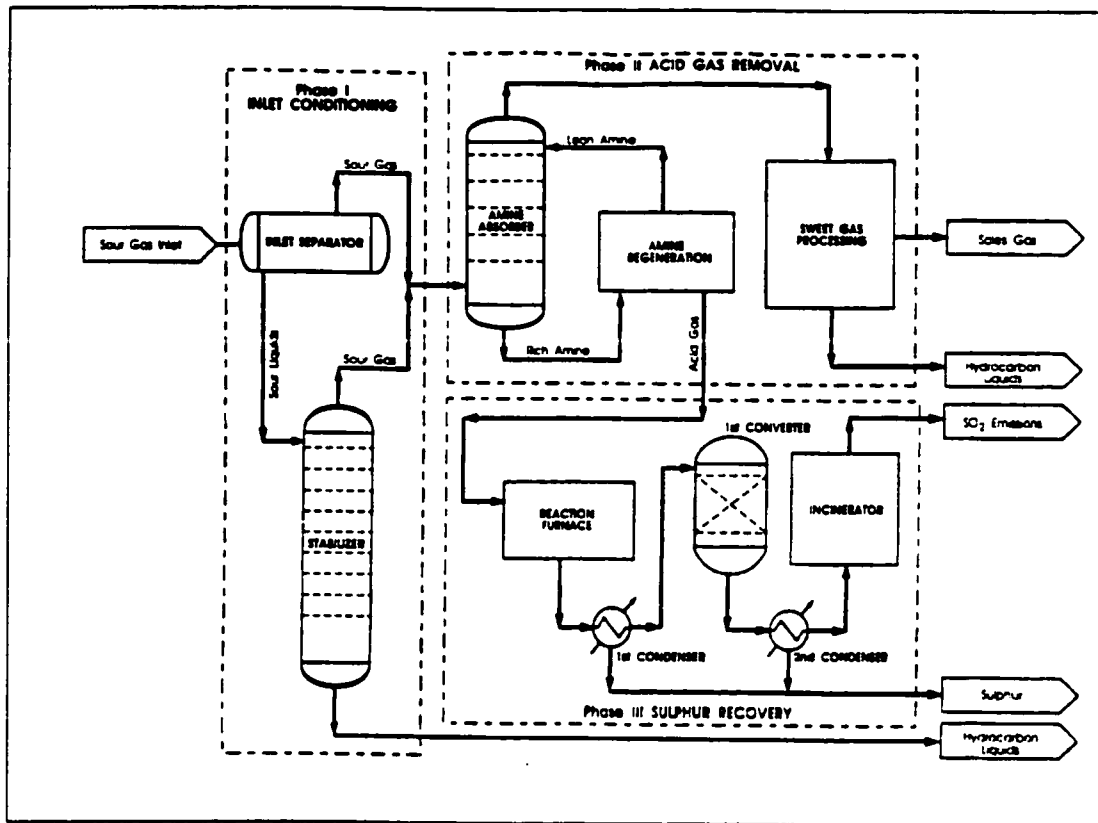


Figure 1.1. General Sour Gas Plant Process Flow Chart (after Environment Canada and CH2M HILL Engineering Ltd., 1993, Reproduced by Permission of the Minister of Supply and Services, 1998)

Sour gas and liquid condensate, comprised of liquid hydrocarbons, and brine (salt-bearing formation water) from production wells in one or more fields, enter the inlet separator where the brine, condensate, particulate and mists are separated from the gas. Dehydration facilities throughout the separation, processing and transportation system remove the water vapor by various means. The most common methods are liquid or dry-bed chemical adsorption, or injection of the dehydrating agent into the gas stream to prevent hydrate formation at various points in the processing stream (Table 1.2). Hydrates are complexes of methane and water which may solidify under appropriate conditions. The wet inlet gas enters the primary scrubber, where liquids are removed by a mist extractor and particulates or solids are removed by gravity settling. The gas then

enters an accumulator section at the base of the glycol contactor, allowing any additional particulate matter to settle out of the stream. The gas flows upward through a series of bubble trays, contacting the lean glycol dehydrating solution circulating downward, then through a mist extractor to remove any remaining free liquids or liquid droplets from the gas. The liquids are directed to the amine facility. The used glycol solution which contains contaminants removed from the gas, enters a flash tank. Here, the absorbed gases are flashed-off to the atmosphere, used as fuel or may be used for stripping gas and the used solution is preheated before finally entering the still column and reboiler system for redistillation and recirculation.

Table 1.2. Agents Commonly Used in Natural Gas Dehydration (Kohl and Riesenfeld, 1979)

Agent	Application
Methanol	injection
Ethylene glycol	injection or column
Diethylene glycol	column
Triethylene glycol	column
Calcium chloride	dry bed
Dessicants (silica gel, silica-based beads, activated alumina, activated bauxite, molecular sieves)	dry bed

The dehydrated gas stream is directed to the sweetening facility where the sour condensate is directed to a low pressure stabilization unit to remove the hydrogen sulphide (H_2S) gas from the condensate. The produced salt water is treated in a sour water stripper, which removes dissolved H_2S , or is disposed of by deep-well injection. Following removal of the H_2S , the sweet (H_2S -'free') condensate is directed to storage while the stripper overhead gas stream, rich in H_2S , is compressed and recombined with the sour inlet gas stream and sent to the amine unit. Gas entering the amine absorber is combined by opposite-direction flows under pressure and low temperature with an aqueous amine solution or other chemical method (Table 1.3) to remove acid gases from the raw gas stream. The sour amine solution, rich in H_2S and carbon dioxide (CO_2) is directed to the low pressure amine flash tank where acid (flash) gas is given off. The amine flash gas is directed to a sulphur recovery unit (or directed to flare), and the rich

amine solution is regenerated. Acid gas dissolved in the amine solution is then driven off in the amine reboiler, which is then either flared or processed by a sulphur recovery unit. To complete the cycle, the hot regenerated amine is pumped, cooled, filtered, and returned to the amine absorber. The sweetened gas exiting the amine absorber may require further conditioning, such as water vapor removal, before it enters the sales gas pipeline.

Table 1.3. Gas Treating Processes (after Petroleum Extension Service, 1974)

Chemical Process Agents	Gases Removed				
	CO ₂	H ₂ S	RHS*	COS	CS ₂
Monoethanolamine (MEA) (15-20% solution)	x	x		x	x
Diethanolamine (DEA) (25-30% solution)	x	x		x	x
Diglycolamine (DGA)	x	x		x	x
Sulfinol (45% diisopropanolamine, 35% sulfolane, 20%water)	x	x	x	x	x
Glycol-Amine	x	x			
Iron Sponge		x			

*RHS = Mercaptans

Other acid gas removal methods include the use of: triethanolamine, methyldiethanolamine, hot potassium carbonate, phosphate, vacuum carbonate, tripotassium phosphate, sodium phenolate, phenoxide, alkacid, and named processes such as Benfield, Catacarb, Estasolvan, Ferrox, Fluor Solvent, Giammarco-Vetrocoke, Lacey-Keller, Manchester, Perox, Rectisol, Seaboard, Selexol, Stretford, Takahax, Thylox, and Townsend (Petroleum Extension Service, 1974; Ecology Audits Inc., 1975).

Before waste gas incineration, acid gases leaving the amine sweetening unit are directed to the sulphur recovery unit to convert H₂S to elemental sulphur for 'tail-gas cleanup'. The acid gases are mixed with air and burned at temperatures of 950° - 1200°C, where one-third of the H₂S is oxidized to sulphur dioxide (SO₂) in an exothermic reaction. The reaction gases are cooled in a waste-heat boiler and as the gases are cooled, about 60 - 65% of the sulphur gases condense to form elemental sulphur. After the remaining gases exit the sulphur condenser, they are directed to the Claus converter, where SO₂ and

H₂S are further reacted over a catalyst at temperatures of 170 - 370°C to form elemental sulphur, water and heat (Kerr *et.al.*, 1976). Sulphur recovery from a single converter can range from 70 - 80%. Higher levels of recovery are obtained by applying more converter and condenser stages in series such that sulphur recoveries of 96 - 98% can be achieved with a three-bed sulphur recovery unit. The recovered elemental sulphur is stored on-site in a liquid sulphur pit, a solid block, or as nuggets. The residual gas, which contains mostly nitrogen, carbon dioxide, and water with small amounts of H₂S, SO₂, and other sulphur-bearing products, is directed to an incinerator stack, where the carbon-, sulphur- and nitrogen- bearing components not recovered in the plant are oxidized through combustion principally to CO₂, SO₂ and NO₂, respectively. This combustion is the principal source of SO₂ emissions from the natural gas processing industry.

The next sections provides an overview of studies addressing the composition of the various waste streams identified and measured at various locations within the gas processing sector. It focuses mainly on the airborne emissions and does not include “land-farmed” wastes or contaminated soils (Table 1.4), even though these may be a significant source of airborne pollutants upon resuspension through weathering, erosion or cultivation (Alberta Environmental Centre, 1996).

Table 1.4. Contaminants Found in Soils from Gulf's Pincher Creek Decommissioned Gas Plant (Alberta Environmental Centre, 1996)

Contaminant	Concentration Range (ppm)	Alberta Tier Criteria for Contaminated Soil (ppm)
Cadmium	0.2 - 4	1
Chromium (total)	30-243	100
Mercury	0.18-6.8	0.2
Zinc	82-1225	120
Polycyclic Aromatic Hydrocarbons (PAH) (total)	3-16,300	1.0
N-substituted PAH	17-25	0.1
Substituted benzenes	210-1850	0.05-1.0
Thiophenes	170-1140	0.1
Phthalates	5-37	30
Polychlorinated Biphenyls	1-1.4	0.5
Diethanolamine	800,000 (amine sump)	Not assigned
Unidentified organics	150-83,000	Not assigned

1.4 Waste Management Practices

Depending upon the configuration of the processing plant, a number of pollution sources can be identified: incineration of tail gas, continuous or intermittent flaring of various hydrocarbon-containing process streams, emergency flaring, venting of gases to atmosphere at various process points (dehydrator reboilers, glycol regenerator vapors), sulphur block dust, burn pits, fugitive emissions (Pervier *et. al.*, 1974; Klemm, 1972), and plant 'burnout' (Kerr *et. al.*, 1977). Pumps driven by natural gas, gasoline or diesel engines produce exhaust emissions (Pervier *et. al.*, 1974; Ecology Audits Inc., 1975). The major source of continuous air emissions are the tail gases going to the incinerator and emitted at the stack. Some smaller volume and continuous or intermittent sources that are directed to flares are emissions from: i) the inlet separator; ii) the stabilizer overhead gas; iii) flash gas from the amine regeneration units; iv) gas from the amine reboiler; and v) sour water stripper.

Limited information is available on the volumes, types of waste or their by-products generated by the sour gas processing sector. One estimate is that Alberta's oil and gas industry sector (exploration, drilling, production and pipeline operations)

produces 150,000 tonnes of hazardous wastes annually and has had a waste inventory of 1.8 million tonnes (David Bromley Engineering Ltd., 1991). Refineries produce 82,500 tonnes annually which comprises approximately 30% of annual hazardous waste production in Alberta (David Bromley Engineering Ltd., 1991). Actual measurements of waste quantities produced in each sour gas sector category have not been located, however estimates have been made by Hawkins *et.al.* (1986) and Wotherspoon and Associates (1988). Annually, the oil and gas industry produces wastes, of which about 50% is deemed hazardous (as defined by the Alberta Hazardous Waste Regulation), in the following amounts and is disposed of by the following methods (Wotherspoon and Associates, 1988):

- 2,160 tonnes of filters of which an estimated 75% was incinerated;
- 14,000 tonnes flare knock-out sludges, of which an estimated 80% was disposed of by landfarming and other methods;
- 1,600 tonnes oily rags, of which an estimated 75% would have been disposed of through methods such as burn barrels;
- 200,000 tonnes of all sludges were in process ponds or flare pits;
- 30,000 tonnes of wash fluid solvents; of which an estimated 10% is stored in ponds on-site and the remaining has either been reclaimed, incinerated or disposed of by other methods; and
- 55,000 tonnes of oil-contaminated soil, of which an estimated 20% is in on-site landfill storage, 30% is in off-site landfills, and 50% has gone to reclaimers.

Hawkins *et.al.* (1986) estimated that for one sour gas plant which processes approximately $1.7 \times 10^6 \text{ m}^3$ raw gas at 10% by volume of H₂S plus CO₂, approximately 350 kg per month of reclaimer bottoms are generated. Filter sludges were estimated to be generated at rates within the same order of magnitude.

Over time, spent or used glycol and amine solutions accumulate contaminants that

interfere with their function. Used amine solutions contain a variety of amine degradation products (Table 1.5), hydrocarbons (0.5 - 2%), phenols (10-50 mg/L), metals (Cr, Pb, Cu, Ni) 5 - 15 mg/L each and oil and grease (0.3 - 0.5%) (Canadian Association of Petroleum Producers [CAPP], 1990). Beasley and Merritt (1992) have provided a brief overview of gas treatment chemicals and their degradation products. Degradation products that were identified include oxazolidones, piperazines plus other undefined nitrogen-containing compounds; salt, asphaltenes, sand, oil, grease, suspended solids, and fine particles of iron sulphide; amine thiosulphates or amine thiocyanates formed when thiosulphates or cyanides are present. The waste bottoms of the amine processor contained about 55% NaCl by weight.

Table 1.5 Amine degradation products that have been identified in amine solutions (after Boyle, 1990; Kim, 1988; Hsu and Kim, 1985; Kennard and Meisen, 1980; Kohl and Riesenfeld, 1979; Oseinton and Knight, 1971)

Amines	Other
aminoethylethanolamine	bis(hydroxyethylaminoethyl)ether
bis(hydroxyethyl)ethylenediamine	N,N'-bis(hydroxyethyl)piperazine
N-(2-hydroxyethyl)ethylenediamine	N,N'-bis(2-hydroxyethyl)piperazine
methyldiethanolamine	N-(2-(N,N-bis(2-hydroxyethyl)amino)ethyl)-N'-2-hydroxyethyl)piperazine
triethanolamine	N,N'-bis(2-hydroxyethyl)glycine
N,N,N,N-tetra(hydroxyethyl)ethylenediamine	N,N'-bis(hydroxyethyl)urea
N,N,N",N"-tetra-(2-hydroxyethyl)diethylenetriamine	thiourea
N,N,N'-tris(2-hydroxyethyl)ethylenediamine	thiuram disulphide
Ketones	diethanolammonium N,N-di-(2-hydroxyethyl)dithiocarbamate
N,N'-bis(hydroxyethyl)imidazolidone	N,N,N',N'-tetra(2-hydroxyethyl)-thiocarbamide
3-(2-(bis(2-hydroxyethyl)-amino)ethyl)-2-oxazolidone	2-diethylaminoethanol
1-(2-hydroxyethyl)imidazolidone	N-(hydroxyethyl)ethyleneimine
3-(2-hydroxyethyl)oxazolidinone	oxazolidine 2-thione
3-(2-hydroxypropyl)-5-methyl-2-oxazolidone	thiazolidine 2-thione
oxazolidinone	alkanolamine salt of dithiocarbamic acid

Amine filters may, in addition to the amine solution remaining within the filter matrix, contain: volatile organics (1%), cyanide (7.5 - 250 mg/kg), thiocyanate (5 - 20,000 mg/kg), sulphide (225 - 4,360 mg/kg), chloride (0.5 mg/kg), vanadium (430-620

mg/kg), arsenic (0.01 - 10.5 mg/kg), cadmium (0.004 - 2.5 mg/kg), chromium (Cr^{6+}) 0.032 - 8.7 mg/kg), lead (0.001 - 445 mg/kg), mercury (0.005 - 9.5 mg/kg), nickel (0.02 - 62 mg/kg), thallium (0.03 - 0.37 mg/kg), oil and grease (0.08 - 9.94%) and amine degradation products (0.03%) (CAPP, 1990). Amine sludges from several gas plants contain the alkanolamine degradation products N-(2-hydroxyethyl)ethylenediamine, bis(hydroxyethyl)ethylenediamine, 1-(2-hydroxyethyl)imidazolidone, in concentrations ranging from 23,000 ppm - 196,000 ppm (Boyle, 1990).

Compounds identified in spent glycol solutions include aromatics from the gas stream and glycol oxidation products such as formic acid, formaldehyde, acetic acid, acetaldehyde, and organic peroxides as intermediate products (Kohl and Riesenfeld, 1979; Curry, 1981). Corrosion inhibitors that are added to the glycol solution include monoethanolamine or sodium mercaptobenzothiazole (Kohl and Riesenfeld, 1979). Agents added to control pH include borax and soda ash (Curry, 1981) and defoamers such as trioctyl phosphate may also be added (Kohl and Riesenfeld, 1979). Glycol filters are reported to contain: ethylene glycol (0.6 - 5.8%), diethylene glycol (800 - 1500 mg/kg), triethylene glycol (2700 - 7500 mg/kg), iron oxide (0.5 - 2.5%), arsenic (0.15 - 0.35 mg/kg), cadmium (0.34 - 4.36 mg/kg), chromium (Cr^{6+}) (0.9 - 50 mg/kg), lead (< 0.01 - 700 mg/kg), mercury (<0.01 - 0.4 mg/kg), nickel (1.96 - 50 mg/kg), total organic and volatiles (34.4- 98.6%), oil and grease (0.6 - 1.8%), and iron sulphide (1.3%) (CAPP, 1990).

Sludges varying in composition are produced at almost every separation phase within a sour gas processing plant. Sludges produced at the amine stage contain: amine degradation products which may comprise up to 60%, total cyanide (up to 200 ppm), arsenic (0.01 - 15 mg/kg), cadmium (0.1 - 950 mg/kg), chromium (Cr^{6+}) (1.0 - 67 mg/kg), lead (0.5 - 1000 mg/kg), mercury (0.01 - 3.5 mg/kg), nickel (0.2 - 35 mg/kg) and sulphur in the form of iron sulphide (0.15 - 0.57%) (CAPP, 1990).

1.5 Incineration and flaring are the two main methods of waste gas disposal.

1.5.1 Incineration

Complete combustion of wastes requires use of equipment which provides an adequate source of oxygen, adequate reaction temperatures, turbulent mixing of air with combustible gases and sufficient residence time to ensure complete oxidation (Canadian Council of Ministers of the Environment, 1992). Kerr *et.al.* (1976a, 1976b, 1976c, 1977) undertook a series of sulphur plant waste gas incineration kinetics and fuel consumption studies. A Claus sulphur plant waste gas stream usually contains the combustible gases: hydrogen, carbon monoxide, hydrogen sulphide, carbonyl sulphide, sulphur vapor, and sulphur liquid (in order of decreasing concentration). Claus waste gas streams were incinerated with added fuel gas and excess oxygen of about 3 - 5 % to attain a stack-top temperature of about 1000°F (538°C) and stack residence time of 4-16 seconds, for oxidation of compounds to carbon dioxide, sulphur dioxide and nitrogen dioxide (Kerr *et.al.*, 1976a). The 1987 Acid Deposition Research Program emissions inventory survey listed 17/42 (40 %) of the sour gas plant's reporting incinerator stacktop temperatures as less than 538 °C (Picard *et.al.*, 1987). Actual stack gas composition will be variable depending upon the processing parameters at each plant. Water vapor may represent a considerable proportion (25%) of the incinerated effluent, however, on a dry gas basis, the incinerated stack gas composition is estimated as: approximately 88% nitrogen, 7% carbon dioxide, 2% sulphur dioxide, and 3.5% oxygen (Klemm, 1972).

In a review of sulphur plant incineration kinetics, Kerr *et.al.* (1975) state that studying incineration processes are difficult due to the complexity of incineration kinetics such as multiple chain initiating, terminating and branching reactions occurring between many species both in the gas phase and on the wall surface, and the wide variety of incinerator designs. Kerr and Paskall (1976c) report that generally, sulphur reacts with hydrocarbons at rates which are orders of magnitude greater than the rate oxygen reacts with hydrocarbons, and that the hydrocarbons in the acid gas would be preserved after the combustion of hydrogen sulphide since hydrogen sulphide reacts with oxygen at a faster

or comparable rate than hydrocarbons with oxygen. Also, these authors report that hydrocarbon contamination of the tail gas stream resulted in significant furnace production of carbon disulphide and lesser amounts of carbonyl sulphide. The carbon disulphide is formed directly from sulphur vapor reacting with any hydrocarbon present in the acid gas feed and the production of carbon disulphide is directly proportional to the hydrocarbon content of the acid gas. The carbonyl sulphide is formed from carbon monoxide reacting with sulphur vapor.

Incinerators may also be used to dispose of: liquid amine wastes, known to contain a variety of amine degradation products (Boyle, 1990); brine from a sour water stripper (Kerr *et.al.*, 1976); and are permitted to be used to dispose of other liquid and solid wastes (CAPP, 1990; Alberta Environmental Centre, 1996). In 1984, the Canadian Petroleum Association Environmental Planning and Management Committee designated incineration as: a preferred method for disposal of treater hay, and process filters; an acceptable method for glycols, degradation products from amine and sulfinol treating; and, subject to special approval, for waste oil sludges (Canadian Petroleum Association, 1984).

As of 1990, incineration is designated a preferred method for non-hazardous wastes including activated carbon, construction debris, crude oil sample bottles, oil-solvent- or condensate- contaminated debris and soil, dessicants, amine-, glycol-, water- and oil- filters, hydrocarbon removal wastes, hydrocarbon-containing lubricating oil, and sludges from the flare pit, fractionator bottoms, sweetening systems, and glycol system (CAPP, 1990). Other substances such as reclaimer drain sludge, process filter washings, and waste liquid catalysts from gas cleanup processes, oily separator sludge, process filters, and liquified propane gas storage tank bottoms may also be incinerated (CAPP, 1990).

1.5.2 Flaring

Flaring has been a traditional method for disposing industrial relief gases on an

intermittent emergency basis or on a continuous low flow rate release basis. A review of flaring technology was undertaken by SKM Consulting Ltd. (1988), which details the flaring technologies available, associated safety concerns, studies on combustion efficiency and summarizes current oil and gas industry flaring practices.

While laboratory studies of stable flames have repeatedly demonstrated combustion efficiencies greater than 98% for a wide variety of combustible gases, assessments of efficiencies for full-scale industrial flares were rarely undertaken. Two studies cited in the SKM Consulting Ltd. Report (1988) measured combustion efficiencies in at several sites in Alberta. An acid gas flare diluted with varying amounts of fuel gas under wind conditions of 1 - 6 m/s was found to have combustion efficiencies of 22 - 100%. Solution gas flare stacks at several locations in the Redwater, Alberta oilfield were found to have H₂S combustion efficiencies in the range of 38 - 100%.

Concerns about the environmental acceptability of flaring as a means of disposing of gas prompted a two-part study undertaken to assess current design and operating practices of flaring, funded by the Research Management Division of Alberta Environment, and Environmental Protection, Environment Canada (Reid, DeBoeck, and Davies, 1988). Part A, the "Review and Assessment of Current Flaring Technology", was completed (SKM Consulting Ltd., 1988) and Part B, the "Summary of Current Oil and Gas Industry Flaring Practices" was not. A draft report dated March 1988 was prepared by the consultants. A final report was not released because of limited funds and the draft report may contain errors and/or omissions which would have been edited out in the final version (personal communication, R.B. DeBoeck, June 1996). As described in the draft report, questionnaires were sent to 426 of a total of an estimated 2500 flare facilities in Alberta to collect information pertaining to the basic facility, details of the flare system, and operations and maintenance. Site visits were also conducted to verify and augment the data collected on the questionnaire. Data, obtained on 318 flare facilities, revealed that although flares are generally designed for a very wide range of operating conditions, the two most common problems are flame-out (loss of flame) and

carry-over of liquids into the flame. The authors indicated that the solution to the flame out problem was elusive despite the fact that numerous design alternatives exist to minimize the problem. Forty-five percent of respondents indicated that flare streams were not analyzed and some facilities were found to operate the flare below recognized minimum heating values. Maintenance of flare systems was commonly done on an as required basis and was attributed to the fact that access is often difficult and that total plant shutdown is required in order to perform maintenance.

1.6 Airborne Compounds Identified Around Sour Gas Processing Facilities

Investigations of incinerator and flare emissions have been undertaken by SCIEX™ (1982), Strosher (1982, 1996), Tollefson and Strosher (1985), Colley *et. al* (1985), Twin Butte Soils and Water Evaluation Task Force (1984), and Gnyp *et. al.* (1983a, b, c, 1986a, b).

1.6.1. The SCIEX™ Study

The SCIEX™ study (1982) used a mobile monitoring laboratory equipped with a TAGA™ 3000 quadrupole mass spectrometry system to assess the feasibility of using it for environmental monitoring in Alberta. The report lists agents tentatively identified from sites around two sour gas processing plants in southern Alberta, Waterton and Hussar. Compounds that were tentatively identified at more than half of the downwind sites and, if available, its estimated minimum concentration based on the analyzer's inherent detection limits, included: ethylenimine, dimethylamine or ethylamine, ethylene glycol, pyrazine or pyridazine or pyrimidine, methylfuran or fragment or 2,3-dimethyl-1,3-butadiene, toluene (5 parts per billion (ppb)), methyl pyridine or aniline (5 parts per trillion (ppt)), cyclohexanone or lactone or maleic anhydride, 2-heptanone, cyclobutyl-1-ethynl ethanol or diaminophenol, 2-(ethylsulfonyl)ethanol, pthalic anhydride (1 ppb), chloride ions fragments (100 ppt), formic acid, and ethyl sulfonic acid.

1.6.2. The Strosher Study

Strosher (1982) used Tenax and Chromosorb 101 adsorbents to retain and concentrate a wide range of gases or vapors (alkanes, alkenes, cyclic compounds, aromatics, oxygenated hydrocarbons, and chlorinated-, nitrogen-, and sulphur-containing compounds) from air in the vicinity of the Gulf-Pincher Creek and Shell-Waterton sour gas processing plants near Pincher Creek. The captured emissions were thermally desorbed or solvent extracted, and analyzed by gas chromatography coupled to a mass spectrophotometer. Aliphatic, aromatic and cyclic hydrocarbons were the major components found in the atmosphere surrounding the gas processing operations while other substances identified were alcohols, amines, formamides, chlorinated hydrocarbons and a sulphur-containing compound. Samples were collected in the vicinity of the gas plants and at a compressor station, which supplied feedstock to the processing plant. In the vicinity of the Gulf-Pincher Creek plant, 42 compounds were identified out of 59 detected, which were almost entirely aliphatic, aromatic and cyclic hydrocarbons. Major contributions were attributed to the di- and tri-methylated benzenes and aliphatic hydrocarbons in the C9-C11 range. One chlorinated hydrocarbon was detected (1,2-dichloroethane). Under simulated plant upset conditions 1 mile downwind, when sales gas was burned, 29 compounds were identified and 18 tentatively identified. The majority of the compounds were aliphatic and aromatic hydrocarbons ranging from C5 - C11. Also included were branched and cyclic compounds as well as benzene compounds with up to 3 methyl substitutions. Also, four nitrogen-containing compounds were tentatively identified of which 3 were amines (ethylamine, methyl-butanamine, and methyl formamide).

At a crosswind site, 45 compounds were detected and 31 tentatively identified. The spectrum of compounds was similar in composition as the downwind site. Also, air at a reclamation site was analyzed to detect fugitive emissions where 35 compounds were detected; the majority of the compounds were similar to those found at the downwind site. The air concentrations, in units of $\mu\text{g}/\text{m}^3$, were: benzene 16.3, methyl benzene 13.4,

octane 3.76, 1,4-dimethyl-benzene 5.04, and nonane 8.72.

Air samples obtained in the vicinity of the compressor station (downwind and adjacent to) contained 18 compounds detected by mass spectrometry, 12 of which were tentatively identified as similar types of hydrocarbon compounds that dominated the emissions in the area. It was noted that only hydrocarbons were detected at the compressor site while compounds containing nitrogen, oxygen, sulphur and chlorine were present in samples collected near the processing plants.

At an upwind location, air was tested to assess background concentrations. Two compounds were detected in low quantities (benzene $0.008 \mu\text{g}/\text{m}^3$ and methyl benzene $0.007 \mu\text{g}/\text{m}^3$). Midway between 2 gas plants, where air was tested to assess residential concentration, seven compounds were identified. All were aliphatic or aromatic hydrocarbons (benzene $1.19 \mu\text{g}/\text{m}^3$; methyl benzene $3.07 \mu\text{g}/\text{m}^3$).

A scientific committee reviewed the SCIEX™ and Kananskis Center for Environmental Research studies (Stroscher, 1982) to provide comments to the Minister of Environment concerning the merits and significance of the reports (Hrudey *et.al.*, 1983). A detailed account of the sampling and analytical methodologies was provided, followed by comparisons of concentration estimates of 14 compounds to Alberta occupational exposure limits. The concentration estimates of the 14 compounds were found to be generally 1000-fold lower and the committee concluded that “although health effects cannot be ruled out, the committee would not expect adverse health effects on the basis of the results reported by these two studies.”

1.6.3. The Tollefson and Stroscher Study

Flare stack sampling was undertaken by Shell Canada through the Energy Resources Conservation Board to collect and analyze trace sulphur compounds when five different gas streams (sales gas, sulphinol contactor overhead, absorber overhead, raw gas and acid gas) were directed to flare at the Shell-Waterton gas plant (Tollefson and Stroscher, 1985). Air samples were also taken upwind to obtain background samples and

at 2, 7.5 and 19 kilometers downwind where odors could be detected. The samples were collected on Tenax, thermally desorbed, trapped on a column immersed in liquid nitrogen, then heated briefly to elute the compounds directly into a gas chromatograph - mass spectrometry system.

Hydrogen sulphide, carbonyl sulphide, carbon disulphide and sulphur dioxide were identified and estimated at concentrations ranging from 30 - 300 ppm, 13 - 90 ppm, 13- 375 ppm, and 275 - >3000 ppm, respectively. The ratio of sulphur dioxide to hydrogen sulphide ranged from 5.3 to 10, which indicated to the authors, the presence of an incomplete combustion process. Additional compounds were found when different gas streams were flared: 23 additional compounds were identified when sales gas was flared; 30 when sulphinol contactor overhead gas was flared; 39 when absorber overhead gas was flared; 74 when raw gas was flared; and 51 additional compounds were identified when acid gas was flared. In all cases, approximately 50% or more of the detected compounds were aromatics with the highest relative abundances of unsubstituted benzene and naphthalene. Fewer aliphatic hydrocarbons were identified and they were also lesser in relative abundance to aromatics. The major portion of the aliphatic compounds identified occurred either as normal straight chain compounds in the range of 7 - 11 carbons in length or methylated cyclohexanes. The sulphur compounds identified were mainly methylated thiophenes, a methylated disulfide, a trithiolane and a methylester of ethylthioacetic acid. The authors concluded that the organic compounds detected were the result of incomplete combustion of flare stack emissions and that some of the gases released were from the knock-out drum. The authors also reported finding a chlorinated hydrocarbon in an ambient air sample whose source was not determined.

1.6.4. The Colley *et.al.* Study (1985)

Following odor complaints near a sour water disposal operation, analysis of the flare stack emissions handling tank vent and treater off-gases was undertaken for

hydrogen sulphide, sulphur dioxide and other compounds. Combustion efficiencies from 15 - 100% were calculated from these results. The concentration of trace organic compounds in the flare stack was between 3-100 $\mu\text{g}/\text{m}^3$.

1.6.5 Strosher's Flaring Emissions Study (1996)

Laboratory, pilot scale and field studies were undertaken to characterize the products of combustion in the emissions from flaring; to determine the extent to which flared gases are left unburned; and to determine which factors contribute to incomplete combustion. Two key findings for the pilot study were that flaring of natural gas in the pilot-sized flare was found to produce up to 100 times the concentrations of low molecular weight aromatics and other hydrocarbons compared to similar laboratory tests; and a total of 188 hydrocarbons were identified in the emissions, many of which were polycyclic aromatic hydrocarbons.

Flaring low levels of sweet solution gas after it passed through the knockout drum was found in field tests to burn with an efficiency of approximately 71%. The efficiency was reduced further to 67% when a 3-4-fold longer flame was produced, and reduced even further to 62% when liquid fuel was added to the stream. The emissions contained between 100 and 150 identified hydrocarbons, which consisted of: i) about 20 times the concentrations of light hydrocarbon gases detected in the pilot study; ii) approximately 10 times the concentration of volatile hydrocarbons such as benzene and other low molecular weight aromatics; and iii) up to 1000 times the concentrations of higher molecular weight compounds including many polycyclic aromatic hydrocarbons. The most abundant compounds found in concentrations exceeding 300 mg/m^3 during the field flare testing were benzene, styrene, ethynyl benzene, naphthalene, ethynyl-methyl benzenes, toluene, xylenes, acenaphthylene, biphenyl and fluorene.

Flaring of solution gas containing 23% hydrogen sulphide and lower amounts of liquid hydrocarbons directed to flare at a sour oilfield battery produced measured combustion efficiencies of 84%, calculated by the carbon mass balance, and 82.4% as

calculated by the sulphur mass balance. Emissions were found to contain over 50% lower concentrations of aromatic hydrocarbons, approximately 20% less aliphatic hydrocarbons and between 50 - 70% less carbon particulate as compared to the emissions from sweet gas flaring. The most abundant sulphur compound, other than sulphur dioxide, was carbon disulphide, followed by some thiophenes, hydrogen sulphide, carbonyl sulphide and other sulphur-containing compounds.

Using theoretical modeling calculations, estimates of the maximum predicted ground level volatile organic compounds (VOC) and polycyclic aromatic hydrocarbons (PAH) concentrations associated with sweet and sour gas flaring were made. Strosher estimated that the occurrence of the largest ground-level concentrations of the identified constituents would occur within a distance of several hundred meters from the flare stack. Sweet gas flares generally produced higher PAH and VOC concentrations than the sour gas flares. Sweet gas flares emitted PAH's that are estimated to be in the range of 1 - 800 ng/m³ for average daily concentrations and annual average concentrations from 0.1 - 30 ng/m³. Sour gas flares emitted PAH concentrations in the range of 3 - 400 ng/m³ daily average and 0.2 - 29 ng/m³ as annual averages. Fluoranthene, anthracene, and pyrene were produced in the largest amounts for the sweet gas flare whereas pyrene, phenanthrene and fluoranthene were produced in the largest amounts for the sour gas flare. Sweet gas flares emitted VOC's in the range of 15 - 2300 ng/m³ as a daily average and <5 - 85 ng/m³ as annual averages. Sour gas flares emitted VOC's in the range of 5 - 345 ng/m³ as a daily average and <5 - 25 ng/m³ as an annual average. Benzene, naphthalene and styrene were in the highest concentration for both flare types.

1.6.6. Trace Element Studies (Gnyp 1983a, b, c, 1986a, b)

Few studies have been undertaken to identify trace elements in sour gas processing streams. A study of trace element emissions from five sour gas plant incinerator stacks was undertaken by A.W. Gnyp and colleagues in 1983. The purpose of the study was to determine whether sour gas plant incinerator stack emit metallic species

that might be implicated in the allegations that sour gas plants were responsible for detrimental health effects on plants, animals, and humans. The emission rates found are listed in Table 1.6. Assuming that the average ambient metal concentrations are equal to the maximum predicted levels from the stack and that an individual inhales 20 m³ of air daily, the authors conclude that "the amounts of aluminum, copper, iron, tin and zinc ingested from the air are negligible in comparison to the estimated daily intake from food sources" (Gnyp *et. al.*, 1983a). Gnyp *et.al.* (1986a, b) measured levels of metals in process streams which, in the event of a plant upset, would be diverted to flare stack discharges at two sour gas plants in Alberta. Aluminum, arsenic, cadmium, chromium, copper, iron, lead, manganese, nickel and zinc were consistently found in six process streams at one plant and antimony, beryllium, boron, lithium, mercury, molybdenum, silver and vanadium were found at least once during a 3-test sampling program. At the second plant, only cadmium, chromium, iron, manganese, and zinc were found consistently in the 6 process streams sampled. Aluminum, antimony, arsenic, beryllium, copper, lead, mercury, nickel, selenium and silver were detected at least once at one or more locations over a wide concentration range of 0.001 - 10 mg/m³.

Table 1.6. Emission Rates of Selected Metals from Five Gas Plant Incinerator Effluents (Gnyp, 1983a)

Element	Emission Rate Range (g/hr)
aluminum	8 - 2390
arsenic	0.2
cadmium	0.7 - 13
chromium	6.6 - 9
copper	1.7 - 14
iron	3.8 - 120
lead	9.9 - 37
nickel	6.6 - 18
titanium	8-186
zinc	1.3 - 45

1.6.7. Cooper and Peake Study (1990)

Cooper and Peake (1990) collected source and ambient particulate data at two sour gas plants near Crossfield, Alberta, to assess the chemical mass balance with the aim of segregating or identifying the relative contributions of multiple emission sources to air quality at a given receptor site. In addition to collecting particulate emissions samples from the incinerator stack, three flare stacks, an inlet compressor stack, prill stack, motor vehicles, and bulk soil and road dust, they also measured the fine, coarse, and PM₁₀ particulate matter concentrations in ambient air at upwind and downwind sites as well as the mass of elemental species associated with each fraction. The chemical mass balance provided no evidence of a direct contribution of fine particle sulphate from the gas plant to the monitoring sites nor of the formation of secondary sulphate from the sulphur dioxide emissions from the gas plant. They found that the City of Calgary rather than the gas plant was the source of the fine particulate sulphate and also found no evidence from the chemical mass balance of a direct contribution of fine particulate nitrate from the processing plant to either of the monitoring sites. For the incinerator emissions, only a low percentage of the particle mass (approximately 20% of the fine, 30% of the coarse and 20% of the total) was explained by the measured chemical species. The deviation was believed to be due to the presence of some elements primarily associated with oxides or carbon species, which were not measured. The incinerator stack emissions consisted primarily of particles less than 2.5 µm giving an average fine to coarse particle mass ratio of 24.9, compared to ratios of 0.041 for road dust and 15.0 for vehicle emissions. The incinerator, prill, flare and inlet compressor stack emissions consisted primarily of fine particle sulphur species, estimated to comprise 17% of the mass, which were assumed to be mostly sulphuric acid. The second-most abundant fine particle species in the incinerator stack fine particulate emissions was organic carbon, which accounted for 1% of the mass.

1.6.8. Other Studies of Natural Gas and Hydrocarbon Combustion Products

1.6.8.1 Particulates

With the exception of the Cooper and Peake (1990) and Gnyp *et. al.* (1983a, b, c, 1986a, b) studies, no others were identified which analyzed particulate composition of flared or incinerator emissions. Other investigators have characterized particulates from various natural gas fired facilities. Fine particle emissions from an exhaust of a natural gas-fired space and water heater has been characterized by Rogge *et.al.* (1993). Organic compounds such as *n*-alkanes, *n*-alkanoic acids, PAH, oxy-PAH, aza arenes, and thia arenes were identified in the exhaust emission. At least 22.5% of the particle mass emitted consisted of PAH, oxy-PAH, aza arenes and thia arenes.

A review of the thermal decomposition products of propylene by Purohit and Orzel (1988) reveals that when combustion occurs around 300 to 700°C, many incomplete combustion products are released, including primarily aliphatic saturated and unsaturated hydrocarbons and some aromatics. When combusted in air at 200 to 600°C, simple and complex aldehydes and ketones were produced in addition to aliphatic and aromatic hydrocarbons. As the temperature and time increase, the proportions of oxygenated and aliphatic hydrocarbons decreases and the proportion of aromatic hydrocarbons increases.

A study of the chemical characteristics of oil refinery plumes in Los Angeles (Parungo *et.al.*, 1980) demonstrated that the refinery operations increase the concentration of aerosols within 16 kilometers downwind and 650 meters aloft in the size range between 0.05 μm and 23.5 μm particle radius. The refinery plumes were found to be strong sources of sulphur dioxide, NO, and NO₂ but the plumes consumed ambient ozone. The sulphate particles were found to have a mode of less than 0.1 μm in diameter, and the inorganic nitrates were found to have a mode between 1 and 10 μm .

1.6.8.2. Chlorine - Containing Compounds

Chlorinated hydrocarbons have been documented as a concern (Energy Resources

Conservation Board Exhibit 57, 1981) and also have been intermittently identified in ambient air around sour gas processing plants in Alberta (SCIEX™, 1982; Strosher, 1982; Beaseley *et.al.*, 1992; Tollefson and Strosher, 1985). They also have been associated with and found in the vicinity of a variety of petroleum processing facilities (Thompson *et.al.*, 1990; Beard *et.al.*, 1993; Todd and Loscutoff, 1993). Chlorinated dioxins and furans were, for the first time, identified by Thompson *et.al.* (1990) in stack emissions and wastewater effluent samples collected from different petroleum refineries. The internal effluent stream containing the dioxins and furans originated from the catalyst regeneration in the reforming process. Catalyst regeneration is achieved by removing the coke deposits by burning and activating the catalyst using chlorinated compounds. The concentration of polychlorinated dibenzodioxins (PCDD's or dioxins) and polychlorinated dibenzofurans (PCDF's or furans) in the stack gas from a continuous regenerator without a scrubber ranged from 0.8 - 3.4 ng/m³ for dioxins and from 1.7 - 120 ng/m³ for furans.

Todd and Loscutoff (1993) identified chlorinated compounds in natural gas-fired utility boilers. While the fuel gas going into the boilers did not contain detectable concentrations of chlorinated compounds, stack sampling results showed 0.8 - 1.2 ppb 1,1,1-trichloroethane, 0.9 ppb tetrachloroethylene at 2/3 and 1/3 plants, respectively.

Eklund *et.al.* (1988) found that combustion of propane in the presence of hydrogen chloride yields a complicated mixture of chlorinated compounds some of which are known to precursors to chlorinated dibenzo -dioxins and -furans and that methane, hydrogen chloride and oxygen formed a wide range of chlorinated organic species in the temperature range 400 - 950°C. The results suggested to the authors that dioxins and furans are formed in a chain of reversible reactions starting with chloromethanes. De Fre and Rymen (1989) found that PCDD and PCDF formed from hydrocarbon combustion in the presence of hydrogen chloride. HCl was injected in concentrations between 150 ppm and 4.5% in gas-oil combustion gases in a domestic burner and an experimental combustion chamber. PCDD's and PCDF's were always

detected in the off-gases. Nestrick *et.al.* (1987) reported that benzene and iron (III) chloride undergo a thermolytic reaction in the presence of a silicate surface at temperatures greater than or equal to 150°C to produce chlorinated dibenzo-p-dioxins and dibenzofurans as well as chlorinated benzenes, chlorinated biphenyls and chlorinated diphenyl ethers. Other semi-volatile products of the reaction they tentatively identified include naphthalene, binaphthalene, anthracene/phenanthrene, diphenylmethane/methylbiphenyls, fluorene, phenylcyclohexane, phenylcyclohexene, xanthene, dihydro-trimethyl-phenylindene, anthracenedione, chloranil, chlorinated toluenes, chlorinated fluorenones, and tetrachlorocyclopentenedione.

Beard *et.al.* (1993) reported that polychlorinated dibenzofurans are formed by chlorination and *de novo* reactions with iron (III) chloride in petroleum refining processes. The presence of dioxins and dibenzofurans in catalytic reforming process was studied however the formation of dioxins and dibenzofurans could not be explained by their experimental results under simulated conditions. The authors speculate that the source of chlorine is from corrosion products on the steel piping of the process plant and note that hydrogen chloride (HCl) and chlorine (Cl₂) react with steel piping surfaces to form iron oxychlorides and chlorides which can catalyze the chlorination of organic compounds or chlorinate them stoichiometrically.

HCl was found in emissions of incinerated petroleum wastes such as process filters, PCB's, treater hay, certain oil-contaminated sludges, amine sludge and sulphinol sludge (Ross and Stewart, 1986). A stack analysis from a prototype incinerator unit burning sour gas plant waste bottoms comprised of oxazolidones, piperazines plus other undefined nitrogen-containing compounds; salt, asphaltenes, sand, oil, grease, suspended solids, and fine particles of iron sulphide; amine thiosulphates or amine thiocyanates, gave an sulphur dioxide concentration of 2.2 mg/m³; NO₂ 94 mg/m³; particulate 19 mg/m³; phenolics 0.05 mg/m³; and chlorinated hydrocarbons 0.099 mg/m³ (Beasley *et.al.*, 1992).

Combustion products of natural gas, oil and coal were tested for dioxins and

furans (Radian Corp., 1987). A single sample of ash collected from a home electrostatic precipitator of natural gas fired forced-air heating system was found to contain 0.6 ng/g 2,3,7,8 - TCDD and 1764 ng/g PCDD.

Conditions conducive to dioxin and furan formation and destruction in heterogenous systems are characterized in a review by Addink and Olie (1993) and are summarized in Table 1.7. The intermittent reports of chlorinated hydrocarbons at some gas processing facilities and the review's key findings, when taken together, strongly suggest that conditions for dioxin and furan production are likely present at gas processing facilities. The presence of chloride ions in the gas processing plants inlet stream (in the brine from the well-head or from well acidification with hydrochloric acid) combined with the finding that chloride salts are present at many stages of the process stream (indicated by its presence in a wide variety of waste materials) and the tendency for chloride to form oxychlorides on the steel piping all provide a continual source of chloride ions within the gas processing system. Thus, at any point where hydrocarbon mixtures are combusted (flares and incinerators), conditions conducive to dioxin and dibenzofuran formation exist.

Table 1.7. Combustion Conditions for Dioxin and Furan Formation (Addink and Olie, 1993)

Parameter	Features
Surfaces	- most surfaces capable but presence of catalyst essential - relative rates of formation: fly ash 1; carbon 0.02; SiO ₂ 0.05; tenax 0.001
Chlorine source	- HCl, Cl ₂ and salts (KCl, NaCl) - CuCl, CuCl ₂ , FeCl ₃ act as catalysts and Cl sources also
Temperature	- 50-150°C optimum for chlorination and dechlorination * - up to 500°C depending upon surface
Catalyst:	- CuCl ₂ , FeCl ₃ , CuCl, CuO, CuSO ₄ , NiO, Zn(NO ₃) ₂ - Cu ions 25times stronger catalyst than Fe
Atmosphere	- O ₂ essential; water vapor gives variable results
Reaction Mechanism	- more than one probably operative; radical initiation by dibenzoyl peroxide increases. PCDD/PCDF formation 5 - 15 times
Optimal conditions	- cooling from 850°C to 100°C in combustion chamber*
PCDD and PCDF Precursors	- aliphatic compounds (2,3-dimethyl-1-butene, propene) - monocyclic aromatic compounds with and without functional groups (benzene, benzaldehyde, benzoic acid, phenol, toluene) - chlorinated aromatic compounds (<i>o,m,p</i> - chlorophenol, 2,4,5-, 2,4,6-, 3,4,5-trichlorophenol, 2,3,4,6- tetrachlorophenol, pentachlorophenol, and 1,2,4,5-tetrachlorobenzene) - anthroquinone derivatives (anthraquinone - 2- carboxylic acid, 2,6-dihydroxyanthraquinone)

* the ADRP survey tabulated stack top temperatures of sour gas processing plant combustion sources in Alberta: exit temperatures ranged from 65 - 982°C for flares and from 370- 604°C for incinerator.

1.7 Summary

A wide variety of air pollutants are expected to be present in the vicinity of sour gas processing plants (Table 1.8), many of which are known toxins (mucous membrane irritants, systemic toxins affecting the nervous, reproductive, and immunologic and other organ systems, as well as mutagens and genotoxins). The toxicological properties are less well known for many of the other agents. Few studies have fully characterized the composition of the various emission sources at sour gas processing plants and the actual space, time and concentration profiles also have not been well characterized.

Table 1.8 Expected Potentially Hazardous Air Emissions From Sour Gas Processing Plants

Process	Airborne Agents Emitted
Tail gas incineration	CO ₂ , SO ₂ , NO ₂ ; lesser concentrations of CO, CS ₂ , COS, hydrocarbons, various metals plus others listed in flaring process depending upon type and composition of process streams directed to incinerator and completeness of combustion process
Continuous, intermittent or emergency flaring of various hydrocarbon-containing process streams (inlet separator, stabilizer overhead gas, flash gas from the amine regeneration units and from the amine reboiler, sour water stripper)	Same as incineration plus mercaptans, thiophenes, sulfones, sulphides, organic acids, CO, maleic anhydride, aldehydes, ketones, alcohols (including phenols) aromatics, VOC's, PAH's, oxy-PAH, aza arenes, and thia arenes, N ₂ O, NO, ammonia, amines, imines, amides, heterocyclic compounds (pyridines), cyanides, metals, HCl, chlorinated hydrocarbons, dioxins and furans.
Fugitive emissions	Alkanes, cycloalkanes, aromatics, VOC's, H ₂ S, mercaptans
Venting of gases to atmosphere at various process points (dehydrator reboilers, glycol regenerator vapors)	Water vapor, alkanes, organic acids, aldehydes, alcohols, ketones, aromatics, VOC's
Sulphur block storage	Elemental sulphur dust, residual H ₂ S, CS ₂
Burn pits	Same as flaring plus coke-containing particulates
Plant 'burnout'	Similar to tail gas incineration plus fine catalyst particulates
Pumps driven by natural gas, gasoline or diesel engines	NO _x , CO, CO ₂ , aldehydes, ketones, alkanes, aromatics, PAH's

Thus, any attempt to monitor exposures to the many compounds will therefore be difficult due to the time-, space- and process-dependent activities. Given these considerations, the compromise made in this study was to focus on one pollutant, sulphur dioxide, for which there were good records and lengthy monitoring data. It is recognized that this approach does not adequately address intermittent exposures from intermittent emissions or to secondary atmospheric transformation products resulting from those emissions. Further work should be undertaken to address these outstanding issues.

Chapter 2 Exposure Assessment Approaches, Dilemmas and Problems

Evaluating the consequences of releasing toxic substances into the environment is one of the most difficult tasks facing people in general and environmental scientists in particular. Not only are cause-and-effect relationships difficult to establish, but the flood of chemicals entering the environment also remains largely invisible and therefore is all too easily overlooked.

Ehrlich, P.R., A.H. Ehrlich, (1996)

Because of the rapid increase in man's population, technology, and consumption, it has not been possible for the relatively small community of atmospheric chemists to keep pace with, or even foresee, the need for more and more quantitative information on air chemistry.

Group Report on Tropospheric Gases, Aerosols and Photochemical Reactions (1982) In: Atmospheric Chemistry, E.D. Goldberg (Ed.), Dahlem Konferenzen, pp 357-372.

The answers I have found serve only to raise a whole new set of questions, which lead only to more problems, some of which we weren't even aware were problems. To sum it all up... in some ways I feel we are as confused as ever, but I believe we are confused on a higher level, and about more important things.

Final remarks made at the 1996 Flaring Symposium Keynote Address by Dr. Charles E. Findley, Deputy Regional Administrator, United States Environmental Protection Agency Region 10, In: Flaring Technology Symposium Proceedings, Feb 21, 1996, Grant MacEwan Community College City Center Campus, Edmonton, Alberta, Canada.

To evaluate whether a particular outcome is associated with a particular exposure, an air pollution epidemiological study designed to examine dose-response relationships should classify study participants, in some manner, on the basis of the exposure to the substance or substances identified as a concern. Ideally, the method for categorizing exposure is based on actual exposure measurements for the time period corresponding to the toxicological properties of the agents of interest. As the previous chapter illustrates however, the air pollution epidemiologist faces a multitude of new factors and many familiar older ones at lower levels capable of adversely affecting health, which should be considered.

This situation presents many dilemmas. In addition to the diurnal cycle for many atmospheric pollutants, in a typical time series for any averaging period, all outdoor air

contaminants have a wide concentration range such that the variation is as wide as the mean value itself (Yee *et.al.*, 1993). At the extremes of the distributions, maximum one-hour average concentrations may be 5 to 10 times the maximum 24-hour averages and about 200 times the expected maximum annual averages (Battelle Pacific Northwest Laboratories, 1979). The variability is mostly due to the inherent variability of the meteorology at a given location. Therefore, to obtain enough samples in each exposure group (for any time period), such that they can be distinguished from each other, very large sample sizes are required because of the pollutant's lognormal distribution and large geometric standard deviation (Hewett, 1995; Armstrong, 1996). Hewett (1995) shows that the accurate estimation of the true arithmetic mean or geometric mean of a single exposure group can require a significant commitment in sampling resources when the pilot study sample size is small or the estimated geometric standard deviation is large. For example, 257 samples would be needed in each group when the true group geometric standard deviation (GSD) is 3.0, the pilot study sample size was 20 and the desired accuracy is 20%. To minimize the sample burden, Hewett (1995) recommends that pilot studies approximate 20 samples, exposure groups devised so that the GSD for each group is as low as possible and that the expectations be relaxed. Sample sizes are greatly reduced if less accuracy is required. In the above example, reducing the accuracy to 30% decreases the group sample size to 114. Further, the methods for determining the precision of lognormally distributed arithmetic mean estimates by confidence intervals are neither well known, nor are accurate for small sample sizes and large geometric standard deviations (Armstrong, 1992).

Roach (1977) and Rappaport (1985) have shown that body burden or tissue concentration can be markedly sensitive to exposure variations. If exposure intensity changes substantially over a time period longer than the elimination half-time from the target tissue, the tissue concentration and exposure intensity will tend to move up or down together. Then, measuring the average exposure intensity during consecutive equal time periods that are approximately twice the elimination half-time in duration will

provide an exposure time profile in which changes in exposure are associated with changes in tissue concentration. Measurements on a finer time scale (shorter averaging times) will not provide additional useful data relative to tissue levels and measurements on a longer time scale (longer averaging times) will provide incomplete information.

In addition to considering toxicological factors, meteorological factors at the site of interest such as frequency of inversions and low wind speeds, and topographical features such as water bodies, valleys, ridges or presence of low lying areas should also be identified and taken into consideration.

Investigators are also usually limited by the methods available to them as well as the sampling and analytical methods' minimum reproducible detection limits. Personal air samples, collected at the breathing zone, are considered to provide the best estimates for inhalation exposure to substances obtained by non-invasive methods. Several commercial suppliers (DuPont®, Dräger®, 3M®, MSA®, Gastec®, Chemsense®, SKC®) have produced dosimeters for the gases (sulphur dioxide, ammonia, hydrogen sulphide) which are designed for use in an occupational setting where, average air pollutant concentrations are one or more orders of magnitude higher than outdoor air. These methods generally have detection limits, which are much higher than that needed for outdoor air pollution studies (National Institute of Occupational Safety and Health [NIOSH] Manual of Analytical Methods, 1994). To compensate, sampling rates may be increased or lengthened and a more sensitive analytical detection method may be chosen. However, co-pollutants and other interferences become more important and the modified method would need to be evaluated prior to use.

As outlined in the previous section, many substances have been identified which are emitted into the air directly from the processing of sour gas and indirectly from contaminated water and soil at many locations in the sour gas processing and distribution system. In an epidemiological study, consideration must also be given to the possible interactive toxicological responses of the mixture. For example, making the simplifying assumption of only one toxicity for each of x and y substances, the 10 possible responses

for a mixture of two compounds are as follows: no response to either chemical; response to x only; response to y only; unrelated responses to both x and y; related additive responses to x and y; potentiation effect of x on y or y on x; synergistic interaction of x on y; and an antagonistic effect of x on y or y on x.

Toxicological interactions between acid aerosols (sulphuric acid, nitric acid, sulphur dioxide, nitrogen dioxide) and other sulphur-containing and nitrogen-containing compounds such as ammonium bisulphate, ammonium sulphate and ammonia have been summarized in a US EPA report (Environmental Criteria and Assessment Office, 1989). Antagonistic (neutralization of acid aerosols with ammonia), additive (sulphur dioxide and sulphuric acid), and synergistic (peak ozone and sulphuric acid aerosols producing pulmonary fibrosis) interactions have all been reported.

Further, in assessing exposure to multiple chemicals, consideration must be given to interactions of the agents in the mixture before, during and after sampling. These effects must be evaluated because of temperature, pressure, and humidity influences, because of artefacts or interactions that can be introduced by co-sampling other chemical agents and because of instability of reactant on the collection medium.

Compared to the total number of known emitted substances, there are very few for which air sampling methods have been developed, evaluated and which have characteristics suitable for use in the field in a large scale epidemiological study of air pollution effects. In a review of air sampling methods available for epidemiological studies to assess exposures to inhaled complex mixtures, Leaderer *et.al.* (1993) found that there are very few methods for substances which are suitable for use and that the development of monitors for exposure assessment purposes has been slow relative to the rate of production and release of new substances into the environment. A 1988 US EPA report of research needs in exposure assessment found that of the 13 pollutant categories which personal monitors are needed, only seven (carbon monoxide, nitrogen dioxide, nicotine, formaldehyde, inhalable particulates, biological aerosols, and house dust) have gone through the development, testing, evaluation, pilot and large field studies such that

they are deemed ready for routine field use (Leaderer *et.al.*, 1993).

Notably absent is the availability of a validated method for a personal sampler for sulphur dioxide, the most common gas emitted from sour gas processing plants. A NIOSH method for sulphur dioxide monitoring in the workplace is available however is requires the use of a battery-powered pump, and is believed to have breakthrough problems associated with it (personal communication, I. Wheeler, June, 1996). While some efforts have been undertaken to develop a sampling device that is suitable for personal exposure assessment (Koutrakis *et.al.*, 1989; Leaderer *et.al.*, 1994), many methods are not suitable for unattended outdoor use in northern climates.

Recently, laboratory and field testing of a passive sulphur dioxide sampler suitable for outdoor exposure assessment purposes was undertaken in Alberta (Tang *et. al.*, 1997). These investigators evaluated effects of some environmental conditions (temperature, wind-speed, relative humidity) on the sampler's performance and found that it corresponded well to concentrations measured by a continuous monitor. However, they did not fully evaluate the possible interactive environmental effects such as the combined effects of other gases, particulates or vapors, nor did they cover the range of all the conditions that the sampler would be exposed to in the outdoor environment such as high wind speeds. NIOSH recommends that samplers intended for outdoor use be evaluated under face velocities up to approximately 9 m/sec (Cassinelli, 1986).

Together, these circumstances make it difficult to assess personal exposures to anything but the most common substances, or to assess the potential confounding effects of other chemicals in a mixture. NIOSH recognized that exposure measurement and evaluation of the results require the use of statistical procedures that consider variations in exposure concentrations caused by sampling, analysis and the environment and has developed guidelines for devising efficient sampling strategies and for the evaluation of measurement data (Leidel *et. al.*, 1977). However, the guidelines were developed with the assumption that an exposure standard is available for comparison purposes. Thus its direct application in an air pollution epidemiological study is limited.

Other investigators have recommended approaches for designing efficient air monitoring networks (Munn, 1970; Noll *et. al.*, 1977; Langstaff *et. al.*, 1987). The approaches these authors describe require prior knowledge of prevailing meteorological conditions and mathematical modelling of the transport and diffusion of pollutants. Geographic, topographic and land use information about the site is also required prior to implementing a monitoring program (Lyons and Scott, 1990).

Eifler *et.al.* (1981) suggested using various plume dispersion models with increasing simplicity and methods for obtaining useful indicator functions which are related to dose for use in community exposure studies. They identify problems whereby the investigator cannot apply the more sophisticated models because of time or cost constraints, or because the necessary data cannot be obtained and propose that several simplifying steps for the Gaussian model be taken. Stinnett *et.al.* (1981) used an emission-weighted distance statistic (the inverse of distance from point sources, weighted by annual average emissions) to create an industrial emissions score for each census tract as a method of categorizing exposures. Yet the use of different approaches to estimate pollutant concentrations in the two air pollution epidemiological studies of the same county produced disparate conclusions (Wong and Bailey, 1993). The authors state that "vastly different conclusions can be reached depending on how the data are derived and used. Furthermore, the models must be tested and validated with actual data... before they are incorporated into any epidemiological analysis."

In an overview of the characteristics of user-oriented models, Angle (1979) states that

"the user of an air quality model needs to understand the components of the 'tool' he is using. He should know in general terms, how the model works, what its limitations are, where problems may arise, and what to do before calling in the specialist, that is, the modeller. It is not intellectually satisfying to rely upon a mysterious 'oracle' or 'black box' about which nothing can be comprehended. Only if the user is comfortable with the general concepts and terminology - if he feels that he understands the model - will he have confidence in the results."

Yet, Angle (1979) also points out that modellers often write the model

documentation for other modellers, emphasizing theoretical and numerical aspects, providing detail that even the informed user may find unintelligible, leading inevitably to wholesale rejection of modelling.

In addition to the issue of clarity, other important user-oriented features of air quality models include simplicity, reliability, appropriateness, and practicability (Angle, 1979). Simplicity is related to clarity in that it refers to the ability of the model to account for natural phenomenon with the fewest variables or parameters. Reliability refers to the ability of a model to make accurate predictions or estimates with known tolerances. Appropriateness refers to the model's time, space, information and resource scales that are suited to the problem, and practicability refers to the resource constraints, such as computer time, that limits a model's use. These features are considered and discussed in Chapter 4.

2.1 Rationale for Approach Taken

Complex mixtures and complex industrial processing operations pose some formidable problems for exposure assessors interested in long term health effects due to many of the factors discussed. Concurrent assessment of time-, space-, activity- and process - dependent events, the key factors which determine exposure, is especially difficult. In addition to Dockery's (1993) recommendation that epidemiologists be creative in their study designs, the call for broad-based advances in study design, exposure assessment, outcome assessment, data analysis and interpretation (Samet and Speizer, 1993; Samet, 1995; Sexton *et. al.*, 1995), attests to the difficulty of the studying complex mixtures.

To evaluate the validity of dispersion models for categorizing exposures and considering the aforementioned factors, the least-cost and most feasible approach was to compare total sulphation values with modelled sulphur dioxide concentrations. The choice of models for comparison purposes was determined by the need for a chronic or long term exposure estimate and was limited primarily by the type of model input data

that was available.

This approach was undertaken with the understanding that the sulphation method is not specific for sulphur dioxide and that other sulphur gases may also be present in the ambient air, collected by the sulphation apparatus and detected by the turbidometric analytical method. Given that hydrogen sulphide is monitored and controlled to a large extent at the processing plants, the assumption was made that sulphur dioxide would be the predominant S-containing gas in ambient air around the processing plants. This assumption was made also with the understanding that other sources of hydrogen sulphide may be present in the surrounding areas (wetlands in summer, well-site-testing, sour gas flaring, farm operations such as manure spreading, or leaks from trucking of hydrogen sulphide containing wastes). These sources are believed to be mostly intermittent, and as such, their effects were expected to show up as outliers in the large data sets. Further, the assumption was made that the influence of the sources would, if present, minimally influence the expected positive correspondence between predicted and observed values.

2.2 Sulphation Plates and Candles

There is a long history of use of the lead dioxide sulphation apparatus going back to 1932 (Meetham, 1961). Singh (1979) has undertaken the most thorough investigation of environmental factors relevant to Alberta's sulphation monitoring program. Other recent and relevant reports include the following: Petroleum Association for Conservation of the Canadian Environment (1980); Sickles and Michie (1984, 1987); Concord Scientific Corp. Report (Davis and Hunt, 1990); and Alberta Research Council Reports (1995, 1996). Together, these and other reports cover many of the analytical (accuracy, precision, sensitivity, specificity) and environmental or sampling (temperature, humidity, wind, shelter geometry) aspects of the sulphation plate or candle method.

A sulphation station consist of a cubical louvered box, usually made out of wood

or occasionally galvanized metal, positioned 1-2 m above ground, with a sulphation cylinder (called a candle) (Figure 2.1) or Huey plate mounted within (Figure.2.2).

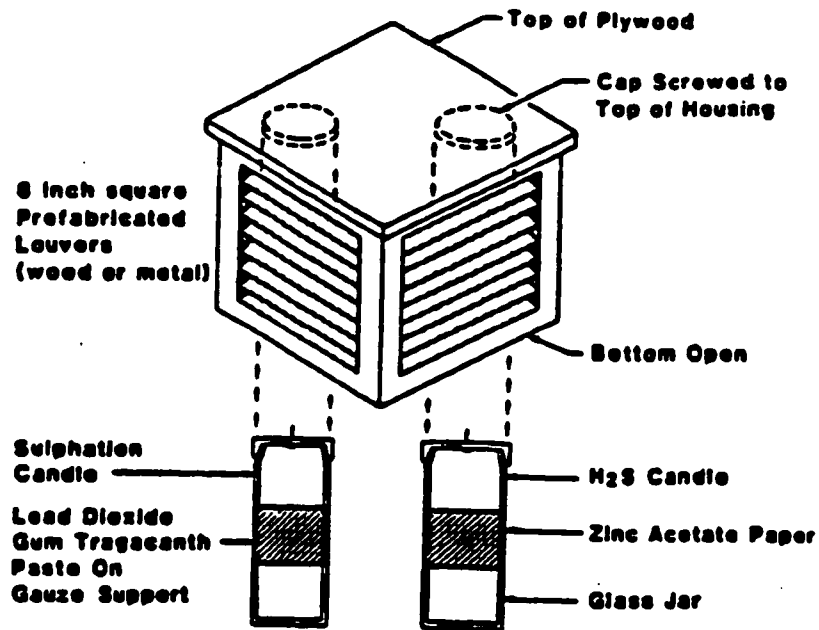


Figure 2.1. Total Sulphation Candle and Holder (after Bertram et. al., 1988)

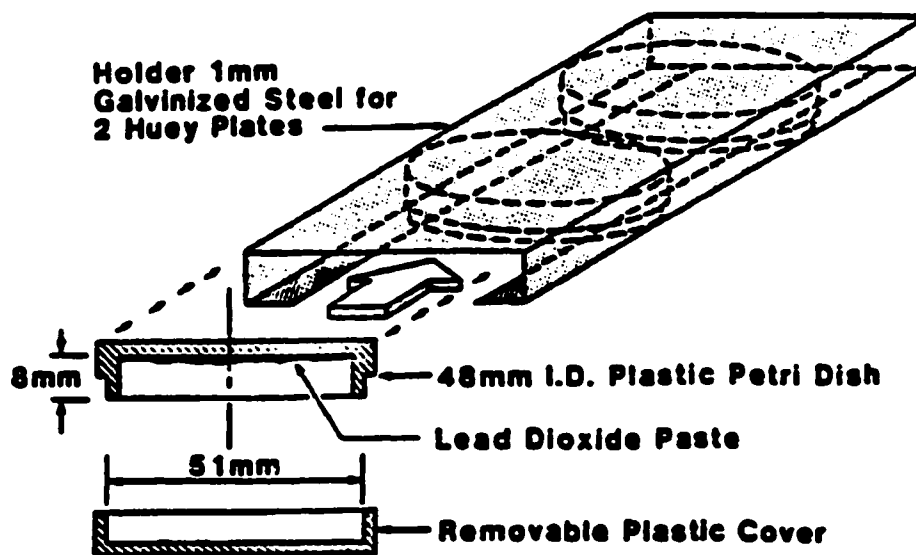
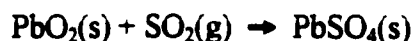


Figure 2.2. Huey Plate Configuration (after Bertram et. al., 1988)

The sulphation candle consists of lead dioxide impregnated gauze wrapped around a glass jar and the Huey plate consists of a plastic petri dish with lead dioxide affixed to the bottom of the dish. Airborne sulphur-containing gases react with the solid phase lead dioxide to form a water-insoluble lead sulphate according to the exothermic reaction:



Measuring airborne sulphur dioxide is based on the rate it combines with solid lead dioxide to form lead sulphate. In the laboratory, the insoluble lead sulphate is converted to soluble lead carbonate with a sodium carbonate solution and heat. The solution is filtered to remove excess lead dioxide particles, the filtrate is acidified, and the sulphate is precipitated as barium sulphate. The sulphate mass is determined by measuring the turbidity of the barium sulphate suspension, compared to standard suspensions using a spectrophotometer, and the total sulphation is then expressed in units of $\text{mg SO}_3/100\text{cm}^2/\text{day}$. The mass of lead sulphate recovered is, up to a certain sulphation level, directly proportional to the quantity of sulphur dioxide coming into contact with the adsorbent. The sulphation rate is linear with concentration for exposure periods for up to 3 months and also varies approximately with 0.4 power of the wind speed (Singh, 1979).

2.2.1 Comparisons Studies of Candles and Huey Plates

There are conflicting reports in the literature as to the agreement between candle and Huey plate sulphation rates. Huey (1968) found that flat plates oriented horizontally give sulphation values on average 18% higher (range 5-27% higher) than the vertically oriented cylindrical candles. Leahey and Legge (1988a) found that Huey plates give 30% higher sulphation values than candles. Field data obtained by Singh (1979) demonstrated an average 45% higher sulphation rate for candles than for plates.

2.2.2 Accuracy

Levadie (1979) reported that the Huey plate values for two sets of 5 spike trials, recoveries ranged between 79 and 115% and averaged 97.5%. Singh (1979) evaluated the accuracy of the turbidometric analytical method by conducting a sulphate recovery analysis and a study of the solution pH effects. The average recovery was 87% of the total sulphate initially present as lead sulphate. The 13% difference was attributed to losses occurring during the digestion and filtration step. The study of solution pH effects demonstrated that errors up to 9% would occur if adjustment of samples and standards to the same pH were not made.

Levadie (1979) reported that the Huey plate values correlated well with average sulphur dioxide concentrations giving a correlation coefficient of 0.8 over the concentration range of 4 - 27 ppb. Stalker *et.al.* (1963) reported that 2- and 24- hourly sulphur dioxide concentrations measured with the tetrachloromercurate method at 7 stations in Nashville correlated well with total sulphation candle giving correlation coefficients of 0.66 to 0.9.

2.2.3 Precision or Reproducibility

Singh (1979) analyzed the precision of the turbidometric analytical method and found that at low sulphate concentrations in the range of 4-10 mg/L, the coefficient of variation (CV) was 15-24% whereas at higher concentrations in the range of 15-60 mg/L, the CV was 1-5%. Within the range of 20 - 200 ppb sulphur dioxide, Sickles and Michie (1984) report a plate-to-plate within-lot precision of +/- 5.3% for high velocity wind speed and +/- 1% for low velocity wind speed; the between-lot precision was +/- 30%. For nine trials of 12 samplers in an outdoor array, Levadie (1979) found the CV ranged from 6.4% to 16.5% with an arithmetic mean of 10%. In agreement with Singh, the higher CV was found for low concentrations in the range of 0.01 - 0.10 mg SO₂/100cm²/day and the low CV was found for high concentrations in the range of 0.2 -

0.6 mg SO₃/100cm²/day. Lynch (1978) reported a mean CV of 5.3% and 98.4 mean % recovery. Eaves and Macauley (1964) compared sulphation results with sulphur dioxide measurement at the same sites made by the hydrogen peroxide method. They found in a set of 800 pairs of readings made at 20 different sites, local sulphur dioxide concentrations could be estimated from sulphation values to within 95% confidence limits of 180 ug/m³ around a mean of 300 ug/m³, which is equivalent to a CV of 30%.

2.2.4 Sensitivity (Minimal Reproducible Detection Limit)

Singh (1979) found that a sulphate concentration of 15 mg/L is the minimal reproducible detection limit for the turbidometric method with a 6% deviation giving a 95% confidence range at this level of 13.2 - 16.8 ppm. This corresponds approximately to a sulphation rate in the range of 0.07 - 0.17 mg SO₃/100cm²/day. Levadie (1979), using a similar analytical method did not determine the sensitivity or the detection limit of the analytical method, but estimated it to be in the range of 4 ppb sulphur dioxide for 24 hours.

2.2.5 Range of Application

The yield of lead sulphate is reported to be proportional to the concentration of sulphur dioxide, for all concentrations, up to one part per thousand (Anonymous, 1974). Noel *et. al.* (1989) demonstrated that the uptake of sulphur dioxide by Huey plates is linear over a 10-fold concentration range of 300 - 3000 µg sulphate/plate and over a range of exposure time of up to 12 weeks. Singh (1979) recommended that the exposure period be extended to a longer period of time, such as three months, to ensure that adequate amounts of sulphate be collected such that the analytical accuracy is in its optimal range.

The uptake of sulphur dioxide is linearly related to concentration until about 15% or 30% of the lead dioxide has reacted (Anonymous, 1974; Wilsdon and McConnell, 1934). Since the volume of solid product is about twice the volume of the solid reactant,

a protective film is formed, which decreases the surface area available and changes the uptake kinetics (Hickey and Hendrickson, 1965). To avoid these possible effects, the authors advise that the exposure and analysis parameters should be kept within the critical loading percentages.

2.2.6 Interferences by Chemical or Physical Agents

2.2.6.1 Chemical agents

The lead dioxide (PbO_2) sulphation method is not specific for sulphur dioxide. Other sulphur-containing compounds react with lead dioxide and may be detected analytically. Hydrogen sulphide reacts with PbO_2 to form lead sulphate (PbSO_4) and consumes PbO_2 at twice the molar rate of sulphur dioxide (Hickey and Hendrickson, 1965). PbO_2 may also react with mercaptans, carbon disulphide and elemental sulphur, reducing the amount available for conversion by sulphur dioxide (Hickey and Hendrickson, 1965) and presumably, will be converted to lead sulphate in the presence of atmospheric oxygen. No references were located which examined the uptake of organic sulphides or sulphur-containing fine particulate matter by lead dioxide.

2.2.6.2 Humidity

There is no significant correlation with relative humidity (Singh, 1979) however the reactivity increases when the lead dioxide surface is wet (Anonymous 1974). Sickles and Mitchie (1984) report a 39% increase in sulphation rate occurring over the range of 16 to 79% relative humidity.

2.2.6.3 Temperature

The reactivity of lead dioxide with sulphur dioxide is reported to increase 1% for a temperature increase of 12.5°F (Anonymous, 1974). Sickles and Mitchie (1984) report a negligible influence of temperature in the range of $5.6 - 27^\circ\text{C}$ and Singh (1979) emphasized that the temperature effects on the sulphation rate are very small.

2.2.6.4 Wind

Several investigators have studied the effects of wind on the total sulphation static monitoring method. In chamber studies done in 1934, Wilsdon and McConnell reported that the ratio of sulphur dioxide concentration to the sulphation rate decreased from 0.3 to 0.03 when the wind speed was increased from 8 m/s to 900 m/s (18 mph - 2.0×10^3 mph; 29 kph - 3.2×10^3 kph). A 1974 report (Anonymous) indicates that at lower wind speeds, the reactivity was not significantly affected under the test conditions of sulphur dioxide concentration of: 30 - 300 ppm and wind speeds of 0.067 - 0.67 mph; 1 - 6 ppm sulphur dioxide and 3.3 - 20.1 mph; and 1 ppm sulphur dioxide and 0.33 - 17.9 mph. However, more recently, both Singh (1979) and Sickles and Mitchie (1984) found that the sulphation rate increased (for both lead dioxide candles and plates) as the 0.4th power of the wind speed.

Further, Singh used a wind tunnel to expose the sulphation plates and candles to sulphur dioxide containing air at constant wind velocities from which he compared measured and predicted transfer assuming that gas phase resistance was the controlling variable. The observations corresponded to the model throughout the wind velocity range of 0.3 to 8.4 m/s. At lower wind velocities where the accuracy of the hot wire anemometer was in question, in the range of 0.18 m/s, the gas phase resistance model under-predicted the sulphation rate by approximately two-fold.

2.2.6.5 Shelter Configuration and Orientation

Singh (1979) consistently found that round shelters resulted in 4 - 17% lower sulphation rates as compared to cubical shelters with approximately equal opening areas. The difference was attributed to the creation of a higher resistance to the free flow of ambient air through the large number of unaligned openings in the round shelter as compared to the long slits of rectangular openings aligned at the same height on all faces for the cubical shelter. Singh (1979) found that as the cubical shelter opening increased,

the sulphation rate increased 25 % for a 6-fold increase in opening area for candles but was unchanged for Huey plates.

Lawrence (1964) found that throughout the external airflow velocity range of 1.5 - 20 mph, the internal airflow values were found to be 41-47% of the external rate for the cubical shelter and 60-67% for the cylindrical shelter. For both shelter designs, the internal airflow values decreased with increasing external speed from 2.5 - 10 mph, but increased with increasing external speed in the range of 1.5 - 2.5 mph. For both the cubical and cylindrical shelter designs, the highest airflow values within the shelter were obtained when the face of the shelter's louvered screen is perpendicular to the direction of airflow and the lowest when a corner of the screen is into the wind.

The total sulphation candles are often housed together with the candles designed for collecting hydrogen sulphide. Theoretically, the position of each candle relative to the predominant wind direction has some bearing on the collection efficiency of the sampler. For example, if a hydrogen sulphide candle is positioned upwind from the sulphation candle within the shelter, the position of the H₂S collector conceivably can alter the air flow through the shelter, producing eddies behind it, and affecting the collection efficiency of the sulphation candle 'behind' or downwind from it. No studies were identified which explored this question, however, Singh (1979) discusses this possibility.

2.2.6.6 Shelter Materials

The static sampler shelters used in Alberta are made out of a variety of materials. Wood shelters are most often used however, galvanized sheet metal may also be used. Non-galvanized metal screens may be placed behind the louvers and metal hinges, which provide the means of interior access. Thus, some discussion of the corrosion effects of sulphur dioxide on metals is warranted. A study of galvanized metal corrosion by sulphur dioxide revealed that the characteristic most influencing inferred dry deposition values was its previous exposure history (Spence *et.al.*, 1993). Deposition of sulphur

dioxide, evaluated by measuring soluble corrosion products, increased with increasing exposure time, decreasing temperature, increasing relative humidity and increasing wind speed. It was also found to be greater for weathered galvanized metal than for new material. Theoretically, increased deposition of sulphur dioxide to the housing material would reduce the amount reaching the static sampler housed inside, leading to a falsely low value.

2.2.7 Field Comparisons

A recent comparison of co-located total sulphation static samplers, selected on the basis of the single criterion of being within 10 meters of one another, showed that, overall, there is weak agreement between the sulphation results produced by industry and government laboratories (Byrne, 1996). Sulphation values at fifteen co-located sites were tested for: equivalency by analysis of correlation, systemic differences, similarity of frequency distributions and equality of medians. While it would be expected that the majority of the test results would be in agreement, overall only 43% of data from co-located sites showed agreement. Only 4 out of 8 data sets (50%) were positively correlated for total sulphation. Comparing the industry and government data sets showed that out of the 15 data sets, six (40%) had significantly different distributions, eight (53%) had medians that were not equal, and 10 (67%) had systematic differences.

The type of chemical adsorbent used (lead dioxide by industry vs. potassium carbonate by government) should not have made a significant difference. Chamber comparisons between the two chemical adsorbents showed good agreement (Bertram *et.al.*, 1988). Some possible explanations are suggested for the discrepancies:

- i) laboratory analytical error associated with the plant sulphation values, as suggested by the wide range of values obtained through a 1995 round robin inter-laboratory quality control program.
- ii) topographical features surrounding the sulphation apparatus may induce air flows adequate to produce micrometeorological variation sufficient to produce discrepant

results. An analyst estimated that 50% of sulphation stations do not meet Alberta Environmental Protection's siting criteria (personal communication, A. Clarke, Chemex Laboratories).

iii) As discussed by Singh (1979), the orientation of the candle or plate relative to the position of the hydrogen sulphide collector within the shelter and the orientation of the shelter relative to the prevailing winds could affect the collection of sulphur-containing gases.

Two overlapping networks of sulphation cylinders in the oil sands region of Alberta were found to give very different results (Leahey and Schroeder, 1985). The poor correspondence was cited as an example of their unreliable performance, however it was found that different lead dioxide powders were used and the discrepancies were explainable by accounting for the particle size differences (Leahey and Legge, 1988a). Comparison of 111 co-located total sulphation devices (PbO_2 plates and PbO_2 cylinders separated by no more than 2 meters) at a sour gas processing plant near Calgary gave a clear linear relationship and a positive correlation ($r = 0.90$) between the measured monthly sulphation rates obtained by the two devices (Leahey and Legge, 1988a).

2.3 Summary

Assessing exposure to single or multiple airborne agents is a not only a difficult undertaking because of technical limitations (method and equipment availability) but also is difficult due to limited information available needed to make appropriate sampling strategy decisions. In essence, as an outcome of these combined problems, the task of assessing exposure is a compromise between the various dilemmas discussed. For this study, the compromise was to use measurements obtained from less than ideal monitoring devices but which were located in extensive networks around sour gas processing plants.

The performance of sulphation devices under a variety of atmospheric conditions is quite well documented. They are inexpensive and useful in qualitatively assessing the

impact of pollution, however, they are generally not highly regarded as a reliable, sensitive or accurate monitoring device. This reputation is most likely due to the combined problems of deficient inter-laboratory quality control, unavailability of a consistent and standard lead dioxide particle size (Leahey and Legge, 1988a), and the influences of wind. In addition to these factors, their non-specificity, or ability to collect many if not all, airborne sulphur-containing compounds, therefore will need to be accounted for in the model comparison study.

Chapter 3.0 Atmospheric Boundary Layer Theory and Pollutant Dispersion Models

"Describing quantitatively the variability of pollution levels in relation to the source conditions that produce it is one of the important outstanding problems in air pollution meteorology" and "recognizing and specifying the innate temporal variability of atmospheric diffusivity is an essential part of a general description of the meteorological aspects of air pollution."

P.J. Barry, 1977

Atmospheric science, contrary to other sciences, is a science where we have to live from synthesis, from putting things together and it is unlike many other fields where a problem is approached by breaking it into tiny pieces. We have to deal with many processes at the same time: turbulent transport, thermodynamics, chemistry and radiation. These processes influence each other and that is where the problem arises. What is going on in the atmosphere is a combination of thermodynamic, chemical and turbulent processes in which each, on its own, is quite well understood, but put together, the interacting system is largely not understood.

We know roughly what the chemical composition of the atmosphere is now, but nobody dares to say what it will be in 50 years, not because we do not understand the science, but because we have a problem of putting it together. That is where we need better links with experimentalists. We use insufficient observations and that is why we, the modelers, have so much freedom: there are no self-correcting observations.

It is the synthesis which is the big problem but I do not agree that there will not be any progress, because 20 years ago the weather prediction was for one day ahead but now it is for six days ahead with equivalent skill. So there is progress. And you can say that physical insight has not changed since that time, but progress has come as an improved understanding of a complex system.

Han van Dop, 1993

3.1 Structure and Dynamics of the Atmospheric Boundary Layer

The atmospheric boundary layer (ABL) also called the boundary layer (BL) or planetary boundary layer (PBL), is the bottom 1 to 4 kilometers of the atmosphere. This layer is directly influenced by the earth's surface through the vertical exchange of momentum, heat and moisture, and responds to surface acting forces with a time-scale of about an hour or less (Stull, 1988, p 2). Surface acting forces include such processes as frictional drag, evaporation, transpiration, heat transfer, pollutant emission, and terrain-induced flow modification. The boundary layer structure and dynamics are determined by the many interacting processes of turbulence, radiation, baroclinity (north-south temperature gradient), advection (horizontal air movement), and divergence (horizontal surface spreading of air under high-pressure centers). Turbulence dominates the vertical and horizontal exchange of momentum, heat, and moisture between earth and atmosphere and determines the dispersion and transport of pollutants to such an extent that it controls all stages and branches of a pollutant's movement from sources to the sinks (Höschele, 1988).

A general conceptual overview of the ABL in relation to land-based point source emissions is provided here. More detailed accounts of ABL structure and dynamics, modelling plume behavior, atmospheric turbulence and air pollution, and Alberta-specific studies are given in Stull (1988), American Meteorological Society (1988), Nieuwstadt and van Dop (1981), and Angle and Sakiyama (1991), respectively.

Four distinct layers make up the ABL: surface, mixed, stable and residual layer (Figure 3.1). The surface layer closest to the earth comprises about 10% of the height of the ABL (the bottom 20 to 200 meters) for both the stable and mixed layers. In this layer, heat conduction, frictional drag, and evaporation from the surface cause substantial changes with height of the mean wind speed, temperature and humidity, whereas turbulent flux and stresses are relatively constant. Surface roughness elements such as forests, cities, and grasses influence air movement in this layer.

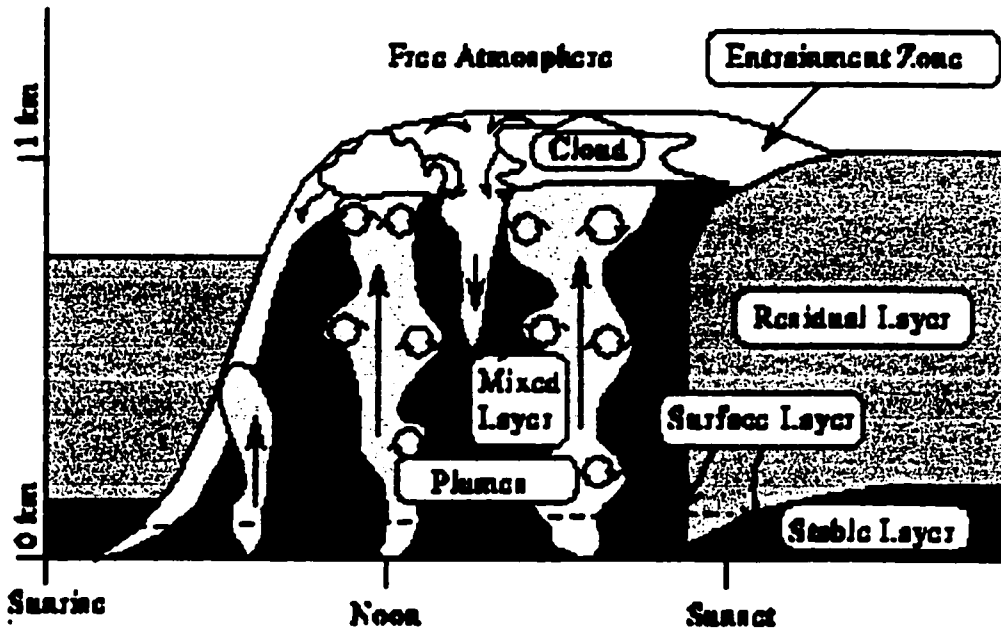


Figure 3.1. Schematic of the boundary layer evolution in fair weather conditions during summer at mid-latitudes (after Piironen, 1994).

The most common mid-latitude fair-weather land-based daytime state and often the urban night time state (Portelli, 1978; p 1) of the ABL is called the mixed layer, the convective boundary layer (CBL) or the unstable boundary layer. Some of the solar energy absorbed by the ground is transferred to the air above by convection. The warmed air parcels, also called thermals or updrafts, form large columns of rising buoyant air, travel upward transporting moisture, heat and aerosols, and coalesce with neighbouring thermals to form vertically coherent updrafts until they lose their momentum or energy (Figures 3.1 and 3.2).

Above this layer is a stable layer, called the entrainment zone, which acts as a lid to the rising thermals, prevents the continued upward motion of thermals, restricts turbulence, and prevents frictional influences from reaching above the ABL.

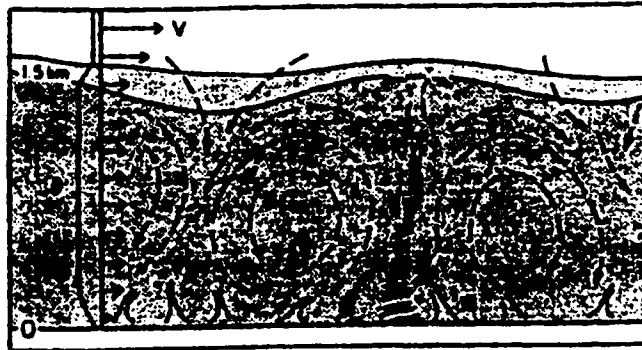


Figure 3.2. Convective boundary layer schematic depicting its large eddies, convective plumes, flat wind profile, and the capping inversion layer (after Wyngaard, 1992).

The convective motion of air leads to significant turbulence, which mixes the air uniformly within the layer producing a mostly uniform pollutant concentration, momentum, temperature, and energy through the depth of the CBL (Stull, 1988; p 13). Turbulence in this layer is characterized by large coherent eddies which scale in size with the CBL depth, typically 1 - 2 kilometers during midday and several hundred meters to 1 kilometer during the night (Figures 3.3 and 3.5). The large eddies have a cycle (ground to ceiling to ground) turnover time on the order of 10 - 30 minutes. Because of these large eddies, plumes from an elevated stack can be released into a downdraft and brought to the surface in high concentration within a few kilometers from the source before substantial diffusion has taken place (Weil, 1988), producing a 'looping' plume formation.

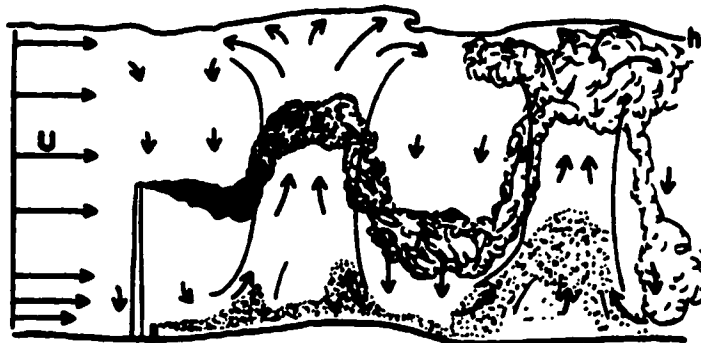


Figure 3.3. Schematic of large eddy diffusion process in the convective boundary layer (after Briggs, 1988)

Dispersion in the ABL is controlled by turbulence, which varies strongly with temperature stratification caused by the atmosphere's vertical temperature structure. The lapse rate, or the change of temperature with height, varies both diurnally and seasonally (Figures 3.4.a and 3.4.b), producing plume profiles as depicted in Figure 3.5. Inverted temperature gradients, where the temperature increases with height may, depending upon the vertical temperature structure, produce both surface-based and elevated inversions, which trap air in those layers. The base height, thickness, strength and persistence all influence the pollution accumulation potential (Angle and Sakiyama, 1991; p 1-32).

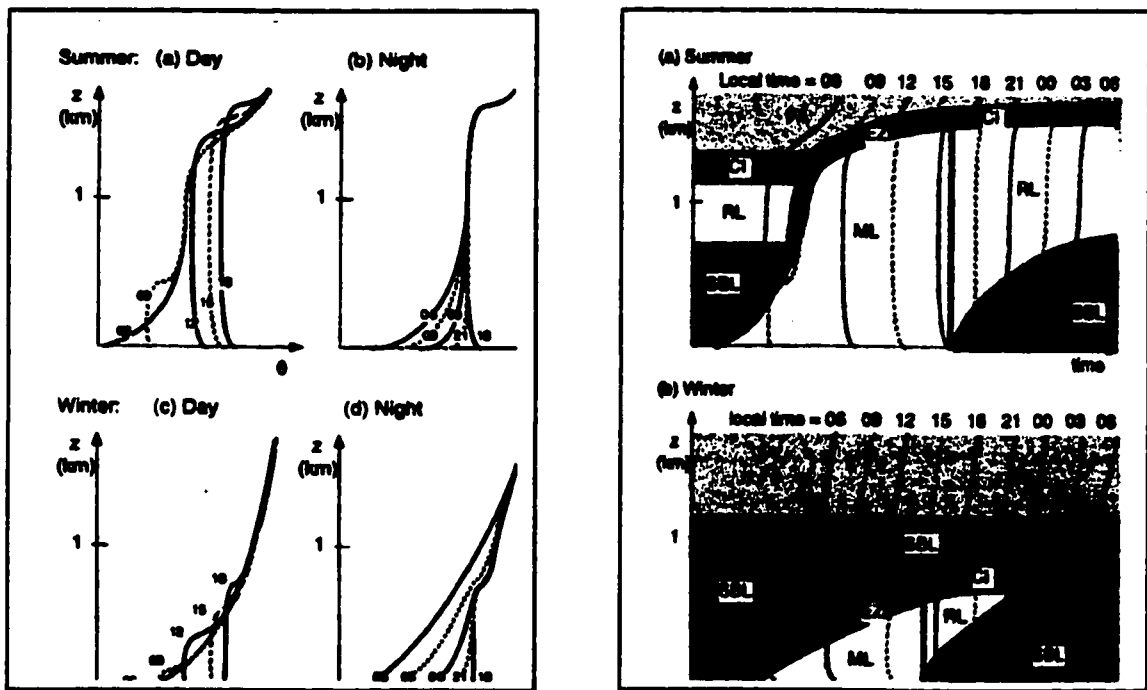


Figure 3.4. Evolution of daily and seasonal temperature profiles (after Stull, 1995).

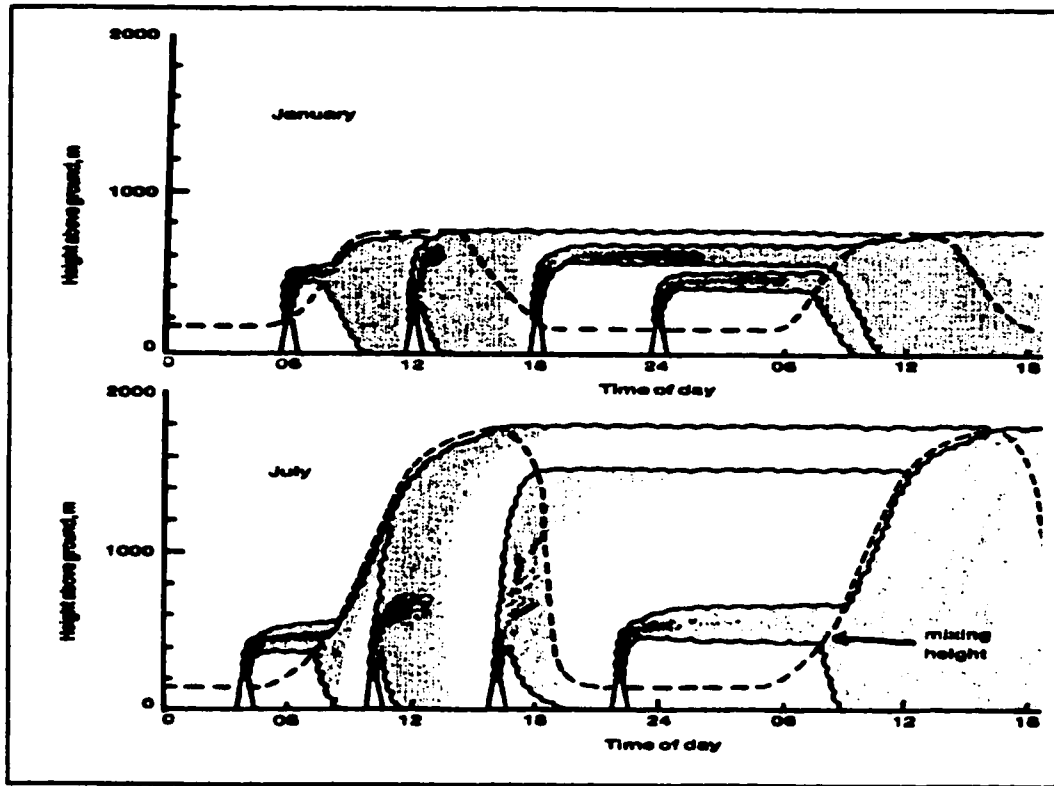


Figure 3.5. Plume dynamics for four different release times in January and July (after Harter, 1985)

Lamb (1984) provides a simple physical description of the earth's daytime air.

The

thermal energy acquired by fluid in contact with the surface results in a decrease in the density of this fluid; and therefore in the presence of a gravitational field, potential energy is acquired which puts the fluid system as a whole in a state of unstable equilibrium. If the fluid is initially at rest and no forces are present that would subsequently induce large-scale horizontal motion, then under conditions first derived by Lord Raleigh, small perturbations can initiate the transformation of the fluid's potential energy into kinetic energy. Such motions are called free convection. In the corresponding situation where the fluid is driven horizontally by some external force, the motions are called forced convection. The latter state is by far the most prevalent in the atmosphere; but atmospheric convection is very often similar in its characteristics to free convection. Generally speaking, the forced convective state of the atmosphere is associated with strong winds and weak surface heating. Within this state there exists the well-known horizontal roll convection regime that is often identified by long, parallel bands of clouds at the top of the boundary layer.

During development of the convective boundary layer, the layer is not uniform.

The rising aerosol-rich thermals are narrow with upward velocities of 1 to 2 m/s,

comprising approximately 40% of the horizontal area. The wider and slower descending air, with maximal downward velocities on the order of 1 m/s, comprise 60% of the horizontal area and consist of “clearer” air. With respect to influences of the thermals at the earth's surface, Stull (1994) notes that researchers who have studied the surface layer recognize that even in calm mean winds, convective circulations can create random gusts near the surface (Figure 3.6). The horizontal gust speed in the surface layer is usually assumed to be on the order of the Deardorff's convective velocity scale (w_c), which is proportional to the one-third power of the surface heat flux and the height of the atmospheric boundary layer (Stull, 1994).

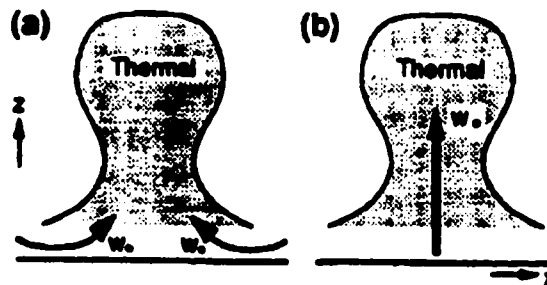


Figure 3.6 Convective circulations have a magnitude on the order of w_c , the Deardorff convective velocity. Such circulations cause (a) surface-layer gusts within the surface layer, and (b) vertical transport out of the surface layer (after Stull, 1994).

In the mid-afternoon when the angle of the sun decreases, the surface heat flux is reduced, convective motion decreases, and the convective boundary layer begins to decay, producing significant changes in the structure of the overlying PBL. The layer formed in this process is called the residual layer. Heat is transferred from the air to the ground, which is then followed by an upward propagation of heat transfer from the air above to the parcel below. As the layer thickens, heat is transferred downward until the turbulence is dampened by the cooler air parcel's tendency to sink back to its original position. The remaining turbulence is of smaller scale than turbulence in the unstable or neutral surface layer. As the convective boundary layer is modified by the reduction of solar radiation from the setting sun, the air retains the temperature, pressure and density

that the well-mixed air had, and forms above the stable layer with a temperature gradient approximating a neutral profile. That is, the lapse rate of the air parcel approximates the lapse rate of the surrounding air such that the air parcel motion will cease and be in equilibrium with the surrounding air. Plumes released into a neutral layer typically have a cone shape (Figure 3.7). This layer is bounded above by a capping inversion, preventing entrainment of air from aloft and, at ground level, above the growing, ground-based inversion layer, the airflow begins to have a layered form as depicted by the shape of the fanning plume (Figure 3.7).

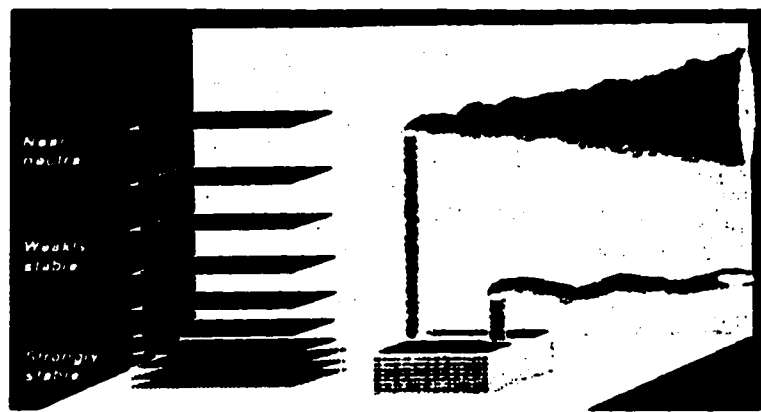


Figure 3.7. The static stability decreases with height in the nocturnal boundary layer, gradually blending into the neutrally-stratified residual layer aloft. Emissions into the stable air fan out in the horizontal with little vertical dispersion other than wavelike oscillations. Emissions in the neutral residual layer air spread with an almost equal rate in the vertical and horizontal, allowing the smoke plume to assume a cone-like shape. (after Stull, 1988).

During the period from sunset to sunrise, a shallow stable boundary layer, called the nocturnal boundary layer, is often formed (Figure 3.8). The winds are light, turbulence is weak and sporadic, eddy sizes are typically on the order of tens of meters or less, and the layer's dynamics is dominated by diffusion. It forms when the solar heating, radiative cooling and the surface friction stabilize the lower portion of the ABL. During this period, the only source of turbulence is shear production, a type of mechanical turbulence, which is produced from the change in wind velocity with height above ground and from the ground's surface roughness (Nieuwstadt and Duynkerke, 1996). This mechanical turbulence produces a logarithmic wind profile next to the earth in

which the horizontal wind speed increases with height above ground. Because of the small eddy sizes in the stable layer, plumes emitted from elevated stacks often remain aloft with negligible surface impact for tens of kilometers (Weil, 1988b; Nieuwstadt and Duynkerke, 1996). The stable boundary layer does not have a well-defined top but slowly merges with the residual layer. The winds aloft may accelerate to produce a nocturnal jet which enhance wind shears and tend to generate turbulence producing short bursts that can cause mixing throughout the stable boundary layer.

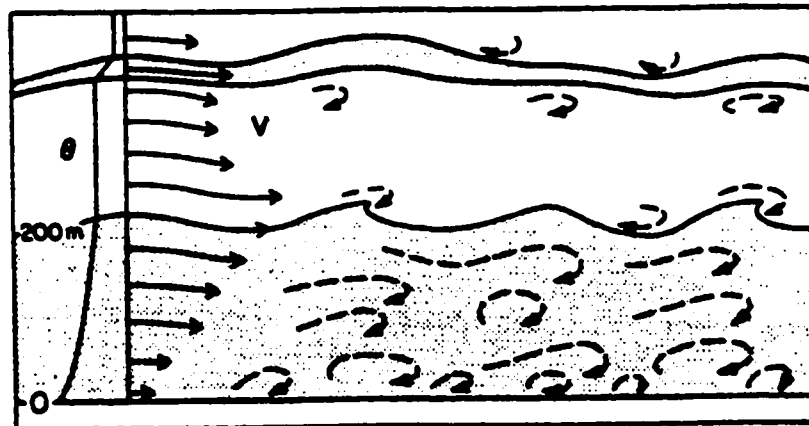


Figure 3.8. Schematic of the stably stratified boundary layer showing its shallow depth, small eddies, and large wind shear (after Wyngaard, 1992).

The structure and evolution of the nocturnal boundary layer is sensitive to characteristics of the local terrain. At the earth's surface, a thin layer of air in contact with the ground forms drainage winds of about 1 m/s at a height of 1 m. These are caused by the colder air adjacent to the ground, flowing downhill under the influence of gravity (Stull, 1988; p 16). The nocturnal boundary layer is considered to have proper conditions for the growth and propagation of internal gravity waves (waves which have an amplitude opposite the force of gravity) which can interact with the turbulence in ways that are not well understood (Wyngaard, 1988; p 41).

Measurement and parameterization of the nocturnal boundary layer turbulence is difficult because of several of its properties (Wyngaard, 1988, p 52; Weil, 1988b). The nocturnal PBL turbulence tends to be intermittent in the surface layer and is

characterized by small velocity fluctuations (~ 0.1 m/s). Parameters such as the surface energy budget, wind aloft, and the PBL depth evolve with time, producing strong vertical inhomogeneities, making the nocturnal PBL less likely than the CBL to be in a quasi-steady state. Although the nocturnal boundary layer is usually stable, it may also be convective when cold air moves over a warm surface, for example during the night in urban areas. Also, turbulence in the stable, stratified PBL is low, requiring more sensitive, lower-noise and faster turbulence-measuring instrumentation.

Many scientists over many decades of study have attempted to understand turbulence. Yet there is no generally accepted way to calculate its structure or its transport properties (Wyngaard, 1992). It is acknowledged that even if the relevant physics of turbulence were understood, a complete mathematical description is not practical (National Acid Precipitation Assessment Program [NAPAP], 1990, p 8-31). Because wind flow patterns that govern transport can be extremely complex and that any detailed description is impossible in practice, describing pollutant transport is believed to be one of the largest uncertainties in estimating source-receptor relationships (NAPAP, 1990, p 8-61). Thus, to study transport of pollutants, investigators are forced to parameterize, or “average” the effect of motions that are not resolved explicitly. The practice of parameterizing aspects of atmospheric behavior leads to the inherent incapability of describing what happens during a specific event and to the introduction of uncertainty and associated errors in the source-receptor relationship (NAPAP, 1990, p 8-31).

3.1.1 Summary

The continually changing processes within the ABL produced from the combined influences of local winds, large scale weather systems, and topography, leads to a wide variety of stack emission plume formations around a continuous elevated point source (Figure 3.9, Table 3.1). A corresponding variety of shifting downwind concentration distribution patterns at ground level are depicted Figure 3.10. The time and location-

dependent behaviour of plumes emitted into the ABL and of the ABL itself influenced by various synoptic scale systems, pose significant challenges for dispersion modellers and air pollution exposure assessors. Especially difficult is determining the degree of atmospheric turbulence, which itself, depends on atmospheric stability. These factors affect the overall behavior and vertical and lateral spread of the plume from a stack. Some of these and other associated difficulties are outlined in subsequent sections.

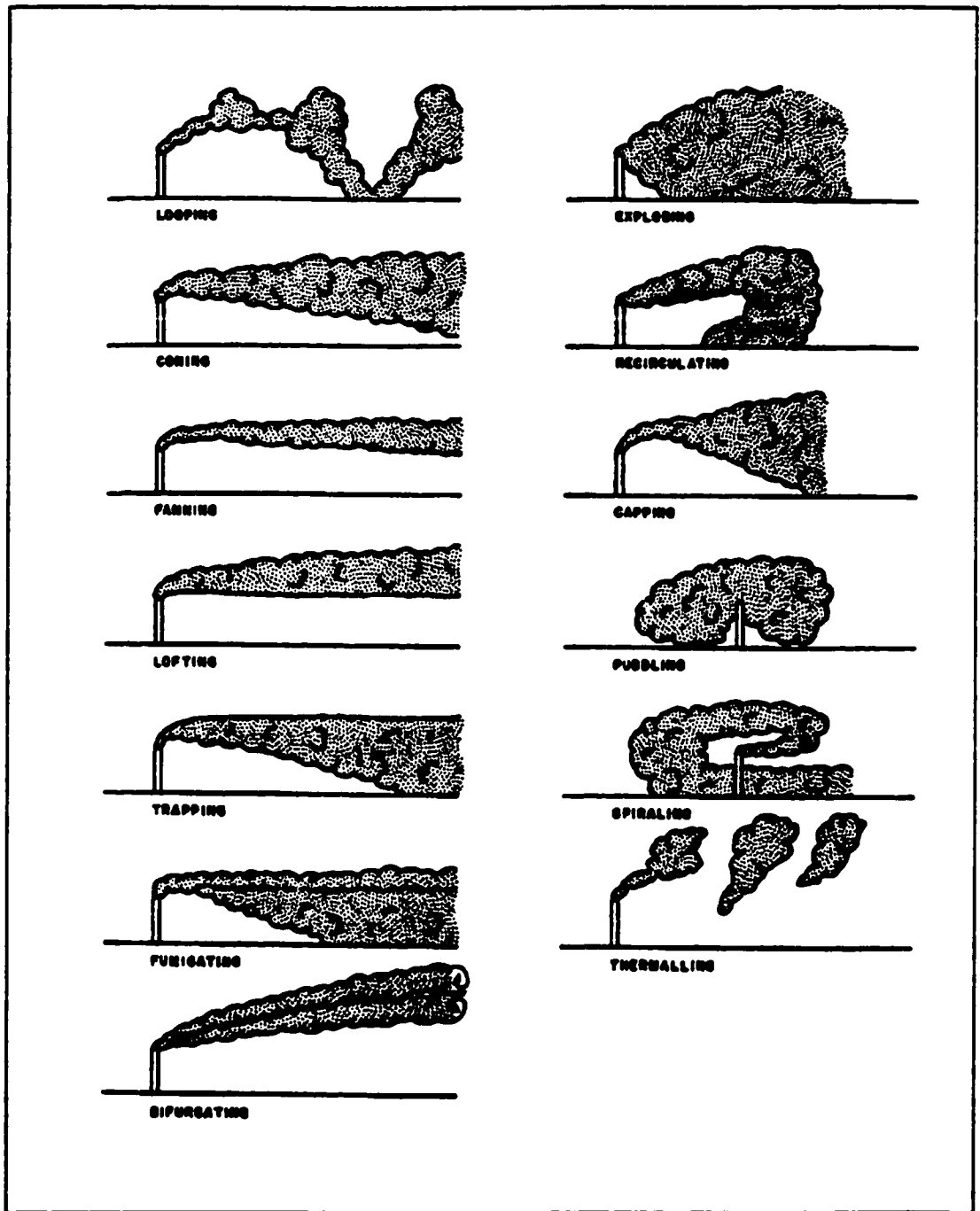
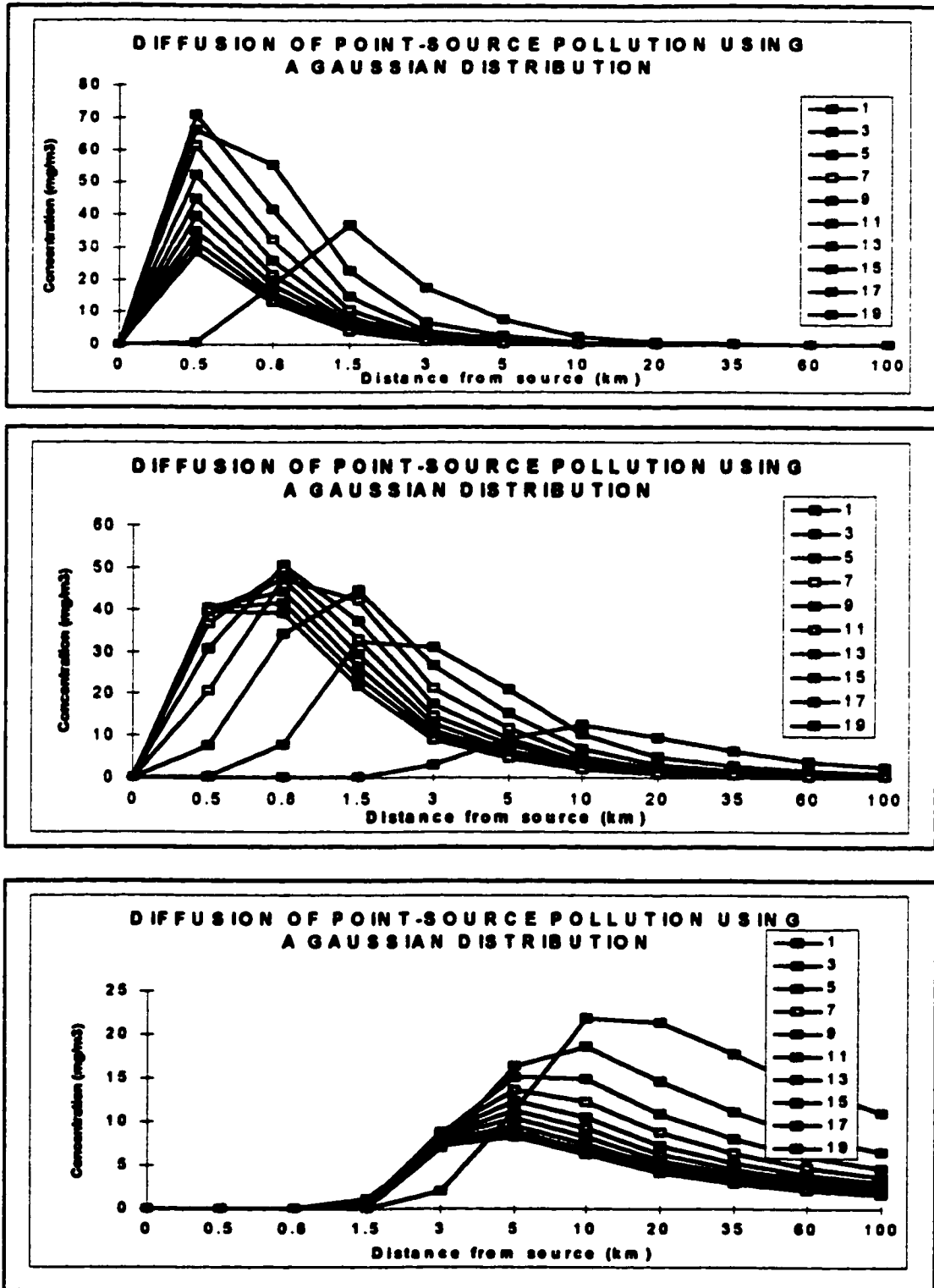


Figure 3.9. Appearance of visible plumes from continuously emitting stacks (after Angle and Sakiyama, 1991)

Table 3.1 Meteorological Conditions Associated with Various Continuous Elevated Point Source Emissions (after Angle and Sakiyama, 1991)

Description of Visible Plume	Occurrence	Turbulence (Stability)	Implication for Ground-Level Concentrations
Looping (convective) concentrations of irregular loops or waves with apparently random sinuous movements.	Daytime with clear skies, light winds and strong solar heating.	Strong thermal turbulence (unstable).	High where loop touches the ground.
Coning - long slender cone.	Strong winds or overcast sky, day or night.	Strong mechanical turbulence (neutral).	Concentrations rise to a maximum and then decrease with distance.
Fanning - narrow, horizontal fan widening but not thickening.	Night and early morning, clear skies and light winds.	Mechanical turbulence damped by thermal stratification (stable).	Dilution within the plume is slow, where plume passes near the surface, high concentrations will occur.
Lofting - coning for some distance, then lower edge becomes horizontal.	Transition from daytime mixing to nocturnal inversion. Night-time, when plume height exceeds inversion depth.	Upper layer has residual turbulence from daytime mixing (neutral or stable). Lower layer has mechanical turbulence damped by thermal stratification (stable).	Plumes in upper layer will produce virtually no ground-level concentrations because the surface-based inversion acts as a barrier.
Fumigating - (inversion breakup); upper edge horizontal, lower edge ragged and swirling to ground.	During transition from nocturnal inversion to daytime mixing. When plume travelling in a stable regime encounters a turbulent internal boundary layer.	Upper layer has little turbulence (stable). Lower layer has mechanical and thermal turbulence (neutral or unstable).	The sudden downward mixing of a fanning plume leads to high concentrations more or less simultaneously along the full length of the plume.
Bifurcating - divides into two rolls.	Later afternoon or early evening with light winds. Large plume buoyancy.	Weak turbulence (near neutral).	Same as coning unless plume rise reduced.
Trapping (limited mixing) - cones or loops and at some distance upper edge becomes horizontal.	Inversion aloft as a result of a frontal zone between air masses; anticyclonic subsidence, or convection.	Upper layer has little turbulence (neutral). Lower layer has mechanical and thermal turbulence (neutral or unstable).	After the plume edge contacts the inversion, upward diffusion is prevented, leading to higher concentrations at ground level.
Puddling (calm subsidence) - mushrooms above stack or drifts in various directions but never leaves the area.	Stagnant air near center or eastern side of anticyclone. Weak pressure gradient, winds light and variable.	Upper layer has little turbulence (stable). Lower layer has weak turbulence (near neutral).	Where the edge of the mushroom touches down, high concentrations are experienced.
Recirculating - travels away at high level and returns at a lower level.	Winds at upper level in opposite direction to those at lower levels.	Mechanical turbulence, strong near the interface between the flow zones (near-neutral).	The returning plume can cause high concentrations near the stack.
Spiralling - coils back on itself.	Light winds and capping inversion. Wind direction changing with altitude or time.	Upper layer has little turbulence (stable). Lower layer has weak turbulence (neutral or slightly unstable).	Because the plume does not leave the area, concentrations can be high.
Capping (wind shear) - plume rise abruptly and prematurely terminated.	Large, sharp changes in wind velocity with altitude.	Strong mechanical turbulence in vicinity of wind change (neutral).	Reduction in rise and strong vertical mixing produces high concentrations.
Exploding - plume expands rapidly in the vertical.	Light wind and clear sky.	Strong thermal turbulence (unstable).	High concentrations close to stack.
Thermalling - plume breaks up in separate masses that rise.	Light wind, strong solar heating. Large plume buoyancy.	Thermal turbulence (unstable).	Ground-level concentrations will be very small.

Figure 3.10 Expected downwind ground level concentration profiles for various wind speeds and atmospheric stabilities: unstable (top); neutral (middle); stable (bottom). Wind speeds (k/h) are in legend.



3.2 Perspectives on Modelling Concepts in the Atmospheric Sciences

Just as relativity eliminated the Newtonian illusion of absolute space and time, and as quantum theory eliminated the Newtonian and Einsteinian dream of a controllable measurement process, chaos eliminates the Laplacian fantasy of a long-term deterministic predictability.

Zeng et.al. (1993)

It seems that nobody has really considered the problem stated by Poincaré [in 1892] until the '60's though the Bénard curls have been deeply studied both on an experimental and theoretical basis. Nobody questioned - and still questions - the fact the organized large motions of molecules appear gently from completely unorganized motions when external parameters (the heat flux in that case) varies continuously in one direction; it is worthwhile noting that the container in which the Bénard's curls appear is not an isolated system.

Marc Pelegrin (1993)

The belief that any statistical specification of the atmosphere can be predicted from initial values using dynamical equations is not well-founded: the equations of dynamical meteorology are empirical equations. Their use is justifiable only in terms of its degree of success, which must therefore be assessed with the same rigour and absence of prejudice as are applied to any other predictive scheme.

G.D. Robinson (1978)

Underlying both descriptive and inferential statistics is the notion of uncertainty. If atmospheric processes were constant, or strictly periodic, describing them mathematically would be easy. Weather forecasting would also be easy, and meteorology would be boring. Of course, the atmosphere exhibits variations and fluctuations that are irregular. This uncertainty is the driving force behind the collection and analysis of the large data sets. It also implies that weather forecasts are inescapably uncertain. The weather forecaster predicting a particular temperature on the following day is not at all surprised if the subsequently observed temperature is different by a degree or two. In order to deal quantitatively with uncertainty it is necessary to employ the tools of probability, which is the mathematical language of uncertainty.

Before reviewing the basics of probability, it is worthwhile to examine why there is uncertainty about the atmosphere. After all, we now have large, sophisticated computer models that represent the physics of the atmosphere. Such models are used routinely for forecasting the future evolution of the atmosphere. These models are deterministic: They do not represent uncertainty. Once supplied with a particular initial atmospheric state (eg. winds, temperatures, and humidities) and boundary forcings (eg. solar radiation, and for some atmospheric models, such fields as sea-surface temperatures), each will produce a single particular result. Rerunning the model with the same inputs will not change that result. In principle, these atmospheric models could provide forecasts with no uncertainty, but do not, for two reasons. First, even though the models can be very impressive and give quite good approximations to atmospheric behavior, they are not complete and are not true representations of the governing physics. An important and essentially unavoidable cause of this problem is that some relevant physical processes operate on scales too small to be represented by these models.

Even if all the relevant physics could be included in atmospheric models, however, we still could not escape the uncertainty because of what has come to be known as dynamical chaos. This is a problem "discovered" by an atmospheric scientist (Lorenz, 1963), and it has become the death knell for the dream of perfect (uncertainty-free) weather forecasts. Simply and roughly put, the time evolution of a non-linear, deterministic dynamical system (eg the equations of atmospheric motion, or of the atmosphere itself) is very sensitive to initial conditions of the system. If two realizations of such a system are started from two only very slightly different initial conditions, the two solutions will eventually diverge markedly. For the case of weather forecasts, imagine that one of these systems is the real atmosphere and the other is a perfect mathematical model of the physics governing the atmosphere. Since the atmosphere is always incompletely observed, it will never be possible to start the mathematical model in exactly the same state as the real system. So even if the model is perfect, it will still be impossible to calculate what the atmosphere will do indefinitely far into the future. Therefore, deterministic forecasts of future atmospheric behavior will always be uncertain, and probabilistic methods will always be needed to adequately describe that behavior.

Daniel Wilks (1995)

Because of the complexity of models, verification is often very difficult. In a simple analytic experiment you can say: "this is my observation, this is my theory," compare them and you can say whether the theory is wrong or right. In complex atmospheric experiments there are often so many parameters involved that it is hard to tell whether you have made a satisfactory model. So, we are often accepting models by consensus. That means that a group of peers agrees on this or that model, or on specific techniques and parameterizations, which are considered to be up to the common standard of knowledge. Therefore, we accept a model which contains pieces of these "agreed" elements as an acceptable model. That is a way of deciding upon model performance which you will not encounter in other sciences.

Han van Dop (1993)

The local structure of the planetary boundary layer can differ greatly from its average structure, and, hence from the structure predicted by even a perfect model. This has been recognized in the dispersion community for some time but, nonetheless, some early work left the impression that one-hour averages, say, removed most of this randomness. Recent data sets show that the scatter in several-hour averages of concentration during convective PBL diffusion experiments is typically so large that one has difficulty differentiating between good and poor models. This was also the case in a recent assessment of rural diffusion models. This cannot but inhibit the building of models with better physics, for what are the rewards of building a better model, if not better predictions?

Wyngaard, J.C. (1985)

Any structural or functional phenomenon that involves the interaction between two or more components may be considered a system (Hall and Day, 1977). A model, even a numerical model, is an abstraction, simplification of a system, or representation of the important properties of any phenomenon (Angle, 1979; Randall and Wielicki, 1997). A model embodies a theory of how some aspect of the world works and provides a basis for making predictions about the outcomes of measurements. Use of mathematical models, such as the Gaussian plume dispersion model, to predict plume dispersion downwind from an elevated point source is an attempt to provide a quantitative cause-effect link between the spatial distribution and intensity of the sources of air pollution and the measured distribution of air quality. However, because of incomplete knowledge of the turbulence structure and limited model testing, use of Gaussian models is "tentative" (Weil, 1988). Yet, in discussions of inherent uncertainty, Venkatram (1979a, b, 1982, 1983, 1988a, b) explains that the details of the stochastic concentration field cannot be predicted - "The best an air quality model can do is to provide an estimate of the average of the concentrations measured during different 'realizations' of the flow", or to "predict the average over a large number of concentrations corresponding to different realizations of an ensemble." An ensemble is defined as a set of experiments corresponding to fixed external conditions. However, to relate the external conditions to measurements that are normally made for modelling applications, the model inputs usually define the ensemble.

It has been recognized since 1977 that an irreducible uncertainty exists. A position paper of the American Meteorological Society (AMS 1977 Committee on Atmospheric Turbulence and Diffusion) states that "the precision of models that use the Pasquill-Gifford curves or that are developed using these observations is closely tied to the scatter of the experimental data bases, including the inherent scatter of meteorological quantities (mean and turbulent winds) that govern the pollutant concentration field. At present, this scatter is irreducible, and dispersion estimates can approximate this degree of scatter only in the most ideal circumstances." This view

continues to have appeal. J.C. Wyngaard (1989, p 4)) states that "broadly speaking, we have found that although improvements of the sort discussed by Weil and Venkatram do result in better model performance, there usually remains a good deal of scatter between model predictions and observations. We now feel that part of this scatter represents an irreducible uncertainty caused by the stochastic nature of the atmosphere. This greatly complicates the model evaluation process ... because we cannot attribute differences between predictions and observations entirely to model errors." Wyngaard (1989, p 52) further states that "there is a growing feeling that air-quality models should predict the inherent uncertainty as well as the mean dispersion, but as yet I do not sense much movement in this direction."

Venkatram (1988, p 310) notes that

the past few years have seen a steady improvement in our understanding of the physics of the planetary boundary layer. Air quality models that have incorporated these advances do show marked improvement over existing models. In spite of these improvements in model performance, it is discouraging to find that the deviations between model predictions and observations are still relatively large. When two models are compared, (one known as CRSTER, based on the Pasquill-Gifford sigma curves developed at least 20 years ago and recommended by the EPA for regulatory applications, and the second model, developed in the Electric Power Research Institute project, based on a recent understanding of dispersion in the convective boundary layer), it is found that the model which incorporates the most recent understanding of dispersion in the CBL performs substantially better than the CRSTER model however r^2 is only 0.34 suggesting that we still cannot explain 66% of the variance between model predictions and observations.

Recently, some air pollution investigators have begun using non-linear methods for evaluating plume dispersion and air pollutant exposure. Sykes and Gabruk (1994) compared a simple fractal (patterns made of the superposition of similar shapes having a range of sizes) generation method using simulated mean statistics with realizations of instantaneous plume cross sections from large-eddy simulations. They found that fractal fields cannot match the realizations precisely however larger-scale features of the plumes are generally well represented by the fractal method. Hatano and Hatano (1997) describe a model of aerosol migration using fractal or self-similar fluctuation of wind speed in an

analysis of daily measurements airborne radionuclide concentration around Chernobyl and conclude that their simple model captures an essential feature of aerosol migration. Salvadori *et.al.* (1996) devised a fractal model to aid in describing the space-time distribution of radioactivity in Northern Italy following the Chernobyl accident and found that the similarities "agree fairly well with the available data". From 19 comparisons at 4 sites, the ratio of predicted to observed daily average concentration of radioactivity ranged between 0.2 and 6.0 with a mean of 1.31 and a standard deviation of 1.24.

McNider *et.al.* (1995) have studied the problem of sensitivity to initial conditions and the limitations of meteorological predictions and measurements. They analyzed a system of ordinary differential equations (analogous to the system of partial differential equations for the nocturnal boundary layer) under first-order closure using non-linear dynamics techniques such as bifurcation analysis (studying a change in the nature of a system's behavior as a parameter is varied). They found that in some parameter regions, multiple equilibria exist and both stable and unstable solution regimes exist with multiple, stable limit or turning points. The authors conclude that the results of their analysis has practical importance to the predictability of the stable boundary layer:

Because of the multivalued solution regime, even slight changes in initial conditions may change the limiting solution as time increases. The results show that the solution of stable boundary layer equations may be indeterminate for certain ranges of imposed geostrophic winds. Practically this means that frost prediction or pollutant dispersion cannot be made with confidence in certain parameter regions. If this type of behavior holds for the full partial differential equation system, it also implies that the addition of physics or numerical sophistication in the system may be irrelevant in improving predictability.

Together, these studies and perspectives give an indication of some of the difficulties faced both by air dispersion model developers and users, and hints at the barriers that will be encountered when attempting to integrate the activities and findings of both groups. For air pollution epidemiologists, whose aim is to have valid, reliable, and sensitive exposure indicators, the implication of these perspectives does not bode well. The naturally occurring atmospheric variability strongly suggests that there are definite limits to the use of air dispersion model outputs. Also it must be acknowledged

that for complex geographic systems, "where individual locations and spatial contexts are essential determinants of agents' interactions with one another and with their landscapes, and of the regional and global phenomenon that emerge, ... a clear understanding of the system components is not sufficient to understand the behavior of the system as a whole" (Dibble, 1997).

3.3 Gaussian Plume Dispersion Theory

The usual starting point for developing an atmospheric dispersion model is the eddy diffusion model, which is mathematically complex, but with some simplifying assumptions can be reduced to the Fickian diffusion equation (Wark, 1998):

$$\frac{dC}{dt} = K_x \left(\frac{\partial^2 C}{\partial x^2} \right) + K_y \left(\frac{\partial^2 C}{\partial y^2} \right) + K_z \left(\frac{\partial^2 C}{\partial z^2} \right) \quad \text{Eq. 3.3.1.}$$

where C is the concentration, t is the time, and K_{ii} quantities are the eddy diffusion coefficients in the three coordinate positions. To allow application of the equation to the atmosphere, additional assumptions are made:

- i) the concentration of the pollutant emanates from a continuous point source
- ii) the process is steady state
- iii) the major transport direction due to the wind is chosen to lie along the x -axis
- iv) the wind speed (u) is chosen to be constant at any point in the x, y, z coordinate system
- v) the transport of pollutant due to the wind in the x -direction is dominant over the downwind diffusion.

With these assumptions, the Fickian diffusion equation reduces to:

$$u \frac{\partial C}{\partial x} = K_y \frac{\partial^2 C}{\partial y^2} + K_z \frac{\partial^2 C}{\partial z^2} \quad \text{Eq. 3.3.2}$$

where, $K_y \neq K_z$. The equation must also satisfy the boundary conditions of:

- i) large concentration at the point source
- ii) zero concentration at great distance from the source
- iii) no diffusion into the surface
- iv) rate of transport of pollutant downwind is constant and equal to the emission rate of the pollutant at the source.

Further assumptions lead to the basic Gaussian model. The Gaussian plume model, the most common air pollution model is based on a simple formula which describes the three-dimensional concentration field generated by a point source under stationary meteorological and emission conditions. The Gaussian plume model is

illustrated in Figure 3.11, where the plume travels toward the positive x-axis.

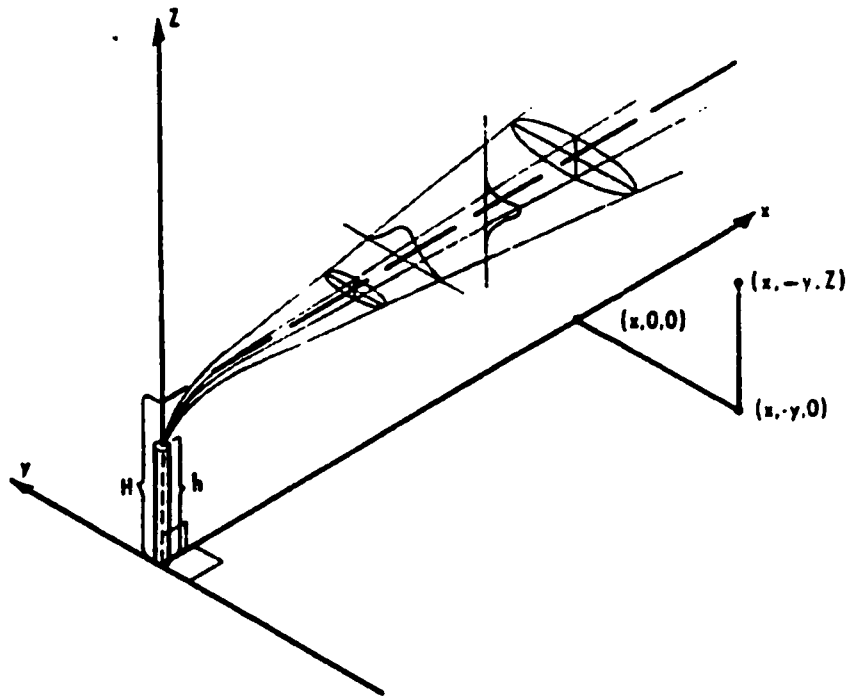


Figure 3.11. Coordinate system showing the Gaussian distributions in the horizontal and vertical directions. (after Turner, 1994).

In a general reference system, the Gaussian plume formula used to calculate ground level concentrations is given in Eq. 3.3.3.

$$C_{(x,r)} = \left(\frac{Q}{2\pi\sigma_y\sigma_z u} \right) \exp \left[-\frac{1}{2} \left(\frac{y}{\sigma_y} \right)^2 \right] \exp \left[-\frac{1}{2} \left(\frac{h_e}{\sigma_z} \right)^2 \right] \quad \text{Eq. 3.3.3}$$

where:

$C_{(x,r)}$ is the concentration at receptor (r) (x, y, z) due to the emissions at source (s) (x_s, y_s, z_s) .

Q is the emission rate

$\sigma_y(j, d)$ and $\sigma_z(j, d)$ are the horizontal and vertical standard deviations of the plume concentration spatial distribution where:

j_y and j_z are the horizontal and vertical turbulence states

d is the downwind distance of the receptor from the source,

u is the average wind velocity vector (u_x, u_y, u_z) at the emission height

h_e is the effective emission plume rise, which is a function of emission parameters, meteorology and downwind distance d and is determined by summing the source height (h_s) and estimated plume rise (Δh) :

$$h_e = h_s + \Delta h \quad \text{Eq. 3.3.4}$$

In addition to the assumptions outlined above, use of the Gaussian model has limitations that affect its applicability for use in epidemiological studies. Some of the assumptions are discussed with respect to this study: i) continuous emissions, ii) conservation of mass, iii) steady state meteorological conditions, iv) Gaussian distribution in the crosswind and vertical directions, v) sampling and averaging time correspondence, and finally, iv) the assumption of the correct use, choice and definition of dispersion parameters.

3.3.1 Continuous emissions

A key assumption is that the emissions are taking place continuously and the rate is not variable over time. The model also assumes that the release and sampling times are long compared with the plume travel time from its source to the receptors. With the exception of turnaround or downtime, processing plant incinerator operation is generally a continuous process, and the emission rate is mostly constant day-to-day. The range of day-to-day emission rate fluctuations, expressed as the mean difference between the daily high and low rates as a percentage of the monthly emission rate was in the range of 1.8 - 3.3 % for all of the processing plants in this study. For all of the plants, the variation in the emission rate did not exceed 12% for 95% of the operating time. This variation was judged to be small and therefore, the assumption of continuous emissions is deemed valid.

3.3.2 Conservation of Mass

During the transport of pollutants from source to receptor, the mass emitted from the source is assumed to remain in the atmosphere, not be removed from the plume through chemical reaction, nor is it lost at the ground surface through reaction,

gravitational settling or impaction as it moves downwind. It is assumed that the material being dispersed is a stable, non-reactive gas or aerosol (effective diameter less than 20 microns) which remains suspended in the air for long time periods. It is also assumed that the earth's surface and the upper atmosphere are complete and perfect reflectors.

Sulphur dioxide is a reactive gas. In Alberta, the average sulphur dioxide lifetime is estimated (from rate constants for the major homogeneous oxidation steps) to be 3.5 days during typical summer conditions and 522 days during winter conditions (Sandu *et al.*, 1980). The oxidation rate of sulphur dioxide in plumes measured at sites in USA varies from less than 0.1% to 16.7% per hour, which equates to a half-life of 3 - 20 days (Harter, 1985). At Fort McMurray, the rate of oxidation to sulphate particles was found to be typically less than 0.5% per hour in February and in the early mornings in June, whereas later in the day in June, the oxidation rate of 2 to 3% per hour was observed (Sandu *et al.*, 1980). Under simulated conditions (to match the diurnal variation of sunlight, near sea level, 40 degrees N latitude, midsummer, 50% relative humidity), a diurnal pattern of oxidation rates was seen. Maximum sulphur dioxide oxidation rates (1-8%/hr) occurred around noon in the lesser polluted air masses and minimum rates (0.01 - 1%/hr) occurred during the night in polluted air masses (Harter, 1985).

For this model comparison study, greater than 90% of the total sulphation stations were within a 10 kilometer radius of the sour gas processing plants and the average wind speeds recorded at the plants range from 5 to 14 kph (1.4 - 3.9 m/s). Thus, under the combined conditions of low wind speed, summertime, and faraway distances significant reductions of sulphur dioxide would be expected to occur.

Fog episodes, agglomeration of particles, and interactions between vegetation and sulphur dioxide may influence the mass that reaches the impact point. In a re-analysis of the Prairie Grass experimental data, obtained from a ground level source, Gryning *et al.* (1983) demonstrated that the earth's surface may not necessarily be a "complete and perfect deflector." Deposition and vegetative uptake of sulphur dioxide led to a 20 - 25% reduction in the ground level concentration at 200 meters from a ground level source.

3.3.3 Steady-State Meteorological Conditions

The Gaussian plume equation is often used to simulate the time-varying concentration field by assuming a series of steady-state conditions. That is, if the hourly emission and meteorological input is known, a steady-state equation can be used repeatedly with the assumption that each hour can be represented by a stationary concentration field. Meteorological conditions are assumed to persist unchanged with time, at least over the time period of transport (travel time) from source to receptor. The assumption of steady state conditions can be more easily met for short time period estimates than for longer period estimates. Thus, it is this assumption that is the most problematic in long term modelling applications since atmospheric flows can never be regarded as stationary or steady for very long and even flows that go undetected by instrumentation have some movement. Further, when the wind is light (approaching zero), the model cannot be applied, and when winds are variable, no mean wind direction can be specified.

Turning of wind with height is also neglected with the Gaussian Model. Wind direction changes with height, turning clockwise up to 20 – 40 degrees, especially under stable conditions. Van Ulden and Holtslag (1985) note that little is known about directional wind shear. Holtslag's 1984 study (cited in Van Ulden and Holtslag, 1985) found that between 20 and 200 meters above the ground, in unstable and near-neutral conditions the turning is small below 200 meters, and in stable conditions, a mean turning angle up to 40 degrees is observed.

3.3.4 Crosswind and Vertical Concentrations Distributions

Gaussian plume dispersion models assume that the time-averaged concentration profiles (over about one hour) at any distance in both the vertical and crosswind directions are well represented by a Gaussian or normal distribution. Over regions of similar surface characteristics, horizontal homogeneity is a reasonable assumption

however, vertical homogeneity does not ever exist because of the earth's surface and the action of buoyancy and gravity forces (Angle and Sakiyama, 1991, p 4-7).

Further, it is assumed that the mean wind direction specifies the x -axis and the wind speed at the height above the ground of the point of release (stack top) represents the diluting wind. This assumption does not correspond to current understanding of air movement in the convective boundary layer. Laboratory and field experiments conducted by Willis and Deardorff (1976, 1981) showed that the centerline of an elevated passive release descends toward the ground, while for a ground level release, the centerline of the plume lifts off from the ground. This plume behavior in the convective boundary layer cannot be properly described with the Gaussian distribution (Venkatram, 1993).

Venkatram (1993) explains:

The vertical distribution of concentrations in the convective boundary layer is related to the properties of the updrafts and downdrafts that form in the buoyancy-driven daytime convective boundary layer. These properties can be described in terms of the distribution of vertical velocities, which displays two unique features. First, in the middle of the boundary layer, the mode of the vertical velocity distribution is negative; the most likely vertical velocity is negative. The second noticeable feature of the CBL is that the downdrafts are coherent enough to assume that a particle released into a downdraft remembers its velocity at release until it hits the ground. These two features give rise to the descent of the centerline of an elevated plume.

Venkatram concludes that use of a symmetric Gaussian distribution rather than the skewed distribution to describe the vertical concentration in the CBL profile underestimates the ground level concentration along the plume centerline by a factor of 1.3. The analysis applies primarily to release heights less than half the mixed layer height and that for larger release heights, the underestimation with the Gaussian formula is greater than a factor of 1.3.

3.3.5 Sampling and Averaging Times

Finally, it is assumed that the averaging time of all quantities measured (mean wind speed, vertical and horizontal plume spread, and concentration) are the same. This is rarely the case. Beychok (1979b) notes that one of the main questions concerning the

Gaussian equation is defining what the calculated concentration really represents. Many different averaging periods are specified. Turner's 1970 Workbook (an EPA publication) states that the equation yields concentrations representing 3 - 15 minute averages. However, Turner's 1994 Workbook assumes that the vertical and crosswind concentration profiles are averaged over about one hour and the vertical spread parameter (σ_z) represents concentrations averaging time periods of about 3 - 10 minutes. The 1977 API publication on air dispersion models states that the concentrations probably represent 10 - 30 minute averages and the US Department of Energy's Handbook on Atmospheric Diffusion (Hanna *et al.*, 1982) states that the standard Pasquill-Gifford curves represent a sampling time of about 10 minutes. Use of one-hour averages now appears to be the most common practice (Federal Register, 1996).

3.4 Use, Choice and Definition of Dispersion Parameters

Another key assumption in Gaussian plume modeling is to assume that the meteorological conditions that determine turbulent diffusion can be characterized by some index or parameter. This section outlines the basis for this premise and discusses the use of various dispersion parameter and schemes.

Turbulence kinetic energy (TKE), as a measure of the intensity of turbulence is usually a starting point for approximations of turbulent diffusion (Stull, 1988). It is one of the most important variables in micrometeorology and is directly related to the transport of momentum, heat and moisture through the boundary layer. The turbulence kinetic energy per unit mass is a measure of the intensity of turbulence, is proportional to the dispersion rate and is the sum of the velocity variances (Stull, 1988, 1995):

$$\frac{TKE}{m} = \frac{1}{2} \left[\overline{(u')^2} + \overline{(v')^2} + \overline{(w')^2} \right] \quad \text{Eq. 3.3.5}$$

where: m = mass

u' = turbulent portion of wind in the x -direction

v' = turbulent portion of wind in the y -direction

w' = turbulent portion of wind in the z -direction

The nature, intensity and type of turbulence, and therefore of dispersion, changes with the magnitudes of terms in the TKE budget. The tendency of turbulent kinetic energy to increase or decrease is given by the following equation (Stull, 1988, 1995):

$$\frac{\Delta TKE}{\Delta t} = A + S + B + Tr + Pc - \epsilon \quad \text{Eq. 3.3.6}$$

where:

$\Delta TKE/\Delta t$ represents the local storage or tendency of TKE.

A is the horizontal movement (or advection) of TKE by the mean wind

S is a mechanical or shear generation (production or loss) term

B is the buoyant production or consumption term, depending on whether the heat flux is positive (during daytime over land) or negative (at night over land).

Tr is the transport by turbulent-scale motions

Pc is a pressure correlation term that describes how TKE is redistributed by pressure perturbations. It is often associated with oscillations in the air such as buoyancy or gravity waves.

ϵ represents the viscous dissipation rate or the rate of conversion of TKE into heat.

The individual terms in Eq. 3.3.6 describe physical processes such as momentum, heat, and moisture transport through the boundary layer that generate turbulence. It is the relative balance of these processes that determines the ability of the flow to maintain turbulence or become turbulent, and thus indicates flow stability. Of the seven terms that make up the TKE equation budget, the buoyant production or consumption term and the mechanical or shear production loss term are the most useful for determining the nature of convection (forced or free) and the intensity of the turbulence (weak or strong) in the atmosphere. The sum of the shear and buoyancy terms determines the turbulence intensity and the ratio of the terms determines the nature of convection (Figure 3.12) (Stull, 1995). On average, buoyant production adds energy directly to vertical motions and shear production adds energy to horizontal turbulent motions (Khanna and Brasseur, 1998). Thus, the strongest buoyancy induced motions are in the vertical velocity component while the strongest shear-induced motions are in the stream-wise velocity component. To represent the mix of mechanical and thermal turbulence, many turbulence

typing schemes have been developed using a variety of methods, such as energy estimations, wind fluctuations (Leung and Liu, 1996), and stability indexes (Sedefian and Bennett, 1980; Angle and Sakiyama, 1991).

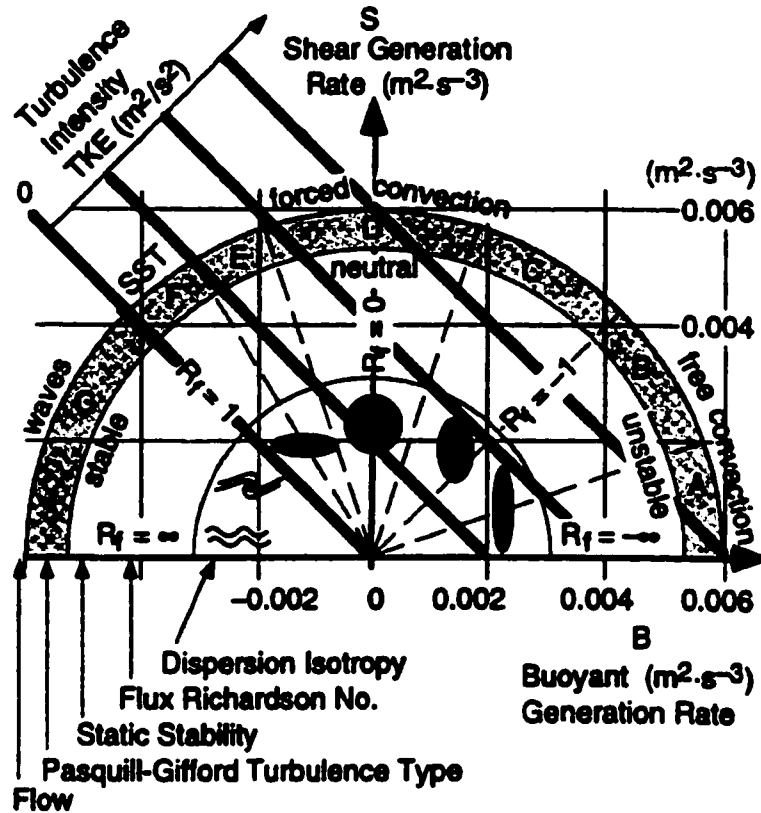


Figure 3.12. Generation rate of turbulent kinetic energy (TKE) by buoyancy (abscissa) and shear (ordinate). Shape and rates of plume dispersion (dark spots or waves). Dashed lines separate sectors of different Pasquill-Gifford turbulence type. Isopleths of TKE intensity (dark diagonal lines). R_f is the flux Richardson number* 1. SST is stably-stratified turbulence. (after Stull, 1995)

Table 3.2 depicts several atmospheric stability classification methods and Figure 3.13 depicts the general qualitative relationships for mid-latitude land masses between the temperature profile, sky conditions, turbulence intensity, and radiation balance as they relate to different measures of atmospheric stability. The relationships depicted in Figure 3.13 are not applicable for snow-covered polar regions during winter. Time of day

* R_f is a dynamic stability parameter that indicates when turbulent flow becomes laminar; also is the ratio of consumption to generation terms of TKE.

provides no indication of stability in these areas (Guenther and Lamb, 1989).

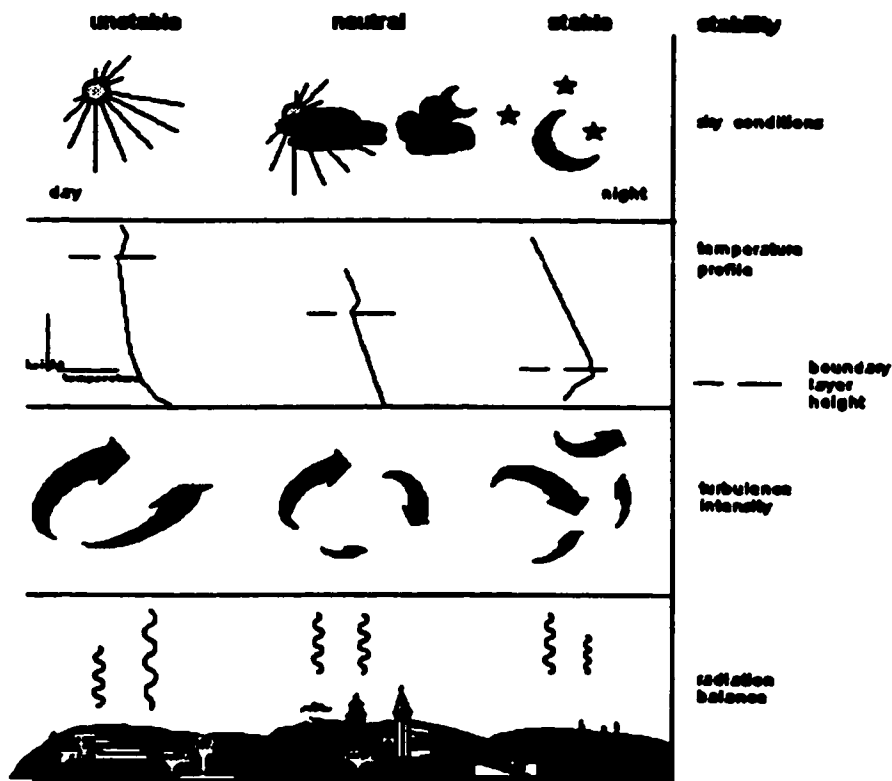


Figure 3.13. Qualitative presentation of atmospheric turbulence intensity, temperature profile, and radiation during unstable, neutral, and stable atmosphere (Cosemans *et al.*, 1996).

Table 3.2. Classification of Atmospheric Stability (after Zannetti, 1990)

Stability Classification	Pasquill Category	σ_h^1 (degrees)	σ_v^1 (degrees)	$\Delta T/\Delta z^2$ ($^{\circ}\text{C}/100\text{m}$)	R_1^3 at 2 meters
Extremely unstable	A	> 22.5	> 11.5	< -1.9	-0.9
Moderately unstable	B	17.5 to 22.5	10.0 to 11.5	-1.9 to -1.7	-0.5
Slightly unstable	C	12.5 to 17.5	7.8 to 10.0	-1.7 to -1.5	-0.15
Neutral	D	7.5 to 12.5	5.0 to 7.8	-1.5 to -0.5	0
Slightly stable	E	3.8 to 7.5	2.4 to 5.0	-0.5 to 1.5	0.4
Moderately stable	F	< 3.8	< 2.4	1.5 to 4.0	[0.8]
Extremely stable	G			> 4.0	

1. Standard deviation of the horizontal (σ_h) and vertical (σ_v) wind direction fluctuation, using highly responsive wind sensor over a period of 15 minutes to 1 hour. The values shown are averages for each stability classification.
2. Temperature change with height above ground.
3. Gradient Richardson number

The American Meteorological Society Workshop on Stability Classification

Schemes and Sigma Curves (Hanna *et. al.*, 1977) noted that the following quantities are required to characterise the horizontal and vertical dispersion, σ_y and σ_z , respectively, in the boundary layer:

- roughness length and friction velocity, as measures of the mechanical turbulence;
- mixing depth and the Monin-Obukhov length (a parameter which reflects the height above ground where the contributions to the TKE from buoyancy forces and from shear stress are comparable) or the heat flux, as measures of the convective turbulence during the daytime; and
- wind speed and the standard deviation of the wind direction fluctuation (σ_θ). The wind vector is needed to specify the transport wind, and σ_θ is required to estimate the horizontal plume spread (σ_y), especially in stable conditions.

Yet the most widely used scheme is the semi-empirical Pasquill turbulence type stability classification which, from the surface wind speed, incoming solar radiation and cloudiness estimates, categorizes the atmospheric stability into six groups ranging from very unstable to stable. To further standardize the classification scheme, Turner incorporated measurements of solar altitude, the angle between the sun's rays and a tangent to the earth's surface at the point of observations, to the classification scheme. For daytime measurements, the solar altitude (the angle between the sun's rays and a tangent to the earth's surface at the point of observation) is measured to define an insolation class and the net radiation index is then determined as a function of insolation class, percentage cloud cover and the cloud ceiling height. For night-time, the net radiation index is determined as a function of cloud cover, and the cloud ceiling height from which the stability class is determined as a function of the net radiation index and the wind speed category at the time and location of the observation (Beychok, 1979a). This scheme (Table 3.3) is used by Environment Canada's Atmospheric Environment Service to produce the Stability Array (STAR) data at airport weather stations (Angle and Sakiyama, 1991).

Table 3.3. Pasquill-Gifford Turbulence Typing Scheme

Mean Surface Wind Speed (m/s)	Daytime Insolation ^{*1}			Night time ^{*2} Cloud Cover	
	Strong*	Moderate	Slight	≥ 4/8 low cloud or thin overcast	≤ 3/8
< 2	A	A to B	B	G	G
2 to 3	A to B	B	C	E	F
3 to 4	B	B to C	C	D	E
4 to 6	C	C to D	D	D	D
>6	C	D	D	D	D

*1 Strong insolation corresponds to sunny midday in mid-summer in England; slight insolation corresponds to similar conditions in mid-winter.

*2 Night refers to the period from one hour before sunset to one hour after dawn.

Draxler (1987) found that the 1964 Turner classification gives the largest frequency of neutral stability (D) cases. Classification by temperature gradient alone, which does not account for the effects of wind shear had the largest number of very unstable cases. However, when temperature gradient and wind shear are used as in the gradient Richardson number, the stability categories showed the largest number of very stable cases.

Erbrink (1991), using a wind fluctuation method, showed that the Pasquill-Gifford-Turner (PGT) method for estimating the stability class results in too many hours with a neutral atmosphere. The wind fluctuation method also found that there are more unstable hours in the daytime and more stable hours at night than the PGT method suggests. The analysis of several hundred hours with wind measurements shows a large decrease in the number of hours with Pasquill D from 70% to only 20% when the wind fluctuation model is applied.

Angle and Sakiyama, (1991) highlight studies undertaken in Alberta by several investigators who have found discrepancies between various stability categorization frequencies:

- Near Edson, compared to STAR data, higher frequencies of neutral and unstable classes using on-site wind fluctuation were found.
- In Calgary, a heat flux profile method gave higher frequencies of unstable classes than STAR data.

- When compared to STAR data from the Edmonton International Airport, the 1973 Briggs scheme, a more simplified scheme devised for small emissions, overestimates, on an annual basis, the frequency of stability classes A and B and underestimates the frequency of D and F stability.
- Monthly distribution of layer stability from one year of acoustic sounder records at Calgary gave total unstable, total stable and total neutral frequencies of 64.9, 28.5 and 6.6 % respectively. This frequency distribution differs significantly from the Calgary International Airport (1972-1976) STAR data of 17.8, 51.9, and 30.4%, respectively.

Davison *et.al.* (1977) found the values for σ_y and σ_z in the Athabasca river valley were consistently higher than the PG curves and suggested that the assignment of a single stability class for a boundary layer with several stabilities in the vertical dimension is not appropriate.

Most stability classifications are based on characteristics of the available data obtained by instruments with differing resolution and accuracy. Druilhet and Durand (1997) reviewed various approaches taken to measure turbulence in the ABL and stated that it is very difficult to make accurate and representative turbulent flux measurements in the surface layer. They note that while turbulence is close to being a random process, it is not exactly, and that for turbulence measurements, 'accuracy' is conditional on factors such as time resolution, sensitivity, frequency response and spatial resolution of the sensor. Sensor measurements may also be influenced by the mounting apparatus itself, producing flow distortion or dampening effects: a one degree misalignment in several 3-component sonic anemometers placed less than one-meter apart and at the same height gave horizontal and vertical plane co-variances ranging from 0.6 to 1.5 times the mean; and direct measurements of temperature fluxes from two instruments separated horizontally by 5 m at 4 m height were compared and found to agreed only within a factor of two for individual runs (cited in Wyngaard, 1988b, p 53).

The wind data obtained from airports is subject to various influences, which can

manifest as sources of error. A traditional meteorological rule of thumb is that a wind measurement should be located at least 100 meters downwind for every upstream roughness change of one meter (Flesch and Wilson, 1993). While the criteria is deemed “quite conservative and economically unrealistic, and a 10 to 1 rule is more accepted,” the airports at High Level, Fort McMurray and Edson do not, or have not in the past, satisfied the 10 to 1 ratio (Flesch and Wilson, 1993). Further, while the topography at airports is generally an extensive uniform flat grassy and asphalt surface, the placement of the anemometer is inconsistent throughout the province’s airport meteorology stations. This inconsistent placement, which varies from grassy areas, airport control tower to an airport hangar roof, is expected to have unpredictable effects on measurements (Flesch and Wilson, 1993), presumably due to the airflow changes induced by the presence of physical structures.

A comparison of methods to measure mixing height under convective conditions (radiosonde, sodar, radar, lidar, and aircraft) have shown that relative differences of the order of 10% or even less can be noticed provided that the capping inversion is not too weak and has a well-defined base (Beyrich, 1997). However, measurements made of a weak capping stable layer or a convective boundary layer that is not perfectly mixed, from different systems and even the analysis of the same potential temperature profile by several experienced meteorologists may easily result in relative differences of 25% or more (Beyrich, 1997). Further, the differences between individual radiosonde point measurements of potential temperature (used to determine the convective boundary layer mean depth) may even approach 100% (Piironen, 1994)

The earth’s surface characteristics also affect the height of the mixed layer and consequently dispersion in the ABL. Carroll (1993) evaluated the degree to which design decisions of a time-dependent one-dimensional model of the planetary boundary layer affect model output variables and found that sensitivity to changes in soil type exceeds any of the design criteria tested. Alapaty *et.al.* (1997) also studied how uncertainty in the specification of surface characteristics affects the processes and structure of a simulated

atmospheric boundary layer using a one-dimensional soil-vegetation-boundary-layer model. They varied five surface parameters: soil texture, initial soil moisture, minimum stomatal resistance, leaf area index and vegetation cover. Variations in these 5 surface parameters had a negligible effect on the simulated horizontal wind fields however they had a significant effect on the vertical distribution of turbulent heat fluxes and on the predicted maximum boundary-layer depth, which varied from about 1400 - 2300 m across 11 simulations. The authors concluded that uncertainties in the specification of the surface parameters can significantly affect the simulated boundary-layer structure in terms of meteorological and air quality model predictions.

These studies clearly demonstrate the significant challenges and barriers to defining and measuring the key atmospheric processes needed to characterize pollutant dispersion. Together, the difficulty, expense, and non-representativeness of direct measurements has led to widespread use of indirect techniques for inferring turbulent fluxes, which may be better than direct techniques in each of these respects (Wyngaard, 1988b).

3.5 Dispersion Parameter Scheme Discrepancies

Significant discrepancies between dispersion typing schemes have been reported. Often, there is a correspondence between median values in each stability class, however the frequency distributions from different schemes are often differ more often than they are found to be similar (Angle and Sakiyama, 1991, p 1-75).

In a brief literature review, Miller and Little (1980) identified nine studies done between 1976 -1978 which showed that the methods for categorizing stability on the basis of various meteorological measurements often gave significantly different stability categorizations when applied to the same meteorological data set. They compared measured and predicted fluorescein tracer concentrations, using three different methods to determine atmospheric stability. Two different sets of vertical temperature gradient measurements and the standard deviation of the wind direction were used to determine atmospheric stability. Although there was a tendency for all three methods to over-predict tracer concentrations in air, they found that the predictions based on the wind fluctuation method for determining atmospheric stability were more accurate than those based on either set of vertical temperature gradient methods.

Kretzschmar and Mertens (1980) showed that for both ground-level and elevated releases, the same meteorological observations give quite different model results when used in nine different turbulence typing schemes. For ground level releases, a factor of 4 difference between the different typing schemes is found at a downwind distance of 1 kilometer, and a factor of 6 difference is found at 10 kilometers. For elevated releases, a factor of 30 is found at 0.5 kilometer, a factor of 10 at 1 kilometer, and a factor of 6 at 10 kilometers.

Irwin (1983) estimated lateral and vertical Gaussian plume dispersion parameters using Cramer's, Draxler's, and Pasquill's schemes and compared them with field data collected at 11 sites. Vertical dispersion parameter comparisons for elevated releases showed that approximately 75% of the estimates were within a factor of two of the measured values for four models but for the Pasquill Gifford model only 19% were

within a factor of two (Irwin, 1983).

In a Washington, D.C. tracer study, Draxler (1987) found that a stability category determined from wind direction fluctuations in combination with Pasquill Gifford dispersion curves were least biased relative to Turner's 1964 or Brigg's 1973 method. Turner's 1964 stability classification provided too few unstable cases during daytime resulting in over-prediction and Brigg's method resulted in an under-calculation by a factor of five.

Carrascal *et.al.* (1993) note that variations in computed ground-level pollutant concentrations resulting from different sigma schemes in a Gaussian Plume model may be as large as several orders of magnitude and conclude that "the accuracy of Gaussian calculations should not be taken for granted."

Mohan and Siddiqui (1997) tested and compared the results of five vertical and horizontal dispersion schemes (Pasquill and Briggs, Irwin, Draxler, Taylor, Hanna) to evaluate the sensitivity of each scheme under various atmospheric stability conditions. They found that the schemes provide "reasonable estimates" of the dispersion coefficient (σ_y) during highly unstable conditions (PG class A and B) however when the atmospheric turbulence decreases and stability increases, the observed data show a random pattern and none of the schemes could satisfactorily represent the observed data.

Regulatory practice has motivated much of the research on dispersion in plume dispersion modelling, and currently, the Gaussian plume equation is the most widely used, assuming lateral and vertical dispersion parameters given by the Pasquill -Gifford - Turner (PGT) curves. The main limitations of the PGT approach are that (Weil, 1988a):

- the curves are based on passive tracer releases from a ground level source and on surface concentrations measured out to only about 800 meters from the source,
- they do not apply to an elevated plume, which has dispersion characteristics quite different from those for a surface release;
- the method does not account for the PBL's vertical structure; and
- the method over-predicts the frequency of neutral conditions during daytime,

when convective or unstable conditions usually exist.

Weil (1988b) suggests that the use of the PGT method is one of the prime reasons for poor model performance and notes that even after criticism at several workshops, the PGT method continues to be used for tall stacks, including those with large heat releases and plume rise. Hanna (1982) notes that the PGT dispersion parameters typically used were "developed from field observations over a limited range of conditions*"; however, "this has not prevented users from extrapolating the curves far outside their range of validity". In a round table discussion (Hanna, 1993), Briggs explains that the

social and regulatory needs are always far beyond the solidly established science, so we are always forced to extrapolate models further than data would permit. An awful example is the extrapolation of Pasquill's original curves 100 times beyond the distance of most of the data - all stable and unstable curves were based on the Prairie Grass experiment, which only extended to 800 meters from the source. But when the regulatory need was for distances of hundreds of kilometers, someone was not afraid of logarithmic coordinates to extend Pasquill's lines rather drastically.

Venkatram (1996) summarizes the status of dispersion parameter use in current modelling activities:

Since [the development of the PGT curves 30 years ago], our understanding of dispersion as well as micrometeorology has progressed to the point that we can get reliable estimates of dispersion from sources in the surface layer. However, the methods to make these estimates have not been incorporated into the practice of modelling primarily because it is generally believed that the PGT curves provide useful concentration estimates that can be used in regulatory decisions.

Although Barry (1977) emphasized the importance of characterizing atmospheric diffusivity, it has been very difficult to do simply since it encompasses many simultaneously interacting processes such as wind, temperature stratification and turbulence. Also, while investigators have developed different approaches using a variety

* The Prairie Grass experiment was conducted in Nebraska (July - August 1956) at a site which was flat, covered with grass stubble 5-6 cm high, and consisted of 70 "runs", each run lasting 10 minutes. SO₂ was released at a height of 46 cm and concentration measurements were made at sampling arc distances of 50, 100, 200, 400 and 800 m from the release point and at 1.5 m above ground (except for the 100 m arc where measurements were made on six towers at heights ranging from 0.5 to 17.45 m). Only the 100 m arc allows a direct calculation of the vertical dispersion from the vertical concentration profile.

of instrumentation to characterize various states of atmospheric stability (standard deviation of angular wind fluctuation, vertical heat flux resulting from surface heating by solar radiation, Richardson number, lapse rate), for certain diffusion typing schemes (the stable and unstable cases) correspondence between schemes has been poor (Kretzschmar and Mertens, 1980). For the same meteorological data set, and within the same diffusion typing or stability classification scheme, important differences in the frequency of occurrence of a given stability class are generated by using a different methodology to determine the stability class at a given time (Kretzschmar and Mertens, 1980).

3.6 Model Validation Studies

Some of the difficulties encountered in verifying, validating or evaluating a model or a component of a model are outlined by Venkatram (1979). Venkatram discusses the difficulty of using concentration estimates to check the validity of the model estimates because of the widely fluctuating concentrations found in the convective boundary layer. The notion of an ensemble average is used to relate “the possibility of identifying a set of experiments which have some quality in common” since the atmosphere can never be completely observed, either in terms of spatial coverage or accuracy of measurements.

Venkatram (1979) presents a method to estimate the expected deviation between measurements representing averages over a limited number of ‘concentration events’ and model predictions, which correspond to ensemble averages. Using the observation that air pollutant concentrations are approximately lognormally distributed, he demonstrates that for an elevated release into a convective boundary layer, more than 50% of concentrations measured under identical meteorological conditions will not meet the factor-of-two criterion commonly used in model validation. The “results indicate that prediction of the maximum concentration (say for supplementary control) under convective conditions is likely to be very unreliable.”

3.6.1. Model Accuracy

The principal value of a good model for epidemiological use lies in its applicability to a wide variety of conditions, allowing accurate concentration predictions when the micrometeorology is not known. Accuracy refers to the deviation of a model's predicted value from the value actually measured in the field. Turner (1992) identified four main factors that affect model accuracy:

- the atmospheric physics and chemistry included in the model;
- the quality of the emission and meteorology input data;
- the time of use to which the model is being put; and
- the inherent uncertainty of the atmosphere.

Many investigators have reviewed or evaluated the accuracy of plume dispersion models over the last 20 years (Hanna *et.al.*, 1978; Miller and Little, 1980; Smith, 1984; Benarie, 1987a, b; Hanna, 1988, 1993; Venkatram, 1988a; US EPA, 1993). The accuracy estimates often apply to concentration averaging times on the order of 10 minutes and to maximum plume centerline concentrations at a given distance. Especially relevant to epidemiological studies is that, in the accuracy evaluations, the observed and predicted maximum may be at different locations (Hanna, 1993). That is, the space, time and concentration comparisons are not coincident. In a review of mathematical models for atmospheric pollutants, The Electric Power Research Institute (Battelle Pacific Northwest Laboratories, 1979) provided point source accuracy estimates for diffusion calculations:

- 10 - 20% under ideal conditions of near field (less than 1 kilometer), short averaging times (min to hr), flat terrain, steady meteorology, surface source;
- 20 - 40% as above except for elevated sources;
- factor of 2 for real world applications: meteorological parameters reasonably well-known and steady with no exceptional circumstances;
- greater than factor of 2; may be as poor as a factor of 10 or more for exceptional circumstances: wakes, buoyant plumes, varied surfaces, such as forests, cities, shorelines, rough terrain, extreme stable and unstable conditions; distances greater than 10 - 20 kilometers.

More recently, in a review undertaken by the US EPA (1993), estimates of model accuracy for various conditions were summarized from the literature (Table 3.4). Thus, based on these summaries, air quality models are expected to be most accurate for long term period averages in urban areas of flat terrain and moderate wind speeds. Additional studies not cited in the US EPA report and more recent studies, which provide more detailed comparisons are discussed to highlight the widely variable model performance. Further, since a wide range of accuracy estimates have been reported which have led to questions about the 'acceptable levels of model performance' (Cox and Tikvart, 1986), some studies of dispersion model accuracy and their correspondence with measured values are also highlighted.

Table 3.4. Estimated Ratios of Predicted to Observed Air Concentrations Using Gaussian Plume Atmospheric Dispersion Models (after US EPA, 1993)

Conditions	Range
Highly instrumented site centerline concentration within 10 km of a continuous point source	
Ground level release	0.8 – 1.2
Elevated release	0.65 – 1.35
Maximum air concentration for elevated releases	0.5 – 1.5
Annual average for a specific point, flat terrain, within 10 km downwind of the release point	0.5 – 2.0
Annual average for a specific point, flat terrain, within 10 – 150 km downwind of the release point	0.25 – 4.0
Specific hour and receptor point, flat terrain, steady meteorological conditions	
Elevated releases without building wake effects	0.1 – 10.0
Elevated releases with building wake effects	0.01 – 100.0
Short-term, surface-level releases with building wake effects using temperature gradient method of estimating atmospheric stability	
Wind speeds over 2 m/s	0.7 – 100.0
Wind speeds under 2m/s	1.0 – 100.0
Short-term, surface-level releases without building wake effects using temperature gradient method of estimating atmospheric stability	
Wind speeds over 2 m/s	0.3 – 10.0
Wind speeds under 2 m/s	1.0 – 100.0
Complex terrain or meteorology (e.g. sea breeze regimes)	
Annual average concentrations	0.1 – 10.0
Short-term releases	0.01 – 100.0
Urban releases	
Annual average concentrations	0.25 – 4.0
Less than 24 hour concentrations	0.1 – 10.0

Good correlation coefficients were found between an urban model's predictions and measured values by Martin (1971) and by Prahm and Christensen (1977). Martin (1971) compared long-term modelled concentration estimates with measured seasonal sulphur dioxide concentrations at 40 sites in an urban setting with uncomplicated topography and found a linear relationship with a correlation coefficient of 0.84. Prahm and Christensen tested a multiple source stationary Gaussian atmospheric dispersion model in the flat urban Copenhagen area for correspondence between measured and computed sulphur dioxide values. They found that the spatial correspondence for 22 receptor points between the computed and measured sulphur dioxide three month-average

concentration gave a linear relationship with a correlation coefficient larger than 0.9. Yet for shorter averaging time periods, using similar methods, Okamoto and Shiozawa (1978) found poorer correlation coefficients. In comparisons of measured and calculated SO₂ concentrations at 12 stations within a highly industrialized area, for hourly data, they found correlation coefficients ranging from 0.20 to 0.58 and for daily data, found correlation coefficients ranging from 0.09 to 0.74.

Venkatram (1980b) described an impingement model to predict dispersion from an elevated source in a convective boundary layer, which incorporated current understanding of dispersion in the mixed layer. In this model, the ground-level concentration distribution is found from an assumed probability density function of the impingement distance, the point where plume segments caught in downdrafts first touch the ground. Venkatram tested it by comparing predictions with measured sulphur dioxide concentrations, obtained by repeated passes across the direction of plume travel by an instrumented mobile van, around two power plants in Maryland and around the INCO smelter in Sudbury, Ontario (Venkatram and Vet, 1981). The studies showed that 80 - 86% of the predictions met the factor-of-two accuracy criterion for all three data sets and a correlation analysis of the logarithms of the observed and predicted concentrations gave correlation coefficients of 0.73, 0.77 and 0.79. Venkatram (1980b) concluded that the model provides rough estimates of one-hour average ground-level concentrations during the period of time when elevated releases are of most concern by assuming that the pollutants are well mixed through the PBL.

Irwin (1983) analyzed the ratio of predicted to observed surface concentrations of an elevated release for four Gaussian plume models using a variety of dispersion schemes. Draxler's scheme gave the smallest mean fractional error in the concentration estimates and the smallest variance of the fractional errors. For unstable stratified conditions, approximately 50% of the estimates were within a factor of 2 for 4 models and only 8% were within a factor of 2 for the Pasquill Gifford model. He found that for elevated releases in unstable conditions between downwind distances of 150 meters and

550 meters, 80% (4/5) of the models had only 21% of estimated values within a factor of two of measured values and the fifth model had 0%. Between 550 meters and 1750 meters downwind, the ratio improved for all the models tested. Four of the 5 models had 64 -71% of estimated values within a factor of two of the measured values and the fifth model had 14%. The Spearman Rank correlation coefficient for these same conditions ranged from 0.337 - 0.439 for 4 models and was 0.063 for the Pasquill Gifford model.

An evaluation of 10 rural Gaussian plume diffusion models was undertaken by an American Meteorological Society committee working with the US EPA (Smith, 1984). Although the models were not considered to be up-to-date scientifically, they were selected on the basis that they were used or submitted to the US Environmental Protection Agency for use for regulatory purposes. The correlation between observations and predictions for all models was very low (range -0.12 to +0.14) and there was no difference between models in their predictive accuracy. The main criticisms of the specific model components pertained to the models':

- failure to include improvements in the modeling of diffusion in the convective boundary layer wherein vertical concentration distributions quickly become non-Gaussian;
- failure of the Gaussian modelling systems to deal with calm and near-calm conditions in a sound scientific manner;
- use of the Pasquill-Gifford expressions which are based on small-scale, short-term, ground level data and have not been shown to apply to elevated sources;
- failure to take account of the variation of turbulent properties with height by use of the Pasquill - Turner method for classifying stability;
- use of the "all or none" concept of plume penetration of elevated inversions wherein the behavior of a plume depends upon the residual buoyancy it has when it reaches the elevated inversion, upon the strength of the inversion, and eventually upon changes in the mixed layer itself;
- use of terrain corrections for difference between receptor height and height of the stack base when they are considered crude and scientifically unproven; and
- failure to adjust for differences between the plume's behavior from low sources and its behavior from high sources.

Smith acknowledged that while the data base they worked with was good quality, on-

site measurements of key factors (wind direction and speed at stack height and above, stability and turbulence at plume elevation, and depth of the mixed layer) which are needed to reliably evaluate model performance were not available.

Weil (1988a) described the main features and performance of several models, which are based on an improved understanding of the convective boundary layer and buoyant plume behavior:

- the Gaussian model with improved formulations of the dispersion parameters;
- the Probability Density Function (PDF) model as modified for plume buoyancy; and
- two other approaches for highly buoyant effluents - Venkatram's impingement model (1980) and Briggs' (1985) model.

The PDF model is based on the probability density function of the vertical velocity, which is non-Gaussian, giving a non-Gaussian predicted vertical concentration distribution. This model assumes that particles released from a fixed source are emitted into a travelling train of organized, long-lived updrafts and downdrafts that are moving with the mean wind speed. The PDF model was in reasonable agreement with surface concentration data for both laboratory and full-scale plumes but for high buoyancy plumes it needs modification to give an adequate description of the crosswind integrated concentration at large distances (Weil, 1988a).

The PPSP model (Weil and Brower, 1984) incorporated σ_y and σ_z expressions, which were based on convective scaling, and differs from conventional Gaussian plume models in four ways (Weil, 1988a):

- Briggs' dispersion curves for elevated releases replace the PG curves for surface releases;
- u/w . (the ratio of wind speed to convective velocity scale) is the stability parameter for daytime instead of the Turner (1964) criteria;
- Briggs' (1975) plume rise formulas for convective conditions are included rather than the pre-1975 formulas, which did not address convection; and
- Briggs' (1984) criteria for estimating plume penetration of elevated inversions are used instead of the 'all-or-none' approach of the CRSTER (a now 'obsolete' US EPA Single Source Dispersion) model.

Comparisons of the PPSP model with ground level concentration values of sulphur

dioxide downwind of Maryland power plants showed that it performed much better than the CRSTER model. The measurements approximated hourly averages along the plume centerline. Sixty-nine percent of the PPSP model predictions were within a factor of 2 of the observed concentrations, and the variance (r^2) explained by the model was 0.58. For the CRSTER model, only 33% of the predictions met the factor of 2 criterion, and r^2 was near zero. The better performance by the PPSP model was attributed primarily to use of the Briggs A sigma z curve and to the modelled distribution of stability - 62%, 30%, 8%, and 0% for the A to D classes, respectively. This distribution is in line with daytime expectations. In contrast, the stability distribution given by the CRSTER model was 1%, 19%, 26% and 53% for stability classes A to D. It was strongly biased toward neutral conditions, which are rather infrequent during daytime.

Venkatram (1993) compared the maximum cross-wind integrated and centerline concentration estimates at ground level for an elevated source in the convective boundary layer using a positively skewed probability density function of vertical velocities with a negative mode with those obtained using the symmetric Gaussian PDF. The positively skewed PDF was used to account for the more frequent downdrafts in the CBL, which better represents the vertical distribution of concentrations in the CBL. Venkatram found that the error associated with the use of the Gaussian PDF is an underestimate of the cross-wind integrated concentration at ground level by a factor of 1.5 and 1.3 for the ground level centerline concentration.

Comparison of a similar PDF model with sulphur hexafluoride ground level concentrations downwind of the Kincaid power plant showed "fair to good agreement on average" (Weil, 1988a). The geometric mean and geometric standard deviation of the C_{pred}/C_{obs} were 1.1 and 2.1 respectively, 68% of the predictions were within a factor of two of the observations, and $r^2 = 0.34$ with large scatter. This performance was better than with the CRSTER model and the Kincaid data set, which gave greater scatter as indicated by a geometric standard deviation of 4.6, fewer predictions within a factor of 2 of the observations (33%), and an r^2 of 0.02.

Al-Khayat *et al.* (1992) compared modelled and measured values of radioactive emissions (^{234}Th) from the Sellafield nuclear fuel fabrication plant in the United Kingdom. A Gaussian plume dispersion model (ISCLT - Industrial Source Complex Long Term model) was able to predict 85% of the observed air concentrations within a factor of four, despite large uncertainties acknowledged in some source parameters. The mean monthly ^{234}Th value at one site gave a correlation coefficient of 0.5. Correlation of the air concentrations at one site with the frequency of winds blowing from the factory to the site was 0.8 based on adjacent meteorological data. Correlation of wind speed and direction with the 5-7 day mean total ^{234}Th concentrations in air at all four sites showed that between 7 and 71% of the variations in concentrations at individual sites could be explained by these meteorological variables. The shape of the predicted zone of enhanced radioactive substances in the atmosphere approximated that of the annual average wind rose for the period but was modified.

Wilson (1993) reviewed the developmental history, formulation, operation and application of the CRSTER and MPTER models. A 1977 EPA study was cited which found the geometric mean of the ratios of predicted to measured second-highest concentrations of the CRSTER model applied to four power plants were as follows: for the one-hour ratios, 1.23 (range from 0.6 - 2.79), and for the 24-hour ratios, 0.68 (range from 0.2 - 2.06). In an evaluation of a complex terrain model, the top 25 observed concentrations paired in time with model predictions, for 1-hour averages, 20% were within a factor of two for all stability classes (Paumier, 1997). For 3-hour averages, 40% were within a factor of two and for 24-hour average, 56% were within a factor of two for all stability classes. This model was only slightly better than the Rough Terrain Dispersion Model which, for all stability classes predicted 24% of 1-hour averages, 16% of 3-hour averages, and 44% of 24-hour averages within a factor of two.

3.7 Summary

Together with the earlier performance summaries, the studies highlighted here further

demonstrate the highly variable performance of air dispersion models. Their ability to predict concentrations corresponding to measurements is inconsistent. Reported correlation coefficients range between no correlation (~ 0) and very good correlation (0.9), and while many of the models appear to predict the peak concentrations quite well, the correspondence between predicted and measured concentrations in both time and space is often poor. Space, time and concentration correspondence is improved with predictions of longer-term averages (daily, monthly, or seasonal), in urban settings, in flat terrain, and with use of convective scaling parameters and wind fluctuation measurements for deriving estimates of horizontal and vertical dispersion.

Chapter 4 Methods

4.1 Dispersion Model Selection and Use

A variety of models and approaches have been recommended by several organizations to estimate airborne pollutant exposure. The Exposure Assessment Group within the US EPA Office of Health and Environmental Assessment state that the Industrial Source Complex Model (a Gaussian dispersion model) is a preferred model for use in exposure assessments from nearby point sources in simple terrain. This is based on availability, general acceptance, ease of use and its extensive range of modelling options (US EPA, 1993, p 14). The long-term version (ISCLT) uses averaging times of 1 month to 1 year. Yet, many years prior, at a combined Environmental Protection Agency and American Meteorological Society workshop in 1984, the Gaussian model was recommended for predicting pollutant concentrations for short time periods, but for long time periods, probability density function and impingement models should be considered (Weil, 1985). While the strongest recommendation was for the use of convective scaling in estimating horizontal and vertical dispersion parameters (σ_x , σ_z) based on the “clear success demonstrated with field, laboratory and numerical data,” the committee could not recommend adoption of these developments due to some of the uncertainties raised (Weil, 1985). Recently however, some of these recommendations have been implemented. A model, called AERMIC Model (AERMOD), which incorporates convective scaling parameters is currently under development to replace the Industrial Source Complex Model Version 3 (Cimorelli, 1996)

For this study, conceptually simple plume dispersion models which predict long-term averages were sought. Simple input requirements and the availability of appropriate input data were also criteria for model selection. Six models were chosen which fulfilled these criteria:

- Industrial Source Complex Long Term (ISCLT3) (US EPA)
- Long - Term Sector Average Model (LTSAM): (Slade, 1968; Hanna, Briggs, and

Hosker, 1982)

- Modified Climatological Model (MCM) (Zannetti, 1990)
- Convective Dispersion Model (CDM) (Venkatram, 1980)
- Mixed Layer Scaling Convective Model (MLSCM) (Stull, 1995)
- Simple Exponential Decay Models (Scott, 1998)

4.1.1 ISCLT3

Industrial source complex long-term (ISCLT3) model-predicted sulphur dioxide concentrations were compared with sulphation values to provide an indication of the model's validity for the purpose of categorizing cattle exposures to sour gas plant emissions in M. Scott's study (1998). This model is endorsed for regulatory use by the United States Environmental Protection Agency.

The ISCLT model uses a Gaussian sector-averaging plume equation as the basis for modeling long-term pollutant concentrations. The area surrounding a continuous source of pollutants is divided into 16 sectors of equal angular width corresponding to those sectors of the seasonal and annual frequency distributions of wind direction, wind speed, and stability provided in the STability ARray (STAR) data. The wind direction input is the frequency of occurrence over a sector, with no information on the distribution of winds within the sector. Monthly emissions from the point source are allocated to the sectors according to the frequencies of wind blowing into the sectors. Concentrations are calculated for user-specified downwind distances, converted to a common coordinate system.

The mean monthly concentration at a given site (X_m) is given by the following (adapted from the ISCLT3 Users Guide (US EPA, 1995)):

$$X_m = \frac{K}{\sqrt{2\pi} R \Delta\theta'} \sum_{i,j,k} \frac{Q_i S_j V_k D}{u_j \sigma_z} \quad \text{Eq. 4.1.1}$$

where:

- K = scaling coefficient to convert calculated concentrations to desired units
- Q = pollutant emission rate (mass per unit time) for the i^{th} wind speed category, the k^{th} stability class and the m^{th} month.
- $\Delta\theta'$ = the sector width (in radians)

- R = radial distance from lateral virtual point source (for building downwash) to the receptor (m)
- x = downwind distance from the source to receptor (m)
- y = lateral distance from the plume axis to the receptor (m)
- S = a smoothing function
- u_i = mean wind speed (m/s) at stack height for the i^{th} wind speed category and k^{th} stability category
- σ_z = standard deviation of the vertical concentration distribution (m) for the k^{th} stability category
- V = vertical term for the i^{th} wind speed category, k^{th} stability category, and m^{th} month (dimensionless)
- D = decay term for the i^{th} wind speed category and k^{th} stability category (dimensionless).

Vertical distribution of the plume is reflected in the term V , which incorporates the stack height, receptor elevation, plume rise, and vertical mixing. The decay term (D) captures the physical or chemical removal of the pollutant, however the model was run in the 'no decay' default.

The model was used to produce monthly predictions of sulphur dioxide concentrations at the specific locations of the sulphation stations around the gas plant. The ISCLT3 model was run on an MS-DOS® (Microsoft Corporation) system where an ASCII input file is submitted with the gas plant specifications, point source stack location, STAR data file, and output file format.

The gas processing plant variables required as inputs for the 11 plants were obtained from the Alberta Energy and Utilities Board (stack height and diameter, exit velocity, and stack top temperature), and from the plant files at Alberta Environmental Protection (monthly SO_2 emissions). Receptor locations were needed as inputs for the model. The sulphation station locations were obtained from the site documentation files and converted to discrete Cartesian coordinates by measuring the distance and direction (degrees from north) from the plant's center and calculating the x- and y-coordinates using trigonometric relationships. The receptor elevation was set as the same as the processing plant and terrain effects were not addressed.

Meteorological data summarized into joint frequencies of occurrence for particular wind speed classes, wind direction sectors, and stability categories are used as

inputs to the ISCLT3 model. Ten-year averages of hourly wind speed, direction and stability class (STAR data) recorded at the airport closest to the sour gas plants were used as meteorological inputs to the model, whereas surface and upper air data were from Edmonton stations for all of the runs. The mixing heights were specified and were applied to all wind speed classes for any given stability class as recommended in the User's Guide:

- a mixing height of 10,000 m was specified for stability classes E and F;
- the mean maximum afternoon mixing heights for Stony Plain, Alberta (Portelli, 1977) were used for the appropriate month for stability classes B, C, and D; and
- for stability class A, the mean maximum afternoon mixing height was multiplied by 1.5.

For each plant, the outputs consisting of point predictions at each sulphation station for the month, were then imported into Microsoft Excel® and compared with the sulphation values and with the wind speed- and vertical velocity-adjusted sulphation values.

4.1.2 Long Term Sector Average Model (LTSAM)

This model is a modification of the formula for crosswind integrated concentration from a continuous emissions point source (Eq. 4.1.2), which is obtained by integrating the Gaussian plume model for a receptor located at ground level (Eq. 4.1.3) with respect to the crosswind distance from source (y) from $-\infty$ to ∞ (Slade, 1968; Hanna, Briggs, and Hosker, 1982):

$$C_{CWI} = \left(\frac{2}{\pi}\right)^{1/2} \left(\frac{Q}{\sigma_z u}\right) \exp\left(-\frac{h_s^2}{2\sigma_z^2}\right) \quad \dots \text{Eq. 4.1.2}$$

$$C_o = \left(\frac{Q}{\pi\sigma_y\sigma_z u}\right) \exp\left[-\left(\frac{y^2}{2\sigma_y^2} + \frac{h_s^2}{2\sigma_z^2}\right)\right] \quad \dots \text{Eq. 4.1.3}$$

where:

C_o = ground level concentration (g/m^3)
 C_{CWI} = cross-wind integrated concentration (g/m^3)

h_e = effective stack height (m)
 h_s = stack height (m)
 Q = SO₂ emission rate (g/s)
 σ_y = standard deviation of the horizontal plume spread (m)
 σ_z = standard deviation of the vertical plume spread (m)
 u = wind speed (m/s)
 x = downwind distance from source to receptor (m)
 y = crosswind distance from source to receptor (m)

The long-period average concentration model incorporates wind rose data, which gives the joint wind-speed and direction frequency distribution of the mean wind, shifts over time and gives a general indication of the meteorological features of that place. To obtain an estimate of the average concentration over a period that is very long compared with that over which the mean wind is computed, the integrated concentration formula is first multiplied by the frequency with which the wind blows toward a given sector and then divided by the width of that sector at the downwind distance of interest ($2\pi x/n$).

$$C = \left(\frac{2}{\pi}\right)^{1/2} \left(\frac{fQn}{2\pi\sigma_z ux}\right) \exp\left(-\frac{h_s^2}{2\sigma_z^2}\right) \quad \dots \text{Eq \# 4.1.4}$$

where:

C = concentration (g/m³)
 f = fraction of the time the wind blows into the sector
 h_s = stack height (m)
 n = number of wind rose sectors
 Q = monthly SO₂ emission rate (g/s)
 σ_z = standard deviation of the vertical plume spread (m)
 u = mean monthly wind speed in the mixed layer (m/s)
 x = distance from source to total sulphation station (m)

An equivalent expression forms the basis for the calculations by Meade and Pasquill (1958) of annual sulphur dioxide concentrations in the vicinity of Staythorpe Power station. These investigators compared the sulphation values derived from lead dioxide candles with predicted concentrations. They found good correspondence between the paired values depicted by a positive linear relationship and also found that the least squares regression equation's y -intercepts were in agreement with the seasonal

background values observed at Staythorpe before the power station began to operate.

The LTSAM model appears to be simple, appropriate for long-term averages, and is practical. It has few input variables that were available and is easily computed with basic computing software. However, with the exception of the one identified study (Meade and Pasquill, 1958), its reliability is not well documented. No other references to its use could be found. Thus, this model may be of questionable reliability or appropriateness.

For the LTSAM, the inputs (Q, f, h, n, u, x) were obtained from the following sources: gas plant files at AEP contained the monthly wind frequency and direction summary (which determined the number of sectors -8 or 16), the monthly sulphur dioxide emission rate, and the distance was determined by measuring the distance and direction from the site documentation maps. The stack height was obtained from the files obtained from the AEUB. Sigma z (σ_z) was calculated three different ways:

- Coefficients derived from Smith's correlations (Pasquill and Smith, 1983) were used:

$$\sigma_z = ax^b \quad \dots \text{Eq. 4.1.5}$$

where values for a and b are listed in Table 4.1.

- Briggs (1973) equation for each Pasquill stability class is given in Table 4.1.
- Weil and Brower (1984) define the stability classes A-D dispersion curves in terms of the wind speed and convective velocity to give the equation:

$$\sigma_z = \left[0.06^2 + (0.56w_c / u)^2 \right]^{0.5} x \quad \dots \text{Eq. 4.1.6}$$

Table 4.1. Coefficients and Formulas Used in Model Calculations

Stability Category	Power Law Plume Spreading Coefficients for σ_z						Wind Speed Power Exponent (p)	
	Smith (1983)				Briggs (1973)		(Irwin, 1979)	
	a		b		open-country conditions		$z_0 = 0.10\text{m}$	$z_0 = 1.0\text{m}$
		$z_0 = 0.10\text{m}$	$z_0 = 1.0\text{m}$	$z_0 = 0.10\text{m}$	$z_0 = 1.0\text{m}$		$z_0 = 0.10\text{m}$	$z_0 = 1.0\text{m}$
A	very unstable	0.28	0.61	0.90	0.83	0.2x	0.08	0.17
B	moderately unstable	0.23	0.54	0.85	0.77	0.12x	0.09	0.17
C	weakly unstable	0.22	0.53	0.80	0.72	$0.08x(1 + 0.0002x)^{-0.5}$	0.11	0.20
D	neutral	0.20	0.46	0.76	0.68	$0.06x(1 + 0.0015x)^{-0.5}$	0.16	0.27
E	moderately stable	0.15	0.35	0.73	0.65	$0.03x(1 + 0.0003x)^{-1}$	0.32	0.38
F	very stable	0.12	0.31	0.67	0.58	$0.016x(1 + 0.0003x)^{-1}$	0.54	0.61

* z_0 = surface roughness length

Since time-dependent stability class measurements were not available from the plant's meteorological data sets, the model calculations were simplified by assuming that a particular stability class predominates for most of the time. For the LTSAM, a stability class-dependent σ_z was required. Stability class D was assumed throughout, based on the most frequently observed stability class (approximately 54%) in Alberta as determined by the insolation method (STAR classification) (Angle and Sakiyama, 1991). When poor correlations were found with this approach, further comparisons of predicted concentrations and observed sulphation values were undertaken using the appropriate dispersion parameters for the stability classes A, B, and C. This was undertaken on the basis that during daytime, convective conditions predominate and that the PGT stability classification scheme has repeatedly been shown to underestimate the frequency of unstable cases.

Wind speed at anemometer height was converted to stack height wind speed by the power law formula:

$$u = u_{ref} (z / z_{ref})^p \quad \text{Eq. 4.1.7}$$

where:

- u = wind speed at stack height (h_s) or vertical height above ground (m/s)
- u_{ref} = wind speed at anemometer height (m/s)
- z = stack height (h_s) or vertical height above ground (m)
- z_{ref} = anemometer height above ground (m)

p = exponent dependent upon atmospheric stability and surface roughness (Table 4.1, Irwin, 1979)

4.1.3 Modified Climatological Model (MCM)

A climatological model, based on the Gaussian plume equation, which takes advantage of the repetition of similar meteorological and emission conditions at several different times by computing long-term concentration averages without performing an expensive hour-by-hour simulation is outlined by Zannetti (1990):

"The assumption is made that a source can operate in N_i different emission conditions and that the meteorology can be described by N_j meteorological classes. Then the general climatological model equation becomes:

$$C = \frac{\sum_{i=1}^{N_i} \sum_{j=1}^{N_j} f_{ij} Q_i \Psi_{ij}}{\sum_{i=1}^{N_i} \sum_{j=1}^{N_j} f_{ij}} \quad \dots \text{Eq. 4.1.8}$$

where:

C is the average concentration in the receptor (r) due to the source in (s) during the period under examination;

f_{ij} is the joint frequency of occurrence, during the same period, of the i -th emission conditions and the j -th meteorological condition;

Q_i is the pollutant emission rate during the i -th emission conditions;

$Q_i \Psi_{ij}$ is the steady-state equation (e.g., the Gaussian plume equation), which gives the concentration in r due to the emission in s with the i -th emission and the j -th meteorological scenarios (Ψ_{ij} is referred to as the 'kernel' of the concentration computation formula). If $N_i \times N_j$ is much smaller than the number of hours of the long-term period under investigation, Eq. 4.7 is computationally faster than the hour-by-hour simulation and, for most practical cases, almost as accurate. Note that the term Ψ_{ij} can be pre-computed for all i and j , thus allowing easy recalculations with different emissions Q_i and/or different meteorology f_{ij} .

The climatological model is generally applied with the following further assumptions:

- The Gaussian plume equation (Eq. 3.1) is used for computing the kernel Ψ_{ij}
- Q is constant (or depends only upon the meteorological condition j)
- The meteorological condition j is given by the combination of a wind direction class, j_1 , a windspeed class j_2 , and a stability class j_3 [i.e., f_{ij} becomes $f(j_1, j_2, j_3)$].
- Because of the high frequency of occurrence of wind blowing in each wind direction sector, a uniform crosswind horizontal concentration distribution is assumed within each downwind sector.
- Receptors are at ground level.

With the above assumptions, Eq. 4.7 becomes:

$$C = \sum_{j_1, j_2, j_3} f(j_1, j_2, j_3) Q(j_1, j_2, j_3) \psi(j_1, j_2, j_3) / \left(\sum_{j_1, j_2, j_3} f(j_1, j_2, j_3) \right) \quad \dots \text{Eq. 4.1.9}$$

where $\psi(j_1, j_2, j_3)$ is the uniform crosswind horizontal Gaussian kernel,

$$\psi(j_1, j_2, j_3) = \left(\frac{2}{\pi} \right)^{0.5} \frac{N_{wd}}{(2\pi\Delta_d)\sigma_z u} \exp \left[-\frac{1}{2} \left(\frac{z_s + \Delta h}{\sigma_z} \right)^2 \right] \quad \dots \text{Eq. 4.1.10}$$

Here,

N_{wd} is the number of wind direction sectors (i.e., $j_1 = 1, 2, \dots, N_{wd}$; generally $N_{wd} = 16$);

$\Delta_d(s, r, j_1)$ is the horizontal downwind distance, between the source and receptor;

$\sigma_z(\Delta_d, j_3)$ is the vertical plume sigma;

$\Delta_h(j_2, j_3)$ is the plume rise;

$u(j_2)$ is the wind speed;

z_s is the source height.

Equation 4.9 can be pre-computed for each j_1, j_2, j_3 , thus providing a fast computational algorithm for C . Clearly Eq. 4.9 must be applied only when the receptor r is downwind of the source s for the wind direction class j_2 (where downwind, in this case, means within a sector of $2\pi/N_{wd}$ angle in the horizontal); otherwise Ψ is equal to zero.

If the plume is uniformly mixed in the mixing layer, Equation 4.9 is further simplified as

$$\psi(j_1, j_2, j_3) = \frac{N_{wd}}{(2\pi\Delta_d)z_i u} \quad \dots \text{Eq. 4.1.11}$$

where

z_i is the mixing height."

The climatological model is modified and simplified further to incorporate the additional assumption that for convective conditions (those conditions under which the plume will most often and most likely encounter the ground level passive sampler), the meteorological conditions are adequately defined by the windspeed frequency and direction:

$$C = \frac{fQn}{2\pi z_i u x} \quad \dots \text{Eq. 4.1.12}$$

where:

C = concentration (g/m^3)

f = fraction of the time the wind blows into the sector
 n = number of wind rose sectors
 Q = monthly SO₂ emission rate (g/s)
 z = mean maximum monthly mixed layer height (m)
 u = mean monthly wind speed in the mixed layer (m/s)
 x = distance from source to total sulphation station (m)

This modified climatological model (MCM) (Eq. 4.12) appears to be simple, appropriate for long-term averages, and practical. Although Zannetti (1990) notes that "several authors have used the climatological Gaussian model successfully" and that "these long-term simulations generally provide better results than the short-term ones, due to error cancellation effects," only one study was located which evaluated the model. Tracy and Meyerhof (1987) compared the air concentrations of uranium-containing dust at eight sites within a 2 km radius around a uranium refinery at Port Hope on Lake Ontario with predictions from a generic version of the Climatological Dispersion Model. The emissions sources had low effective release heights in the range of 0.1 - 28 m. They used 10-year STAR data from a location 60 km away and found a linear relationship very near to a line of perfect fit between the measured and predicted values (slope, y-intercept and r not given). In this study, the unmodified Climatological Dispersion Model appeared to perform well. However the simplified version, as modified here, may still also be of questionable reliability.

The inputs to the MCM (Q, f, n, x) were the same used for the LTSAM. The mean maximum monthly mixing heights (z) for Edmonton, obtained from Portelli (1977) (Table 4.2), were used for all of the plant data sets.

Table 4.2. Monthly mean maximum afternoon mixing heights (meters above surface) at Edmonton (Stony Plain), Alberta for the four-year period between July 1965 and June 1969.

Month	Mean Maximum (Afternoon) Mixing Heights at Edmonton (Stony Plain) (m)
January	227
February	295
March	696
April	1578
May	2396
June	2185
July	1954
August	1563
September	1322
October	998
November	420
December	208

4.1.4 Convective Dispersion Model (CDM)

Venkatram (1980) and Venkatram and Vet (1981) described a convective dispersion model (CDM) for an elevated source in a convective boundary layer that incorporated some of the more recent understanding of dispersion in the mixed layer:

$$C = \frac{0.9Q}{w_c z x} \quad \dots \text{Eq. 4.1.13}$$

where:

- C = concentration (g/m^3)
- Q = monthly SO_2 emission rate (g/s)
- w_c = maximum convective velocity scale (m/s)
- x = distance from source to total sulphation station (m)
- z = mean maximum monthly mixed layer height (m)

This model differs from the others in that it incorporates a convective scaling parameter (w_c). The convective velocity scale is a value that incorporates the two variables known to be important for free convection: buoyancy flux at the surface and the mixed layer height. Because thermals rise until they hit the stable layer capping the mixed layer, their size scales to the height of the mixed layer. The buoyancy associated

with the strong heat flux into the air fuels the thermals and the magnitude of the vertical velocity fluctuations in thermals is on the same order as the convective velocity scale.

Deardorff (1970 a,b) first suggested the use of convective scaling for atmospheric applications when he found that it ordered velocity and temperature variances produced in the most convection-dominated runs of his numerical boundary-layer model. When the variances were non-dimensionalized with convective scaling parameters, they agreed well with aircraft turbulence measurements (Briggs, 1985). Deardorff and Willis (1974, 1976) performed a series of laboratory simulations of diffusion from continuous point sources in conditions corresponding to free convection and used scaling methods to make their results applicable to the atmosphere. They showed that the height of the mixed layer and the convective velocity scale are the ruling parameters for dispersion of pollutants emitted at heights much greater than the thickness of the shear-dominated surface layer. Hicks (1985) also concluded that the convective velocity scale (w_c) is the dominant scale characterizing the vertical dispersion under specific conditions, corresponding roughly to conditions that are more convective than Pasquill's C conditions (for mixing height values on the order of 1000 m.). Thus, use of the convective scaling parameter has no validity in neutral or stable boundary layers (Briggs, 1988).

In the upper part of the planetary boundary layer (when the height above ground is greater than one-tenth the inversion height or mixed layer depth), the turbulent velocities σ_u and σ_w (standard deviation of the horizontal and vertical wind velocity, respectively) are proportional to the convective velocity scale (w_c) (Venkatram, 1980):

$$w_c = \left(\frac{g}{T_0} H_0 z_i \right)^{1/3} \quad \dots \text{Eq. 4.1.14}$$

where:

- g is the acceleration due to gravity (9.8 m/s²)
- H_0 is the surface kinematic heat flux (K m/s)
- T_0 is the average temperature of the mixed layer (K)
- z_i is the mixed layer height (m)

Venkatram's model was chosen for several reasons. Mathematically, it is a

simple model. The data and parameters necessary for the model were available from the processing plants and the literature. It incorporates convective scaling parameters as suggested by the 1985 EPA-AMS workshop participants. It was tested on three sets of data (Dickerson and Morgantown power plants in Maryland and INCO's nickel smelter in Sudbury, Ontario) and the results were found to be "very encouraging" (Table 4.3) (Venkatram and Vet, 1981).

Table 4.3. Summary of Model Testing for the Dickerson, Morgantown and Sudbury Data Sets.

Data Set	No. of data points	% meeting factor-of-two criterion	Mean value and standard deviation of C(obs)/C(pred) ³	Linear regression observations ¹			Logarithmic regression observations ²		
				r ²	a	b	r ²	a	b
Dickerson	26	85	0.98 (0.34)	0.70	-0.15	0.98	0.74	0.9	1.00
Morgantown	22	86	1.20 (0.37)	0.65	18.86	0.87	0.80	2.21	0.84
Sudbury	25	80	1.02 (0.27)	0.53	9.95	1.00	0.60	0.89	1.02

¹ Linear regression equation: C(observed) = a + b C(predicted)

² Logarithmic regression equation: C(observed) = a[C(predicted)]^b

³ Filtered data set meeting the factor-of-two criterion used

The model is simple, requiring fewer input variables than any of the other models, is practicable, and is reliable for 1-hour average daytime concentration predictions. Although the model performed well against hourly sulphur dioxide concentrations, it was believed to be appropriate for predicting long-term averages because of typical plume behaviour during day and night. The convective state predominates during the day and the plume from an elevated stack would reach the ground to encounter the sampler, whereas during the night time, typically, the stable state would lead to the incinerator plume remaining aloft, travelling past the sampler undetected.

The inputs to the CDM (Q, z, x) were the same as for the MCM. A simplified practical method (Venkatram, 1978, 1980) for calculating the maximum daily convective velocity scale is as follows:

$$w_c = Bz \quad \dots \text{Eq. 4.1.15}$$

where:

$$B = \text{constant of } 1.07 \times 10^{-3} \text{ s}^{-1}$$

z = mean maximum monthly mixed layer height (m)

The constant, 1.07×10^{-3} , derived from the work of Venkatram (1980) (cited in Angle and Sakiyama, 1991, p 2-12) for northeastern Alberta in the months of May through September, was used for all months. This value differs slightly from a theoretical value of $1.12 \times 10^{-3} \text{ s}^{-1}$ and from a measured mean value of $1.18 \times 10^{-3} \text{ s}^{-1}$ (with a coefficient of variation of 0.23) derived from a 1973 Minnesota boundary layer field experiment (Venkatram, 1978, Kaimal et al., 1976).

The mean maximum monthly mixed layer height (z) for Edmonton, obtained from Portelli (1977), was used for all of the plant data sets (Table 4.2).

4.1.5 Mixed Layer Scaling Convective Model (Stull, 1995)

The mixed layer scaling model incorporates the key concepts revealed by the laboratory findings of Willis and Deardorff (1978) and the numerical predictions of Lamb (1978). That is that the dispersion and behavior of a near-surface plume release is distinct from the behavior of an elevated plume, rising first then levelling off, as compared to an elevated plume which descends first, rises some and then levels off (Figure 4.1). Scaling techniques (mathematical methods based on similarity theory that are used to non-dimensionalize other variables) were used to demonstrate that the results were consistent from widely different investigations.

The presence of updrafts and downdrafts partially account for the plume behavior. Release of material into the base of an updraft begins rising almost immediately whereas that released into downdrafts remains near the ground and moves horizontally. For elevated releases, the greater horizontal area coverage of downdrafts (and therefore a greater probability of a release into one) and the tendency to be long-lived, accounts for the plumes descent.

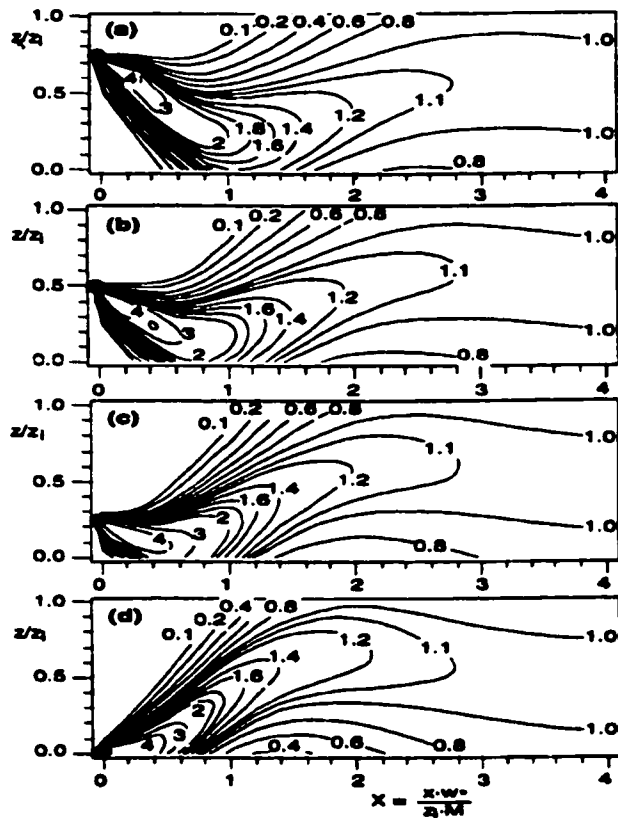


Figure 4.1. Isopleths of dimensionless crosswind-integrated concentration in a convective mixed layer. Dimensionless source heights (z/z_1) indicated by the black circle are as follows: (a) 0.75, (b) 0.5, (c) 0.25, (d) 0.025. (after Stull, 1995)

This model uses variables that are normalized by free convection scales. The relevant physical variables are:

- c = pollutant concentration
- c_y = cross-wind integrated concentration
- Q = pollutant emission rate (g/s)
- U = mean wind velocity (m/s)
- x = distance of a receptor downwind of the stack (m)
- z = height of a receptor above ground (m)
- z_{cl} = height of plume centerline (center of mass) above ground (m)
- z_s = stack-top height or source height (m)
- σ_y = lateral standard deviation of pollutant (m)
- σ_z = vertical standard deviation of pollutant (m)
- σ_x = vertical standard deviation of cross-wind integrated pollutant concentration (m).

The relevant mixed-layer scaling variables are:

z_i = depth of the convective mixed layer (m)
 w_* = Deardorff convective velocity (m/s)

The relevant dimensionless scales are:

$$C = \frac{cz_i^2 U}{Q} = \text{dimensionless concentration} \quad \text{Eq. 4.1.16}$$

$$C_y = \frac{c_y z_i U}{Q} = \text{dimensionless crosswind integrated concentration} \quad \text{Eq. 4.1.17}$$

$$X = \frac{xw_*}{z_i U} = \text{dimensionless downwind distance} \quad \text{Eq. 4.1.18}$$

$$Y = \frac{y}{z_i} = \text{dimensionless crosswind (lateral) distance of receptor from centerline} \quad \text{Eq. 4.1.19}$$

$$Z_{CL} = \frac{z_{CL}}{z_i} = \text{dimensionless plume centerline height} \quad \text{Eq. 4.1.20}$$

$$Z_s = \frac{z_s}{z_i} = \text{dimensionless source height} \quad \text{Eq. 4.1.21}$$

$$\sigma_{yd} = \frac{\sigma_y}{z_i} = \text{dimensionless lateral standard deviation} \quad \text{Eq. 4.1.22}$$

$$\sigma_{zdc} = \frac{\sigma_{zdc}}{z_i} = \text{dimensionless vertical standard deviation of crosswind-integrated concentration} \quad \text{Eq. 4.1.23}$$

The pollutant concentration downwind of a source during convective conditions is calculated in three-steps (adapted from Stull, 1995; p 317-320):

1) the plume centerline height is calculated as:

$$Z_{CL} \approx 0.5 + \frac{0.5}{1 + 0.5X^2} \cos \left[2\pi \frac{X}{\lambda} + \cos^{-1}(2Z_s - 1) \right] \quad \text{Eq. 4.1.24}$$

where λ is the dimensionless wavelength parameter = 4.

2) the crosswind integrated concentration is calculated using an algorithm which is calculated at equally spaced heights between the ground to the top of the mixed layer. A first guess of a dimensionless crosswind integrated concentration (C_y) as a function of dimensionless height Z is as follows:

$$C_y' = \exp \left[-0.5 \left(\frac{Z - Z_{CL}}{\sigma_{zdk}'} \right)^2 \right] \quad \text{Eq. 4.1.25}$$

where:

the prime indicates a first guess, and

$$\sigma_{zdk}' = aX \quad \text{Eq.4.1.26}$$

with $a \approx 0.25$.

The average over all the heights Z (between 0 and 1) is determined from:

$$\overline{C_y}' = \frac{1}{n} \sum_{k=1}^n C_y' \quad \text{Eq. 4.1.27}$$

where:

index k corresponds to height z .

The revised estimate for the dimensionless crosswind integrated concentration at any height is calculated:

$$C_y = \frac{C_y'}{\overline{C_y}'} \quad \text{Eq. 4.1.28}$$

3) the dimensionless concentration is calculated using:

$$C = \frac{C_y}{(2\pi)^{1/2} \sigma_{yjd}} \exp \left[-0.5 \left(\frac{Y}{\sigma_{yjd}} \right)^2 \right] \quad \text{Eq. 4.1.29}$$

where:

$$\sigma_{yjd} \approx bX \quad \text{Eq. 4.1.30}$$

and $b \approx 0.5$.

The pollutant concentration is then calculated by:

$$c = \frac{CQ}{z_i^2 U} \quad \text{Eq. 4.1.31}$$

The input variables used for this model (Q , u , z , x) were the same as for the LTSAM and for the CDM (w_s). The algorithm for the dimensionless crosswind integrated concentration was obtained in an Excel® spreadsheet format from R. Stull. This model's algorithms produce isopleths of dimensionless cross-wind integrated concentration that match the observations of Deardorff, Willis and Lamb better than most others (personal communication, R. Stull, 1998).

4.1.6 Exponential Decay Model

An exponential decay model, similar to the Potential Mapping (Pot Map) function

used in M. Scott's (1998) study to categorize exposures, was compared to adjusted and unadjusted sulphation values. To assess their correspondence with sulphation observations, the total mass of sulphur dioxide emitted from the processing plant's stack was calculated (with and without regard to wind direction frequency) as a function of the square of the sulphation station distance from the plant. Use of this function is based on an expected exponential decay relationship between the downwind ground level concentration and distance from the stack (see Figure 3.10).

4.2 Sour Gas Plant Data

Sour gas processing plants were selected using the following general criteria:

- presence of an on-site meteorological station for wind speed and direction measurements;
- a network of at least six total sulphation static samplers in the vicinity of the plant;
- a location relatively isolated from other adjacent oil and gas activities such as well-site flaring and minimally affected by regional air pollution sources such as urban centers or agriculture, and;
- a recent and complete data set.

Of the 201 licensed sour gas plants in Alberta, 11 plants met these criteria. All eleven processing plants had sulphur recovery facilities. No exclusion criteria were set to identify or screen out 'poor quality' data. However, in extracting the data from the files, an effort was made to obtain whatever quality control information was available on file. Information collected, although not consistently obtained from all plants were anemometer calibration reports, total sulphation analytical recovery reports, and manual stack sampling reports.

Monthly sulphur dioxide incinerator emissions, monthly total sulphation values, and monthly wind speed and direction frequency data was obtained from sour gas plant reports on file at the offices of Alberta Environmental Protection (AEP) and entered into Excel® spreadsheets. Each processing plant's monthly

incinerator stack emissions data (stack height, stack diameter, exit velocity, and exit temperature) was obtained from reports submitted to the Alberta Energy and Utilities Board (M. Scott, 1998). Due to the intermittent nature of flaring and the difficulty of identifying the time of flare activity with the wind conditions at the time, emissions from flare stacks were not added to the total stack emissions value.

Site documentation and maps showing the layout of the sulphation station network, in relation to the meteorology trailer and plant were also obtained from AEP. The distance and direction of each sulphation station from the processing plant, obtained directly from the site documentation maps, were used as inputs for each model.

In addition to the data sets obtained from AEP, an additional data set for Plant No. 14 (designated as 14a), was obtained from the West Whitecourt Study report (Legge, *et al.*, 1988) and examined for correlation between total sulphation and predicted concentrations. Plant emissions and sulphation data were available from the report for the period between 1967 and 1983, however wind speed and direction data was not available from the plant site. Instead, the 10-year average wind speed and direction frequency distribution from the adjacent airport (27 km away) was used as inputs for the models. The meteorology, sulphation station network, and emissions features for each plant are summarized in Table 4.4.

Table 4.4. Meteorology, Total Sulphation Station (TSS) Network and Sour Gas Processing Plants' Emissions Summary

Plant No.	SO ₂ Emission Rate (tonnes/mon) (SD)	Distance to airport with STAR data (km)	General Physical Features of Area	Monthly Wind Speed (km/h) (range)	Mean % Time Calm	No (%) of TSS in		Down-wind* Frequency (%)	Months of Complete Meteorological, Emissions and TSS Data
						Net-work	Down-wind* Sectors		
1	500 (51)	7	flat agriculture	15 (10-20)	<1	13	6 (46)	45 (28)	22 1/95 - 10/96
2	217 (78)	97	flatforest	5 (3-7)	5	20	5 (25)	57 (8)	43 3/93 - 9/96
3	516 (325)	128	mountain valley	14 (5-18)	<1	20	17 (85)	65 (58)	46 1/93 - 10/96
5	496 (75)	73	hilly, forest; adjacent lake, river	8 (5-8)	1	38	23 (61)	38 (38)	37 4/93 - 7/93; 1/94 - 9/96
6	1582 (282)	54	forest; adjacent river	7 (4-9)	1	26	11 (42)	62 (55)	55 1/93 - 7/93; 9, 11, 12/93; 7/94 - 9/96
7	115 (23)	42	flat; agriculture	13 (7-17)	<1	6	3 (50)	44 (26)	24 7/93 - 6/94; 7/95 - 6/96
8	227 (49)	58	flat; agriculture	12.5 (8-16)	<1	16	7 (44)	47 (47)	43 1/93 - 7/96
9	363 (65)	67	flat; agriculture	14 (10-18)	<1	20	12 (60)	50 (50)	29 1/93 - 1/95; 3/95 - 5/95
10	160 (30)	123	flat; forest; adjacent creek	5 (3-8)	18	8	1 (13)	51 (11)	61 1/93 - 6/93; 9/93 - 4/94; 7/94 - 9/96
11	106 (26)	115	flat; forest; adjacent river	10 (6-12)	<1	8	3 (38)	52 (16)	22 1/93 - 6/93; 6/94 - 7/95; 7/96 - 9/96
14	598 (108)	27	flat; forest	11 (5-13)	<1	25	4 (16)	78 (40)	25 Jan 95 - Sep 96
14a	1276 (895)	27	flat; forest	9 (6-13)	26	4	4 (100)	Nd	204 Jan 67 - Jan 83

*Downwind is defined as the 5 sectors in which the wind blows most of the time (the 5 most frequent sectors of the 16 sectors into which the wind blows)

Nd = not determined

SD = one standard deviation

TSS = total sulphation station

4.3. Total Sulphation Data

Monthly total sulphation values were obtained from the plant files at Alberta Environmental Protection and entered into Excel® spreadsheets. Values reported as less than the detection limit were entered as the detection limit value.

Total sulphation values were also adjusted for the influence of wind by applying a corrective formula derived from the work of Singh (1979). For both sulphation candles and plates, Singh compared model-predicted correlation factors, which calculated the mass transfer rate from the gas phase resistance, with experimentally derived values throughout the range of 0.3 to 8.4 m/s. The wind speed (u) and associated experimental correlation factors ($CF = \text{ppm}/(\text{mgSO}_3/\text{dm}^2/\text{day})$) were plotted for both candles and plate data sets and a curve-fitting program was run (SPSS®, 8.0) to obtain the constants b_0 and b_1 . A power law curve with the form:

$$CF = b_0 u^{b_1} \quad \dots \text{Eq. 4.3.1}$$

yielded r^2 of 0.999 for Singh's candle data set and the r^2 value was 1.000 for the Huey plate data set. The constants b_0 and b_1 for the candle data set were 0.0355 and -0.4145 and for the plate data set, the constants were 0.0391 and -0.4916, respectively. These constants were averaged because the type of sulphation device used by each plant was not indicated on the laboratory reports, yet were both devices were known to be in use. The constants were used as indicated in Eq. 4.3.2.

$$C = S(0.0373u^{-0.453})2620 \quad \dots \text{Eq. 4.3.2}$$

where,

$C = \text{SO}_2$ concentration, $\mu\text{g}/\text{m}^3$

$S =$ monthly total sulphation value, $\text{mgSO}_3/100\text{cm}^2/\text{day}$

$u =$ average monthly wind speed (m/s) travelling to the sector where the sulphation static sampler is located.

The average monthly wind speed measured at the plant's monitoring trailer (usually 10 m.) was converted to the wind speed at the height of the sulphation station (usually 1.5 m) by the log wind profile power law (Eq. 4.1.6 and Table 4.1). Because site-specific stability estimates were not available, stability class D was assumed for the full exposure period.

In addition to adjusting for the horizontal wind speed, the total sulphation values

were also adjusted for vertical velocity effects. This was done on the basis that both buoyancy- (responsible primarily for vertical motions) and shear-induced motions (responsible principally for horizontal air movement) often exist together but their interactive effects are poorly understood (Kanna and Brasseur, 1998). It is known that even in calm mean winds, convective circulations can create random perturbation gusts near the surface and that the horizontal gust speed in the surface layer is usually assumed to be of the order of the convective velocity scale (w_c) Stull (1994). Panofsky et al. (1977) and Kaimal (1978) found that large-scale downdrafts create horizontal sweeping motions, producing horizontal fluctuations that scale with the mixed layer scales of w_c and z_m , thereby strongly influencing the near-ground horizontal velocity field. Thus, the vertical movement of air in daytime was thought to influence the sulphation values and a correction for its influence was included.

Effects of downdrafts in the convective layer that may affect the total sulphation values were adjusted for by replacing the wind speed (u) with the estimated convective velocity scaling parameter (w_c), obtained from Eq. 4.14 into Eq 4.15.

4.4 Plume Rise Considerations

Plume rise estimates for each plant's incinerator stack at each static sampler location were made using the methods of Briggs (1969, 1975). The Briggs' formulations (1969) suggest that the buoyancy (Eq. 4.4.3), momentum (Eq. 4.4.2) and sum of cubes formula (Eq. 4.4.1) can be used for estimating transitional rise in all cases (Wilson, 1994):

$$\Delta H = (\Delta h_m^3 + \Delta h_b^3)^{1/3} \quad \text{Eq. 4.4.1}$$

where:

$$\Delta h_m = 1.6 \frac{F_m^{1/3}}{U_c^{2/3}} x^{1/3} \quad \text{Eq. 4.4.2}$$

$$\Delta h_b = 1.6 \frac{F_b^{1/3}}{U_c} x^{2/3} \quad \text{Eq. 4.4.3}$$

$$F_m = \frac{\rho_s}{\rho_a} v_s^2 r_s^2 \quad \text{Eq. 4.4.4}$$

$$F_b = g \left(\frac{\rho_a - \rho_s}{\rho_a} \right) v_s r_s^2 \quad \text{Eq. 4.4.5}$$

where:

- ΔH = total plume rise (m)
- Δh_m = plume rise from momentum (m)
- Δh_b = plume rise from buoyancy (m)
- ρ_s = plume density (g/m^3)
- ρ_a = air density (g/m^3)
- v_s = stack exit velocity (m/sec)
- r_s = stack exit radius (m)
- g = acceleration due to gravity (9.807 m/sec^2)
- U_c = wind speed in boundary layer (m/s)

4.5 Statistical Analysis

The correlation coefficients were calculated using the non-parametric statistical test, the Spearman's rank correlation (SPSS® Version 8.0). This test statistic (r_s) squares the difference between the rank of an object in one sample and its rank in the second sample. It does not assume a Gaussian distribution and is insensitive to extreme values. A perfect positive correlation ($r_s = +1$) means that the two samples rank each object identically, while a perfect negative correlation ($r_s = -1$) means that the ranks of the two samples have an exactly inverse relationship and values between -1 and +1 denote less than perfect correlation (Harnett, 1982).

Seasonally based ensemble averages for modelled and measured total sulphation values were obtained by: i) partitioning the area surrounding the plant into 2 kilometer concentric rings; ii) dividing the rings into 16 sector quadrants corresponding to the 16 wind directions; and iii) averaging the total sulphation values, the wind speed - adjusted total sulphation values, the convective velocity - adjusted total sulphation values and the model-predicted concentrations for all of the stations located within that quadrant for seasonal groupings of winter (December, January, February), spring (March, April, May), summer (June, July, August) and fall (September, October, November).

Chapter 5.0 Results, Discussion, Conclusions and Recommendations

In this chapter, the various model predictions are presented and compared to the sulphation values, the wind-speed-adjusted total sulphation values and the convective velocity scaling parameter-adjusted values. Between-model and between-processing plant comparisons are made. The results are discussed in the context of topography, general and seasonal meteorology of the processing plant sites. Implications of the findings for air pollution epidemiologists are also discussed.

5.1 Model-Predictions and Total Sulphation Comparisons

The scatter plots of the wind speed-corrected total sulphation and the model-predicted sulphur dioxide concentration for all of the sulphation stations in the entire sulphation network around each gas plant are given in Figures 5.1 through 5.12. The Spearman Rank correlation coefficients (r_s) for the model-predicted concentrations and the adjusted and unadjusted sulphation values are given in Table 5.1 and Figure 5.25. Before discussing the results, an overview of the processing plants' estimated overall plume rise, general meteorology and topography of the area surrounding the plants is given.

5.2. Processing Plant Characteristics

5.2.1 Plume Rise

Buoyant hot plumes may or may not rise to substantial heights depending upon atmospheric conditions. Strong inversions with large potential temperature gradients greatly reduce plume rise. A plume may completely penetrate a ground-based inversion layer, which may then block dispersion of pollutants back to the ground. The plume may also partially penetrate an elevated inversion layer or a thick ground-based inversion layer or the plume may become completely embedded within an elevated inversion which can lead to a fumigation event when the inversion layer is broken up by rapid solar heating. In Alberta at 05:00 hrs, ground-based inversions are present more than 80% of the time in summer and 60% of the time in

winter; at 17:00 hrs, inversions occur less than 5% in spring and summer and about 40% in winter (Angle and Sakiyama, 1991, p 1-33). Thus, plumes which do not penetrate the inversion layer may spread slightly horizontally and minimally vertically in the stable layer and, upon breakup, produce increased ground level concentrations. Also, emissions released at ground level will remain near the ground under stable conditions to also produce high concentrations.

The stack height and estimated mean plume rise (with respect to the sulphation station location) for each processing plant is presented in Table 5.2. The estimated average plume rise for each plant varies widely. The largest, about 500 to 700 m. (Plants 5, 6, and 10), indicate that for much of the time the emissions at these plants would reach the top of the mixed layer during spring and fall and less frequently in the summer. Under these circumstances, the pollutants may or may not reach the ground for some distance. Because Gaussian models do not incorporate algorithms for plume rise to the top of the atmospheric boundary layer, the model predictions at these plants are expected to correspond poorly with observations.

Table 5.2. Estimated Plume Rise For Sour Gas Processing Plants' Incinerator Stacks

Plant	Stack Height (m)	ΔH Mean Estimated Plume Rise (meters) (SD)
1	122	225 (120)
2	76.2	432 (216)
3	91.5	170 (120)
5	70.1	644 (356)
6	141.7	763 (816)
7	68.8	98 (26)
8	73.5	252 (155)
9	91.4	186 (138)
10	30.5	529 (182)
11	114.3	121 (56)
14	122	291 (223)

5.2.2 Wind Speed

The Gaussian plume dispersion model is unable to deal with low wind conditions. Pollutant concentration predictions around plants with low average wind

speeds are therefore expected to be poor. Four plants stand out from the group. Plants 2, 5, 6, and 10 recorded monthly average wind speeds in the range of 5 - 8 k/h and calm periods 5, 1,1, and 18% of the time, respectively. In contrast, the remaining plants recorded average wind speeds in the range of 10 - 15 k/h and calm periods less than 1 percent of the time.

5.2.3 Sulphation Station Network Density and Layout

The location of the static samplers relative to the predominant wind direction should not, in theory, affect the correspondence between the prediction and observations since these relations are incorporated within the models. However, placement of the samplers at sites in directions in which the wind blows infrequently, will give many low sulphation values and values below the sulphation method's analytical detection limit. The range of observed (and predicted) values will then likely be narrow and, at the same time the scatter of the values wide due to the analytical method's poor accuracy at the lower end of its analytical range. Under these circumstances, any correspondence will be less apparent than if a wide range of observations was included and the accuracy of the analytical method was high. Only three plants (Nos. 3, 6, 9) have at least 50% of the sulphation stations in a principally downwind direction (defined as the five most frequent sectors into which the wind blows). Three plants stand out as having few stations located downwind: No. 2 with 8%, No. 10 with 11%, and No. 11 with 16% of the stations in the network in the principal downwind directions (Table 4.4). Plant No. 2 also has the highest proportion (52%) of sample results reported as less than the detection limit.

5.2.4 Topography

The models used in this study assume that the turbulence statistics do not vary in horizontal space within the boundary layer. For processing plants located in flat terrain with small or moderate landscape heterogeneities, this assumption will most likely be fulfilled. Any local heat flux perturbation such as rivers or lakes, which affect the mean circulation, can affect dispersion. It is therefore expected that the best

correspondence between predicted and observed concentrations would most likely be found most often where the terrain is flat with small and few topographic elements such as valleys, hills, water bodies or ridges. With the exception of three processing plants (No. 3 is located in a mountain valley, No. 6 is located beside a river, and No. 5 is located beside a lake), the remaining processing plants are located in "mostly" flat agricultural or forested areas. Yet Plants 1, 7, 8, and 9 are also located on the edge of the foothills and as such, may be influenced by both chinooks and mountain winds. Mountain winds produce a re-circulation zone extending to 150 km east of the Rocky Mountains and up to 1 km above ground. They are characterized by a marked diurnal variation - southeast in the afternoon and northwest at night (Angle and Sakiyama, 1991, p 1-95). These same four plants are also located within the 100 - 200 km chinook band along the eastern slopes of the Rocky Mountains. Chinooks are warm, dry, gusty winds from the mountains accompanied by rapid temperature changes. They are accompanied by regions of high turbulence (which may produce a type of fumigation event), a circular region of reverse flow, or a rotor, further east on the prairie, and formation of intense inversions. The average frequency of chinook occurrence in Calgary, based on five years of data, was 17.8 events per month (with a range of 2 to 29) for the period of October to March, and an average of 13.5 days per month (range 2 - 20). Chinook layers have been observed 2.7% of the time in November, 17.1% of the time in December, and 3.3% of the time in February (Angle and Sakiyama, 1991, 1-97). It is unlikely that the requirement of a horizontally homogenous atmosphere will be fulfilled due to the combined presence of these topographic features and the frequency of the meteorological phenomenon near these plants. Thus, correspondence between model predictions and observations is expected to be less than ideal for these processing plants.

In summary, taking the meteorological, topographical and plant plume rise estimates into consideration, it is anticipated that Plant Nos. 2, 5, 6, and 10 would give the poorest correspondence between the model predictions and the total sulphation values because of their: relatively high plume rise (Plant Nos. 5, 6, and 10); low average wind speed (2, 5, 6, and 10); and low proportion of downwind

samplers (2, 10, and 11). Also, as Plant No.3 is located in mountainous terrain and 1, 7, 8, and 9 are situated where mountain wind systems may significantly influence dispersion, the only plant that is expected to provide the best site conditions for comparing modelled to measured concentrations is Plant No. 14.

5.3 Between-Model Comparisons

Even though seasonally grouped or ensemble averages were compared, it is known that model-predicted ensemble averages can deviate substantially from observations, which represent members of the ensemble, and the deviation will occur even if the model can predict the 'true' ensemble average. Therefore, a correlation analysis is not a foolproof method of evaluating a model's performance especially if the variance of the observations is comparable to the expected variance between measurements and model predictions, which are not unusual situations in air pollution modelling (Venkatram, 1981). Further, because neither the static sulphation sampler values nor the plume dispersion models are gold standards (the most accurate and reproducible quantification methods available), only general comparisons can be made between them (van Dop, 1993).

For the paired variables and ensemble averages, the correlation coefficients (r_s) varied widely, between -0.5 to +0.9, across all of the plant data sets. With the exception of the ISCLT3, where the correspondence between ensemble averages tended to worsen when compared to the single point estimates of total sulphation and wind-speed adjusted total sulphation, the r_s for the seasonally grouped ensemble averages for the remaining models were only slightly improved. The correlation coefficients tended to improve mostly between the ensemble averaged convective velocity adjusted total sulphation and the CDM and MCM models and tended to worsen mostly between the convective velocity adjusted total sulphation and the ISCLT3 model. These combinations gave the poorest and the best overall correspondence across all of the plant data sets: the poorest correlation coefficients were found with the ISCLT3 while the best were found with the CDM and MCM.

Neither the MLSCM nor the simple exponential decay model (simulating the

Potential Mapping function) appeared to provide significant improvement in correspondence compared to the other models. The Pot Map model corresponded best to the same three plants which gave the best model correspondence overall (Nos. 3, 10, 14a), indicating further that topographic features and the receptor locations play a key role in the relationship.

Only one sour gas plant's data set (No. 3) consistently gave positive correlation coefficients (in the range of 0.3 to 0.7), for all of the model-predicted (with the exception of the ISCLT3) and measured and adjusted total sulphation values. This processing plant is located in a mountain valley. This geographical feature is believed to contribute to greater pollutant accumulation because mountain valley walls produce wind channelling through the valley and also confine horizontal dispersion producing a greater likelihood for encounter with the sulphation device.

5.3.1. ISCLT3

No statistically significant positive correlation coefficients were found with the ISCLT3 model for any of the plant data sets, and surprisingly, some small statistically significant negative correlation coefficients were found. The poorest correspondence was found at all of the plants with the convective velocity corrected sulphation values.

The low and negative r_c values found in this study are consistent the findings of Smith (1984) however are inconsistent with the findings of Al-Khayat *et. al.* (1992). In Smith's review of several Gaussian dispersion models performance (1984), correlation coefficients ranging between -0.12 and +0.14 were reported, whereas Al-Khayat *et. al.* (1992), using the ISCLT3 'standard' model at a site in England found a correlation of 0.72.

In all of the plant data sets, the ISCLT3 model under-predicts the monthly concentration as indicated by the clustering of data points below the line of unity (Figures 5.1(f) - 5.27(f)), which are consistent with the findings of Al-Khayat *et. al.* (1992). They found that the ISCLT3 under-predicts actual monthly average concentrations overall by 3-fold. The under-predictions were greatest in the spring

and summer (March through August) ranging from 3.3-fold to 7.1-fold. During fall and winter (September through February), under-predictions ranged from 1.2- to 4.4-fold. The good correspondence may be due to several factors: use of meteorological data from a nearby airport (15 km away); use of Pasquill Gifford stability class scheme, which was originally derived from data collected at England; and use of a wide range of concentrations covering several orders of magnitude observed at one site only 0.95 km from the plant. It is known that the Pearson Product Moment correlation test statistic is sensitive to the range of concentrations covered (Westgard, 1973).

A possible explanation for the poor correlation coefficients found in this study is use of off-site meteorological data (wind speed, direction and stability class frequencies) from airports that are between 7 km and 128 km away. However, since the predictions for processing plants which were near to adjacent airport STAR data (Plants 1 and 14, 7 and 27 km away, respectively) corresponded poorly to sulphation values and to the adjusted sulphation values (r , between -0.05 and -0.34), this explanation can be eliminated. Thus, other explanations for the poor correspondence are considered. They include the known limitations of Gaussian plume dispersion modelling and dispersion parameter selection. All of these limitations are all believed to contribute to the errors: the invalid assumptions of atmospheric homogeneity; constant wind speed, and Gaussian distribution in the vertical direction; use of dispersion parameters that are biased towards neutral stability when unstable conditions are prevalent (Weil, 1988a; Erbrink, 1991); and the invalid assumption that the errors in short term sub-models going into longer term averages will more or less cancel each other (Benarie, 1987a, b).

5.3.2. Long Term Sector Average Model (LTSAM)

Compared to the ISCLT3 model, moderately improved correlation coefficients were found for 9 of the 12 plant data sets with the LTSAM when convective conditions were assumed (Stability Class A) for all time. Only slightly improved correlation coefficients were found for 6 of the 12 plant data sets when neutral

conditions (Stability Class D) were assumed. For five of the twelve plant data sets (Nos. 1, 2, 11, 14, 14a), the correspondence improved when convective conditions were assumed to predominate as compared to the assumption that neutral conditions predominate. The correlation coefficients showed no change for the remaining seven plant data sets (Nos. 3, 5, 6, 7, 8, 9, 10). The improved correlation coefficients found with the assumption of convective conditions (Stability Class A) is consistent with the findings of Erbink (1991) and suggest that the convective conditions may occur more frequently than the PGT scheme indicates.

Use of Weil and Brower's vertical dispersion parameter in the LTSAM model improved the r , for the paired point estimates slightly as compared with the Smith or Briggs Stability Class A dispersion parameters. A slightly greater improvement, although not consistent across the plants, was found with the seasonal ensemble averages.

5.3.3. Convective Dispersion Model (CDM) and the Modified Climatological Model (MCM)

For both the CDM and MCM models, a well-mixed atmospheric boundary layer is assumed. The models are considered together here. Correspondence between measured total sulphation values and model predictions varied widely between the plant data sets, with r , ranging between 0.05 and 0.70 (Table 5.1). Five of the plant data sets (Nos. 1, 3, 7, 14, and 14a) gave positive correlation coefficients ranging between 0.4 and 0.6. Correspondence between measured total sulphation values and predictions for the remaining plants was low.

The correspondence improved for all the plant data sets when the total sulphation values were adjusted for wind effects using the convective velocity scaling parameter. Recall that the adjustment was made on the basis of the following rationale. During free convection, which occurs under conditions of light to calm winds when the surface temperature is warmer than the air temperature, buoyant thermals transport heat, moisture, and momentum from the surface upward into the boundary layer (Stull, 1994). It is expected that these conditions occur most

frequently during the daytime in summer, less frequently in spring and fall, and little or not at all under snow-covered winter conditions. Buoyancy-induced motions tend to form concentrated regions of high magnitude positive vertical velocity fluctuations in the updrafts with broad regions of weaker negative vertical velocity fluctuations in downdrafts (Wyngaard, 1985; Khanna and Brasseur, 1998). The turbulent fluctuations of vertical velocity both within and outside of the thermals may themselves be larger than the mean thermal updraft velocity (Lenschow and Stephens, 1980). These regions of upward- and downward-moving air, which extend throughout the boundary layer depth maintain a strong vertical coherence, strongly influencing the near-ground horizontal velocity field (Khanna and Brasseur, 1998). In an evaluation of ground-surface heat flux patchiness on CBL development using large eddy simulation, Avissar and Schmidt (1998) found that the total kinetic energy is maximal near ground level and near the top of the CBL. Recall that the turbulence kinetic energy per unit mass of air (TKE) gives an overall measure of turbulence intensity and is proportional to the summed velocity fluctuation variances (Stull, 1995). These vertical and horizontal motions tend to scale with the mixed layer scales, the convective velocity parameter (w_*) and the mixed layer height (z_i). (Khanna and Brasseur, 1998; Panofsky *et al.*, 1977; Kaimal, 1978). Businger and Oncley (1990) have suggested that the mass flux velocity is proportional to the standard deviation of the vertical velocity fluctuations. The sulphation value can be considered a type of flux measurement, representing the transfer of a quantity of sulphur-containing compounds onto a surface area over a period of time. The mass transfer of gaseous sulphur compounds to the sulphation device is limited by gas phase resistance (Singh, 1979) primarily through the molecular diffusivity parameter. Yet turbulence is several orders of magnitude more effective at transporting quantities than is molecular diffusivity (Stull, 1988). An increase in turbulence of 10% was enough to decrease boundary layer resistance by 22% in one study which measured the resistance to evaporation from wet paper cylinders as a function of turbulent intensity (Nobel, 1974). Finally, Singh (1979) noted that the gas phase resistance model underestimated the sulphation rate by approximately two-fold at low

wind velocities (in the range of 0.18 m/s where the accuracy of the hot wire anemometer was in question). Taken together, these findings suggest that use of the convective velocity scaling parameter, which scales with the velocity fluctuations, may be justified to adjust for effects of vertical air movement on the sulphation device.

Correcting the total sulphation for vertical velocity effects gave clearly improved correlation coefficients, compared to the sulphation and the wind-speed adjusted sulphation value, for all the plant data sets for both models. Ensemble averaged values for almost all of the Plants (exceptions are Plant No. 6 and 9) gave correlation coefficients in the range of 0.5 - 0.7 (Table 5.1). For most of the plants' scatterplots, there is generally a linear relationship between the CDM- and MCM-model predicted concentrations and the convective velocity adjusted sulphation value (Figures 5.13 through 5.24).

Plant Nos. 2 and 3 display an aggregation of data points at low concentration. These clusters represent sulphation values at the detection limit and the corresponding model predictions for periods that the plants were shut down. During plant shutdown periods, the emission rates (Q) were set at arbitrary low values so that predicted concentrations could be calculated.

For all of the plant scatter-plots, however, there is a wide spread of data points which at best covers a range of about 10 to 100-fold around the line of best fit, indicating large random errors. This wide scatter is consistent with Draxler's (1987) Washington tracer study. When the measured and predicted 8-hr average concentrations at three sites 14-40 km away were paired in space and time, the scatter ranged over two orders of magnitude. This wide spread illustrates the stochastic variability associated with the atmosphere that Wyngaard (1988) and others have referred to.

5.4. Comparisons of Sulphation Values, Wind Speed-Adjusted- and Convective Velocity Adjusted Values

An adjustment of the total sulphation values for the effects of wind was

undertaken based on the work of Singh (1979) and Sickles and Richie (1984). This was done with the concern that incorporating similar values in each of the variables violates the assumptions of independence, which could lead to artificially elevated correlation coefficients. This may occur by incorporating the wind speed value in both the dependent variable (the model prediction), and the independent (wind speed adjusted sulphation value) variable. It was expected that if an artefactual increase were to occur that it would show up as a consistent increase in the r_s , relative to the correlation with the uncorrected total sulphation value, across all of the plant data sets. A consistent increase in the correlation coefficient was not seen using the wind-speed adjusted sulphation values across all of the plants. This observation reduces the concern for producing falsely increased correspondence with use of the wind speed to correct the total sulphation value. However, lack of an increased correspondence may be because the wind speed is not a major contributor to the models' predictive power. This suggestion is consistent with Venkatram's CDM, which omits wind speed altogether.

The same concern is warranted with the use of the convective velocity scaling parameter to correct the total sulphation values. It is derived from the mean monthly mixing height (z), which is also found in the MCM and twice in the CDM model (in the derivation of w_c and as z). In contrast, there were clear improvements in the correlation coefficients across all the plant data sets for the CDM and MCM models using the convective velocity corrected sulphation value. After adjusting the sulphation values for the estimated convective velocity, a vertical velocity value derived from the mean maximum mixed layer height, the correlation coefficients for the CDM, MCM, LTSAM with Weil and Brower's vertical dispersion parameter, for all of the plants, improved. The correlation improved for the MLSCM for Plants 1, 2, 5, 6, 8, 10, and 14. The best correlation coefficients obtained with the CDM and MCM models, in the range of 0.5 - 0.7, are close to Venkatram's (1988) and Wyngaard's (1989) estimate of the best that can be expected for prediction, because of an "irreducible uncertainty caused by the stochastic nature of the atmosphere."

The CDM and MCM models are believed to provide better correspondence

between predicted and observed values than the LTSAM or the ISCLT3 model for several reasons. First, the models both assume that the convective boundary layer is well mixed, which has been shown to be mostly correct by consistent daytime vertical profiles of temperature, wind speed, water vapor and pollutant concentration above the surface layer (Stull, 1988). Second, the assumption that the convective state contributes most to the sulphation value is believed to be reasonable due to the behavior of daytime air motion. Solar heating of the ground produces rising thermals which will bring the plume (mixed with ambient air if caught in an updraft or not mixed if caught in a downdraft) to the ground to encounter the sulphation apparatus. During the night, due to the stable layers that are formed, the plume emanating from the stack remains aloft and is not expected to or rarely will encounter the sulphation apparatus. The impact of ground level or fugitive emissions however cannot be ruled out. They are likely to remain at ground level to encounter the sulphation device during this period also. Third, for the ISCLT3, use of meteorological data derived from airports that are some distance away from the processing plants, that are perhaps not representative of the plant site, is expected to introduce additional errors. Yet, even for plants that were close to airports (Nos. 1 and 14), the correspondence was poor. The wind speed and direction data were obtained at the plant-site for the LTSAM, CDM and MCM models, minimizing although not necessarily eliminating the potential for introducing errors by using meteorological data from nearby stations. Complete anemometer calibration reports were located in the files for only 6 of the 11 plants and not all of the reports indicated full functional status.

Overall, the correlation coefficients obtained with the MCM and CDM models are also much improved as compared to those found in the literature, with those obtained with the EPA-endorsed model (ISCLT3), and also approach what has been suggested to be a limit for predictability. The possibility that the improved correspondence may be due to the artefact of using the mixing height in both the independent and dependent variables however cannot be ruled out. Further work should be undertaken to explore this relationship using independent measures of concentration and mixing height.

5.5 Ensemble Average Correspondence

To minimize the scatter known to be associated with measurements, and allow more reliable model comparisons, ensemble averages were calculated based on distance, direction and seasonal groupings of the data. Averaging in this fashion is expected to improve the correspondence between the models' predictions and observations, or at least assist in the identification of the better-performing models. The correlation coefficients were calculated for seasonally grouped data for each plant data set. Ensemble averages were derived from the grouping of all of the sulphation stations within a 2-kilometer radial quadrant and compared with the mean of the model predictions for those locations within that radial quadrant. The Spearman rank correlation coefficients for each season and each plant are presented in Figures 5.26 (a) through (k).

Correspondence between the ISCLT3 model and the sulphation values tended to worsen overall whereas they tended to improve slightly for the remaining models. The convection-based models (CDM, MCM, LTSAM with Stability Class A vertical dispersion parameter), as expected, generally gave higher correlation coefficients for spring, summer and fall periods, however Plants 6, 7, 8 and 9 are exceptions.

5.6 Identification of Other Sources of Errors

To evaluate the contribution of possible errors within the sulphation data sets, attempts were made to gather quality control documentation for the total sulphation method from the analytical laboratories. The method's accuracy is not equivalent throughout its analytical range. Between-run and within-lab accuracy for the total sulphation method is reported to be in the range of 25% at the low end of the analytical range and in the range of 6% in the middle to high end of the analytical range (Singh, 1979). This variation is quite small relative to the variation in wind speed and direction measurements. Further, each plant's sulphation analysis was performed by one analytical laboratory. Given these considerations, the laboratory results are believed to be reliable and any analytical errors are believed to contribute

minimally to the observed overall poor correlation. However, because a 1995 round robin study indicated a wide range of values in an inter-laboratory recovery evaluation of spiked samples (personal communication, H. Bertram, 1997), analytical errors cannot be ruled out.

5.7 Implications of Dispersion Modelling for Exposure Assessment Purposes in Air Pollution Epidemiology

Plume dispersion models are known to provide poor predictions for the three dimensions of concentration, space and time (Wilson and Arulanandam, 1996). However, for this study, it was anticipated that, with longer averaging times, large data sets and comparison with seasonally grouped averages, a model's ability to predict concentrations in both space and time might prove to be adequate for chronic exposure assessment in epidemiological applications. Use of an exposure indicator that correlates well with and corresponds perfectly to the true value is ideal. For measures less than ideal, compensation can be made by increasing sample size, by repeating the measurements, by incorporating different measures of the same variable, or by mathematical correction of measurement error (Rosner *et. al.*, 1990)

The various modelling approaches, as they have been applied in this study, overall, corresponded poorly and inconsistently with both ensemble-averaged- total sulphation values (which would be expected to reduce the variance in the point data) and with the single point measures of sulphation and wind speed adjusted sulphation values. However, the consistency of the scatter-plot patterns for a single plant across models suggests that the general features of the site itself is a more important aspect with regard to correspondence between model predictions and observations.

Adjusting the total sulphation values for the effects of the vertical velocity induced by free convection improved the correspondence for the LTSAM with the Weil and Brower vertical dispersion parameter, the MCM, and the CDM.

Comparisons of the ISCLT3 Gaussian plume model predictions with total sulphation values, wind speed adjusted values, or convective velocity adjusted values showed no or negative correlation at all of the plants. These findings raise the

question of whether Gaussian plume dispersion models in general, and in particular, the ISCLT3 model, should be recommended for use in assessment of long term exposure.

The correspondence between the MCM, CDM predictions and the total sulphation values was good (r , approximately or greater than 0.5) for four plants, Nos. 1, 3, 7, and 14. The r , is deemed 'good' in the context of the statements made by Wyngaard (1988b) and Venkatram (1988b). That is, even though model performance has improved with incorporation of variables that more accurately represent atmospheric behavior, there usually remains a good deal of scatter between model predictions and observations and the scatter represents an irreducible uncertainty caused by the stochastic nature of the atmosphere.

The remaining processing plants' poor correspondence between model predictions and observations may be partially explained by their location (in complex topography or nearness to the Rocky Mountains), their average plume rise, the overall meteorology of the surrounding area (low average wind speeds), or the inadequate distribution of sulphation samplers. Thus, after eliminating the plants expected to have poor correspondence, the plant expected to have the best correspondence based on its location and meteorology (No. 14) was found to have the best prediction-observation correspondence. Good correspondence between the model predictions and observations for some of the plant sites is encouraging and suggests that the use of models in epidemiological studies may be undertaken with some confidence. However, given that the correspondence was consistently good at only two out of eleven plants suggests that their use should be restricted to sites that have flat topography, are without influence of larger wind systems, and are in areas where average wind speeds are moderate (not low).

The air pollution epidemiologist still encounters the problem of the wide scatter found in any series of point estimates even for sites that meet these criteria. While sample sizes can be increased to account for a desired level of accuracy and a desired detectable difference level, the effects of the large random error inherent in the model predictions reduces the investigator's ability to discern small differences

between study groups. The net effect of using of a mediocre or poor exposure indicator or one that has low correspondence with the true exposure, is to underestimate the true relative risk by a significant margin. For example, when the true relative risk is 5.0, use of an exposure indicator that is correlated with the true value by 0.5, reduces the measured relative risk to 1.4 - 2.0 depending upon the method of calculation (De Klerk *et.al.*, 1989; Rosner *et. al.*, 1990). Further, even when the sample size is increased to compensate for misclassification errors, the effects estimate is progressively biased toward the null (Walker and Blettner, 1985). Thus, a relationship, if present between the exposure and outcome, may go unrecognized, undetected or underestimated when one truly exists. As such, these circumstances, pose significant challenges and dilemmas for the design and interpretation of air pollution epidemiological studies.

5.8 Conclusions and Recommendations

While the aim of an air dispersion model is to estimate pollutant concentrations in space and time as a function of the emissions, meteorological and geophysical conditions, in their actual application, performance varies widely. Many are capable of predicting peak concentrations without regard to location or time, however few are able to accurately predict all three dimensions. Correspondence improves with predictions of longer-term averages (daily, monthly, or seasonal), in urban settings and in flat terrain, with use of convective scaling parameters and wind fluctuation measurements for deriving estimates of horizontal and vertical dispersion.

For epidemiological studies, efforts should be undertaken to ensure that the chosen model produces predictions corresponding to measurements at the location of interest. Yet, the assessment of model accuracy is made very difficult by the natural atmospheric variability or as Scorer described 'the unending succession of different cases' such that model errors cannot be easily distinguished from the inherent atmospheric variability. The wide scatter between measured and observed values found in this study and in the literature not only makes model evaluation difficult, it also suggests that there is a limit to model predictability due to the inherent stochastic

nature of the atmosphere. This wide scatter of paired data points somewhat limits the use of models for epidemiological purposes.

Overall, the correspondence between the total sulphation values and the wind speed adjusted total sulphation values and model predictions was consistently poor (ISCLT3) to inconsistently fair (all other models). Simple dispersion models, such as the Modified Climatological Model and Convective Dispersion Model which incorporate assumptions of complete mixing in the convective boundary layer provided the best correspondence overall. They predicted concentrations for monthly averages that are positively correlated in time and space with the total sulphation values. These models also corresponded well with the convective velocity-corrected monthly sulphation values for all of the plants. A positive linear correspondence was found for all of the plant data sets, suggesting that use of the CDM or the MCM model is valid in a variety of settings. The correspondence occurs for conditions of flat terrain, moderate wind speeds, and is unaffected by mountain wind systems. Thus, they may be used to categorize exposures with more confidence than the ISCLT3 or any of the comparison models. The correspondence between the MCM- and CDM-predicted sulphur dioxide concentrations and convective velocity corrected sulphation values were much improved compared to the ISCLT3. This finding suggests that the US EPA recommendations for use of the ISCLT3 model for exposure assessment purposes should be revisited.

The epidemiologist using dispersion models for categorization purposes, however, must not only compensate for the large random error that is inherent in the model predictions and in any air measurement series but also prior to use, ensure the model is capable of producing predictions which correspond to actual observations. Because the ISCLT3 dispersion model and the Potential Mapping model used in Scott's (1998) cattle study corresponded poorly to the sulphation values and to the adjusted sulphation values, the first and main recommendation is to repeat the analysis using either the MCM or CDM described here. These models are shown to provide significantly better correspondence under a variety of topographical conditions, indicating that they are capable of providing more reliable exposure

estimates as compared to the ISCLT3 or Potential Mapping models.

Finally, this study has identified some of the many problems facing air pollution epidemiologists attempting to design a study to explore causal relationships. Among the many difficulties, the major issues are shortages of: validated air sampling and analytical methods for use in remote environments; inter-laboratory quality control programs; dispersion model performance evaluations; meteorological measurements that are reliable and representative of sites of interest; and information on the wide variety of chemical agents and sources in the ambient environment. Efforts should be undertaken to address these deficiencies.

Figure 5.1. Plant # 1 – Scatter Plots of Wind-Speed Corrected Total Sulphation ($\mu\text{g}/\text{m}^3$) (x-axis) and Model-Predicted SO_2 Concentrations ($\mu\text{g}/\text{m}^3$) (y-axis); (a) CDM; (b) MCM; (c) LTSAM - Weil and Brower σ_2 ; (d) LTSAM -Smith Stability Class A σ_2 ; (e) MLSCM; (f) ISCLT3; the solid line indicates the line of best fit.

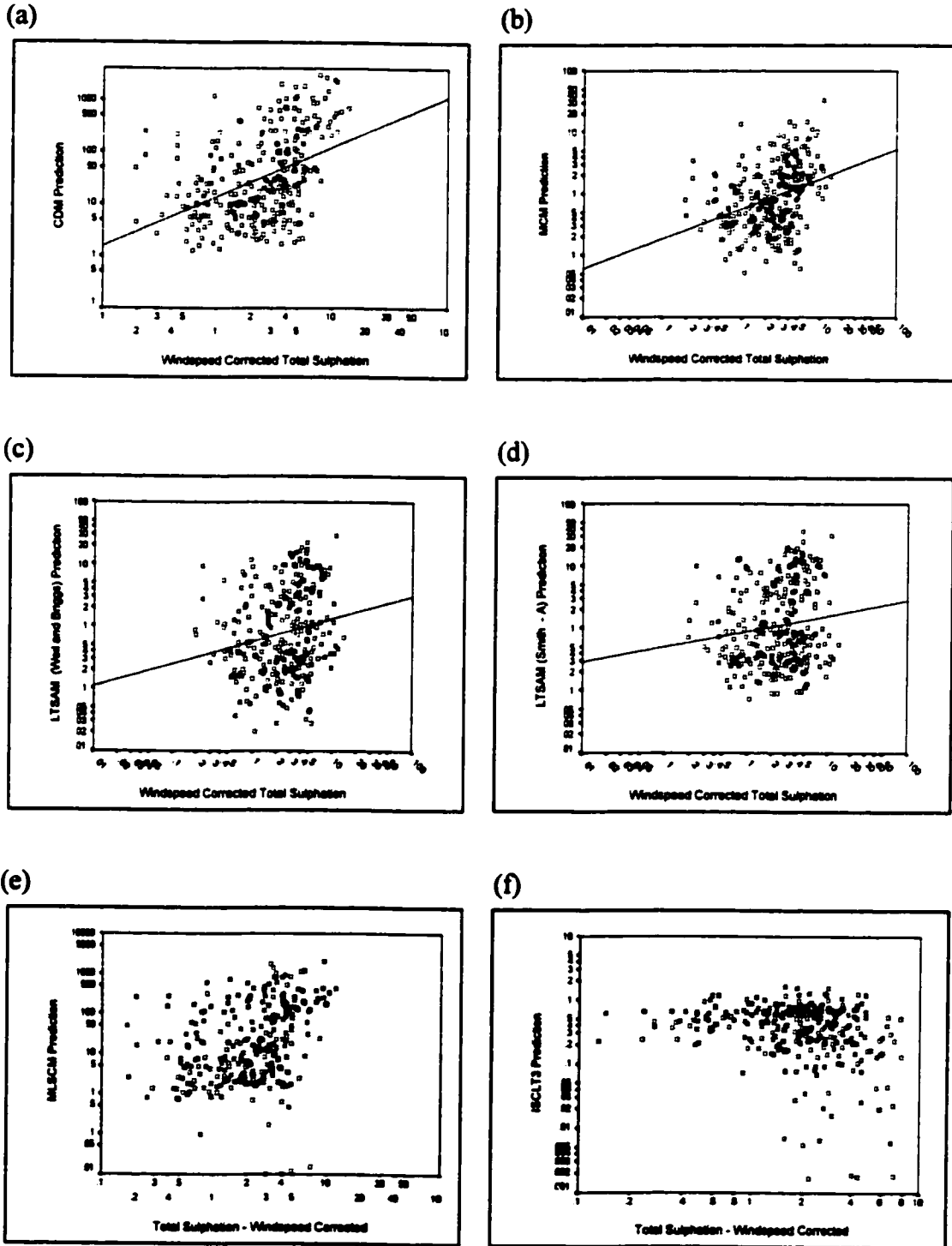


Figure 5.2. Plant # 2 - Scatter Plots of Wind-Speed Corrected Total Sulphation ($\mu\text{g}/\text{m}^3$) (x-axis) and Model-Predicted SO_2 Concentrations ($\mu\text{g}/\text{m}^3$) (y-axis); (a) CDM; (b) MCM; (c) LTSAM- Weil and Brower σ_z ; (d) LTSAM - Smith Stability Class A σ_z ; (e) MLSCM; (f) ISCLT3.

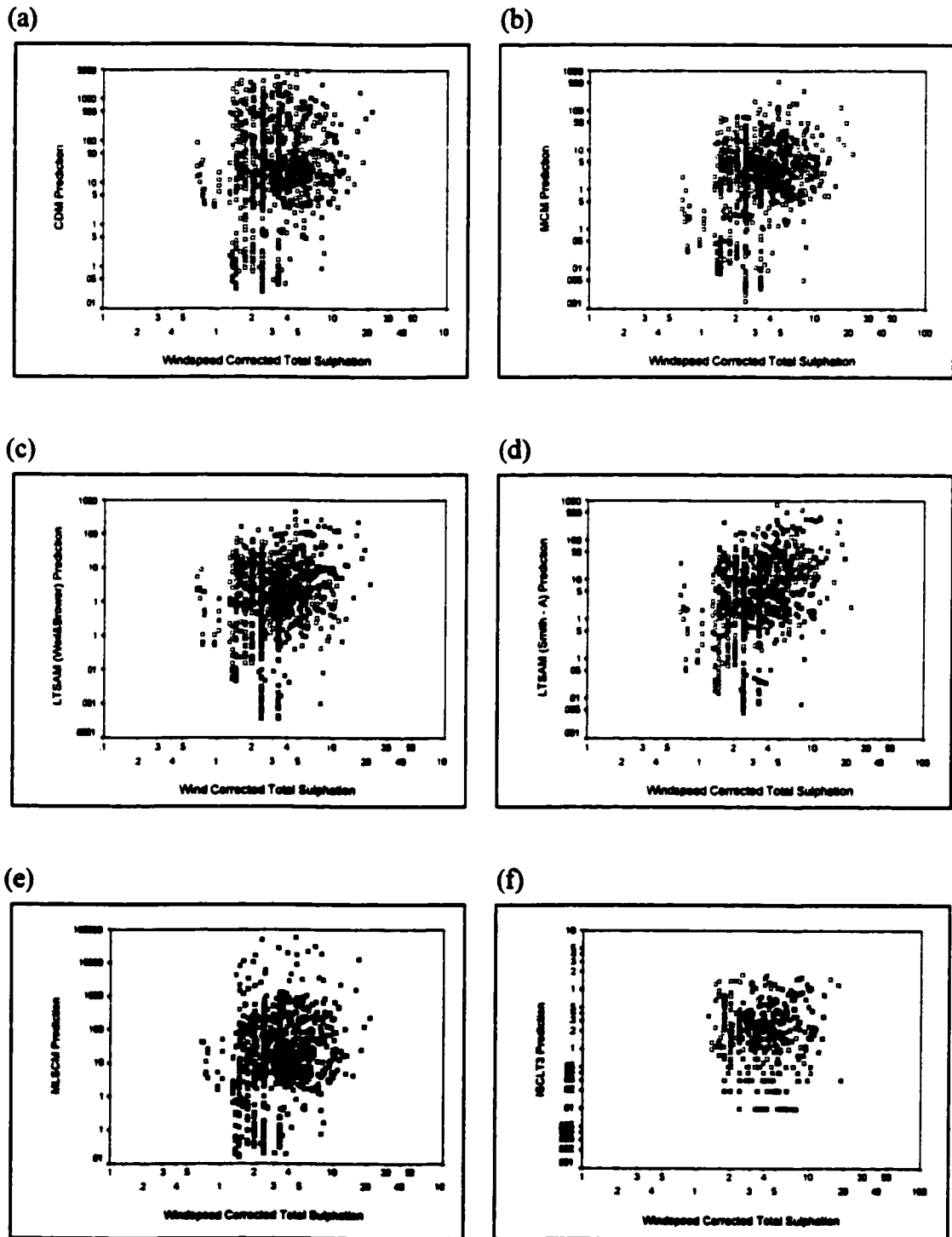


Figure 5.3. Plant # 3 – Scatter Plots of Wind Speed Corrected Total Sulphation ($\mu\text{g}/\text{m}^3$) (x-axis) and Model-Predicted SO_2 Concentrations ($\mu\text{g}/\text{m}^3$)(y-axis); (a) CDM; (b) MCM; (c) LTSAM - Weil and Brower σ_z ; (d) LTSAM - Smith Stability Class A σ_z ; (e) MLSCM ; (f) ISCLT3; the solid line indicates the line of best-fit.

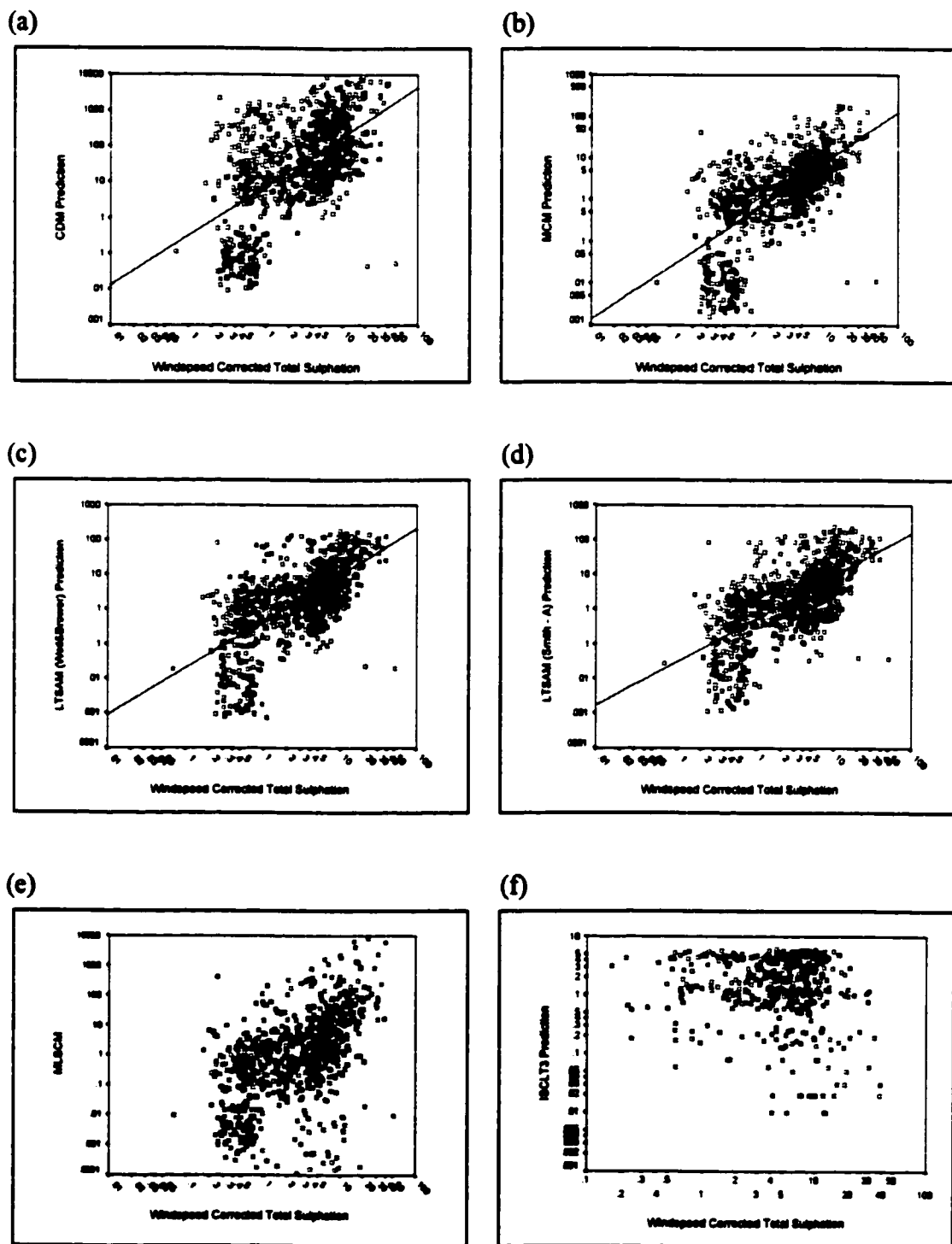


Figure 5.4. Plant # 5 - Scatter Plots of Wind Speed Corrected Total Sulphation ($\mu\text{g}/\text{m}^3$) and Model-Predicted SO_2 Concentrations ($\mu\text{g}/\text{m}^3$) (a) CDM; (b) MCM; (c) LTSAM with Weil and Brower σ_z ; (d) LTSAM with Smith Stability Class A σ_z ; (e) MLSCM; (f) ISCLT3.

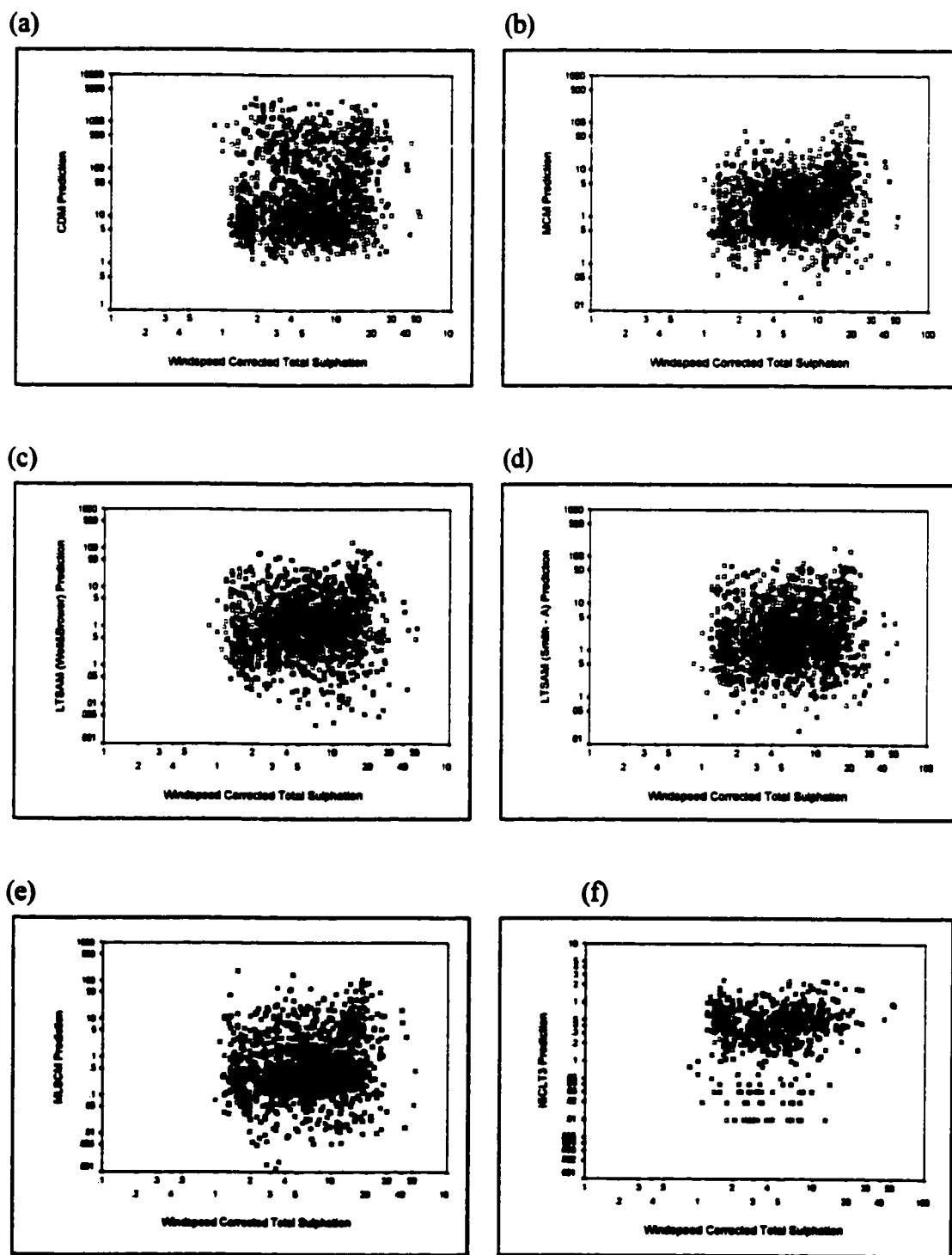


Figure 5.5. Plant # 6 - Scatter Plots of Wind Speed Corrected Total Sulphation ($\mu\text{g}/\text{m}^3$) (x-axis) and Model-Predicted SO_2 Concentrations ($\mu\text{g}/\text{m}^3$) (y-axis); (a) CDM; (b) MCM; (c) LTSAM with Weil and Brower σ_z ; (d) LTSAM with Smith Stability Class A σ_z ; (e) MLSCM; (f) ISCLT3.

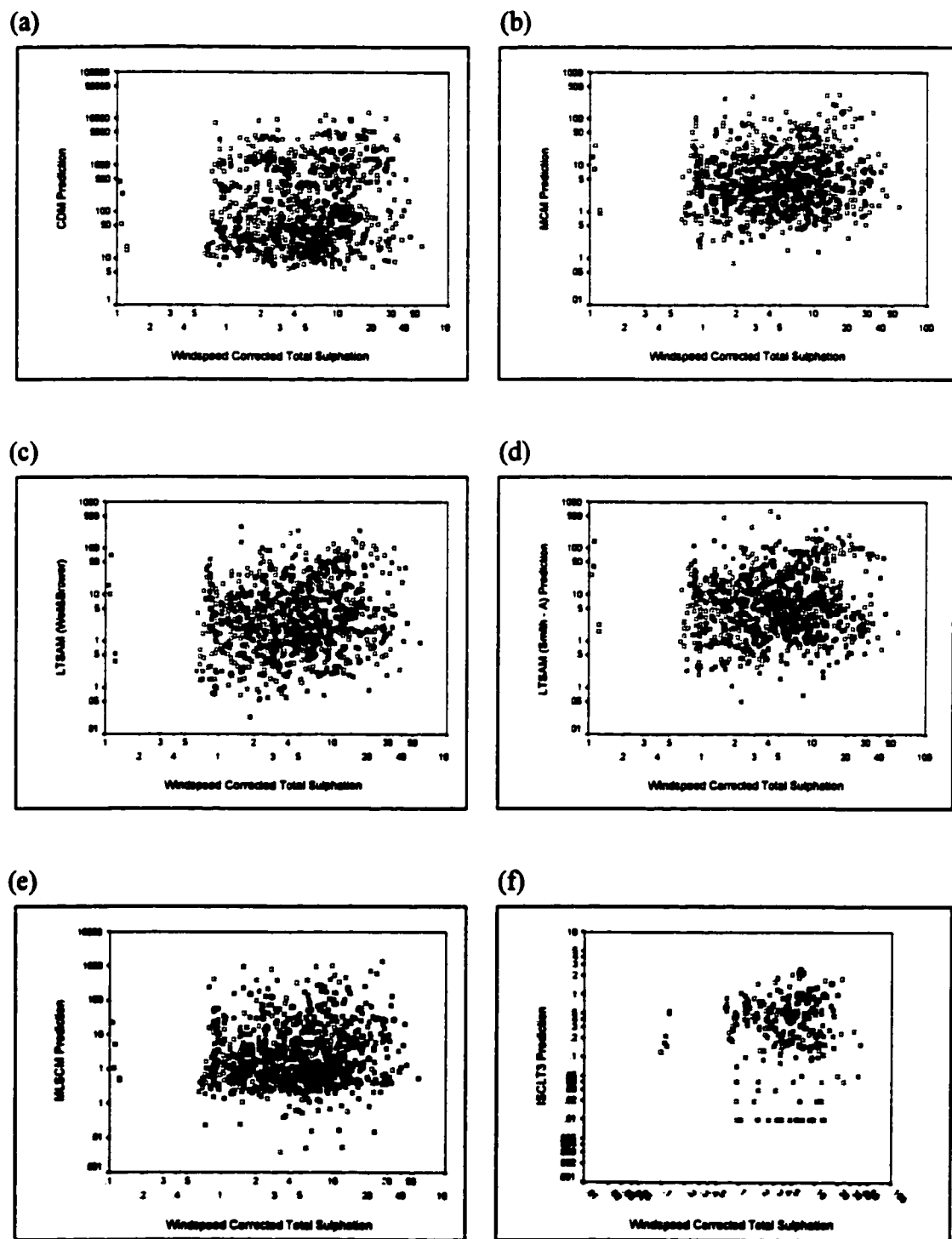


Figure 5.6. Plant # 7 – Scatter Plots of Wind Speed Corrected Total Sulphation ($\mu\text{g}/\text{m}^3$) (x-axis) and Model-Predicted SO_2 Concentrations ($\mu\text{g}/\text{m}^3$) (y-axis); (a) CDM; (b) MCM; (c) LTSAM with Weil and Brower σ_z ; (d) LTSAM with Smith Stability Class A σ_z ; (e) MLSCM; (f) ISCLT3; the solid line indicates the line of best-fit.

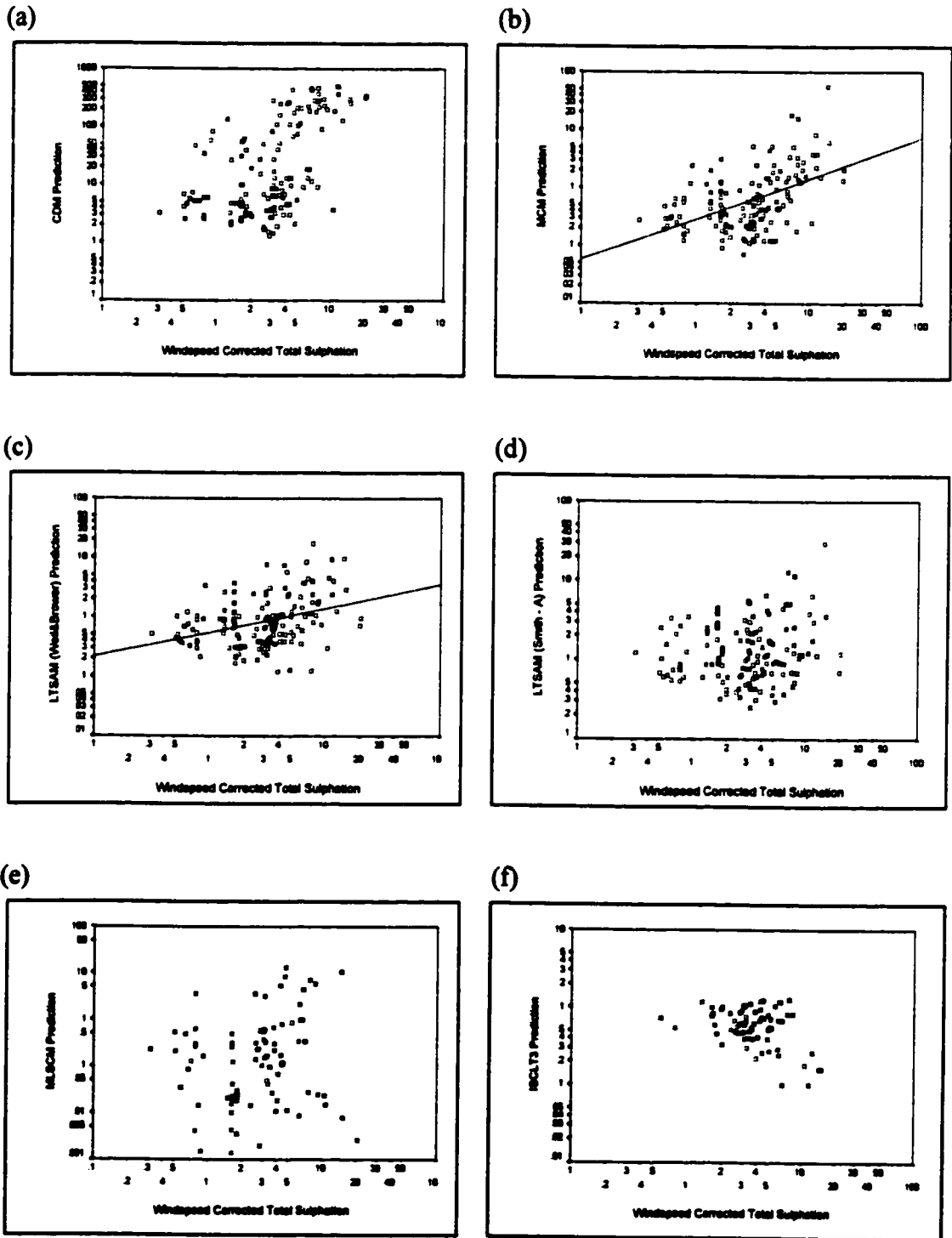


Figure 5.7. Plant # 8 – Scatter Plots of Wind Speed Corrected Total Sulphation ($\mu\text{g}/\text{m}^3$) (x-axis) and Model-Predicted SO_2 Concentrations ($\mu\text{g}/\text{m}^3$) (y-axis); (a) CDM; (b) MCM; (c) LTSAM with Weil and Brower σ_z ; (d) LTSAM with Smith Stability Class A σ_z ; (e) MLSCM; (f) ISCLT3.

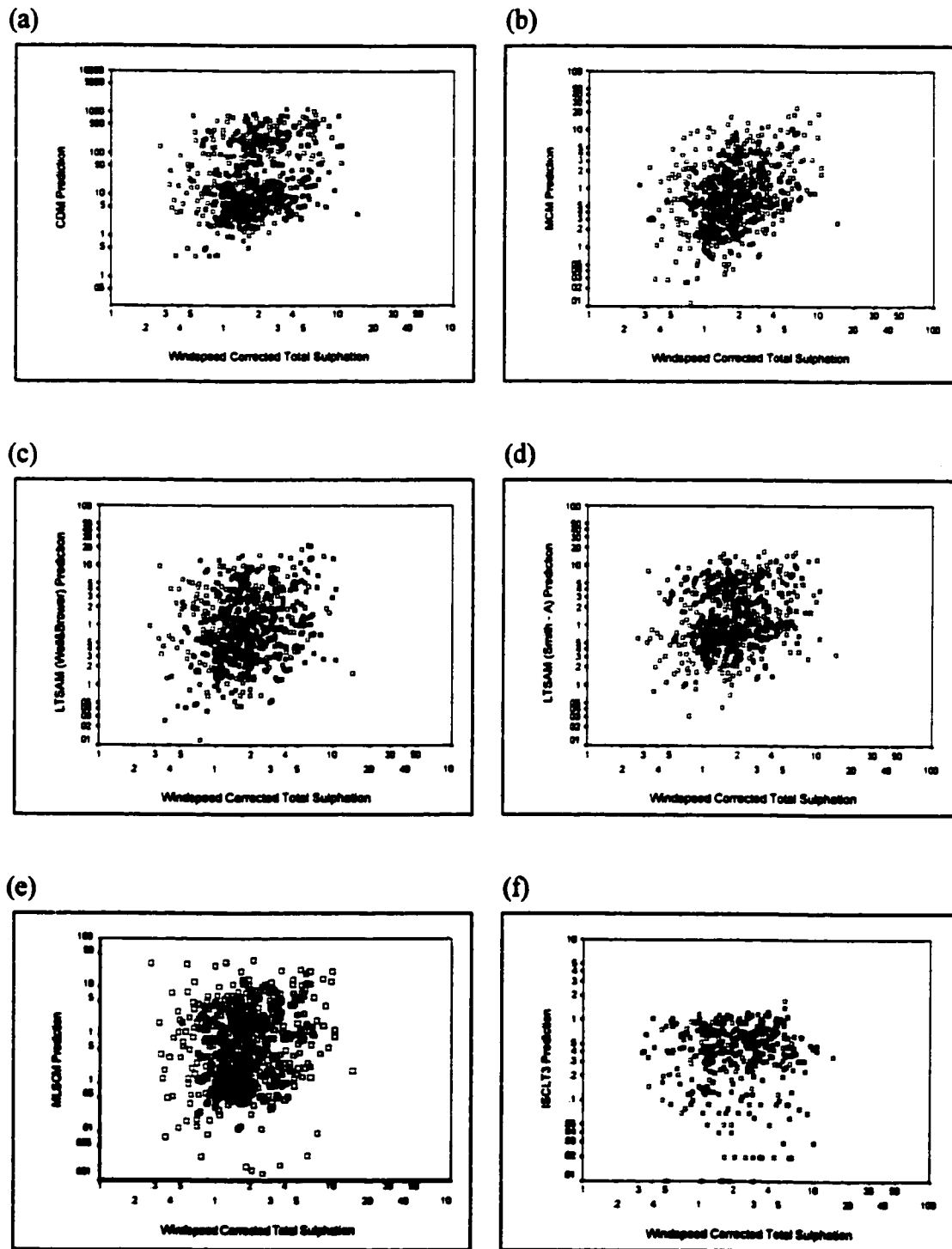


Figure 5.8. Plant # 9 – Scatter Plots of Wind Speed Corrected Total Sulphation ($\mu\text{g}/\text{m}^3$) (x-axis) and Model-Predicted SO_2 Concentrations ($\mu\text{g}/\text{m}^3$) (y-axis); (a) CDM; (b) MCM; (c) LTSAM with Weil and Brower σ_z ; (d) LTSAM with Smith Stability Class A σ_z ; (e) MLSCM; (f) ISCLT3.

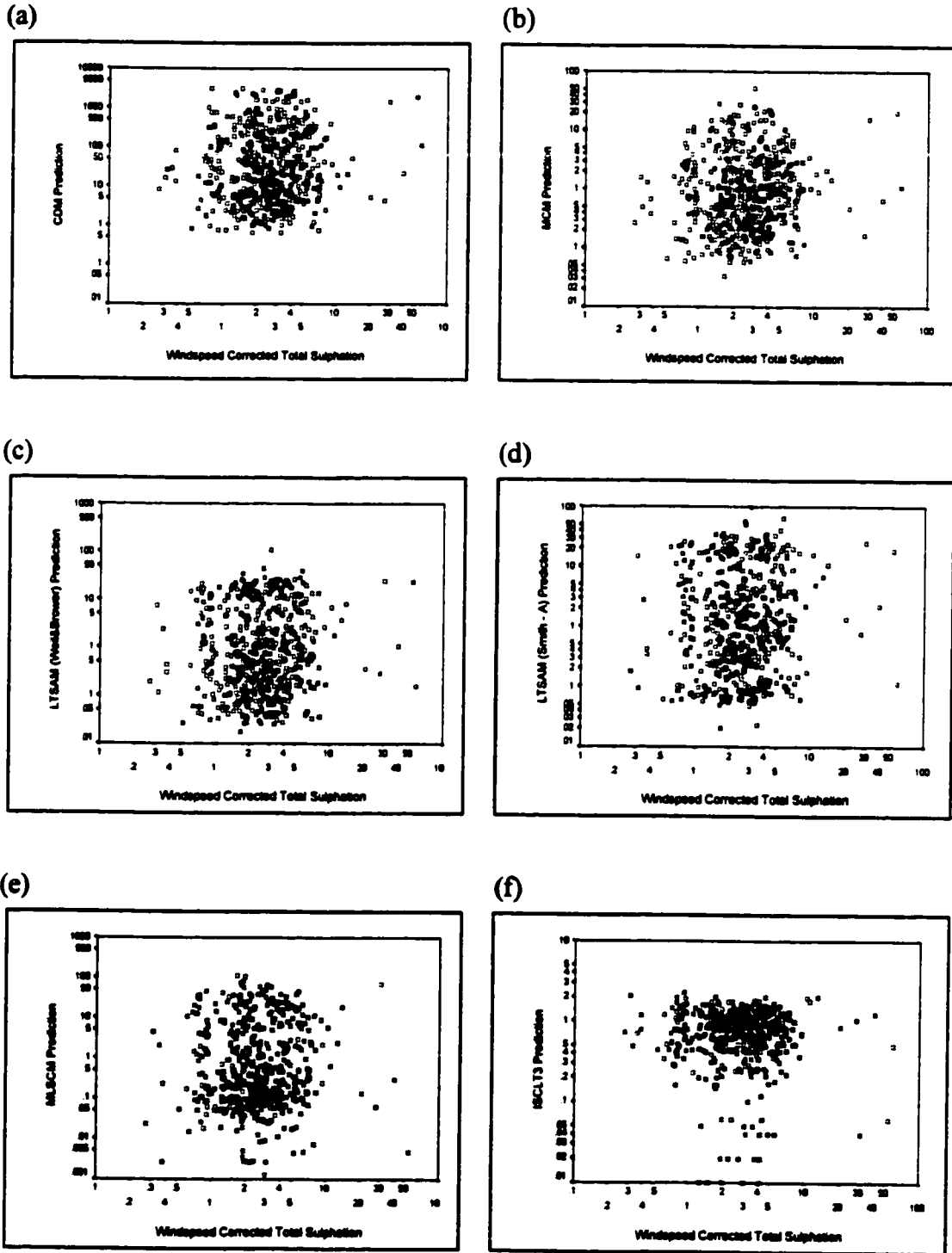


Figure 5.9. Plant # 10 – Scatter Plots of Wind Speed Corrected Total Sulphation ($\mu\text{g}/\text{m}^3$) (x-axis) and Model-Predicted SO_2 Concentrations ($\mu\text{g}/\text{m}^3$) (y-axis); (a) CDM; (b) MCM; (c) LTSAM with Weil and Brower σ_z ; (d) LTSAM with Smith Stability Class A σ_z ; (e) MLSCM; (f) ISCLT3; the solid line indicates the line of best-fit.

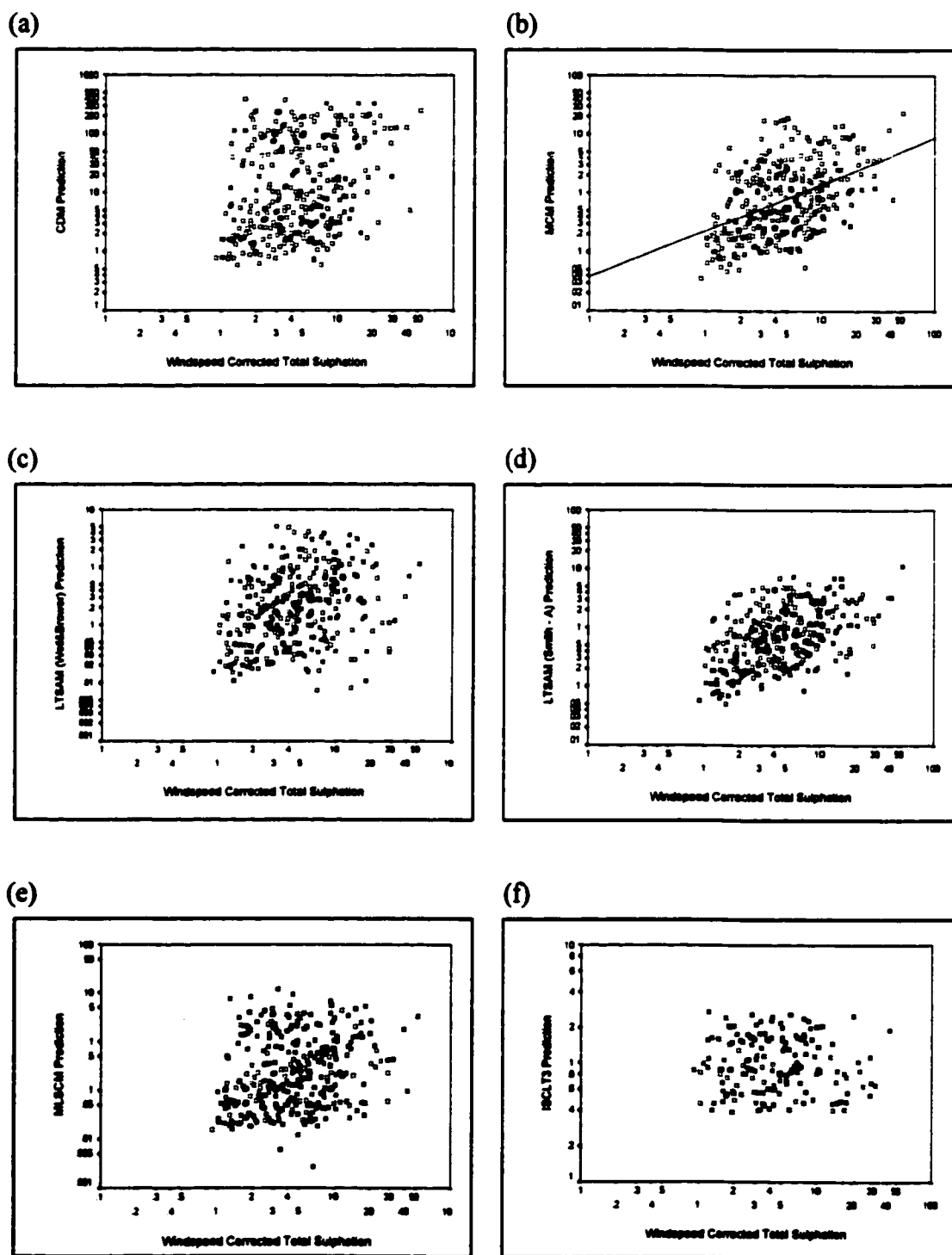


Figure 5.10. Plant # 11 – Scatter Plots of Wind Speed Corrected Total Sulphation ($\mu\text{g}/\text{m}^3$) (x-axis) and Model-Predicted SO_2 Concentrations ($\mu\text{g}/\text{m}^3$) (y-axis); (a) CDM; (b) MCM; (c) LTSAM with Weil and Brower σ_z ; (d) LTSAM with Smith Stability Class A σ_z ; (e) MLSCM; (f) ISCLT3.

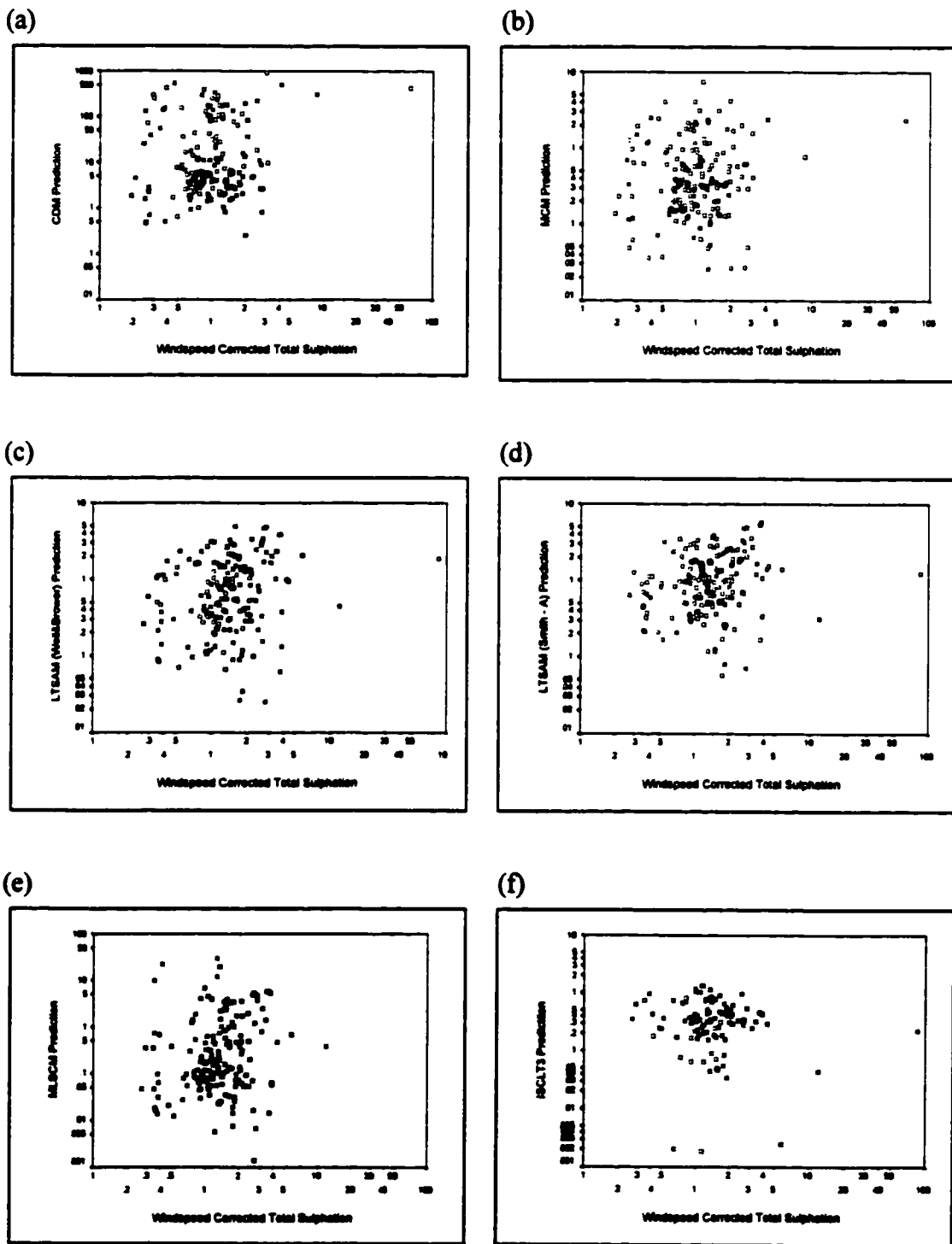


Figure 5.11. Plant # 14 – Scatter Plots of Wind Speed Corrected Total Sulphation ($\mu\text{g}/\text{m}^3$) (x-axis) and Model-Predicted SO_2 Concentrations ($\mu\text{g}/\text{m}^3$) (y-axis); (a) CDM; (b) MCM; (c) LTSAM with Weil and Brower σ_z ; (d) LTSAM with Smith Stability Class A σ_z ; (e) MLSCM; (f) ISCLT3.

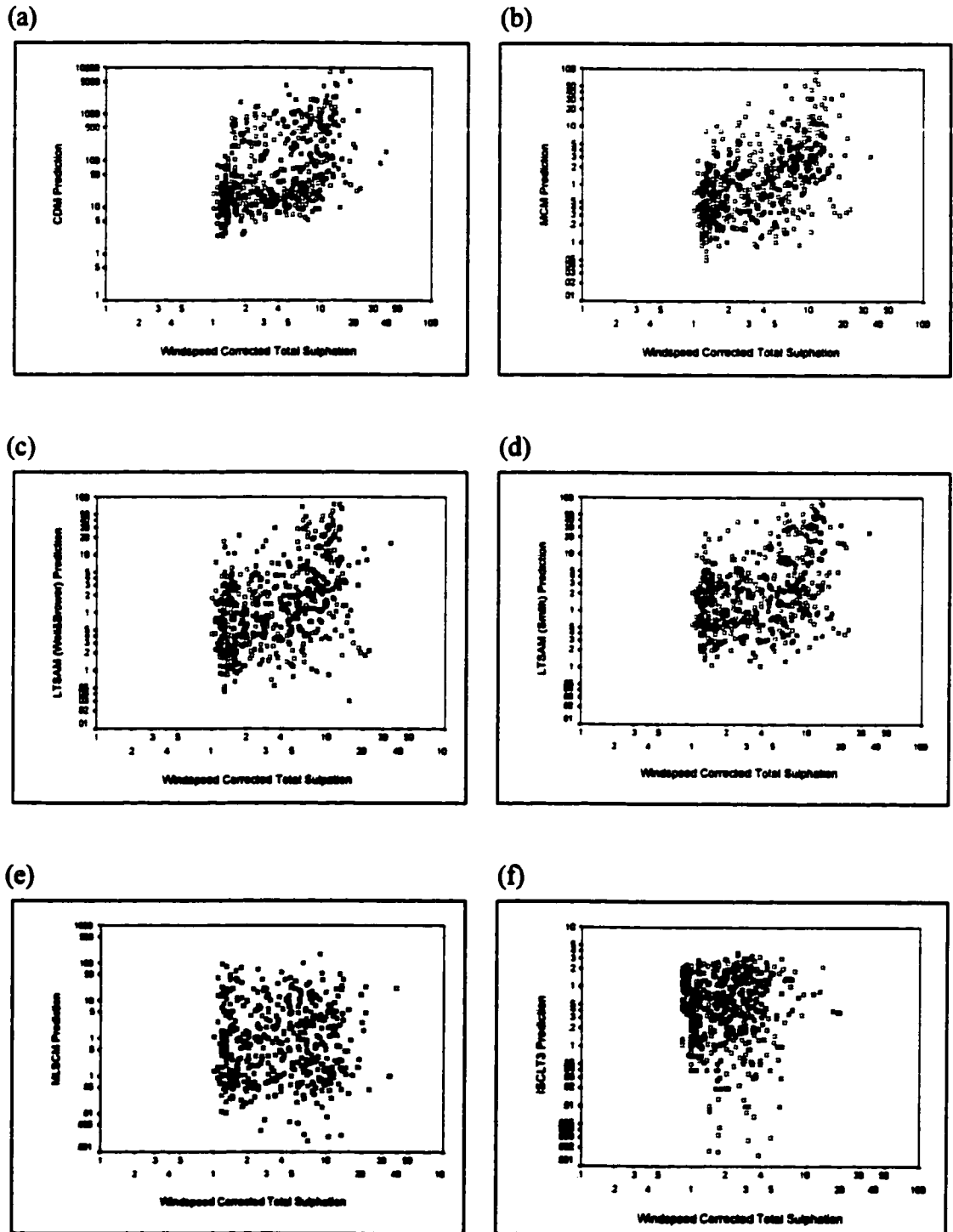


Figure 5.12. Plant # 14a - Scatter Plots of Wind Speed-Corrected Total Sulphation ($\mu\text{g}/\text{m}^3$) (x-axis) and Model-Predicted SO_2 Concentrations ($\mu\text{g}/\text{m}^3$) (y-axis); (a) CDM; (b) MCM; (c) LTSAM with Weil and Brower σ_z ; (d) LTSAM with Smith Stability Class A σ_z ; (e) MLSCM; the solid line indicates the linear regression line of best-fit.

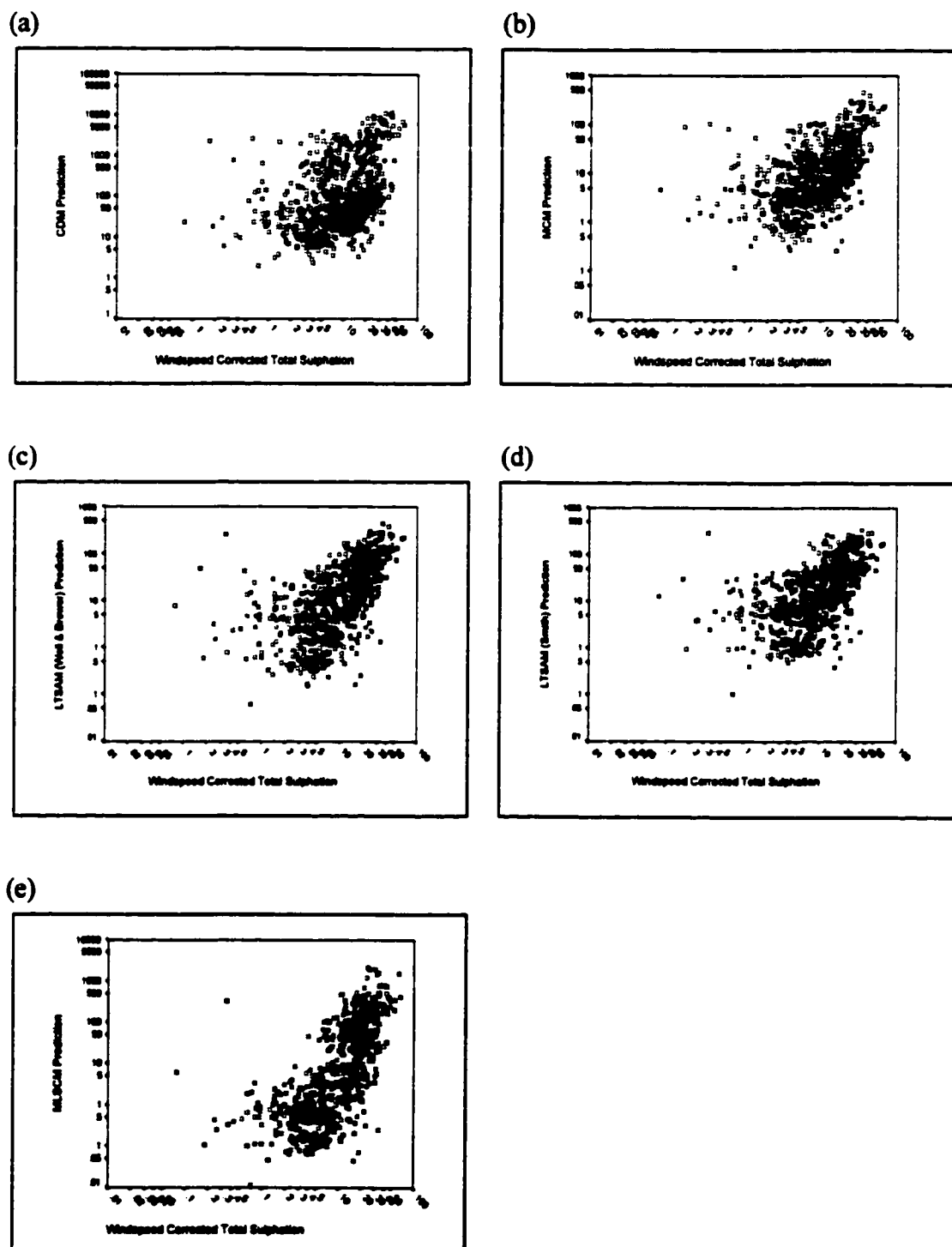


Figure 5.13. Plant #1 - Scatter Plots of Convective Velocity-Corrected Total Sulphation ($\mu\text{g}/\text{m}^3$) (x-axis) and Model-Predicted SO_2 Concentrations ($\mu\text{g}/\text{m}^3$) (y-axis); (a) CDM; (b) MCM; (c) LTSAM with Weil and Brower σ_z ; (d) LTSAM with Smith Stability Class A σ_z ; (e) MLSCM; the solid line indicates the linear regression line of best-fit.

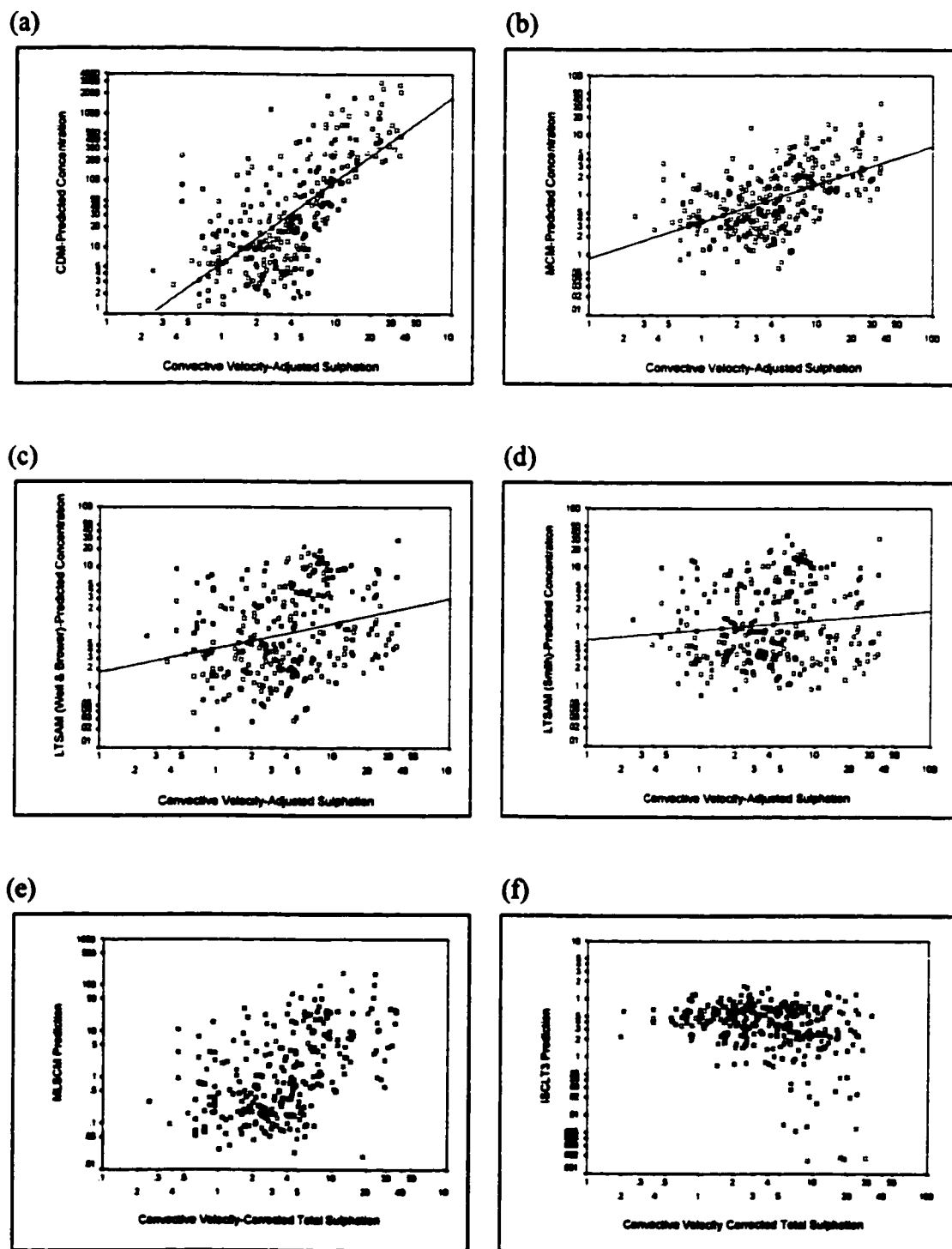


Figure 5.14. Plant #2 - Scatter Plots of Convective Velocity-Corrected Total Sulphation ($\mu\text{g}/\text{m}^3$) (x-axis) and Model-Predicted SO₂ Concentrations ($\mu\text{g}/\text{m}^3$) (y-axis); (a) CDM; (b) MCM; (c) LTSAM with Weil and Brower σ_z ; (d) LTSAM with Smith Stability Class A σ_z ; (e) MLSCM; (f) ISCLT3; the solid line indicates the linear regression line of best-fit.

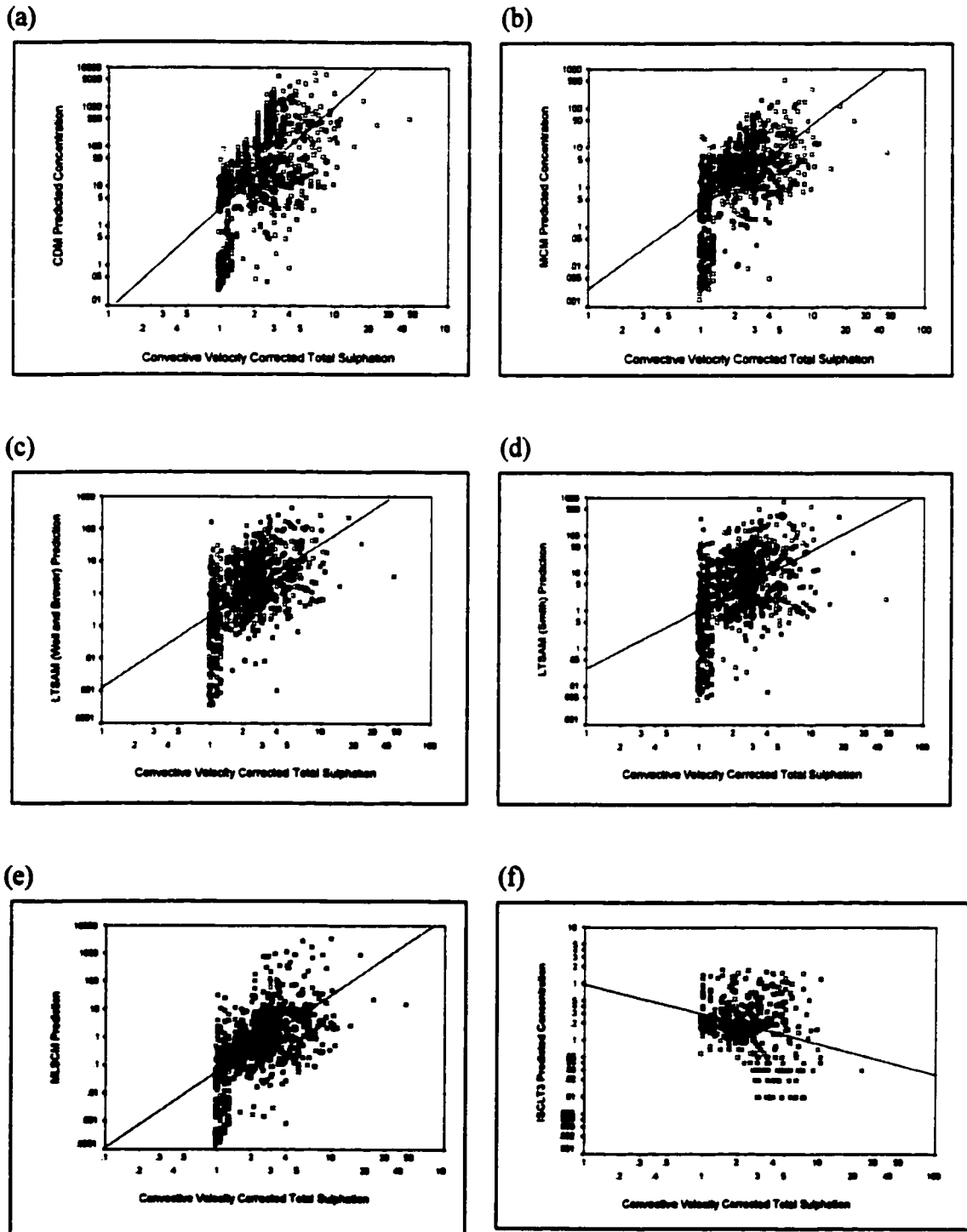


Figure 5.15. Plant #3 - Scatter Plots of Convective Velocity-Corrected Total Sulphation ($\mu\text{g}/\text{m}^3$) (x-axis) and Model-Predicted SO₂ Concentrations ($\mu\text{g}/\text{m}^3$) (y-axis); (a) CDM; (b) MCM; (c) LTSAM with Weil and Brower σ_z ; (d) LTSAM with Smith Stability Class A σ_z ; (e) MLSCM; (f) ISCLT3; the solid line indicates the line of best-fit.

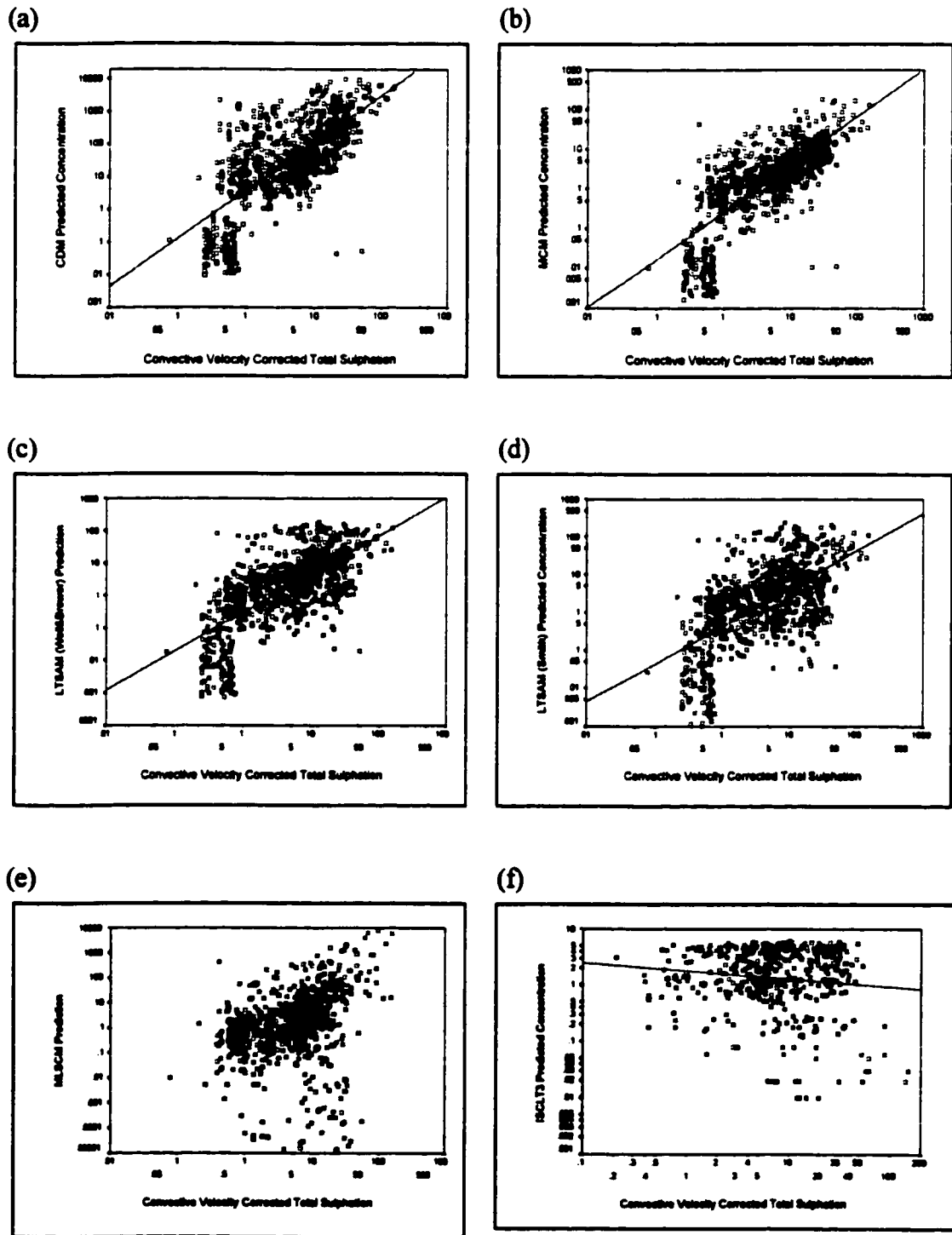


Figure 5.16. Plant #5 - Scatter Plots of Convective Velocity-Corrected Total Sulphation ($\mu\text{g}/\text{m}^3$) (x-axis) and Model-Predicted SO₂ Concentrations ($\mu\text{g}/\text{m}^3$) (y-axis); (a) CDM; (b) MCM; (c) LTSAM with Weil and Brower σz ; (d) LTSAM with Smith Stability Class A σz ; (e) MLSCM; (f) ISCLT3; the solid line indicates the linear regression line of best-fit.

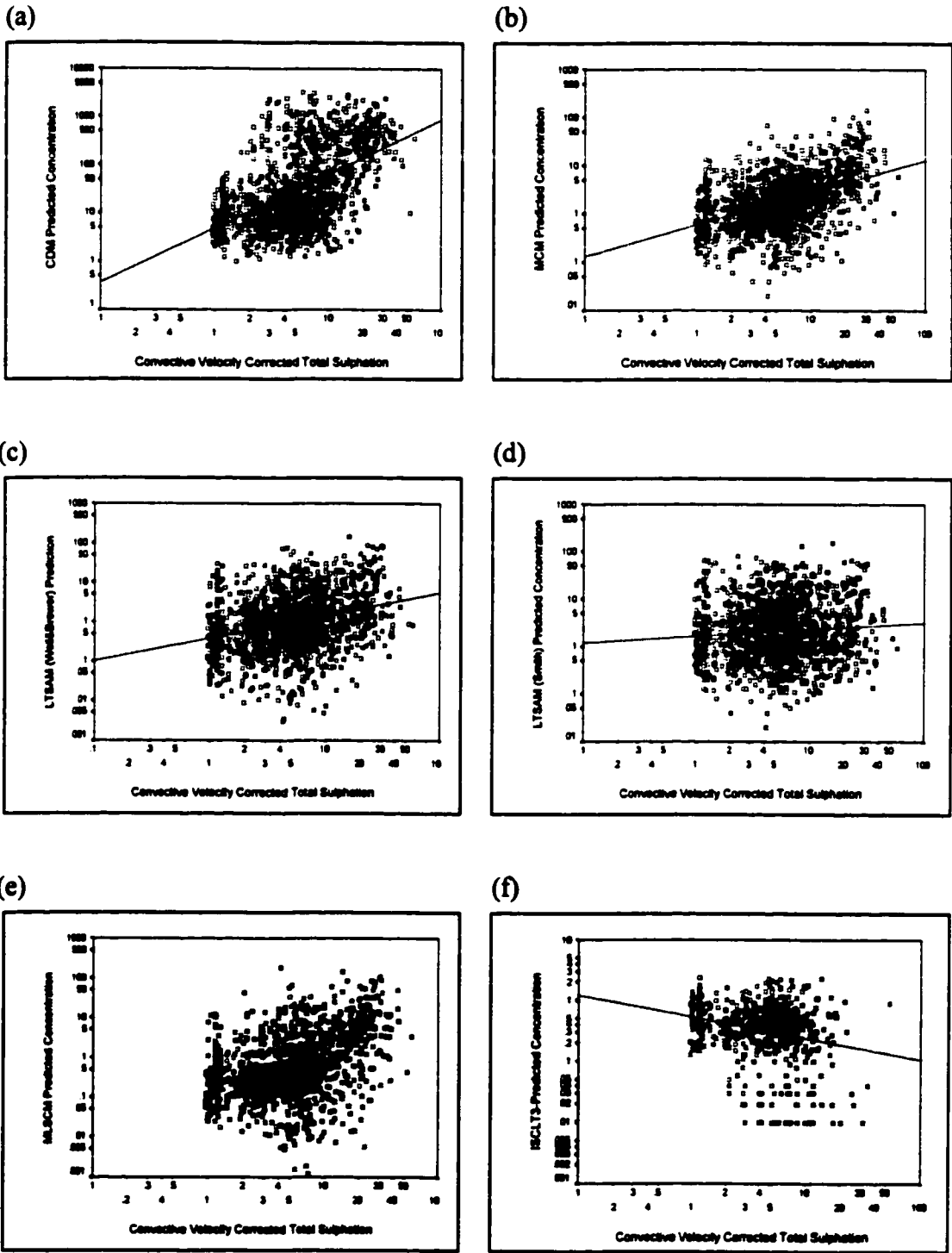


Figure 5.17. Plant #6 - Scatter Plots of Convective Velocity-Corrected Total Sulphation ($\mu\text{g}/\text{m}^3$) (x-axis) and Model-Predicted SO₂ Concentrations ($\mu\text{g}/\text{m}^3$) (y-axis); (a) CDM; (b) MCM; (c) LTSAM with Weil and Brower σ_z ; (d) LTSAM with Smith Stability Class A σ_z ; (e) MLSCM; (f) ISCLT3; the solid line indicates the linear regression line of best-fit.

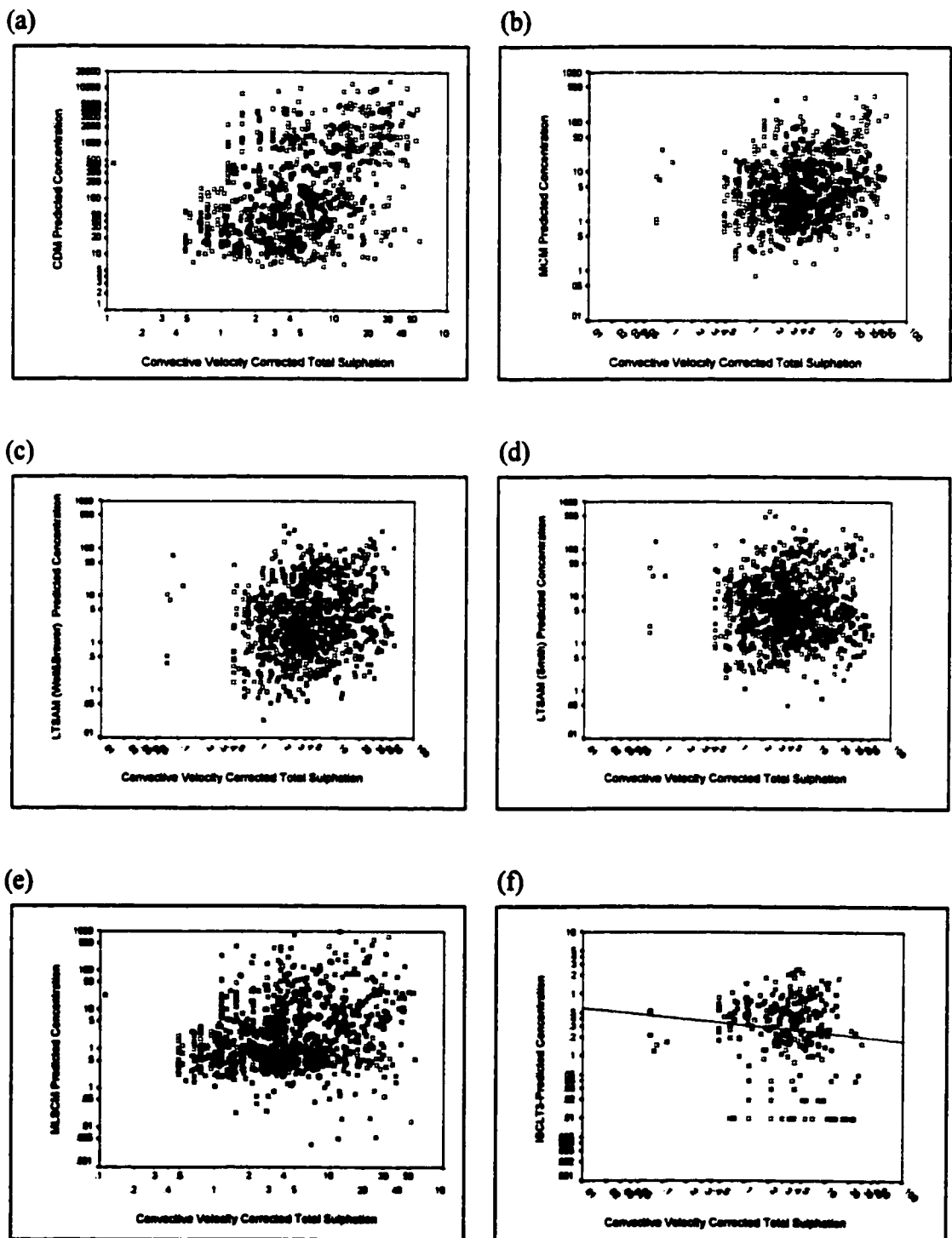


Figure 5.18. Plant #7 - Scatter Plots of Convective Velocity-Corrected Total Sulphation ($\mu\text{g}/\text{m}^3$) (x-axis) and Model-Predicted SO_2 Concentrations ($\mu\text{g}/\text{m}^3$) (y-axis); (a) CDM; (b) MCM; (c) LTSAM with Weil and Brower σ_z ; (d) LTSAM with Smith Stability Class A σ_z ; (e) MLSCM; (f) ISCLT3; the solid line indicates the linear regression line of best-fit.

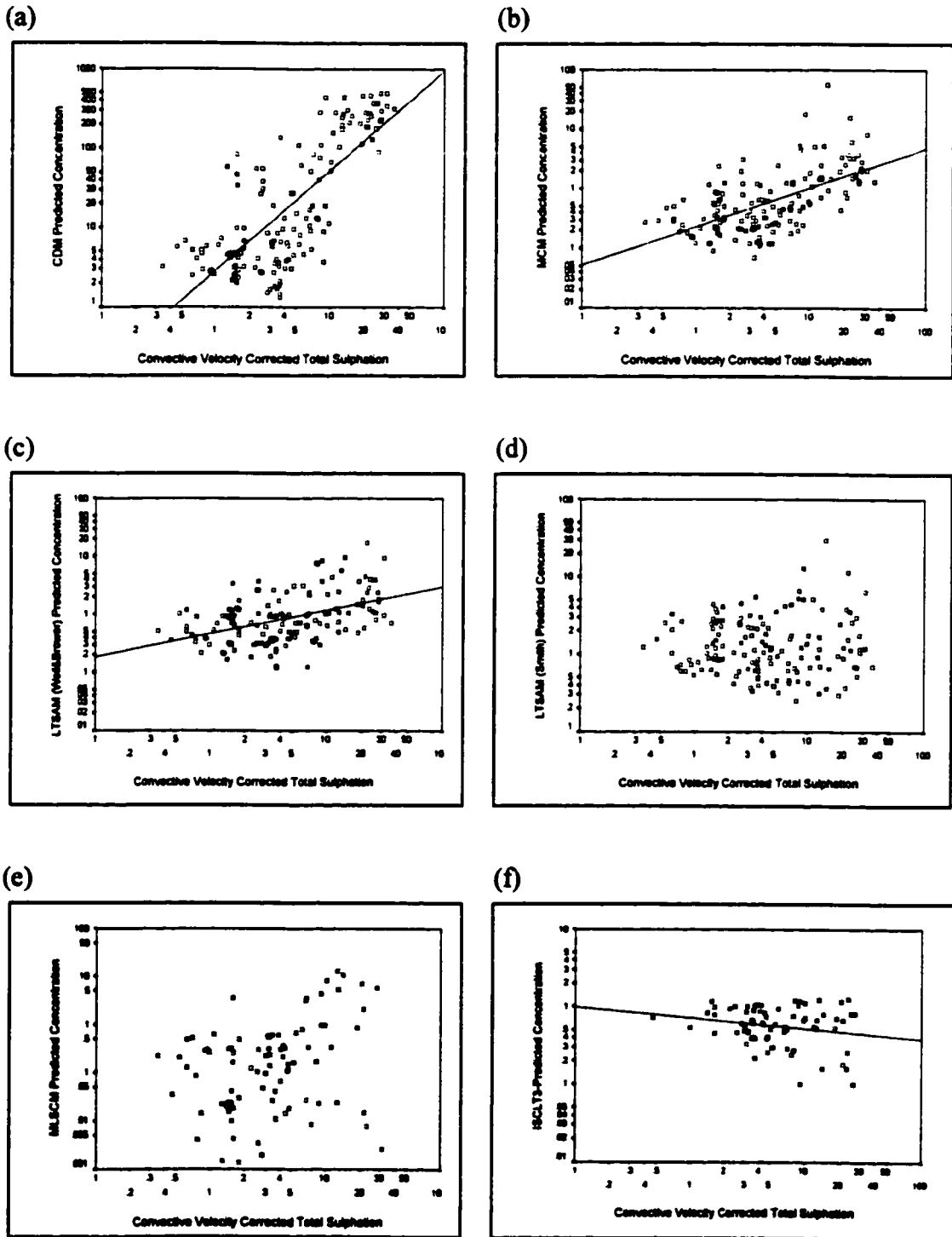


Figure 5.19. Plant #8 - Scatter Plots of Convective Velocity-Corrected Total Sulphation ($\mu\text{g}/\text{m}^3$) (x-axis) and Model-Predicted SO_2 Concentrations ($\mu\text{g}/\text{m}^3$) (y-axis); (a) CDM; (b) MCM; (c) LTSAM with Weil and Brower σ_z ; (d) LTSAM with Smith Stability Class A σ_z ; (e) MLSCM; (f) ISCLT3; the solid line indicates the linear regression line of best-fit.

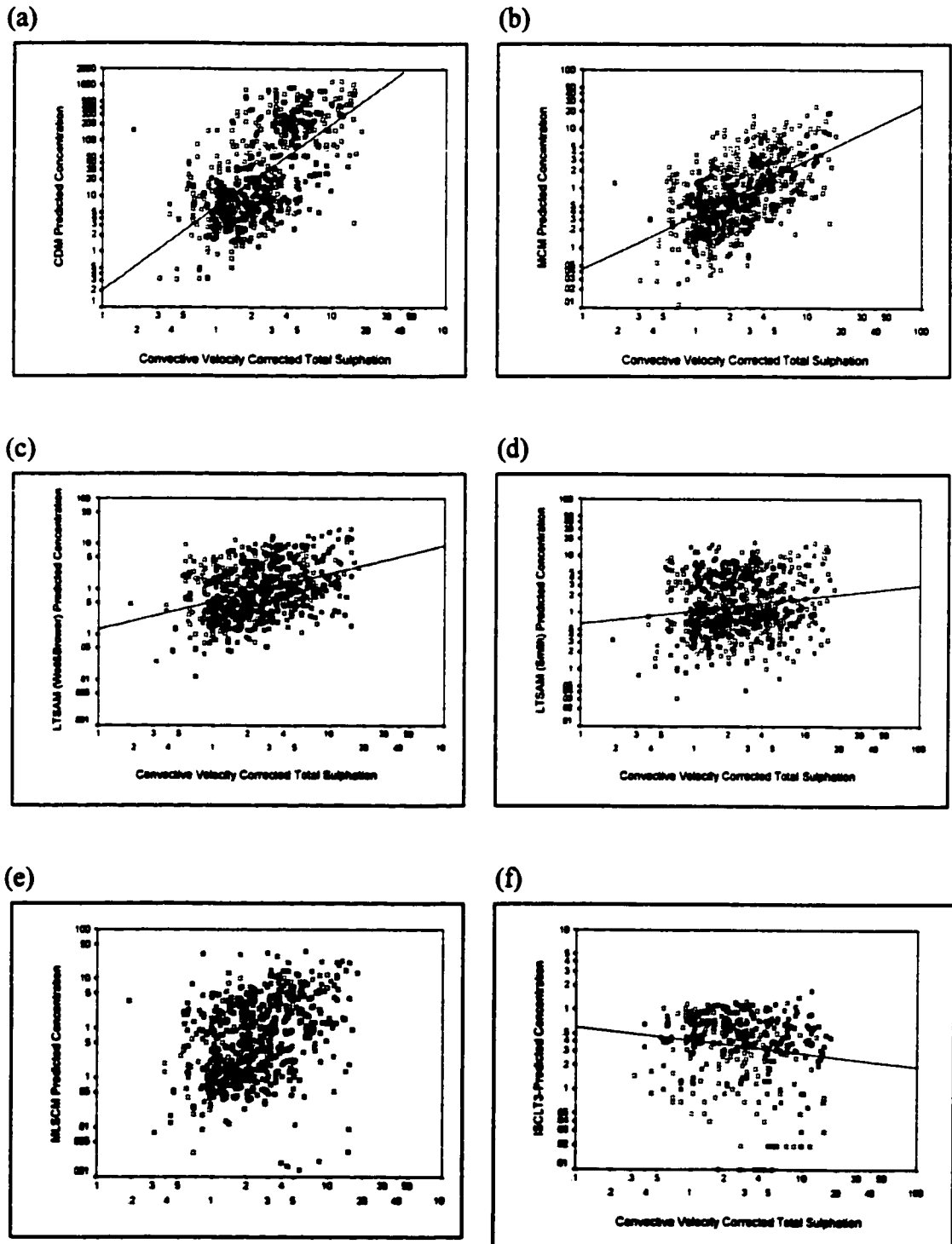


Figure 5.20. Plant #9 - Scatter Plots of Convective Velocity-Corrected Total Sulphation ($\mu\text{g}/\text{m}^3$) (x-axis) and Model-Predicted SO₂ Concentrations ($\mu\text{g}/\text{m}^3$) (y-axis); (a) CDM; (b) MCM; (c) LTSAM with Weil and Brower σ_z ; (d) LTSAM with Smith Stability Class A σ_z ; (e) MLSCM; (f) ISCLT3; the solid line indicates the linear regression line of best-fit.

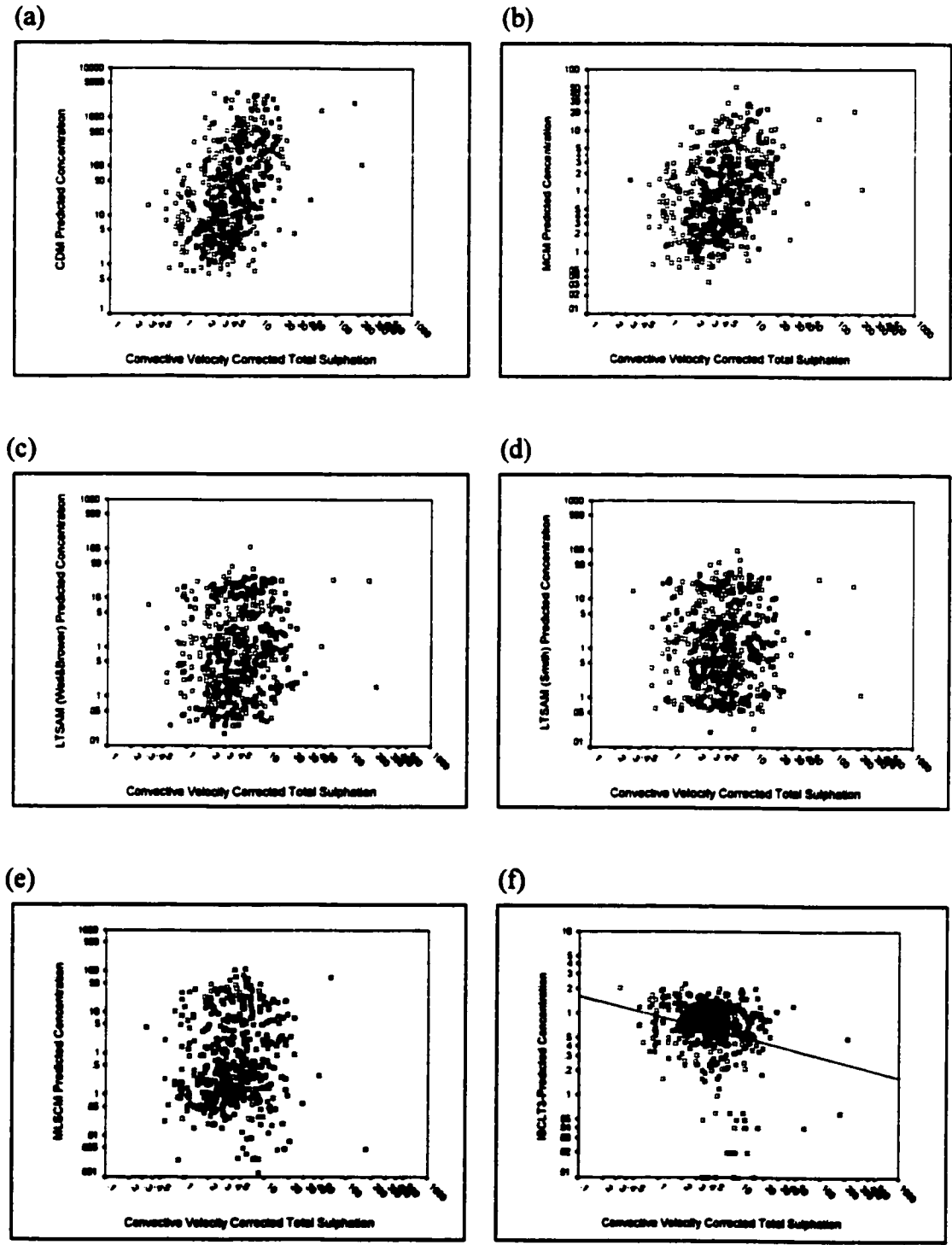


Figure 5.21. Plant #10 - Scatter Plots of Convective Velocity-Corrected Total Sulphation ($\mu\text{g}/\text{m}^3$) (x-axis) and Model-Predicted SO₂ Concentrations ($\mu\text{g}/\text{m}^3$) (y-axis); (a) CDM; (b) MCM; (c) LTSAM with Weil and Brower σ_z ; (d) LTSAM with Smith Stability Class A σ_z ; (e) MLSCM; (f) ISCLT3; the solid line indicates the linear regression line of best-fit.

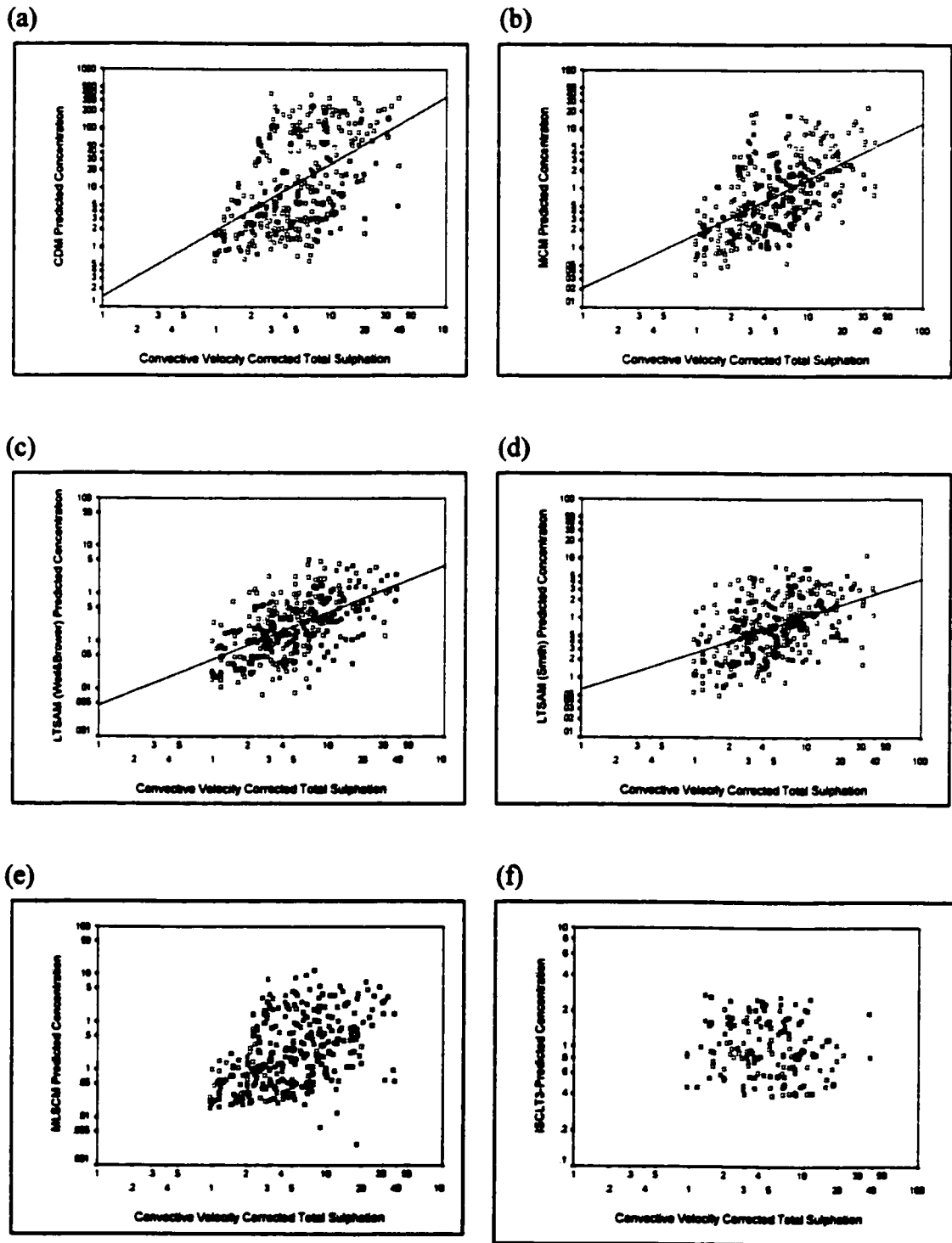


Figure 5.22. Plant #11 - Scatter Plots of Convective Velocity-Corrected Total Sulphation ($\mu\text{g}/\text{m}^3$) (x-axis) and Model-Predicted SO₂ Concentrations ($\mu\text{g}/\text{m}^3$) (y-axis); (a) CDM; (b) MCM; (c) LTSAM with Weil and Brower σ_z ; (d) LTSAM with Smith Stability Class A σ_z ; (e) MLSCM; (f) ISCLT3; the solid line indicates the linear regression line of best-fit.

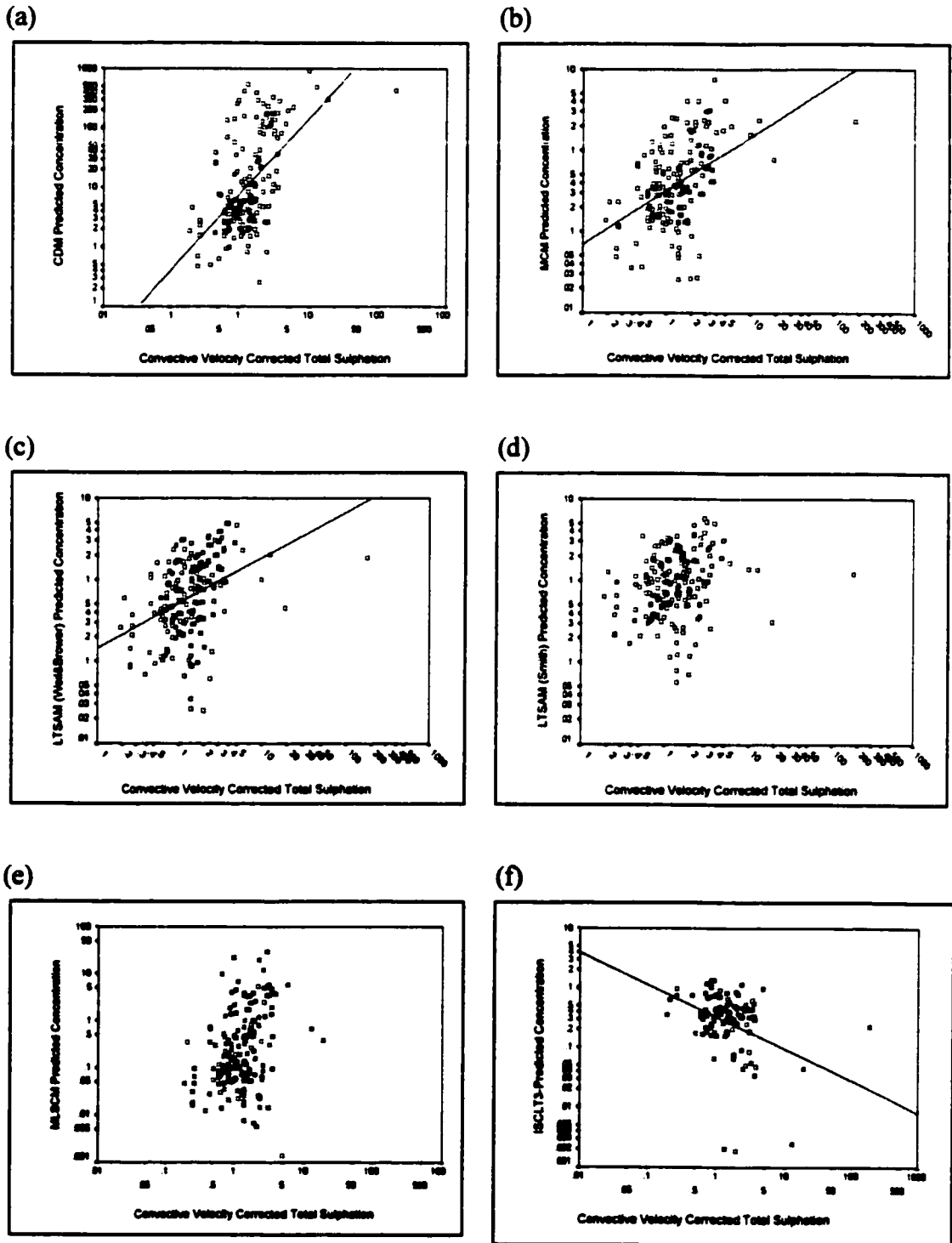


Figure 5.23. Plant #14 - Scatter Plots of Convective Velocity-Corrected Total Sulphation ($\mu\text{g}/\text{m}^3$) (axis) and Model-Predicted SO₂ Concentrations ($\mu\text{g}/\text{m}^3$) (y-axis); (a) CDM; (b) MCM; (c) LTSAM with Weil and Brower σ_z ; (d) LTSAM with Smith Stability Class A σ_z ; (e) MLSCM; (f) ISCLT3; the solid line indicates the linear regression line of best-fit.

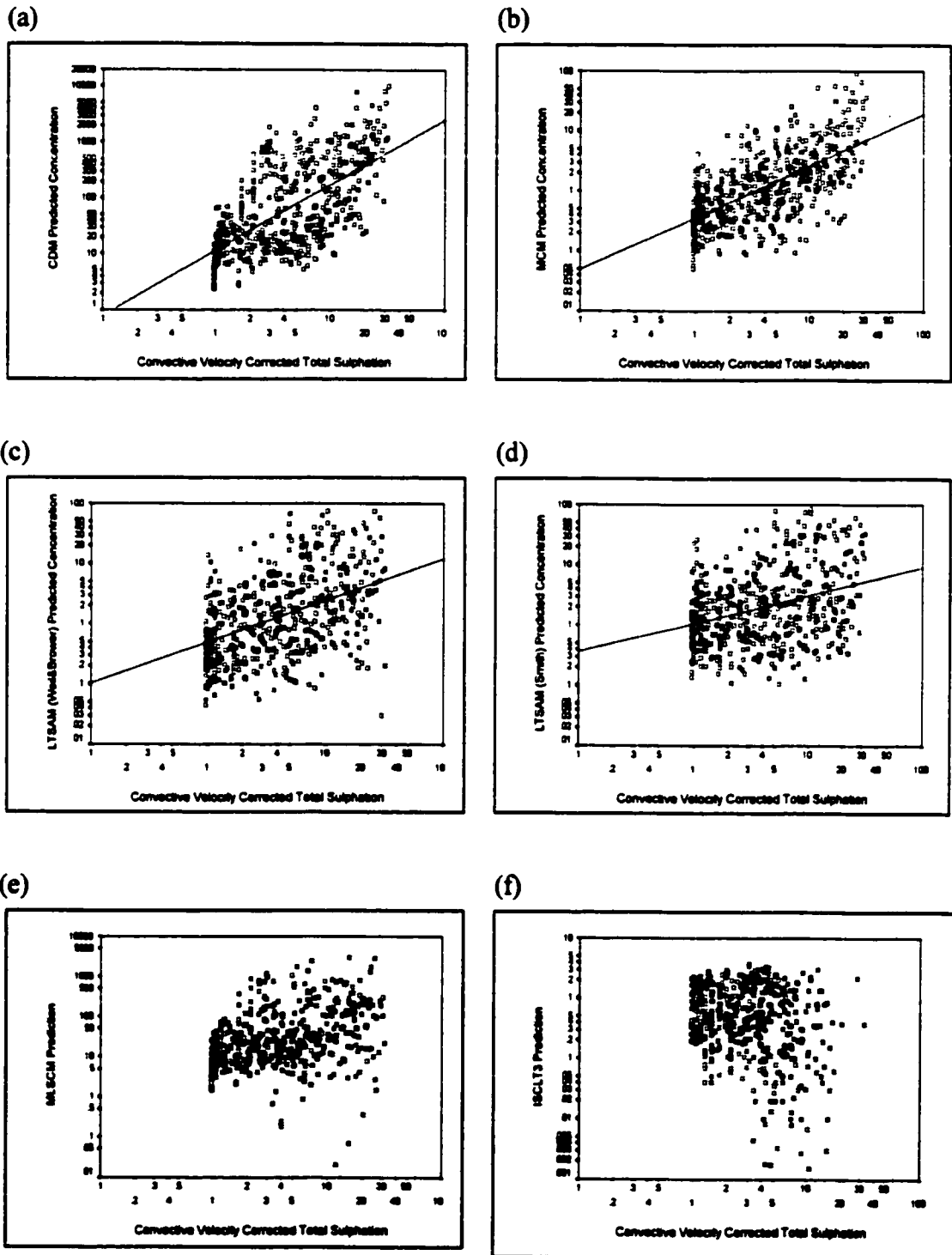


Figure 5.24. Plant #14a - Scatter Plots of Convective Velocity-Corrected Total Sulphation ($\mu\text{g}/\text{m}^3$) (x-axis) and Model-Predicted SO₂ Concentrations ($\mu\text{g}/\text{m}^3$) (y-axis); (a) CDM; (b) MCM; (c) LTSAM with Weil and Brower σ_z ; (d) LTSAM with Smith Stability Class A σ_z ; the solid line indicates the line of best-fit.

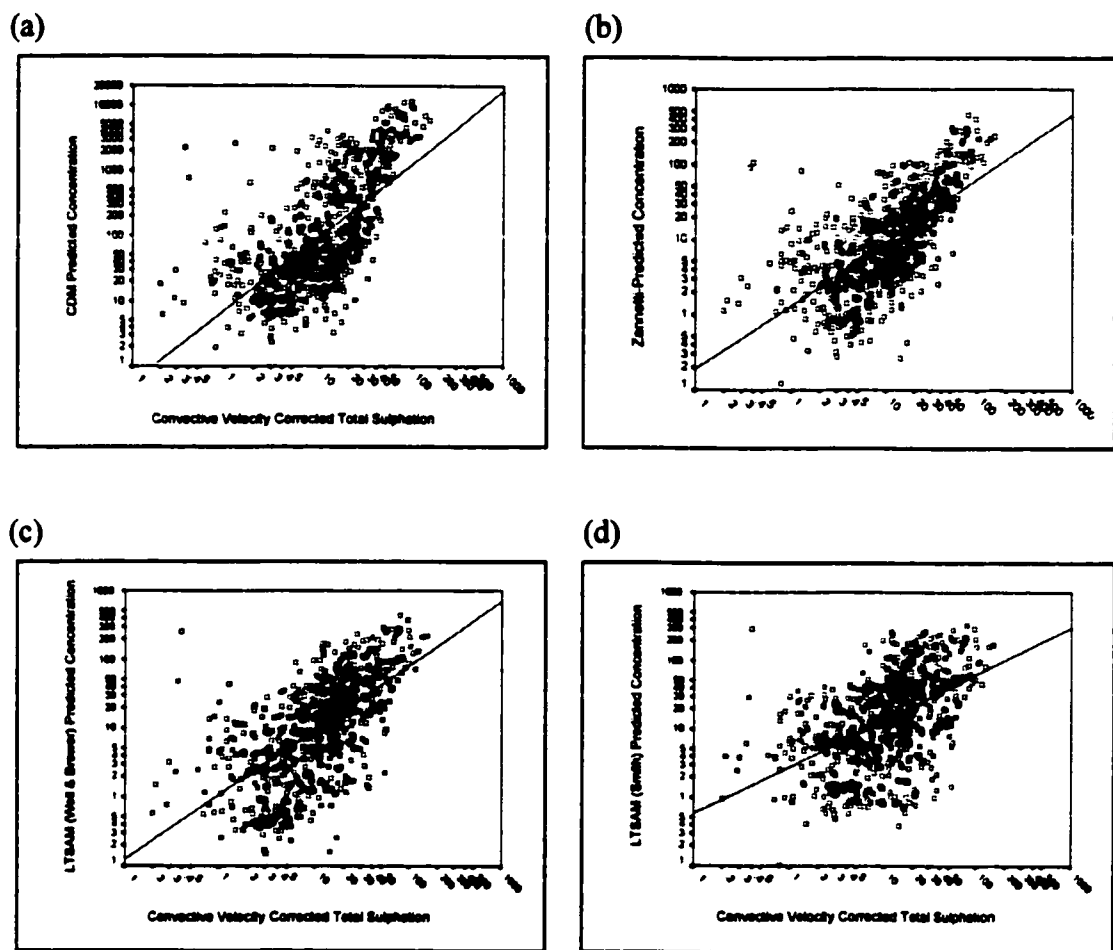


Table 5.1. Spearman Rank Correlation Coefficients Between Model-Predictions and Total Sulphation (top row), Wind Speed-Corrected Sulphation (middle row), and Convective Velocity - Corrected Total Sulphation (bottom row). Coefficients greater than 0.5 and less than -0.3 are highlighted.

Plant	ISCLT3			LTSAM						MCM		CDM		MLSCM		Pot-map	
	P	E	ND	Well & Brower	Smith-SC-A	Smith-SC-D	Briggs-SC-A	Briggs-SC-D	P	E	P	E	P	E			
1	-0.18**	0.17*	Nd	0.25**	0.31*	0.15**	0.29*	0.02	0.03	0.16**	0.28*	-0.03	-0.04	0.40**	0.47**	0.28**	0.05
	-0.22**	0.29**	Nd	0.32**	0.27	0.13*	0.25	-0.00	-0.02	0.14**	0.24	-0.06	-0.12	0.39**	0.47**	0.26**	0.03
	-0.29**	0.38**	Nd	0.29**	0.34*	0.14	0.27	0.00	0.02	0.12*	0.26	-0.05	-0.06	0.35**	0.43**	0.35**	0.03
2	0.04	0.29	Nd	0.32**	0.40**	0.26**	0.40**	0.23**	0.24	0.36**	0.40**	0.17**	0.09	0.20**	0.08	0.08	0.22**
	0.03	0.09	Nd	0.33**	0.32*	0.20**	0.21	0.13**	0.11	0.32**	0.21	0.24**	-0.08	0.27**	0.11	0.14**	0.04
	-0.03**	0.24**	Nd	0.30**	0.41**	0.28**	0.32*	0.28**	0.20	0.41**	0.32*	0.18**	0.04	0.04	0.27**	-0.09	0.12**
3	-0.01	Nd	Nd	0.35**	0.42**	0.29**	0.32*	0.23**	0.24	0.36**	0.42**	0.18**	0.09	0.20**	0.08	0.08	0.22**
	-0.10*	Nd	Nd	0.36**	0.43**	0.30**	0.32*	0.24**	0.25	0.37**	0.43**	0.19**	0.10	0.21**	0.09	0.09	0.23**
	-0.06	Nd	Nd	0.37**	0.44**	0.31**	0.33*	0.25**	0.26	0.38**	0.44**	0.20**	0.11	0.22**	0.10	0.10	0.24**
5	0.07	-0.17*	Nd	0.38**	0.45**	0.32**	0.34*	0.26**	0.27	0.39**	0.45**	0.21**	0.12	0.23**	0.11	0.11	0.25**
	-0.23*	-0.20*	Nd	0.39**	0.46**	0.33**	0.35*	0.27**	0.28	0.40**	0.46**	0.22**	0.13	0.24**	0.12	0.12	0.26**
	-0.28*	-0.25**	Nd	0.40**	0.47**	0.34**	0.36*	0.28**	0.29	0.41**	0.47**	0.23**	0.14	0.25**	0.13	0.13	0.27**
6	0.00	-0.01	Nd	0.41**	0.48**	0.35**	0.37*	0.29**	0.30	0.42**	0.48**	0.24**	0.15	0.26**	0.14	0.14	0.28**
	0.01	-0.07	Nd	0.42**	0.49**	0.36**	0.38*	0.30**	0.31	0.43**	0.49**	0.25**	0.16	0.27**	0.15	0.15	0.29**
	-0.25**	-0.22**	Nd	0.43**	0.50**	0.37**	0.39*	0.31**	0.32	0.44**	0.50**	0.26**	0.17	0.28**	0.16	0.16	0.30**
7	-0.01	-0.09	Nd	0.44**	0.51**	0.38**	0.40*	0.32**	0.33	0.45**	0.51**	0.27**	0.18	0.29**	0.17	0.17	0.31**
	0.17	-0.24	Nd	0.45**	0.52**	0.39**	0.41*	0.33**	0.34	0.46**	0.52**	0.28**	0.19	0.30**	0.18	0.18	0.32**
	-0.08	-0.10	Nd	0.46**	0.53**	0.40**	0.42*	0.34**	0.35	0.47**	0.53**	0.29**	0.20	0.31**	0.19	0.19	0.33**
8	0.10	0.31*	Nd	0.47**	0.54**	0.41**	0.43*	0.35**	0.36	0.48**	0.54**	0.30**	0.21	0.32**	0.20	0.20	0.34**
	0.08	0.24**	Nd	0.48**	0.55**	0.42**	0.44*	0.36**	0.37	0.49**	0.55**	0.31**	0.22	0.33**	0.21	0.21	0.35**
	-0.11	0.32*	Nd	0.49**	0.56**	0.43**	0.45*	0.37**	0.38	0.50**	0.56**	0.32**	0.23	0.34**	0.22	0.22	0.36**
9	-0.01	-0.08	Nd	0.50**	0.57**	0.44**	0.46*	0.38**	0.39	0.51**	0.57**	0.33**	0.24	0.35**	0.23	0.23	0.37**
	0.01	-0.03	Nd	0.51**	0.58**	0.45**	0.47*	0.39**	0.40	0.52**	0.58**	0.34**	0.25	0.36**	0.24	0.24	0.38**
	-0.14**	-0.28*	Nd	0.52**	0.59**	0.46**	0.48*	0.40**	0.41	0.53**	0.59**	0.35**	0.26	0.37**	0.25	0.25	0.39**
10	-0.04	-0.29	Nd	0.53**	0.60**	0.47**	0.49*	0.41**	0.42	0.54**	0.60**	0.36**	0.27	0.38**	0.26	0.26	0.40**
	-0.05	0.39**	Nd	0.54**	0.61**	0.48**	0.50*	0.42**	0.43	0.55**	0.61**	0.37**	0.28	0.39**	0.27	0.27	0.41**
	-0.14	0.42**	Nd	0.55**	0.62**	0.49**	0.51*	0.43**	0.44	0.56**	0.62**	0.38**	0.29	0.40**	0.28	0.28	0.42**
11	-0.05	-0.20	Nd	0.56**	0.63**	0.50**	0.52*	0.44**	0.45	0.57**	0.63**	0.39**	0.30	0.41**	0.29	0.29	0.43**
	-0.00	-0.27	Nd	0.57**	0.64**	0.51**	0.53*	0.45**	0.46	0.58**	0.64**	0.40**	0.31	0.42**	0.30	0.30	0.44**
	-0.26**	0.46**	Nd	0.58**	0.65**	0.52**	0.54*	0.46**	0.47	0.59**	0.65**	0.41**	0.32	0.43**	0.31	0.31	0.45**
14	-0.05	-0.11	Nd	0.59**	0.66**	0.53**	0.55*	0.47**	0.48	0.60**	0.66**	0.42**	0.33	0.44**	0.32	0.32	0.46**
	-0.12*	-0.19	Nd	0.60**	0.67**	0.54**	0.56*	0.48**	0.49	0.61**	0.67**	0.43**	0.34	0.45**	0.33	0.33	0.47**
	0.24**	0.44**	Nd	0.61**	0.68**	0.55**	0.57*	0.49**	0.50	0.62**	0.68**	0.44**	0.35	0.46**	0.34	0.34	0.48**
14a	Nd	Nd	Nd	0.62**	0.69**	0.56**	0.58*	0.50**	0.51	0.63**	0.69**	0.45**	0.36	0.47**	0.35	0.35	0.49**
	Nd	Nd	Nd	0.63**	0.70**	0.57**	0.59*	0.51**	0.52	0.64**	0.70**	0.46**	0.37	0.48**	0.36	0.36	0.50**
	Nd	Nd	Nd	0.64**	0.71**	0.58**	0.60*	0.52**	0.53	0.65**	0.71**	0.47**	0.38	0.49**	0.37	0.37	0.51**

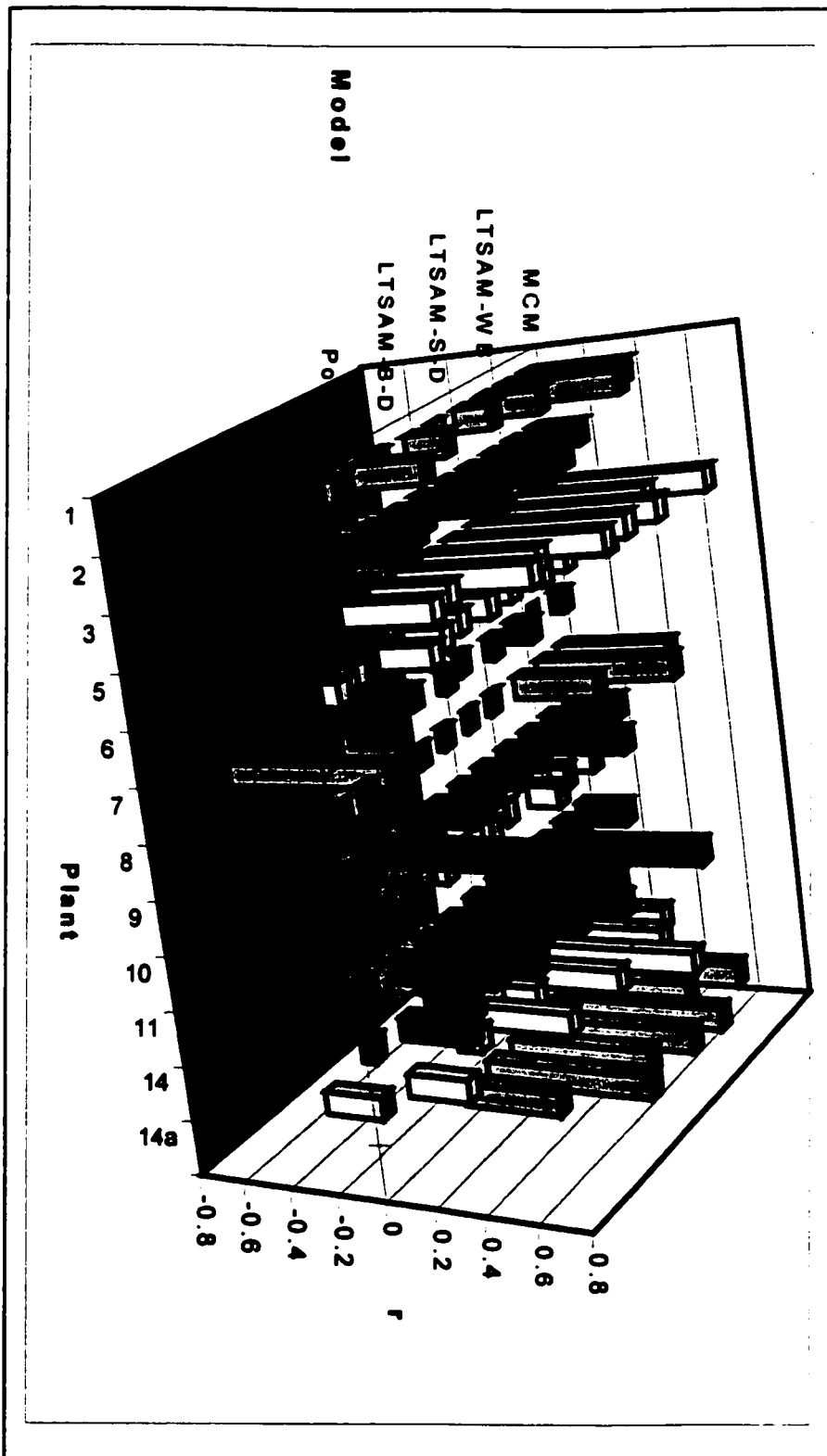
SC-A - stability class A; SC-D - stability class D; P - paired observed and predicted values; E - seasonally grouped ensemble averages; Nd - not determined
 * correlation is significant at the 0.01 level (two-tailed); ** correlation is significant at the 0.05 level (two-tailed)

NOTE TO USERS

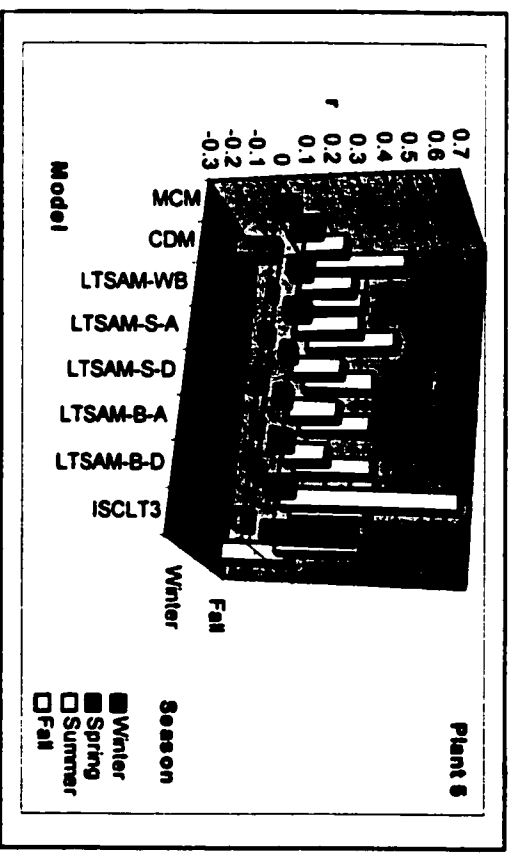
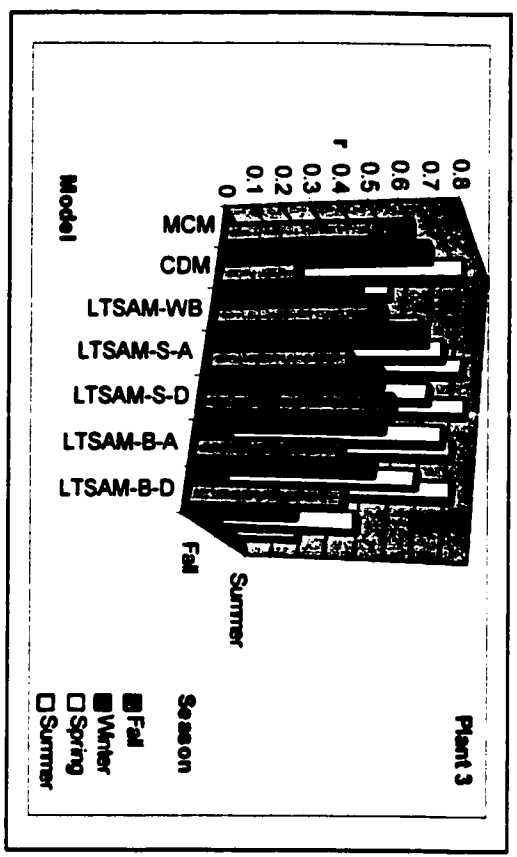
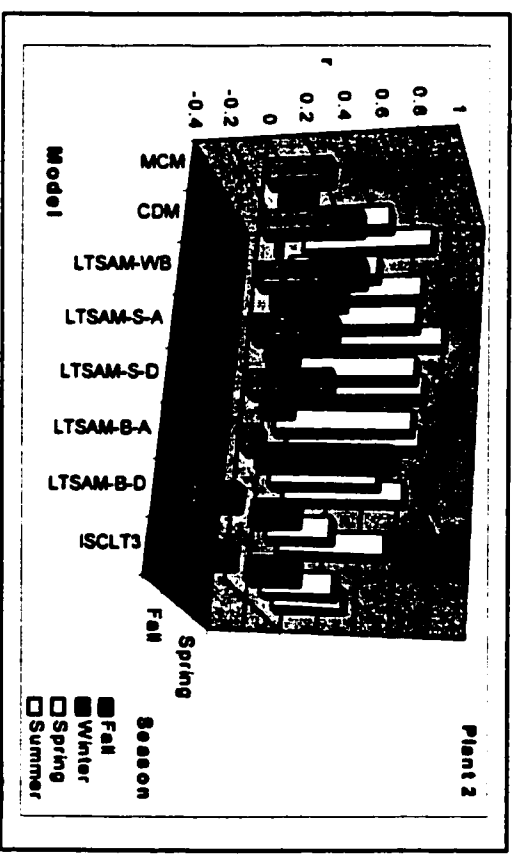
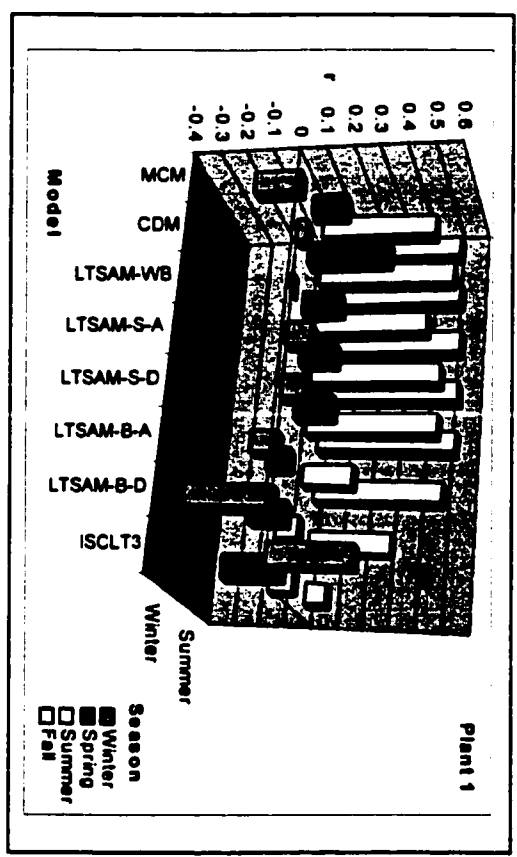
Page(s) not included in the original manuscript are unavailable from the author or university. The manuscript was microfilmed as received.

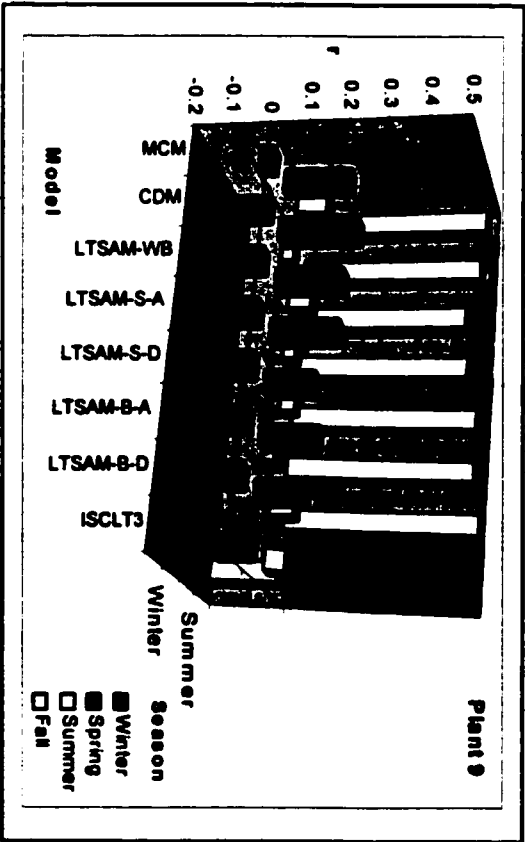
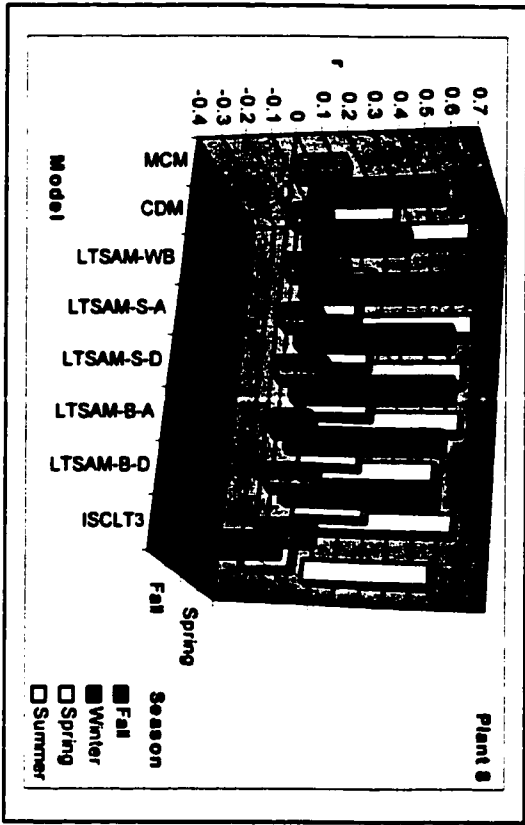
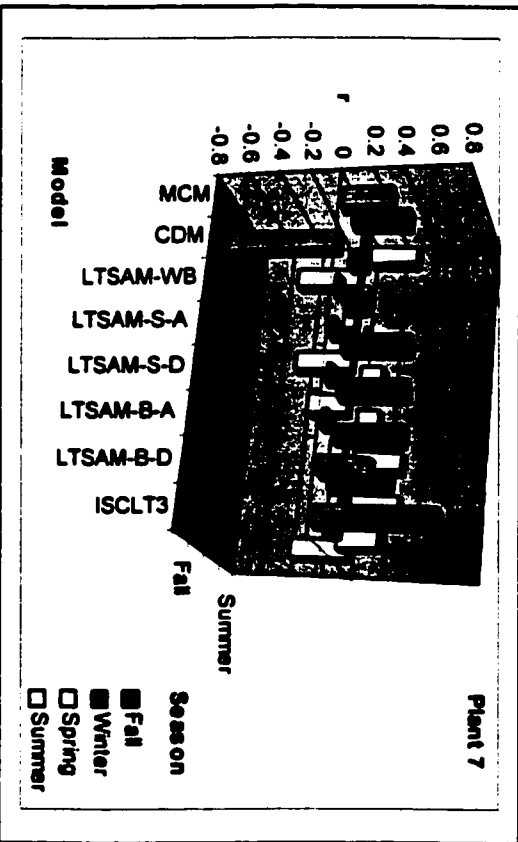
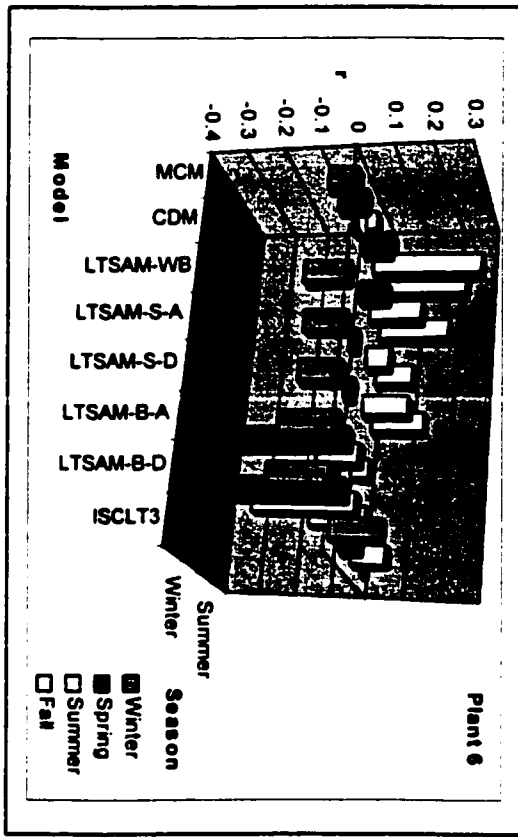
UMI

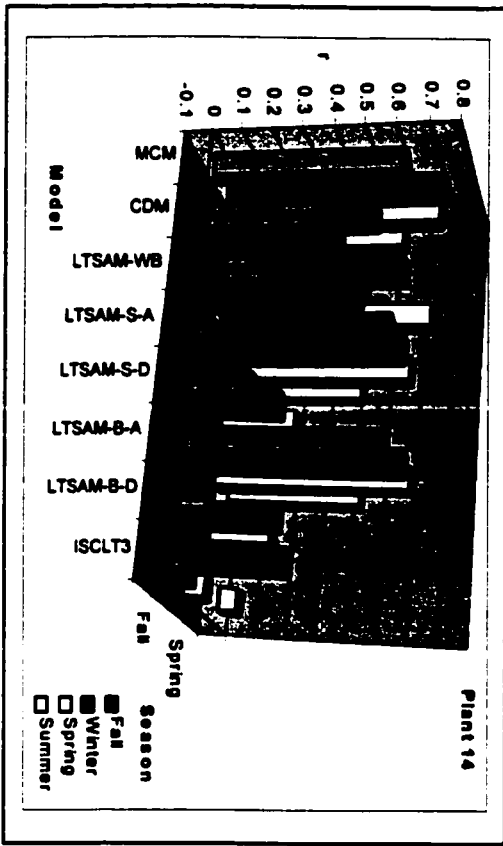
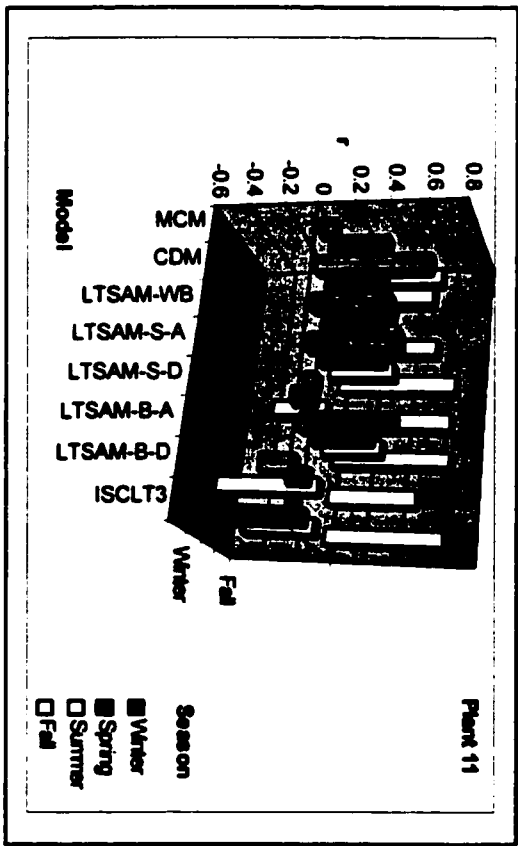
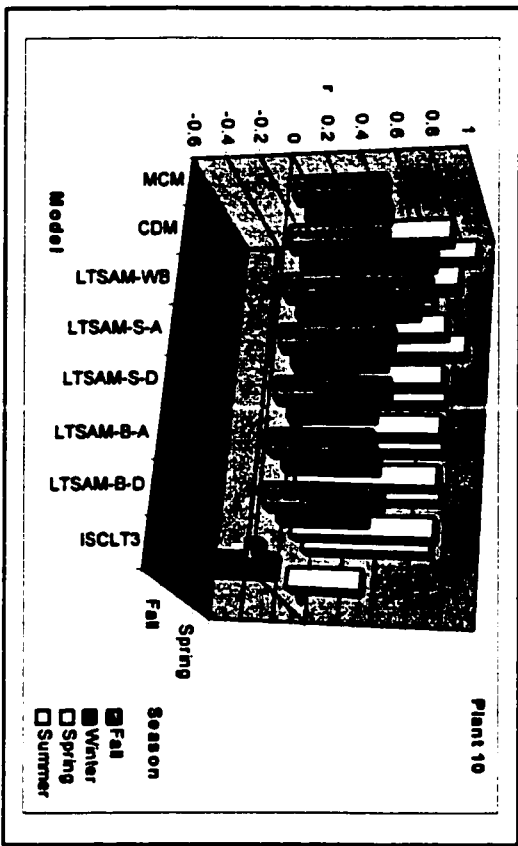
Figure 5.25. Correspondence Between Model Predictions and Total Sulphation Values Across Sour Gas Processing Plants



Figures 5.26. Seasonally Grouped Ensemble Average Predictions and Total Sulphation Ensemble Averages







References

- Addink, R., K. Olie, (1995) Mechanisms of Formation and Destruction of Polychlorinated Dibenzo-p-dioxins and Dibenzofurans in Heterogenous Systems, *Environmental Science and Technology*, Vol. 29, No. 6, pp 1425 - 1435.
- Al-Khayat, T.A.H., B. Van Eygen, C.N. Hewitt, M. Kelly (1992) Modelling and Measurement of the Dispersion of Radioactive Emissions From a Nuclear Fuel Fabrication Plant in the U.K., *Atmospheric Environment*, Vol. 26A, No. 17, pp 3079 - 3087.
- Alapaty, K., S. Raman, D.S. Niyogi. (1997) Uncertainty in the Specification of Surface Characteristics: A Study of Prediction Errors in the Boundary Layer, *Boundary-Layer Meteorology*, Vol. 82, pp 473-500.
- Alberta Environmental Centre, (1996) Cattle and the Oil and Gas Industry in Alberta: A Literature Review with Recommendations for Environmental Management, July, 1996, Calgary, Alberta: Alberta Cattle Commission.
- Alberta Research Council (1995) An Evaluation of Passive Sampling Systems - A Report to Alberta Environmental Protection, 1494-A9503.
- Alberta Research Council (1996) Development and Application of Passive Sampling Systems in Alberta- A Report Prepared for The Clean Air Strategic Alliance.
- American Meteorological Society (1977) Accuracy of Dispersion Models - A Position Paper of the AMS 1977 Committee on Atmospheric Turbulence and Diffusion, *Bulletin of the American Meteorological Society*, Vol. 59, No. 8, pp 1025-1026.
- American Meteorological Society (1988) Lectures on Air Pollution Modeling, A. Venkatram and J.C. Wyngaard (Eds.), Boston, 390 pp.
- Angle, R.P., S.K. Sakiyama (1991) Plume Dispersion in Alberta, Standards and Approvals Division, Alberta Environment, Edmonton, Alberta, 428 pp.
- Angle, R.P. (1979) Air Quality Modelling and User Needs, Prepared for the Alberta Oil Sands Environmental Research Program by Alberta Environment, Air Quality Control Branch, AOSERP Report 74, 34 pp.
- Anonymous (1974) Background Document Concerning Sulphur Recovery and Sulphur Emissions at Gas Processing Plants in Alberta (Draft), Standards and Approvals Division.
- Anonymous, (1984) Technical Report - Twin Butte Soils and Water Evaluation Task Force.
- Anonymous, (1995) National Pollutant Release Inventory Summary Report, Cat # EN40-495\1-1995.
- Armstrong, B.G., (1992) Confidence Intervals for Arithmetic Means of Lognormally Distributed Exposures, *American Industrial Hygiene Association Journal* Vol. 53, No. 8, pp 481-485.
- Armstrong, B. (1996) Optimizing Power in Allocating Resources to Exposure Assessment in an Epidemiological Study, *American Journal of Epidemiology*, Vol. 144, pp 192-197.

Barry, P.J. (1977) Stochastic Properties of Atmospheric Diffusivity, In: Sulphur and its Organic Derivatives in the Canadian Environment, National Research Council of Canada, NRC Associate Committee on Scientific Criteria for Environmental Quality, Publication No. NRCC 15015 of the Environmental Secretariat, pp 313 - 358.

Battelle Pacific Northwest Laboratories (1979) Mathematical Models for Atmospheric Pollutants Appendix D: Available Air Quality Models, Electric Power Research Institute - EA-1131, Research Project 805.

Beard, A., K.P. Naikwadi, W. Karasek, (1993) Formation of Polychlorinated Dibenzofurans by Chlorination and de novo Reactions with FeCl₃ in Petroleum Refining Processes, Environmental Science and Technology, Vol. 27, No. 8, p 1505.

Beasley, T., D. Merritt (1992) Construction and Demonstration of a Portable Chemical Processing Unit for Purifying and Recovering Waste Gas Treating Chemicals from the Petroleum Industry, for the Technology Development Branch, Environmental Protection, Conservation and Protection, Environment Canada, Report EPS 3/PN/1.

Benarie, M. M. (1987a) Air Pollution Modelling Operations and Their Limits, In: Mathematical Models for Planning and Controlling Air Quality, Proceedings of an October 1979 HASA Workshop, G. Fronza and P. Melli (Eds.), Pergamon Press, Oxford, pp 109 - 115.

Benarie, M.M.(1987b) Editorial: The Limits of Air Pollution Modelling, Atmospheric Environment, Vol. 21, No. 1, pp 1-5.

Berkowicz, R., E. Lyck, P.A. Larsen, J.S. Markvorsen, S. Dalager, A.B. Jensen (1988) Evaluation of a Model Performance with Data From a Large Power Plant, In: Environmental Meteorology, K. Grefen and J. Löbel (eds.), pp 93 - 114.

Bertram, H. L., C.B. Christensen, V.I. Hannak, (1988) Developments in Passive Monitoring of Ambient Sulphur Dioxide, Internal Report, Air Analysis and Research Group, Alberta Environmental Center, Vegreville, Alberta.

Beychok, M.R. (1979a) Meteorological Data, In: Fundamentals of Stack Gas Dispersion, pp X-1-9.

Beychok, M.R. (1979b) How Accurate Are Dispersion Predictions? Hydrocarbon Processing, October, pp 10-17.

Beyrich, F. (1997) Mixing Height Estimation From Sodar Data - A Critical Discussion, Atmospheric Environment, Vol. 31, No. 23, pp. 3941-3953.

Borchardt, J.K. (1989) Chemicals Used in Oil-Field Operations, In: Oil-Field Chemistry, Enhanced Recovery and Production Stimulation, J.K. Borchardt, T.F. Yen Eds., American Chemical Society, Washington DC., pp 1-54.

Boulerice, M., W. Brabant (1969) New Lead Dioxide Support for the Measurement of Sulphation, Journal of Air Pollution Control Association, Vol. 19, No. 6, pp 432-434.

Boyle, C.A. (1990) Petroleum Waste Management: Amine Process Sludges, for the Canadian Petroleum Association and Environment Canada.

- Briggs, G.A. (1985) Analytical Parameterizations of Diffusion: the Convective Boundary Layer. *Journal of Climate and Applied Meteorology*, Vol. 24, pp 1167 - 1186.
- Briggs, G. (1988) Analysis of Diffusion Field Experiments, In: *Lectures on Air Pollution Modeling*, Eds: A. Venkatram, J.C. Wyngaard, American Meteorological Society, Boston, pp 63 - 117.
- Briggs, G. (1993a) The Round Table Discussion: Interactions and Feedback Between Theory and Experiment, *Boundary-Layer Meteorology*, Vol. 62, pp 435-448.
- Briggs, G..A. (1993b) Final Results of the CONDORS Convective Diffusion Experiment, *Boundary-Layer Meteorology*, Vol. 62, pp 315- 328.
- Brown, M.J., S.P. Arya, W.H. Snyder (1993) Vertical Dispersion from Surface and Elevated Releases: An Investigation of a Non-Gaussian Plume Model, *Journal of Applied Meteorology*, Vol. 32, pp 490 - 505.
- Brown, R.A. (1991) *Fundamentals of Fluid Dynamics*, In: *Fluid Mechanics of the Atmosphere*, Academic Press Inc.
- Brown, R.D. (1981) *Health and Environmental Effects of Oil and Gas Technologies: Research Needs, A Report to the Federal Interagency Committee on the Health and Environmental Effects of Energy Technologies*, July 1981, MTR-81W77.
- Businger, J.A., S.P. Oncley (1990) Flux Measurement With Conditional Sampling, *Journal of Atmospheric and Oceanic Techniques*, Vol. 7, pp 349 - 352.
- Byrne, C.A. (1996) *An Evaluation of Industry and Government Total Sulphation and Hydrogen Sulphide Exposure Data Across Alberta*, Alberta Environmental Protection.
- Canadian Association of Petroleum Producers (1990), *Production Waste Management Handbook for the Alberta Upstream Petroleum Industry*, December.
- Canadian Association of Petroleum Producers (1992) *A Detailed Inventory of Methane and Volatile Organic Emissions From Upstream Oil and Gas Operations in Alberta*, Vol. I - Overview of the Emission Data, Vol. II - Development of the Inventory, Vol. III - Results of the Field Validation Program.
- Canadian Council of Ministers of the Environment (1992) *National Guidelines for Hazardous Waste Incineration Facilities - Design and Operating Criteria*, Volume 2.
- Canadian Petroleum Association - Environmental Planning and Management Committee (1984) *Waste Disposal Guidelines for the Petroleum Industry*.
- Carrascal, M.D., M. Puigcerver, P.Puig (1993) Sensitivity of Gaussian Plume Model to Dispersion Specifications, *Theoretical and Applied Climatology*, Vol. 48, pp 147-157.
- Carroll, J.J. (1993) Sensitivity of PBL Model Predictions to Model Design and Uncertainties in Environmental Inputs, *Boundary-Layer Meteorology*, Vol 65, pp 137 - 158.
- Cassinelli, M.E., R.D.Hull, J.V. Crable, A.W. Teass (1986) Protocol for the Evaluation of Passive Monitors, In: *Diffusive Sampling: an alternative approach to workplace air monitoring: the proceedings of an international symposium, Luxembourg, Sept 22-26, 1986*, eds: A. Berlin, R.H. Brown, K.J. Saunders, pp 190-202.

Caughey, S. J., J.C. Wyngaard, J.C. Kaimal (1979) Turbulence in the Evolving Stable Boundary Layer, *Journal of Atmospheric Sciences*, Vol 36, pp 1041 - 1052.

Chadwick, M.J., J.C.I. Kuylenstierna (1992) Effects of Acidic Depositions on Living Organisms, *International Journal of Environment and Pollution*, Vol 2, No. 1/2, pp 23 - 42.

Chalmers, G.A. (Ed.) (1997) A Literature Review and Discussion of the Toxicological Hazards of Oilfield Pollutants in Cattle, Alberta Research Council, Vegreville, AB, 1997, ARCV97-R2, 440 pp.

Chatwin, P. (1993) Round Table Discussion: Interactions and Feedback Between Theory and Experiment, *Boundary-Layer Meteorology*, Vol 62, pp 435-448.

Cheng, L., R.P. Angle (1996) Model-Calculated Inter-annual Variability of Concentration, Deposition, and Transboundary Transport of Anthropogenic Sulphur and Nitrogen in Alberta, *Atmospheric Environment*, Vol 30, No. 23, pp 4021 - 4030.

Cimorelli, A.J., S.G.Perry, R.F. Lee, R.J.Paine, A. Venkatram, J.C. Weil, R.B. Wilson, Current Progress in the AERMIC Model Development Program, Report No. 96-TP24B.04, 28 pages.

Colley, D.G., Rutberg, R.J., Smolarski, G.M., Jackson, R.P. (1985) Oil and Gas Fugitive Emissions - Testing and Combustion, In: *Proceedings of the Fifth Annual Technical Meeting of the Air Pollution Control Association - Canadian Prairie and Northern Section*, June 1985, Calgary, Alberta.

Cooper, J.A., E. Peake (1990) Source Apportionment Studies Near Crossfield, Alberta, In: *Acidic Deposition: Sulphur and Nitrogen Oxides*, Eds: A.H. Legge, S.V. Krupa, Lewis Publishers Inc., pp 347 - 380.

Cottle, M., T. Guidotti (1990) Process Chemicals in the Oil and Gas Industry: Potential Occupational Hazards, *Toxicology and Industrial Health*, Vol 6, No. 1, p 41-56.

Cox, W.M., Tikvart, J.A. (1986) Assessing the Performance Level of Air Quality Models, In: *Air Pollution Modeling and Its Application V*, Eds: C. De Wispelaere, F.A. Schiemeier, N.V. Gillani, Plenum Press, New York, p 425-439.

Curry, R.N. (1981) *Fundamentals of Natural Gas Conditioning*, PennWell Books, PennWell Publishing Company, Tulsa, Oklahoma, 118 pages.

David Bromley Engineering (1983) Ltd. (1991), *Hazardous Waste Volumes and Residual Wastes in the Province of Alberta*, prepared for Chem-Security (Alberta) Ltd.

Davis, C.S., Hunt, J.E. (1990) Evaluation of Methods for Measuring Dry Deposition and Recommendations for Establishing a Regional Dry Deposition Monitoring Network in Alberta, 162 pages.

Davison, D.S., C.C. Fortems, K.L. Grandia (1977) The Application of Turbulence Measurements to Dispersion of a Large Industrial Effluent Plume, In: *Joint Conference on Applications of Air Pollution Meteorology*, November 29 - December 2, 1977, Salt Lake City, Utah.

De Klerk, N.H., D.R. English, B.K. Armstrong (1989) A Review of the Effects of Random Measurement on Relative Risk Estimates in Epidemiological Studies, *International Journal of Epidemiology*, Vol. 18, No. 3, pp 705 - 712.

- Deardorff, J.W. (1970a) Preliminary Results From Numerical Integrations of the Unstable Boundary Layer. *Journal of the Atmospheric Sciences*, Vol. 27, pp 1209 - 1211.
- Deardorff, J.W. (1970b) Convective Velocity and Temperature Scales for the Unstable Boundary Layer, *Journal of Atmospheric Sciences*, Vol. 27, pp 1211 - 1213.
- Deardorff, J.W., and Willis, G.E. (1974) Computer and Laboratory Modelling of the Vertical Diffusion of Nonbuoyant Particles in the Mixed Layer, *Advanced Geophysics*, Vol. 18B, Academic Press, pp 187- 200.
- Deardorff, J.W., G.E. Willis (1984) Ground Level Concentration Fluctuations From a Buoyant and a Non-Buoyant Source Within a Laboratory Convectively Mixed Layer, *Atmospheric Environment*, Vol. 18, No 7, pp 1297 - 1309.
- Deardorff, J.W. (1985) Laboratory Experiments on Diffusion: The Use of Convective Mixed-Layer Scaling, *Journal of Climate and Applied Meteorology*, Vol. 24, pp 1143 - 1166.
- De Fre, R., T. Rymen (1989) PCDD and PCDF Formation From Hydrocarbon Combustion in the Presence of Hydrogen Chloride, *Chemosphere*, Vol. 19, No 1, pp 331 - 336.
- Dibble, C. (1997) Geographic Modeling with Computational Laboratories, URL: <http://www.ncgia.ucsb.edu/~cath/geocomp97.html>.
- Dockery, D.W. (1993) Epidemiologic Study Design for Investigating Respiratory Health Effects of Complex Air Pollution Mixtures, *Environmental Health Perspectives Supplements*, Vol. 101, Suppl. 4, December, pp 187 - 191.
- Draxler, R.R. (1987) Accuracy of Various Diffusion and Stability Schemes over Washington, D.C., *Atmospheric Environment*, Vol. 21, No. 3, pp 491-499.
- Druilhet, A., P. Durand (1997) Experimental Investigation of Atmospheric Boundary Layer Turbulence, *Atmospheric Research*, Vol. 43, pp 345-388, 1997.
- Eaves, A., R.C. Macaulay (1964) Sulphur Dioxide Pollution: Statistical Analysis of Results From Adjacent Lead Dioxide and Hydrogen Peroxide Instruments, *International Journal of Air and Water Pollution*, Vol. 8, pp 645-655.
- Ecology Audits, Inc. (1975) Atmospheric Emissions Survey of the Sour Gas Processing Industry, EPA-450/3-75-076.
- Ehrlich, P.R., A.H. Ehrlich, (1996) Fables about Toxic Substances, In: *Betrayal of Science and Reason - How Anti-Environmental Rhetoric Threatens Our Future*, Island Press/Shearwater Books, Washington D.C., p 153.
- Eifler, C.W., S.S. Stinnett, P.A Buffler (1981) Simple Models for Community Exposure from Point Sources of Pollution, *Environmental Research*, Vol. 25, pp 139-146.
- Eklund, G., J.R. Pedersen, B. Stromberg (1988) Methane, hydrogen chloride and oxygen form a wide range of chlorinated organic species in the temperature range 400 - 950C., *Chemosphere*, Vol. 17, No 3, pp 575 - 586.

Environment Canada and CH2M HILL Engineering Ltd. (1993) Evaluation of Options to Reduce Sulphur Dioxide Emissions From the Natural Gas Processing and Tar Sands Industries, Report EPS 2/PN/2.

Environmental Conservation Authority (1972) Environmental Effects of the Operation of Sulphur Extraction Gas Plants in Alberta, Report and Recommendations.

Environmental Conservation Authority (1973) Environmental Effects of the Operation of Sulphur Extraction Gas Plants in Alberta - Summary of the Public Hearings.

Environmental Criteria and Assessment Office, US Environmental Protection Agency (1989) An Acid Aerosols Issue Paper: Health Effects and Aerometrics, EPA-600/8-88-005F.

Environmental Protection Agency, Guideline on Air Quality Models (Revised), EPA - 450/2-78-027R (Appendix W of 40 CFR Part 51).10.1 - 10.7.

Environmental Protection Agency, On-Site Meteorological Program Guidance for Regulatory Modeling Applications, EPA-450/4-87-013.

Erbrink, J.J. (1991) A Practical Model for the Calculation of σ_y and σ_z for Use in an On-line Gaussian Dispersion Model for Tall Stacks Based on Wind Fluctuations, Atmospheric Environment, Vol. 25A, No 2, pp 277-283.

Erisman, J.W., C. Beier, G. Draaijers, S. Lindberg (1994) Review of Deposition Monitoring Methods, Tellus, 46B, 79-94.

Energy Resources Conservation Board Exhibit No 57 (1981) Answer to Undertaking of Edward Lewis Jones, P.Eng., In Reference to ERCB Application No. 810092 -- Shell Canada Resources Ltd., Jumping Pound Gas Processing Plant, November 23, 1981.

Federal Register: (August 12, 1996) Rules and Regulations, Part II, United States Environmental Protection Agency, 40 CFR Parts 51 and 52, Appendix W to Part 51--Guideline on Air Quality Models, Vol. 61, No. 156, pp 41837-41894.

Flesch, T.K., J.D. Wilson (1993) Extreme Value Analysis of Wind Gusts in Alberta, A Joint Publication of Forestry Canada and the Alberta Land and Forest Services pursuant to the Canada-Alberta Partnership Agreement in Forestry, Geography Dept., University of Alberta, Project No. A-8033-107.

Gifford, F.A. (1981) Estimating Ground-Level Concentration Patterns from Isolated Air-Pollution Sources: A Brief Summary, Environmental Research, Vol.. 25, pp 126-138.

Gnyp, A.W., C.C. St.Pierre (1983a) Trace Element Emission Study at Selected Sour Gas Plant Incinerator Stacks, Presentation at 66th Canadian Chemical Conference, Chemical Institute of Canada, June 5-8, 1983, Calgary, Alberta.

Gnyp, A.W., C.C. St. Pierre, D.S. Smith, S. Viswanathan (1983b) A Trace Element Study at Selected Sour Gas Plant Incinerator Stacks in the Province of Alberta. Strachan-Gulf Oil Canada Ltd.; Ram River - Canterra Energy Ltd; Jumping Pound - Shell Canada Ltd., Industrial Research Institute of the University of Windsor, Windsor, Ontario, Canada.

Gnyp, A.W., C.C. St. Pierre, D.S. Smith, S. Viswanathan (1983c) A Trace Element Study at Selected Sour Gas Plant Incinerator Stacks in the Province of Alberta, Waterton-Shell Canada Resources Ltd., Pincher

- Creek-Gulf Oil Canada Ltd., Industrial Research Institute of the University of Windsor, Windsor, Ontario, Canada.
- Gnyp, A.W., C.C. St.Pierre, D.S. Smith, S. Viswanathan (1986a) A Trace Element Study of Process Streams with Potential Discharge to Flare Stacks at Selected Sour Gas Plants in the Province of Alberta, The Industrial Research Institute of the University of Windsor, Windsor, Ontario, Canada, Prepared for the Energy Resources Conservation Board.
- Gnyp, A.W., C.C. St. Pierre, D.S. Smith, S. Viswanathan (1986b) A Trace Element Study of Process Streams with Potential Discharge to Flare Stacks at Selected Sour Gas Plants in the Province of Alberta, The Industrial Research Institute of the University of Windsor, Windsor, Ontario, Canada.
- Gryning, S.E., P. van Ulden and S.E. Larsen (1983). Dispersion From a Continuous Ground Level Source Investigated by a K-model, Quarterly Journal of the Royal Meteorological Society, Vol. 109, pp 355-64.
- Guenther, A. and B. Lamb (1989) Atmospheric Dispersion in the Arctic: Winter-Time Boundary-Layer Measurements, Boundary-Layer Meteorology, Vol. 49, pp 339 - 366.
- Hall, C.A.S., and J.W. Day, Jr. (1977) Systems and Models: Terms and Basic Principles. Chapter 1, In: Ecosystem Modelling in Theory and Practice. John Wiley and Sons, New York, pp 6-36.
- Hammond, L.K., L.R.J. Wessman (1973) Kaybob South - Plants I and II, Gas Processing/ Canada, January - February, pp 28-33.
- Hanna, S.R., G.A. Briggs, J. Deardorff, B.S. Egan, F.A. Gifford, F. Pasquill (1977) AMS Workshop on Stability Classification Schemes and Sigma Curves - Summary of Recommendations, Bulletin of the American Meteorological Society, Vol. 58, pp 1305 - 1309.
- Hanna, S.R., T.V.Crawford, W.B. Bendel, J.W.Deardorff, T.W. Horst, G.H. Fichtl, D. Randerson, S.P.S. Arya and J.M. Noorman (1978) Accuracy of Dispersion Models - A Position Paper of the AMS 1977 Committee on Atmospheric Turbulence and Diffusion, Bulletin of the American Meteorological Society, Vol. 59, No 8, pp 1025 - 1026.
- Hanna, S.R., Briggs, G.A., Hosker, R.P. (1982) Handbook on Atmospheric Diffusion (DOE/T1C-1123; DE82002045), Technical Information Center, US Department of Energy.
- Hanna, S.R. (1982) Review of Atmospheric Diffusion Models for Regulatory Applications, Technical Note No. 177, World Meteorological Organization, Secretariat of the World Meteorological Organization, Geneva, Switzerland.
- Hanna, S.R. (1988) Air Quality Model Evaluation and Uncertainty, Journal of the Pollution Control Association, Vol. 38, pp 406 - 412, 1988.
- Hanna, S.R. (1993) Uncertainties in Air Quality Model Predictions, Boundary-Layer Meteorology, Vol. 62, pp 3-20.
- Harnett, D.L. (1982) Nonparametric Statistics, In: Statistical Methods, Third Edition, Addison-Wesley Publishing Co., Don Mills, Ontario, pp 693-728.
- Harter, P. (1985) Sulphates in the Atmosphere, IEA Coal Research ICTIS/TR30, 155 pages.

- Hasse, L. (1993) Turbulence Closure in Boundary-Layer Theory - An Invitation to Debate, Boundary-Layer Meteorology, Vol. 65, pp 249-254.**
- Hatano, Y., N. Hatano (1997) Fractal Fluctuation of Aerosol Concentration Near Chernobyl, Atmospheric Environment, Vol. 31, No 15, pp 2297 - 2303.**
- Hawkins, J.G., Trotter, D.M., Riddle, M.J. (1986) Characterization of Gas Plant Sludges, In: Petroleum Waste Management "A Western Perspective" Conference and Exhibition, January 22&23, 1986, Calgary Convention Centre, Presented by Canadian Petroleum Association & Info-Tech, A Division of Oilweek.**
- Hewett, P. (1995) Sample Size Formulae for Estimating the True Arithmetic or Geometric Mean of Lognormal Exposure Distributions, American Industrial Hygiene Association Journal, Vol. 56, pp 219-225.**
- Hickey, H.R., E.R. Hendrickson (1965) A Design Basis for Lead Dioxide Cylinders, Journal of the Air Pollution Control Association, Vol. 15, No. 9, pp 409-414.**
- Hicks, B. B. (1985) Behavior of Turbulent Statistics in the Convective Boundary Layer, Journal of Climate and Applied Meteorology, Vol. 24, pp 607-614.**
- Hicks, B.B. (1987) Some Limitations of Dimensional Analysis and Power Laws, Boundary-Layer Meteorology, Vol. 14, pp 567-569.**
- Holtslag, A.A.M. (1984) Estimates of Diabatic Wind Speed Profiles from Near Surface Weather Observations, Boundary-Layer Meteorology, Vol. 29, pp 225 - 250.**
- Höschele, K. (1988) Adequate Meteorological Measurements as a Prerequisite for the Assessment of Air Pollution, In: Environmental Meteorology, K.Grefen and J.Löbel (eds), Kluwer Academic Publishers, pp 1-8.**
- Hrudey, S.E., J.W. Markham, B.G. Kratochvil, R.K. Shaw, R.R. Orford (1983) Scientific Methodology Assessment Committee Report.**
- Hsu, C.S., C.J. Kim (1985) Diethanolamine (DEA) Degradation Under Gas-Treating Conditions, Industrial Engineering Chemical Products Research and Development, Vol. 24, pp 630 - 635.**
- Huey, N.A. (1968) The Lead Dioxide Estimation of Sulphur Dioxide Pollution, Journal of the Air Pollution Control Association, Vol. 18, No. 9, pp 610-611.**
- Hunt, J.C.R. (1981) Some Connections Between Fluid Mechanics and the Solving of Industrial and Environmental Fluid-Flow Problem, Journal of Fluid Mechanics, Vol. 106, 103-130.**
- Irwin, J.S. (1983) Estimating Plume Dispersion - A Comparison of Several Sigma Schemes, Journal of Climate and Applied Meteorology, Vol.. 22, pp 92-114.**
- Irwin, J.S., J.O. Paumier (1990) Characterizing the Dispersive State of Convective Boundary Layers for Applied Dispersion Modeling, Boundary-Layer Meteorology, Vol. 53, pp 267-296.**

Jendritzky, G., K. Bucher (1992) Medical-Meteorological Fundamentals and Their Utilization in Germany, In: Proceedings of The Weather and Health Workshop, Nov 19 – 20, 1992, Ottawa, Ontario, Canada, A. Maarouf (Ed).

Kaimal, J.C., Wyngaard, J.C., Haugen, D.A., Cote, O.R., Izumi, Y., Caughey, S.J., and C.J. Readings, (1976) Turbulence Structure in the Convective Boundary Layer. *Journal of the Atmospheric Sciences*, Vol. 33, pp 2152 - 2169.

Kaimal, J.C., (1978) Horizontal Velocity Spectra in an Unstable Surface Layer. *Journal of the Atmospheric Sciences*, Vol. 35, pp 18-24.

Karim, G.A., R.D. Rowe, E.L. Tollefson (1985) A Review of Flaring in the Sour Gas Industry With Particular Reference to the Emission of Pollutants. A Study Undertaken for the Environmental Protection Service of Environment Canada Under Contract OSG84-00242.

Kellert, S. H. (1993) *In the Wake of Chaos: Unpredictable Order in Dynamical Systems*, University of Chicago Press.

Kennard M.L., A. Meisen (1980) Control DEA Degradation, Hydrocarbon Processing, April, pp 103 - 106.

Kerr, R.K., H.G. Paskall, L.C. Biswanger (1975) Sulphur Plant Waste Gases: Incineration Kinetics and Fuel Consumption, A Summary Report of an Investigation Commissioned by the Government of Alberta, Department of Environment.

Kerr R., H.G. Paskall, L.C. Biswanger (1976a) Sulphur Plant Waste Gases - Incineration Kinetics and Fuel Consumption, *Energy Processing Canada*, Mar-Apr, pp 32 - 40.

Kerr, R.K., H.G. Paskall, N. Ballash (1976b) Claus Process: Catalytic Kinetics Part 1 - Modified Claus Reaction, *Energy Processing Canada*, September - October, pp 66 - 72.

Kerr, R.D., H.G. Paskall (1976c) Claus Process: Catalytic Kinetics Part 2 - COS and CS₂ Hydrolysis, *Energy Processing Canada*, November - December, pp 38 - 44.

Kerr, R.D., H.G. Paskall, N. Ballash (1977) Claus Process: Catalytic Kinetics Part 3 - Deactivation Mechanisms Evaluations and Catalyst, *Energy Processing Canada*, January - February, pp 40 - 51.

Khanna, S., J.G. Brasseur (1998) Three-Dimensional Buoyancy- and Shear-Induced Local Structure of the Atmospheric Boundary Layer, *Journal of the Atmospheric Sciences*, Vol. 55, pp 710 - 743.

Kim C.J. (1988) Degradation of Alkanolamines in Gas-Treating Solutions: Kinetics of Di-2-propanolamine Degradation in Aqueous Solutions Containing Carbon Dioxide, *Industrial Engineering and Chemical Research*, Vol. 27, pp 1-3.

Klemm, R.F. (1972) Environmental Effects of the Operation of Sulphur Extraction Gas Plants, Submitted to Environment Conservation Authority.

Kohl, A.L., F.C. Riesenfeld (1979) *Gas Purification*, Third Edition, Gulf Publishing Company, Book Division, Houston, 825 pages.

- Koutrakis, P., A.M. Fasano, J.L. Slater, J.D. Spengler, J.F. McCarthy, B.P. Leaderer (1989) Design of a Personal Annular Denuder Sampler to Measure Atmospheric Aerosols and Gases, *Atmospheric Environment*, Vol. 23, No 12, pp 2767 - 2773.
- Kretzschmar, J.G., I. Mertens (1980) Influence of the Turbulence Typing Schemes Upon the Yearly Average Ground-Level Concentrations Calculated by Means of a Mean Wind Direction Model, *Atmospheric Environment*, Vol. 14, pp 947-951.
- Lamb, R.G., (1978) A Numerical Simulation of Dispersion From an Elevated Point Source in the Convective Planetary Boundary Layer, *Journal of the Atmospheric Sciences*, Vol.. 33, 2152 - 2169.
- Lamb, R.G. (1984) Diffusion in the Convective Boundary Layer, In: *Atmospheric Turbulence and Air Pollution Modelling*, Eds: F.T.M. Nieuwstadt and H. van Dop, D. Reidel Publishing Company, Boston, pp 159 - 229.
- Langstaff, J., C. Seigneur, M-K. Liu, J. Behar, J.L. McElroy (1987) Design of an Optimum Air Monitoring Network for Exposure Assessments, *Atmospheric Environment*, Vol. 21, pp 1393-410.
- Lawrence, E.N. (1964) The Measurement of Atmospheric Sulphur Compounds Using Lead Dioxide, *International Journal of Air and Water Pollution*, Vol. 8 pp 381-388.
- Leaderer, B.P., P.J. Liroy, J.D. Spengler (1993) Assessing Exposures to Inhaled Complex Mixtures, *Environmental Health Perspectives Supplements*, Vol. 101, Suppl. 4, Dec., pp 167-177.
- Leaderer, B.P., P. Koutrakis, J.M. Wolfson, J.R. Sullivan (1994) Development and Evaluation of a Passive Sampler to Collect Nitrous Acid and Sulphur Dioxide, *Journal of Exposure Analysis and Environmental Epidemiology*, Vol. 4, No 4, pp 503-522.
- Leahey, D.M., M. Schroeder (1985) Sulphur, In: *Atmospheric Emissions Monitoring and Vegetation Effects in the Athabasca Oil Sands Region*. Syncrude Canada Ltd., Environmental Research, 1985-5.
- Leahey, D.M., A.H. Legge (1988a) Evaluation of Passive Monitors as a Means of Assessing SO₂ and H₂S Pollution at Fortress Mountain and Crossfield, Alberta, A Report Prepared for The Acid Deposition Research Program.
- Leahey, D.M., A.H. Legge (1988b) The Use of Sulphation Information to Evaluate Models of Sulphate Deposition, Prepared for presentation at the CPANS/APCA Annual Meeting, Calgary, AB, May 16-17, 1988.
- Legge, A.H., J. Corbin, J. Bogner, M. Strosher, H.R. Krouse, E.J. Laishley, R.D. Bryant, M.J. Cavey, C.E. Prescott, M. Nosal, H.U. Schellhase, T.C. Weidensaul, and J. Mayo (1988) Acidification in a Temperate Forest Ecosystem: The Role of Sulphur Gas Emissions and Sulphur Dust - A Final Report Submitted to the Whitecourt Environmental Study Group, 399 pages.
- Legge, A.H., S.V. Krupa (Eds.) (1990), *Acidic Deposition: Sulphur and Nitrogen Oxides - The Alberta Government/Industry Acid Deposition Research Program (ADRP)*, Lewis Publishers, 1990, 659 pages.
- Leidel, N.A., K.A., Busch, J.R. Lynch, (1977) *Occupational Exposure Sampling Strategy Manual*, National Institute for Occupational Safety and Health, 132 pages.

- Leung, D.Y.C, C.H Liu (1996) Improved Estimators for the Standard Deviations of Horizontal Wind Fluctuations, *Atmospheric Environment*, Vol. 30, No. 14, pp 2456-2461.
- Levadie, B. (1979) Sampling and Analysis of Atmospheric Sulphur Dioxide with the Lead Dioxide Plate (Huey Plate), *Journal of Testing and Evaluation*, Vol. 7, pp 61-67.
- Liang, S.F., C.V. Sternling, T.R. Galloway (1973) Evaluation of the Effectiveness of the Lead Peroxide Method for Atmospheric Monitoring of Sulfur Dioxide, *Journal of the Air Pollution Control Association*, Vol. 23, No 7, pp 605 - 607.
- Lillie, L.E. (1992) Introduction, In: *Effects of Acid Forming Emissions: Proceedings of an International Workshop*, 334 pp, R.W. Coppock and L.E. Lillie (ed.). Alberta Environmental Center, Vegreville, Alberta, AECV92-P2.
- Lott, R.A. (1985) SO₂ Concentrations Near Tall Stacks, *Atmospheric Environment*, Vol. 19, No. 10, pp 1589 - 1599.
- Lynch, A.J., N.R. McQuaker, M. Gurney (1978) Calibration Factors and Estimation of Atmospheric SO₂ and Fluoride by Use of Solid Adsorbents, *Environmental Science and Technology*, Vol. 12, No. 2, pp 169 - 173.
- Lyons, T.J., W.D. Scott (1990) *The Atmospheric Boundary Layer*, In: *Principles of Air Pollution Meteorology*, Bellhaven Press, London.
- Martin, D.O. (1971) An Urban Diffusion Model for Estimating Long Term Average Values of Air Quality, *Journal of Air Pollution Control Association*, Vol. 21, pp 16-23.
- McNider, R.T., D.E. England, M.J. Friedman, X. Shi (1995) Predictability of the Stable Atmospheric Boundary Layer, *Journal of the Atmospheric Sciences*, Vol. 52, No. 14, pp 1602 - 1614.
- Meade, P.J., F. Pasquill (1958) A Study of the Average Distribution of Pollution Around Staythorpe, *International Journal of Air Pollution*, Vol. 1, pp 60 - 70.
- Meetham, A.R. (1961) *Atmospheric Pollution - Its Origins and Prevention*, Pergamon Press, London.
- Mennen, M.G., H.J.M.A. Zwart, J.E.M. Hogenkamp, J.W. Erisman (1996) Flow Distortion Errors Caused by Rigid Obstacles in Dry Deposition Measurement Systems, *Boundary-Layer Meteorology*, Vol. 81, pp 353- 371.
- Meyers, T.P., D.R., Matt, D.D. Baldocchi, B.B. Hicks (1988) On the Use of Measurements and Models of Dry Deposition, *Air Pollution Control and Hazardous Waste Management 81st Annual Meeting of APCA*, Dallas, Texas, June 19-24.
- Mohan, M., T.A. Siddiqui (1997) An Evaluation of Dispersion Coefficients for Use in Air Quality Models, *Boundary-Layer Meteorology*, Vol. 84, pp 177-206.
- Miller, C.W., C.A. Little (1980) Accuracy of Gaussian Plume Dispersion Model Predictions as a Function of Three Atmospheric Stability Classification Calculations, *Health Physics*, Vol. 39, November, pp 773 - 783.

Mullins, B.J., D.E. Solomon, G.L. Austin, L.M. Kacmarcik, (Ecology Audits Inc.) (1975) Atmospheric Emissions Survey of the Sour Gas Processing Industry, Report No. EPA-450/3-75-076.

Munn (1970) Design of Air Quality Monitoring Networks, Macmillan, London.

National Acid Precipitation Assessment Program (1990), NAPAP Report 8, Relationships between Atmospheric Emissions and Deposition/Air Quality.

National Pollutant Release Inventory Summary Report (1995) Canadian Environmental Protection Act, Environment Canada, Minister of Public Works and Government Services Canada.

Nestrick *et al.* (1987) Thermolytic Surface-Reaction of Benzene and Iron (iii) chloride to form chlorinated DBPD and DBF's, Chemosphere, Vol. 16, No 4, pp 777 - 790.

Neumann, J. (1977) Averaging for Wind Speed in a Given Direction in the Concentration Equation for Pollutants, Journal of Applied Meteorology, Vol. 16, pp 1097-1100.

Nieuwstadt, F.T.M., H. van Dop (Eds.) (1984) Atmospheric Turbulence and Air Pollution Modelling - A Course Held in The Hague, 21-25 September, 1981, D. Reidel Publishing Company, Dordrecht. 358 pages.

Nieuwstadt, F.T.M., P.G. Duynkerke (1996) Turbulence in the Atmospheric Boundary Layer, Atmospheric Research, Vol. 40, pp 111-42.

NIOSH Manual of Analytical Methods (1994), 4th ed., DHHS (NIOSH) Publication 94-113, Eller, P. & Cassinelli, M., Eds.

Noel, D., J-J. Hechler, H. Roberge (1989) Performance of Sulphation and Nitration Plates Used to Monitor Atmospheric Pollutant Deposition in a Real Environment, Atmospheric Environment, Vol. 23, No 3, 603-609.

Noll, K.E., T.L. Miller, J.E. Norco, R.K. Rauffer (1977) An Objective Air Monitoring Site Selection Methodology For Large Point Sources, Atmospheric Environment, Vol. 11, pp 1051 - 1059.

Noll, K.E., T.L. Miller (1977). Air Monitoring Survey Design, Ann Arbor Science, Ann Arbor, 296 pp.

Okamoto, S., Shiozawa, K. (1978) Validation of an Air Pollution Model for the Keihin Area, Atmospheric Environment, Vol. 12, pp 2139 - 2149.

Osenton, J.B., A.R. Knight (1971) Sweetening Agent Losses Explored, Canadian Gas Journal Gas Processing/Canada, March - April, pp 30 - 33.

Panofsky, H.A., H. Tennekes, D.H. Lenschow, J.C. Wyngaard, (1977) The Characteristics of Turbulent Velocity Components in the Surface Layer Under Convective Conditions, Boundary Layer Meteorology, Vol. 11, pp 355- 361.

Parungo, F.P., R.F. Puschel, D.L. Wellman, (1980) Chemical Characteristics of Oil Refinery Plumes in Los Angeles, Atmospheric Environment, Vol. 14, pp 509-522.

Paumier, J.O., S.G. Perry, D.J. Burns (1992) CTDMPPLUS: A Dispersion Model for Sources Near Complex Topography, Part II: Performance Characteristics, Journal of Applied Meteorology, Vol. 31, pp 646 - 660, July.

Pelegrin, M. (1993) Introduction to Lecture Series 191 on Non Linear Dynamics and Chaos, Advisory Group for Aerospace Research and Development, North Atlantic Treaty Organization.

Personal communication, H. Bertram, Alberta Research Council (previously Alberta Environmental Center), Vegreville, 1997.

Personal communication, A. Clarke, Analyst, Chemex Laboratories, Edmonton, 1996.

Personal communication, R.B. DeBoeck, Senior Mechanical Engineer, Titan Projects, Ltd., Consulting Engineers, Calgary, 1996

Personal communication, I. Wheeler, Industrial Hygienist, Certified Industrial Hygiene Consulting Ltd., Calgary, 1996.

Pervier, J.W., R.C. Barley, D.E. Field, B.M. Friedman, R.B. Morris, W.A. Schwartz (1974) Survey Reports on Atmospheric Emissions From the Petrochemical Industry, Volume II, Prepared for Environmental Protection Agency, Office of Air and Water Programs, Office of Air Quality Planning and Standards, EPA-450/3-73-005-b, April 1974.

Petroleum Extension Service (1974) Texas Education Agency, Committee on Vocational Training and Gas Processors Association, Plant Processing of Natural Gas.

Picard, D.J., D.G. Colley, D.H. Boyd (1987) Emission Data Base: Emission Inventory of Sulphur Oxides and Nitrogen Oxides in Alberta, Prepared for the Acid Deposition Research Program by Western Research, Division of Bow Valley Resource Services Ltd., Calgary, Alberta, Canada, ADRP-A-3-87.

Picard, D.J., D.G. Colley, A.H. Legge (1990) Anthropogenic Sources of Acidic and Acidifying Air Pollutants in Alberta, In: Acidic Deposition: Sulphur and Nitrogen Oxides, A.H. Legge and S.V. Krupa (Eds.) Lewis Publishers, pp 413 - 431.

Picard, D.J., B.D. Ross, D.W.H. Koon (1992) A Detailed Inventory of CH₄ and VOC Emissions From Upstream Oil and Gas Operations in Alberta, Vols. 1, 2, 3, Prepared for the Canadian Petroleum Association, Calgary, Alberta.

Piironen, A.K. (1994) Analysis of Volume Imaging Lidar Signals, PhD Thesis, University of Joensuu, Department of Physics, URL: http://lidar.ssec.wisc.edu/papers/akp_thes/thesis.htm, 77 pages

Prahn, L.P., M. Christensen, (1977) Validation of a Multiple Source Gaussian Air Quality Model, Atmospheric Environment, Vol. 11, pp 791 - 795.

Portelli, R.V. (1978) Mixing Heights, Wind Speeds, and Ventilation Coefficients for Canada, Climatological Studies Number 31, Fisheries and Environment Canada, Atmospheric Environment, Minister of Supply and Services Canada.

Purohit, V., R. A. Orzel (1988) Polypropylene: A Literature Review of the Thermal Decomposition Products and Toxicity, Journal of the American College of Toxicology, Vol. 7, No. 2, pages 221-242, 1988.

Radian Corp. (1987). National Dioxin Study Tier 4 Combustion Sources: Engineering Analysis Report, Prepared for US Environmental Protection Agency, NTIS #PB88-120704, Sept 1987.

- Randall, D.A., B.A. Wielicki (1997) Measurements, Models, and Hypotheses in the Atmospheric Sciences, Bulletin of the American Meteorological Society, Vol. 78, No 3, pp 399-406.
- Rappaport, S.M. (1985) Smoothing of Exposure Variability at the Receptor: Implications for Health Standards, Annals of Occupational Hygiene, Vol. 29, pp 201-214.
- Reid, C.M., B. DeBoeck, M.J.E. Davies (1988) A Study of Current Flaring Practices Used in Oil and Gas Production in the Province of Alberta, (Draft) RMD 86-24, March.
- Rider, P.E., C.C Rider, R.N. Coming (1977) Studies of Huey Sulfation Plates at High Ambient SO₂ Concentrations, Journal of the Air Pollution Control Association, Vol. 27, No 10, pp 1011-1013.
- Roach, S.A. (1977) A Most Rational Basis for Air Sampling Programmes, Annals of Occupational Hygiene, Vol. 20, pp 65-84.
- Robinson, G.D. (1978) Weather and Climate Forecasting as Problems in Hydrodynamics, Monthly Weather Review, Vol. 106, pp 448-457.
- Rogge, W.F., L.M. Hildemann, M.A. Mazurek, G.R. Cass (1993) Sources of Fine Organic Aerosol. 5. Natural Gas Home Appliances, Environmental Science and Technology, Vol. 27, pp 2736 - 2744.
- Rosner, B., D. Spiegelman, W.C. Willett (1990) Correction of Logistic Regression Relative Risk Estimates and Confidence Intervals for Measurement Error: The Case of Multiple Covariates Measured With Error, American Journal of Epidemiology, Vol. 132, No. 4, pp 734-745.
- Rosner, B., D. Spiegelman, W.C. Willett (1992) Correction of Logistic Regression Relative Risk Estimates and Confidence Intervals for Random Within-Person Measurement Error, American Journal of Epidemiology, Vol. 136, No. 11, pp 1400 1409.
- Ross, W.K., Stewart, G.R. (1986) Incineration of Wastes From the Petroleum Industry - A Program Sponsored and Largely Funded by CPA, In: Petroleum Waste Management "A Western Perspective" Conference and Exhibition, Jan 22,23, 1986. Calgary Convention Center, Presented by Canadian Petroleum Association and Info-Tech, A Division of Oilweek.
- Salvadori, G., S.P. Ratti, G. Belli (1996) Modelling the Chernobyl Radioactive Fallout (I): A Fractal Approach in Northern Italy, Chemosphere, Vol. 33, No 12, pp 2347-2357.
- Samet, J.M. (1995) What Can We Expect From Expect From Epidemiologic Studies of Chemical Mixtures? Toxicology, Vol. 105, pp 307-314.
- Samet, J. M., F. E. Speizer (1993) Introduction and Recommendations: Working Group on Indoor Air and Other Complex Mixtures, Environmental Health Perspectives Supplements, Vol 101, Suppl. 4, December, pp 143-147.
- Sandu, H.S., H.P. Sims, R.A. Hursey, W.R. MacDonald, B.R. Hammond (1980) Environmental Sulphur Research in Alberta: A Review, Alberta Department of the Environment.
- SCIEX™ (1982) Air Quality Surveys in Alberta Using the TAGA 3000 Mobile Laboratory.
- Scorer, R.S. (1968) Air Pollution, Pergamon Press, Oxford, London.

Scorer, R.S (1973) *Pollution in the Air - Problems, Policies and Priorities*, Routledge & Kegan Paul, London.

Scorer, R.S.(1980), *Book Review, Clean Air*, Vol. 10, 148-149.

Scott, H.M.(1998) *Effects of Air Emissions From Sour Gas Plants on the Health and Productivity of Beef and Dairy Herds in Alberta, Canada*, PhD. Thesis.

Sedefian, L., E. Bennett (1980) *A Comparison of Turbulence Classification Schemes*, *Atmospheric Environment*, Vol. 14, pp 741-750.

Sexton, K., B.D. Beck, E. Bingham, J.D. Brain, D.M. DeMarini, R.C. Hertzberg, E.J. O'Flaherty, J.G. Pounds (1995) *Chemical Mixtures From a Public Health Perspective: The Importance of Research for Informed Decision Making*, *Toxicology*, Vol. 105, pp 429 - 441.

Sickles, J.E., R.M. Michie (1984) *Investigation of the Performance of Sulphation and Nitration Plates*, EPA-600/3-84-073, US EPA, June.

Sickles, J.E., R.M. Michie (1987) *Evaluation of the Performance of Sulphation and Nitration Plates*, *Atmospheric Environment*, Vol. 21, No 6, pp 1385 - 1391.

Singh, C. (1979) *Experimental Evaluation of Variables Affecting the Lead Dioxide Method for Monitoring of Sulphur Dioxide*, Master of Science Thesis, Department of Chemical Engineering, University of Alberta, Edmonton, AB.

SKM Consulting Ltd (1988) *Review and Assessment of Current Flaring Technology*, for Environmental Protection, Conservation and Protection, Environment Canada, Western and Northern Region in Association with Government Industry Consultative Committee on Flaring, February, 1988.

Smith, M.E. (1984) *Review of the Attributes and Performance of 10 Rural Diffusion Models*, *Bulletin of the American Meteorological Society*, Vol. 65, No 6, pp 554-558.

Spence, J.W., F.W. Lipfert, S. Katz (1993) *The Effect of Specimen Size, Shape, and Orientation on Dry Deposition to Galvanized Steel Surfaces*, *Atmospheric Environment*, Vol. 27A, No 15, pp 2327-2336.

Spitzer, W.O.(1986) McGill Inter-University Research Group, *The Southwestern Alberta Medical Diagnostic Review*, Calgary, Acid Deposition Research Program, June.

Stalker, W.W., R.C. Dickerson, G.D. Kramer (1963) *Atmospheric Sulfur Dioxide and Particulate Matter - A Comparison of Methods of Measurements*, *Journal of the American Industrial Hygiene Association*, Vol. 14, pp 68 - 79.

Steward, R.W.(1979) *The Atmospheric Boundary Layer*, World Meteorological Organization.

Stinnett, S.S., P.A. Buffler, C.W. Eifler (1981) *A Case-Control Method for Assessing Environmental Risks from Multiple Industrial Point Sources*, *Environmental Research*, Vol. 25, pp 62-74.

Stroscher, M.(1982) *Trace Organic Compounds in the Atmosphere Near Industrial Development*, Report to Alberta Environment, February 16.

- Stroscher, (1996) M., Investigations of Flare Gas Emissions in Alberta, A Final Report to Environment Canada, Conservation and Protection, the Energy and Utilities Board, and the Canadian Association of Petroleum Producers (DRAFT), August.
- Stull, R.B. (1988) An Introduction to Boundary Layer Meteorology, Kluwer Academic Publishers, Dordrecht, 666 pages.
- Stull, R.B. (1994) A Convective Transport Theory for Surface Fluxes, Journal of the Atmospheric Sciences, Vol. 51, No 1, pp 3 - 22.
- Sykes, R.I., R.S. Gabruk (1994) Fractal Representation of Turbulent Dispersing Plumes, Journal of Applied Meteorology, Vol. 33, pp 721- 732.
- Tang, H., B. Brassard, R. Brassard, E. Peake (1997) A New Passive Sampling System for Monitoring SO₂ in the Atmosphere, Field Analytical Chemistry and Technology, Vol. 1, No 5, pp 307-314.
- Tennekes, H. (1978) Turbulent Flow in Two and Three Dimensions, Bulletin of the American Meteorological Society, Vol. 59, pp 22-28.
- Thomas, F.W., Davidson, C.M (1961) Monitoring Sulfur Dioxide with Lead Peroxide Candles, J. Air Poll. Control Ass., Vol. 11, p. 24.
- Thompson, T.S., R.E., Clement, N. Thornton, J. Luyt (1990) Formation and Emission of PCDDs/PCDFs in the Petroleum Refining Industry, Chemosphere, Vol. 20, Nos 10 - 12, pp 1525-1532.
- Todd, D.F., W.V. Loscutoff (1993) An Overview of CARB-Adopted Source Test Methods for Toxic Compounds and Results of Testing Natural Gas-Fired Utility Boilers, In: Managing Hazardous Air Pollutants, Eds: W. Chow, K.K. Connor, EPRI TR-101890, Lewis Publishers, Boca Raton, pp 66 - 72.
- Tollefson, E.L., M.T. Stroscher (1985) An Investigation of Flare Stack Emissions From a Sour Gas Plant, In: Proceedings of the 1985 Joint Annual Meeting - Canadian Prairie and Northern Section and Pacific Northwest International Section of the Air Pollution Control Association, Nov 13-15, Calgary AB.
- Tracy, B.L., D.P. Meyerhof (1987) Uranium Concentrations in Air Near a Canadian Uranium Refinery, Atmospheric Environment, Vol. 21, No. 1, pp 165-172.
- Turner, D.B. (1964) A Diffusion Model for an Urban Area, Journal of Applied Meteorology, Vol. 3, No 1, pp 83-91.
- Turner, D.B. (1992) Will Accuracy of Air Quality Simulation Models be Improved Soon? In: Health and Ecological Effects, Papers from the 9th World Clear Air Congress Towards the Year 2000: Critical Issues in the Global Environment, Montreal, Quebec, Canada, Aug 30 - Sept. 4, 1992.
- Turner, D.B. (1994) Workbook of Atmospheric Dispersion Estimates - An Introduction to Dispersion Modeling, Second Edition, Lewis Publishers, Boca Raton.
- Turner, D.B. (1997) The Long Lifetime of the Dispersion Methods of Pasquill in US Regulatory Air Modeling, Journal of Applied Meteorology, Vol. 36, pp 1016 - 1020.
- Turner, J.M., Sholtes, R.S.(1971) Laboratory Evaluation of the Sulfation Plate for Estimation of Atmospheric Sulfur Dioxide, Presented at Air Pollution Control Association 64th Annual Meeting

Twin Butte Soils and Water Evaluation Task Force (1984) Technical Report Twin Butte Soils and Water Evaluation Task Force.

United States Environmental Protection Agency (1989) An Acid Aerosols Issue Paper - Health Effects and Aerometrics, Office of Health and Environmental Assessment, EPA/600/8-88/005F.

United States Environmental Protection Agency (1991) Handbook: Control Technologies for Hazardous Air Pollutants, PB92-141373, National Technical Information Service.

United States Environmental Protection Agency (1991), Office of Toxic Substances, "Toxics in the Community", The 1989 Toxics Release Inventory National Report, EPA 560/4-91-014, Washington, DC, USA.

United States Environmental Protection Agency (1993) Selection Criteria for Mathematical Models Used in Exposure Assessments: Atmospheric Dispersion Models, EPA/600/8-91/038.

United States Environmental Protection Agency (1995) User's Guide for the Industrial Source Complex (ISC3) Dispersion Models, Volumes 1 and 2, EPA Publication Nos. EPA-454/B-95-003a & b. U.S. Environmental Protection Agency, Research Triangle Park, NC. (NTIS Nos. PB 95-222741 and PB 95-222758, respectively)

United States Environmental Protection Agency Support Center for Regulatory Air Models Website (<http://www.epa.gov/ttn/scram>)

United Technology and Science Inc. (1980) Origin and Fate of Emissions of Sulphur Compounds From Petroleum Refineries - A Literature Review, Pace Report No. 80-2, Prepared for Petroleum Association for Conservation of the Canadian Environment.

van Duuren, H., J.J. Erbrink (1988) Modelling Dispersion of Air Pollutants Emitted by Power Stations Using Fluctuations of Wind Direction, In: Environmental Meteorology, K.Grefen, J. Lobel (eds), pp 497-513.

van Dop, H. (1993) Round Table Discussion: Interactions and Feedback Between Theory and Experiment, Boundary-Layer Meteorology, Vol. 62, pp 435-448.

van Ulden, A.P., A.A.M. Holtslag, (1985) Estimation of Atmospheric Boundary Layer Parameters for Diffusion Applications, Journal of Climate and Applied Meteorology, Vol. 24, pp 1196 - 1207.

Venkatram, A. (1978) Estimating the Convective Velocity Scale for Diffusion Applications, Boundary-Layer Meteorology, Vol. 15, pp 447-452.

Venkatram, A. (1979a) The Expected Deviation of Observed Concentrations from Predicted Ensemble Means, Atmospheric Environment, Vol. 13, pp 1547 - 1549.

Venkatram, A. (1979b) A Note on the Measurement and Modelling of Pollutant Concentrations Associated with Point Sources, Boundary-Layer Meteorology, Vol. 17, pp 523-536.

Venkatram, A. (1980a) Evaluation of the Effects of Convection on Plume Behavior in the AOSERP Study Area. Prepared for the Alberta Oil Sands Environmental Research Program. AOSERP Report 95, 75 pages.

- Venkatram, A. (1980b), Dispersion From an Elevated Source in a Convective Boundary Layer, *Atmospheric Environment*, Vol. 14, pp 1- 10.
- Venkatram, A., R. Vet (1981) Modelling of Dispersion from Tall Stacks, *Atmospheric Environment*, Vol. 15, No 9, pp 1531-1538.
- Venkatram, A. (1982) A Framework for Evaluating Air Quality Models, *Boundary-Layer Meteorology*, Vol. 24, pp 371-385.
- Venkatram, A. (1983) Uncertainty in Predictions From Air Quality Models, *Boundary-Layer Meteorology*, Vol. 27, pp 185-196, 1983.
- Venkatram, A., R. Paine (1985) A Model to Estimate Dispersion of Elevated Releases into a Shear-Dominated Boundary Layer, *Atmospheric Environment*, Vol. 19, No 11, pp 1792 - 1805.
- Venkatram, A. (1988a) Inherent Uncertainty in Air Quality Modelling, *Atmospheric Environment*, Vol. 22, No 6, pp 1221 - 1227.
- Venkatram, A. (1988b) Topics in Applied Dispersion Modelling, In: *Lectures on Air Pollution Modelling*, A. Venkatram, J.C. Wyngaard, (Eds.), American Meteorological Society, pp 267-322.
- Venkatram, A. (1993) Estimates of Maximum Ground-Level Concentration in the Convective Boundary Layer - The Error in Using the Gaussian Distribution, *Atmospheric Environment*, Vol. 27A, No. 14, pp 2187 - 2191.
- Vranka, R.G., G.E. Watkin (1993) Effects of Deposition Velocities on Predicted Health Risks, In: *Managing Hazardous Air Pollutants*, W.Chow, K.K. Connor Eds., EPRITR - 101890, Lewis Publishers, Boca Raton.
- Venkatram, A. (1996) An Examination of the Pasquill-Gifford-Turner Dispersion Scheme, *Atmospheric Environment*, Vol. 30, No 8, pp 1283 - 1290.
- Wakkers, P.J.M., H. Hellendoorn, G.J. Op De Weegh, W. Heerspink (1975) Applications of Statistics in Clinical Chemistry - A Critical Evaluation of Regression Lines, *Clinica Chimica Acta*, Vol. 64, pp 173 - 184.
- Walker, A.M., M. Blettner (1985) Comparing Imperfect Measures of Exposure, *American Journal of Epidemiology*, Vol. 121, No 6, pp 783 - 790.
- Wark, K. (1998) Dispersion of Pollutants in the Atmosphere, In: *Air Pollution, Its Origin and Control*, pp 143 - 167.
- Weil, J.C. (1985) Updating Applied Diffusion Models, *Journal of Climate and Applied Meteorology*, Vol. 24, No 11, pp 1111 - 1130.
- Weil, J.C. (1988a) Dispersion in the Convective Boundary Layer, In: *Lectures on Air Pollution Modeling*, A. Venkatram, J.C. Wyngaard, (Eds), American Meteorological Society, pp 167-222.

- Weil, J.C. (1988b) Atmospheric Dispersion - Observations and Models, In: Flow and Transport in the Natural Environment: Advances and Applications, W.L. Steffen, O.T. Denmead (Eds), Springer-Verlag, Berlin, pp 352-379**
- Weil, J.C., R.I. Sykes, A. Venkatram (1992) Evaluating Air-Quality Models: Review and Outlook, Journal of Applied Meteorology, Vol 31, pp 1121-1145.**
- Weil, J.C., L.A. Corio, R.P. Brower (1997) A PDF Dispersion Model for Buoyant Plumes in the Convective Boundary Layer, Journal of Applied Meteorology, Vol. 36, pp 982 - 1003.**
- Westgard, J.O., M. Hunt (1973) Use and Interpretation of Common Statistical Tests in Method-Comparison Studies, Clinical Chemistry, Vol. 19, No 1, pp 49 - 57.**
- Wilks, D. S. (1995) Uncertainty About the Atmosphere, In: Statistical Methods for the Atmospheric Sciences, Academic Press, Inc., pp 2 - 4.**
- Willis, G.E., and J.W. Deardorff (1976) A Laboratory Model of Diffusion into the Convective Planetary Boundary Layer, Quarterly Journal of the Royal Meteorological Society, Vol. 102, pp 427 - 445.**
- Willis, G.E., and J.W. Deardorff (1981) A Laboratory Study of Dispersion From a Source in the Middle of the Convectively Mixed Layer, Atmospheric Environment, Vol. 15, pp 109 - 117.**
- Wilsdon, B.H., F.J. McConnell (1934) The Measurement of Atmospheric Sulphur Pollution by Means of Lead Peroxide, Journal of the Society of Chemical Industry, Dec., pp 385 - 388.**
- Wilson, D. (1994) Predicting Pollutant Concentrations in the Atmosphere, Class Notes.**
- Wilson, D., S. Arulanandam (1996) Uncertainty in Air Pollution Dispersion Models, Dealing with Uncertainty in Risk Assessment and Risk Management Pre Conference Workshop, Eighth Annual Conference of the International Society for Environmental Epidemiologists, Aug 17-21, Edmonton, AB.**
- Wilson, R.B. (1993) Review of Development and Application of CRSTER and MPTER Models, Atmospheric Environment, Vol. 27B, No. 1, pp 41-57, 1993.**
- Wong, O., W.J. Bailey (1993) Cancer Incidence and Community Exposure to Air Emissions from Petroleum and Chemical Plants in Contra Costa County, California: A Critical Epidemiological Assessment, Journal of Environmental Health, Vol. 56, No. 5, pp 11-17.**
- Working Group on Benzene Emissions From Glycol Dehydrators (1997) Best Management Practices for the Control of Benzene Emissions From Glycol Dehydrators, 22 pages.**
- World Health Organization (1979) Environmental Health Criteria for Sulfur Oxides and Suspended Particulate Matter.**
- Wotherspoon and Associates (1988) The Canadian Petroleum Association, Industry Waste Survey, Canadian Petroleum Association Publication, September, 1988.**
- Wyngaard, J. C. (1985) Structure of the Planetary Boundary Layer and Implications for its Modeling, Journal of Climate and Applied Meteorology, Vol. 24, No 11, pp 1131 - 1142.**

Wyngaard, J. C. (1988a) Introduction, In: Lectures on Air Pollution Modeling, A. Venkatram, J.C. Wyngaard, Eds., American Meteorological Society, pp 1-7.

Wyngaard, J. C. (1988b) Structure of the PBL, In: Lectures on Air Pollution Modeling, A. Venkatram, J.C. Wyngaard, Eds., American Meteorological Society, pp 9-61.

Wyngaard, J.C. (1992) Atmospheric Turbulence, Annual Reviews of Fluid Mechanics, Vol. 24, pp 205 - 233.

Yee, E., P.R. Kosteniuk, G.M. Chandler, C.A. Biltoft, J.F. Bowers (1993) Recurrence Statistics of Concentration Fluctuations in Plumes within a Near-Neutral Atmospheric Surface Layer, Boundary-Layer Meteorology, Vol. 66, pp 127-153.

Zannetti, P. (1990) The Climatological Model, In: Air Pollution Modeling - Theories, Computation Methods and Available Software, Van Nostrand Reinhold, New York, pp 162-165.

Zeng, X., R.A. Peilke, R. Eykhold (1992) Estimating the Fractal Dimension and the Predictability of the Atmosphere, Journal of the Atmospheric Sciences, Vol. 49, No 8, pp 649 - 659.

Zeng, X., R.A. Peilke, R. Eykhold (1993) Chaos Theory and its Application to the Atmosphere, Bulletin of the American Meteorological Society, Vol. 74, pp 631-644.